2020-04-29

Novel Approaches to Fight Prion Diseases

Thapa, Simrika

UNIVERSITY OF CALGARY

Novel Approaches to Fight Prion Diseases

by

Simrika Thapa

A THESIS

SUBMITTED TO THE FACULTY OF GRADUATE STUDIES

IN PARTIAL FULFILMENT OF THE REQUIREMENTS FOR THE

DEGREE OF DOCTOR OF PHILOSOPHY

GRADUATE PROGRAM IN VETERINARY MEDICAL SCIENCES

CALGARY, ALBERTA

APRIL, 2020

ABSTRACT

Prion diseases are fatal neurodegenerative disorders caused by PrP^{Sc}, the misfolded and infectious isoform of the cellular prion protein (PrP^{C}). Currently, no preventive or therapeutic measures are available. In this work, we focused on therapeutic and prophylactic strategies against prion infections. In the therapeutic approach, we targeted cellular pathways and investigated the role of the quality control (QC) proteins, ERp57 and VIP36, on prion propagation. We found that the overexpression of ERp57 or VIP36 significantly reduced PrP^{Sc} levels in persistently prion-infected cells and decreased the susceptibility of uninfected cells to *de novo* prion infection. Moreover, lentiviral-mediated overexpression of ERp57 prolonged the survival of prion-infected mice. Mechanistically, we found that ERp57 overexpression reduced endoplasmic reticulum (ER) stress. To translate this proof-of-concept into potential drug therapy, we investigated the anti-prion effect of Sephin1, shown to prolong the phosphorylation of eIF2α and lower ER stress in the cells. In persistently prion-infected neuronal cells, we found that treatment with Sephin1 markedly reduced PrP^{Sc} levels. Moreover, Sephin1 reduced ER stress-induced PrP aggregates in cells and significantly extended the survival of prion-infected mice. These data provide the basis for targeting these cellular pathways as novel anti-prion therapy.

In our prophylactic approach, we hypothesized that active vaccination is useful to contain chronic wasting disease (CWD), a contagious and expanding prion disease of cervids. Here, we vaccinated transgenic mice expressing elk prion protein with adjuvant CpG alone, or one of four recombinant PrP (rPrP) immunogens: deer dimer (Ddi), deer monomer (Dmo), mouse dimer (Mdi), and mouse monomer (Mmo). After challenging the animals with CWD prions intraperitoneally, we found that all vaccinated groups had longer survival times than the CpG

control group. Interestingly, the Mmo-immunized group revealed that survival was extended by 60%. We also observed 28.4% and 24.1% prolongation in Dmo and Ddi groups, respectively. Our preliminary study in reindeer showed substantial humoral immune response induced by Mdi and Ddi, and the sera from the Ddi-vaccinated reindeer significantly reduced CWD prions in a cell culture model. Taken together, this study describes potential vaccine candidates against CWD. However, their protective effect in the natural cervid host needs further investigation.

PREFACE

This thesis is presented as a manuscript-based thesis, including three manuscripts that have already been published in peer-reviewed journals. I am first author on all three. For the animal experiments done in this study, the Canadian Council for Animal Care (CCAC) guidelines were strictly followed, in addition to the University of Calgary Health Sciences Animal Care Committee (HSACC) approval. The permission from the journals and co-authors was taken to include the following published work in this thesis.

The following manuscripts are included in this thesis.

1. Chapter 2 is published in *The Journal of Biological Chemistry* and is reproduced here as:

   Thapa S, Abdulrahman BA, Abdelaziz DH, Lu L, Aissa MB and Schatzl HM. 2018. Overexpression of quality control proteins reduces prion conversion in prion-infected cells. *The Journal of Biological Chemistry*, 293(41): 16069–16082.

   This chapter contains my original work with technical assistance from Dr. Basant A. Abdulrahman and Dr. Dalia H. Abdelaziz. Dr. Li Lu conducted the immunofluorescence experiment and Dr. Manel Ben Aissa performed the cloning experiments and prepared the plasmids.

2. Chapter 3 is published in the *Journal of Molecular Neurobiology* and is reproduced here as:

   Thapa S*, Abdelaziz DH*, Abdulrahman BA and Schatzl HM. 2020. Sephin1 Reduces Prion Infection in Prion-Infected Cells and Animal Model. *Molecular Neurobiology*. https://doi.org/10.1007/s12035-020-01880-y (* represents shared authorship)

   This chapter contains an original idea and a study design that I developed. The experimental study was later developed in close collaboration with Dr. Dalia H. Abdelaziz. I analyzed the data and wrote the manuscript. Dr. Abdelaziz and I worked together to test two

compounds (Sephin1 and Metformin) for their anti-prion efficacy *in vitro* and *in vivo*, of which the results for Sephin1 are presented here. We performed the animal experiment together. Dr. Basant A. Abdulrahman offered technical support.

3. Chapter 4 is published in *The Journal of Biological Chemistry* and is reproduced here as:

   Abdelaziz DH*, **Thapa S***, Brandon J, Maybee J, Vankuppeveld L, McCorkell R and Schatzl HM. 2018. Recombinant prion protein vaccination of transgenic elk PrP mice and reindeer overcomes self-tolerance and protects mice against chronic wasting disease. *The Journal of Biological Chemistry*, 293 (51): 19812-19822, except for the "Result" and "Discussion" sections. I have re-written these two sections to maintain the original concept that was presented in the peer-reviewed manuscript. All of the co-authors have given their consent for the changes in the text (* represents shared authorship).

   I am a shared first author in this manuscript. I developed and co-wrote this chapter in close collaboration with Dr. Dalia H. Abdelaziz. Together, we initiated the CWD vaccination in transgenic mouse models, monitored the animals, determined the terminal disease stage, performed the sampling, and analyzed the brain and spleen samples in immunoblots and RT-QuIC. Dr. Abdelaziz performed ELISA. I performed the immunoblotting for the cell culture studies. Dr. Robert McCorkell, Jenna Brandon, Justine Maybee, and Lauren Vankuppeveld conducted the reindeer vaccination and did the reindeer *Prnp* genotyping.

ACKNOWLEDGEMENTS

All the praise be to the Almighty. I am grateful for His endless blessings, constant guidance, help, and protection.

First, I would like to acknowledge the Faculty of Veterinary Medicine (UCVM) at the University of Calgary for providing me with the opportunity to pursue my PhD and inspiring me continuously throughout the program.

To begin with, I would like to mention my supervisor, Prof. Hermann Schaetzl, who has made the foremost contribution to my academic life. His tremendous support and guidance have made my PhD journey smooth and very comfortable. I still remember the day when he motivated me to believe that I could earn my PhD and inspired me to pursue my dream of an academic career, though I was struggling with decision-making about what was next after the completion of my Master's degree. I really admire his extraordinary supervision, constant guidance, thoughtful criticism, optimistic attitude, and inspiration, which have been invaluable for my productivity and successful achievements. He is my source of inspiration, the one who has provided me tremendous support to conduct my research enthusiastically, gain new learning experiences, and develop professional, communication, and writing skills. I am very fortunate to have such a dedicated and knowledgeable person as my PhD supervisor. I really want to thank you, Hermann, for your guidance, encouragement, immense support, inspiration, patience, and excellent supervision for all these years.

Next, I would like to extend my sincere gratitude to my supervisory committee members, Dr. Sabine Gilch, Dr. Guido van Marle, and Dr. Tuan Trang, for their constant support and guidance, which have always helped me to improve my work. My mentors were always welcoming and open for discussions. Their critical comments have indeed helped me to improve my scientific

reasoning and skills. I am very grateful to all my supervisory committee members for their willingness to give me time whenever I needed and for helping me with my academics and research. Thank you so much to each one of you for your dedication and full mentoring throughout my PhD years. I will always remember your commitment and kindness.

Special thanks goes to Dr. Carla Coffin and Prof. Glen Telling for their time and kind willingness to be on my committee as examiners.

I would like to thank all my past and present lab members, Samia, Dalia, Basant, Li, Su, Cristobal, Waqas, Maria, Pearl, Ginny, Chris, Tahir, Rupali, Antonia, Shubha, Lilian, Bukola, and Govinda, for their constant help and tremendous support. I am indebted for the suggestions they have always provided to help improve my work, and for their excellent collaborations, which have created a positive lab environment. Specifically, I would like to thank Dr. Dalia Abdelaziz, whom I have worked with in different projects in the lab (particularly on the CWD vaccine project). She is a very dedicated researcher and I have learned a lot from her. Whenever I encountered problems, she was always there to advise and help me in optimising and solving them. I will always remember the long chats we used to have while spending long hours in the animal facility during experimental procedures. I really appreciate her help, support, advice, time, and effort. I really enjoyed working with her on a team and I feel proud that our team was quite productive in terms of generating data. Next, I would like to thank Dr. Basant Abdulrahman, from whom I initially learned cell culture techniques. I really admire her optimistic nature and dedication to work. I am really thankful to her for all the suggestions, help, support, and time she has given me. I am also thankful to Dr. Li Lu for performing immunofluorescence experiments, Ginny Cheng for preparing the necessary recombinant PrP protein (for RT-QuIC), and Dr. Manel Ben Aissa for cloning the plasmid constructs. I express my gratitude to Dr. Robert McCorkell, and the summer students, Jenna,

Justine, and Lauren, for performing the reindeer vaccination study. I want to thank Dr. Samia Hannaoui and Chris Chang for helping me to revise my thesis.

I am really grateful to all the vets and staff of the Animal Resource Centre (ARC), especially Dr. Lillian Oribhabor and Bukola Alli, for taking very good care of our animals and for their kindness. I am very grateful to Dr. Frank Visser from the Hotchkiss Brain Institute (HBI) Molecular Core facility for preparing the lentiviruses used in my animal study. Also, I would like to acknowledge Dr. Nathalie Daude from the Histopathology facility at the Centre for Protein Misfolding Diseases at the University of Alberta for performing the histological staining and analysis. I am grateful to the Academic Copy Editing service at the University of Alberta, especially Debby Waldman, for reviewing chapter 1 and 5 for grammer, puntuations and language clarity. I am also thankful to Dr. Careem, Dr. Czub, Dr. van Marle, Dr. van der Meer, and Dr. Coffin and all their lab members for their help and willingness to share lab resources and equipment. Also, thanks goes to the Virology, Infection Biology, and Neurodegenerative Disease groups at the University of Calgary.

I would also like to express my gratitude to Dr. Jacob Thundathil (present Associate Dean of Graduate Education), Dr. John Matyas (past Associate Dean of Graduate Education), Kasia Wojdyla (Graduate Program Administrator), and Mina Ojaghi (Graduate Program Coordinator) from the UCVM Office of Graduate Education for their constant support, guidance, encouragement, and help. Also, I am very grateful to the University of Calgary Eyes High, the Killam Trusts, and Alberta Innovates-Health Solutions (AIHS) for awarding me doctoral fellowships and supporting me financially during my PhD. Also, I would like to thank Alberta Prion Research Institute (APRI) for their humongous support with the funding and travel grants.

Next, I am very much grateful to Samia, my sister and my best friend. Thanks for being beside me in all the ups and downs. I just want to tell you, Sam that I love you and you are my family. Also, I want to thank my dear and close friends, Shubha, Bahja, Hanaa, Rkia, and Mahua for supporting me and always being there for me.

Lastly, I would like to thank my family for all their support and for making me what I am today. I am indebted to my parents who have constantly fought against various situations and been through hardships just to give me a better life and all possible opportunities. Their unconditional love and care are my biggest strengths and source of inspiration, and are indeed precious in my life. Also, I would like to thank my husband, Salman, for filling my life with love and joy. He is so supportive, loving, caring, and patient, and he just makes me happy all the time. I cannot imagine my life without him. Thanks a lot for making my life so smooth, enjoyable, and full of happiness. I am also thankful to my sister, Bhumika, who loves me unconditionally and has always sacrificed everything for me since our childhood. Also, I am grateful to my sister in-law, Sakufa, for all her constant support, unconditional love, understanding, and prayers. I am thankful to my beautiful nephew and nieces, Zaiyan, Manha, and Afsah for filling my life with their smiles and happiness. I am also grateful to Tania for her love and support. Last but not the least, I am thankful to my in-laws for being so supportive and encouraging. I feel blessed to have such a loving family. I love you all so much.

Thank you very much.

Simrika Thapa

DEDICATION

To my beloved Mom and Dad,

To my loving husband, Salman,

To my supportive family, friends and mentors

TABLE OF CONTENTS

LIST OF TABLES

LIST OF FIGURES

LIST OF ABBREVIATIONS

A	Alanine
AAV	Adeno-associated virus
AD	Alzheimer’s disease
ALS	Amyotrophic lateral sclerosis
ARC	Animal Resource Centre
ATF4	Activating transcription factor 4
ATF6	Activating transcription factor 6
Aβ	Amyloid beta
BBB	Blood brain barrier
BH	Brain homogenate
BSA	Bovine serum albumin
BiP	Binding immunoglobulin protein
BSE	Bovine spongiform encephalopathy
C	Cysteine
C-BSE	Classical bovine spongiform encephalopathy
CCAC	Canadian Council for Animal Care
CD	Circular dichroism
CHOP	C/EBP homologous protein
CJD	Creutzfeldt-Jakob disease
CNS	Central nervous system
CNX	Calnexin

COCS	Cerebellar organotypic-cultured slices
CPD	Camel prion disease
CRT	Calreticulin
CSF	Cerebrospinal fluid
CWD	Chronic wasting disease
D	Aspartic acid
Ddi	Deer dimer recombinant PrP
Dmo	Deer monomer recombinant PrP
DOC	Sodium deoxycholate
dpi	Days post-infection
DSE	Disease-specific epitope
DY	Drowsy TME prion strain
E	Glutamic acid
EDTA	Ethylenediaminetetraacetic acid
EEG	Electroencephalogram
eIF2α	Eukaryotic translation initiation factor 2α
ELISA	Enzyme-linked immunosorbent assay
ER	Endoplasmic reticulum
ERAD	Endoplasmic reticulum-associated degradation
EUE	Exotic ungulate spongiform encephalopathy
F	Phenylalanine
FBS	Fetal bovine serum

fCJD	Familial Creutzfeldt-Jakob disease
FFI	Fatal familial insomnia
FTIR	Fourier transform infrared spectroscopy
G	Glycine
GAGS	Glycosaminoglycans
GALT	Gut-associated lymphoid tissues
GdnHCl	Guanidine hydrochloride
GPI	Glycophosphatidylinositol
GSS	Gerstmann-Strausler-Scheinker
H	Histidine
h	hours
H&E	Hematoxylin and eosin
HBI	Hotchkiss Brain Institute
HD	Hydrophobic domain
HEK	Human embryonic kidney
hGH	Human growth hormone
HSACC	Health Sciences Animal Care Committee
HSP	Heat shock protein
HY	Hyper TME prion strain
ic	Intracerebral
iCJD	Iatrogenic Creutzfeldt-Jakob disease
IHC	Immunohistochemistry
ip	Intraperitoneal

IRE1	Inositol requiring enzyme 1
K	Lysine
kDa	Kilodalton
L	Leucine
LDH	Lactate dehydrogenase
LTP	Long-term potentiation
M	Methionine
MAPK	Mitogen-activated protein kinase
MBM	Meat and bone meal
Mdi	Mouse dimer recombinant PrP
MEF	Mouse embryonic fibroblast
min	minutes
Mmo	Mouse monomer recombinant PrP
MS	Multiple sclerosis
N	Asparagine
NaPTA	Sodium phosphotungstic acid
N-CAM	Neural cell adhesion molecule
NMR	Nuclear magnetic resonance
OD	Optical density
OR	Octapeptide repeat
ORF	Open reading frame
P	Proline
PD	Parkinson’s disease

PDI	Protein disulfide isomerase
PE	Phosphatidylethanolamine
p-eIF2α	Phosphorylated eIF2α
PERK	Protein kinase (PKR)-like endoplasmic reticulum kinase
PIPLC	Phosphatidylinositol-specific phospholipase C
PK	proteinase K
PKA	Protein kinase A
PLGA	Polylactic-co-glycolic acid
PMCA	Protein Misfolding Cyclic Amplification
PNS	Peripheral nervous system
p-PERK	Phosphorylated PERK
PrP^{C}	Cellular prion protein
PrP^{Sc}	Pathological prion protein
Q	Glutamine
QC	Quality control
R	Arginine
RAMALT	Rectoanal mucosa-associated lymphoid tissue
RESET	Rapid ER stress-induced export
RFU	Relative ThT fluorescence unit
ROS	Reactive oxygen species
rPrP	Recombinant prion protein
$rPrP^{Sc}$	PK-resistant PrP^{Sc}

RT	Room temperature
RT-QuIC	Real-time quaking-induced conversion
S	Serine
sc	Subcutaneous
sCJD	Sporadic Creutzfeldt-Jakob disease
SD	Standard deviation
SDS-PAGE	Sodium dodecyl sulfate-polyacrylamide gel electrophoresis
SEM	Standard error of mean
sFI	Sporadic fatal insomnia
SP	Signal peptide
$sPrP^{Sc}$	PK-sensitive PrP^{Sc}
SSBP/1	Scrapie brain pool 1
Tg	Transgenic
TGN	Trans-Golgi Network
ThT	Thioflavin T
TME	Transmissible mink encephalopathy
TSE	Transmissible spongiform encephalopathy
UCVM	University of Calgary Faculty of Veterinary Medicine
UGGT	UDP-glucose:glycoprotein glycosyltransferase
UPR	Unfolded protein response

UPS	Ubiquitin-proteasome system
V	Valine
vCJD	Variant Creutzfeldt-Jakob disease
VPSPr	Variably protease-sensitive prionopathy
WT	Wild-type
XBP-1	X-box binding protein1
Y	Tyrosine

CHAPTER 1:

INTRODUCTION TO PRION DISEASES AND BACKGROUND FOR THE STUDY

1.1. Prion diseases

Prion diseases are the transmissible spongiform encephalopathies (TSEs) characterized by a distinctive spongiform appearance (shown in Fig. 1.1), subsequent to neuronal loss, and astrogliosis in the brain histology. Unlike other neurodegenerative diseases, TSEs affect both animals and human [1-5]. As per today, these disorders are always fatal. The naturally occurring TSEs in animals include scrapie in sheep and goats, bovine spongiform encephalopathy (BSE) in cattle, chronic wasting disease (CWD) in cervids, transmissible mink encephalopathy (TME) in mink, and feline spongiform encephalopathy in cats [6]. Most recently, TSE has been identified in dromedary camels as camel prion disease (CPD) [7]. In humans, TSEs are referred to as Creutzfeldt-Jakob disease (CJD), which can be either sporadic (sCJD), genetic, or acquired [8, 9]. sCJD is the most common form of CJD. Inherited forms, such as Gerstmann-Strausler-Scheinker (GSS), familial CJD (fCJD), and fatal familial insomnia (FFI), are very rare [8, 9]. Acquired prion diseases occur due to an exogenous source of infection from TSE-contaminated tissues and material. Some examples are Kuru, iatrogenic CJD (iCJD), and variant CJD (vCJD) [8, 9]. The list of prion diseases with their etiology is summarized in Table 1.1.

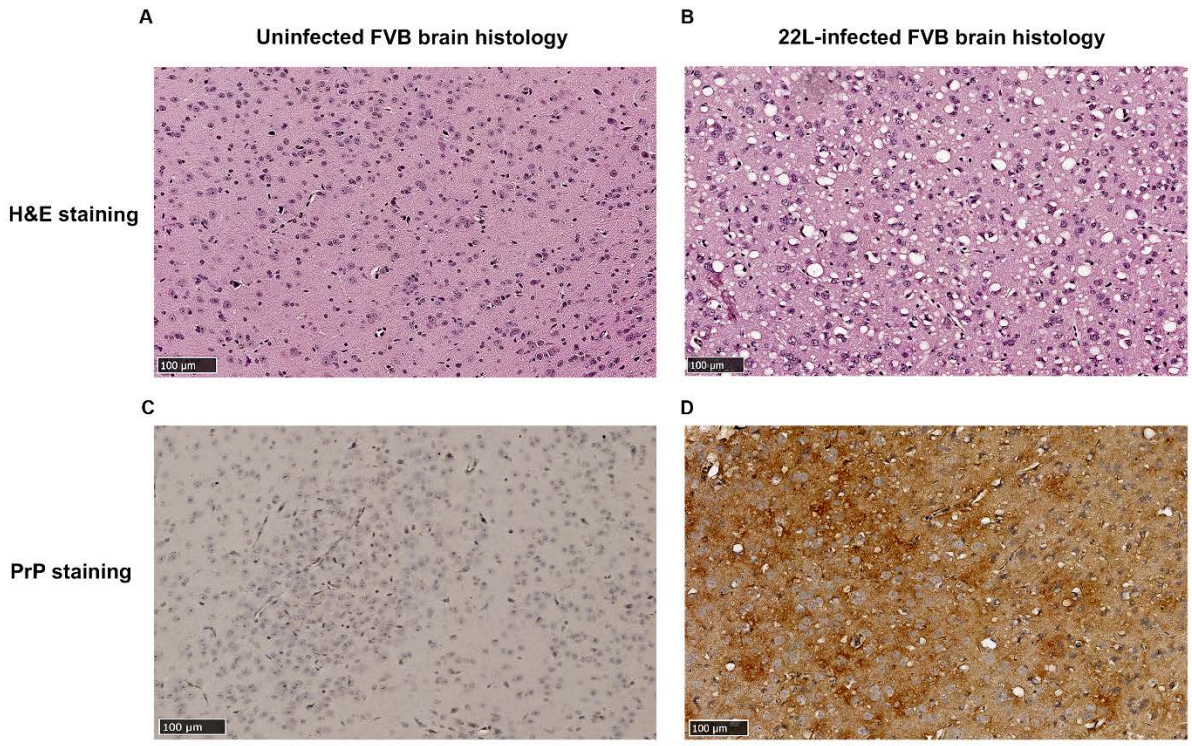

Figure 1.1. Histopathology of brain from FVB mouse either uninfected or infected intracerebrally with mouse-adapted 22L prion strain. Hematoxylin and eosin (H&E) staining of brain sections from the uninfected mouse (A), and 22L-infected mouse (B) with spongiform appearance in prion-infected brain. Immunohistochemistry (IHC) staining of brain sections from uninfected (C) and 22L-infected (D) mice using anti-PrP SAF83 antibody showed PrP^{Sc} accumulation in prion-infected brain.

Table 1. 1. List of human and animal prion diseases indicating the affected species and origin of infection. CJD: Creutzfeldt-Jakob disease; iCJD: iatragenic CJD; vCJD: variant CJD; sCJD: sporadic CJD; fCJD: familial CJD; GSS: Gerstmann-Strausler-Scheinker; FFI: Fatal familial insomnia; BSE: Bovine spongiform encephalopathy; CWD: Chronic wasting disease; TME: Transmissible mink encephalopathy; FSE: Feline spongiform encephalopathy; CPD: Camel prion disease

	Host	**Type**	**Prion Disease**	**Origin/Etiology**
Human prion disease	Human	Acquired	Kuru	Consumption of infected organs (cannabalism rituals)
			iCJD	Infection due to prion contamination via organ transplant such as cornea, dura mater, and human growth hormone (hGH)
			vCJD	Consumption of BSE-contaminated beef
		Sporadic	sCJD, sporadic fatal insomnia (sFI), variably protease-sensitive prionopathy (VPSPr)	Origin unknown, most probably spontaneous conversion of PrP^{C} to PrP^{Sc} or somatic mutation
		Inherited	fCJD, GSS, FFI	Mutations in the *PRNP* gene encoding host prion protein, PrP^{C}
Animal prion disease *	Sheep and goat		Scrapie	Origin unknown, most probably spontaneous conversion or somatic mutation. However, once animals are affected, effective horizontal transmission is possible via environmental shedding
	Cattle		BSE	Origin unknown, most probably spontaneous conversion or somatic mutation. However, it was transmitted through TSE-contaminated meat and bone meal

	Cervids		CWD	Unknown origin, most probably spontaneous conversion or somatic mutation. However, once affected, effective horizontal transmission is possible via urine, feces, saliva, and environment
	Mink		TME	Originated from Scrapie or BSE through food contamination
	Cats, captive wild cats		FSE	Originated from BSE
	Exotic zoo animals, e.g. nyala, kudu, gemsbok		Exotic ungulate spongiform encephalopathy (EUE)	Originated from BSE
	Dromedary camel		CPD	Origin unknown, most probably spontaneous conversion or somatic mutation.

***** Whereas classical animal prion diseases are acquired by infection, atypical scrapie and atypical BSE are now considered sporadic prion diseases.

Prion diseases are caused by the misfolded, infectious, self-replicating, and aggregation-prone isoform, PrP^{Sc}, of the normal host cellular protein, PrP^{C} [1-3]. As a ubiquitous protein, PrP^{C} is widely expressed in peripheral tissues such as lymphoid tissues, heart, liver, kidney, intestinal tract, and epithelium, yet it is mainly expressed in the central nervous system (CNS) [10, 11]. The main hallmark of prion diseases is the accumulation of PrP^{Sc} in the CNS as shown in Fig. 1.1 D [5]. In 1982, Dr. Stanley Prusiner gave the name “prions” (pathological PrP conformer) to the small, proteinaceous, and infectious components of the scrapie-causing agent devoid of nucleic acid [1]. Similar phenomena of accumulating misfolded proteins and “prion-like” mechanisms are observed in other neurodegenerative diseases [12]. This includes Alzheimer’s disease (AD), caused by the deposition of amyloid-β in the brain, resulting in plaque formation; and Parkinson’s disease (PD), in which Lewy bodies develop in the brain due to the accumulation of misfolded α-

synuclein [12]. However, prion diseases are unique among other neurodegenerative diseases due to their transmissibility between and within species, including zoonotic transmission from animals to humans as in the case of vCJD [13, 14]. There is currently no treatment or preventive prophylaxis available for prion diseases.

1.2. Protein-only hypothesis: Protein as a pathogenic agent

In 1967, J.S. Griffith speculated that the scrapie agent could be a self-replicating protein, rather than a slow virus as it was believed, and proposed most possible ways of protein self-replication process [15]. In support of Griffith's hypothesis, Stanley Prusiner proposed the "protein-only hypothesis" and described the scrapie agent as a proteinaceous infectious particle [1]. Prions were resistant to various nucleic acid damaging treatments; however, they were prone to inactivation with protein-denaturing reagents [1, 16]. In early 80s, the infectious, proteinaceous amyloid or prions from a scrapie-infected hamster brain were successfully isolated using sucrose-gradient-based ultracentrifugation, further supporting the protein-only hypothesis [17, 18]. Further, the scrapie-infected hamster prions were resistant to proteinase K (PK) digestion, and yielded a 27-30 kDa resistant protein in the sodium dodecyl sulfate-polyacrylamide gel electrophoresis (SDS-PAGE), unlike that of a similar fraction from an uninfected brain [17, 18]. These extraordinary experimental series demonstrated the protein nature of the scrapie agent. These discoveries earned Dr. Prusiner the Nobel Prize in Physiology and Medicine in 1997. Further attempts made to sequence the PrP 27-30 fraction revealed that the prion agent is encoded by a cellular gene [19, 20]. Surprisingly, both in normal and infected hamster brains, the single PrP-related gene (*Prnp*) was found with similar levels of associated mRNA and the same primary structure of encoded PrP [19, 21]. The protease-resistant PrP was termed PrP^{Sc}, the "Sc" for

scrapie; and its cellular counterpart was termed PrP^{C}, the "C" for cellular prion protein, both with distinct biochemical properties [22].

The successful discovery of the *Prnp* gene opened a new dimensional platform for further research on a protein as a causative agent. The development of PrP-knockout mice, denoted as $Prnp^{0/0}$ or $Prnp^{-/-}$, provided full support for the protein-only hypothesis [23, 24]. Such mouse lines, with no PrP expression, were resistant to prion disease after prion inoculation, suggesting the inevitable role of PrP^{C} in prion propagation [23, 24]. Besides, the humoral stimulation only in PrP-knockout mice by prions, unlike in a normal host, was reported as an indication that PrP^{Sc} was non-immunogenic in nature, and shared the same primary structure as the host PrP^{C} [24].

The protein-only hypothesis is now widely accepted concept and prions, responsible for causing prion diseases, are seen as infectious, misfolded proteins that possess no genetic material. Substantial evidence supporting the hypothesis was presented further after the generation of infectious *de novo* prions *in vivo* and *in vitro* in a number of experiments [25-30]. These evidences include the successful generation of infectious synthetic amyloid fibrils prepared from the bacterial-expressed NH_2-terminally (N-terminal) truncated (89-230) rPrP [25]. When inoculated into transgenic (Tg) mice overexpressing mouse PrP (89-231), the fibrils caused neurological disease accompanied by PK-resistant PrP accumulation in the brain. The fibrils were further transmitted on second passage to wild-type (WT) and Tg mice [25]. Next, the *in vitro* prion amplification technique, Protein Misfolding Cyclic Amplification (PMCA), was used to generate infectious prions by seeding the uninfected brain homogenate (BH) as PrP^{C} substrate with prion-infected BH [26, 31]. Further, Supattapone's and Soto's groups generated spontaneously *de novo* infectious prions using PMCA in the absence of pre-existing infectious seed [27, 28]. The development of spontaneous prion disease in a gene knock-in transgenic mouse model expressing

FFI-associated mutant PrP under *Prnp* promotor further added an evidential basis to the prion hypothesis [32].

A unanimously convincing experiment in favor of the prion hypothesis was reported by Ma's group. Utilizing the PMCA technique, *de novo* highly infectious prions were generated *in vitro* from unseeded bacterial-expressed rPrP in the presence of different cofactors and, when inoculated, these prions serially transmitted prion disease in WT mice [29, 30, 33]. Later, researchers were successful in preparing synthetic cross-beta-sheet amyloid prions from rPrP subjected to an annealing step in the presence of normal BH or bovine serum albumin (BSA) [34]. These synthetic prions, when inoculated into hamsters, resulted in prion disease with a unique clinical neuropathology including a large amount of PrP^{Sc} deposits, a very long incubation period, and slow disease progression [34].

1.3. Different prion diseases

1.3.1. Human prion diseases

Human prion diseases are quite rare compared to other infectious diseases, and the disease incidence is approximately 1.5 in 1 million people per year [9]. Of human prion diseases, sCJD is the most common (85-90 % of cases). About 10-15% are genetic (including fCJD, FFI and GSS), and the acquired form (iCJD and vCJD) represents 2-5% of all cases [9].

The classical clinical presentation of sCJD includes rapid progressive dementia, behavioural abnormalities, ataxia, and eventual myoclonus [8]. The sCJD disease phenotype is classified based on polymorphism at codon 129 (methionine (M)/ valine (V)) of the human *PRNP* gene and types of PrP^{Sc} [35]. The ante-mortem detection of biomarkers like 14-3-3, neuron-

specific enolase and tau in patients' cerebrospinal fluid (CSF) is one of the tools for CJD diagnosis. However, these tests are non-specific and a tissue biopsy is necessary for confirmation [36, 37].

Genetic prion diseases consist of fCJD, FFI and GSS and occur due to mutations in the human *PRNP* gene [38]. The most common form is fCJD, which is associated with ataxia, myoclonus, and other motor features [8]. The neuropathology of fCJD is quite similar to that of sCJD, exhibiting spongiform changes, neuronal loss and gliosis, and PrP^{Sc} accumulation in the form of granular or plaque-like deposits [38]. Glutamic acid (E) substitution to lysine (K) at codon 200 in the *PRNP* gene, E200K is the most common mutation [38]. Interestingly, the aspartic acid substitution to asparagine at codon 178 (D178N) mutation-associated phenotype is found to be dictated by a *PRNP* polymorphism at codon 129. Homozygous V at 129 with a D178N mutation results in fCJD [39]. FFI is a rare form of genetic prion disease associated with a D178N mutation along with a 129MM polymorphism in the *PRNP* gene with neuropathology predominantly confined in the thalamus, and which presents with severe progressive insomnia [40]. GSS is another genetic prion disease associated with *PRNP* mutations such as proline (P) to leucine (L) substitution at codon 102 (P102L), P105L, and alanine (A) to valine substitution at 117 (A117V), and mainly presents as a slow progressive disease with ataxia and motor dysfunction [8, 41].

vCJD was first reported in the United Kingdom (UK) and was suspected to occur due to the zoonotic potential of BSE prions to transmit to humans via the consumption of BSE-contaminated food products [42]. Several epidemiological studies were performed following the vCJD incidence in the UK, which linked the BSE epizootic as the cause of vCJD [43, 44]. Subsequent mouse transmission experiments showed that the lesion profiles in the mouse brain caused by vCJD prions were similar to those produced by BSE prions and different from those produced by sCJD prions, confirming that the vCJD and BSE prions were a single strain [13, 14].

Additionally, unlike sCJD, vCJD occurs in much younger patients and the PrP^{Sc} found in the lymphoreticular system along with CNS have been reported [8, 45]. The clinical presentation usually consists of early psychiatric onset followed by cognitive and cerebellar dysfunction and myoclonus [46]. The polymorphism at codon 129 in the human *PRNP* gene is found to play a significant role in vCJD susceptibility; all vCJD patients until now, except two heterozygous cases, had homozygous M at codon 129, suggesting a partial protective effect of valine exerted on the BSE prions [47]. Moreover, acquired cases of vCJD reported due to blood transfusions from preclinical vCJD-infected donors, and the surveillance data describing the latent vCJD in the lymphoreticular system in some people in the UK, have raised a significant public health risk [48-51].

iCJD is an acquired prion disease of human-to-human transmission nature. A corneal transplant was associated with the first case of iCJD in 1974 [52]. There have been several reports of iCJD occurring through CJD-infected corneal transplants, blood product transfusions, dura mater graft transplants, cadaveric human pituitary growth hormone, and contaminated electroencephalogram (EEG) electrodes and surgical instruments [53].

Kuru is another acquired form of human prion disease found epidemic in the Fore population residing in the Eastern Highlands of Papua New Guinea and the neighbouring linguistic groups in the late 1950s [54, 55]. It is the first human prion disease shown to be experimentally transmitted to the chimpanzees [56]. Kuru is associated with the act of endocannibalism practiced by these communities as a part of mortuary feast for paying respect to the deceased relatives by consuming their dead bodies [55]. The consumption of tissues from a sCJD-affected individual was hypothesized to be the cause of the kuru epidemic [57]. Later, the transmission studies in rodent model showed that the strain properties of kuru prions were similar to sCJD [58]. Moreover,

following the cease of the act of endocannibalism after 1956, the cases of kuru declined and the kuru epidemic was later eradicated [55]. There was no kuru patient born after 1956. After the cessation of kuru transmission, the study of cases until the end of the disease epidemic in mid 2000 suggested that the incubation period of kuru can be more than 50 years [55]. The clinical symptoms includes progressive cerebellar ataxia, parkinsonian tremors, joint pain, choreiform, and athetoid movements, however, dementia is rare [55]. Mostly women and children population were found affected, and there was report of only 2% of the cases in adult males [59].

1.3.2. Animal prion diseases

Some animal prion diseases are listed below. These include scrapie in sheep and goats, BSE in cattle, TME in mink, FSE in cats and captive wild cats, and CWD in cervids.

1.3.2.1. Scrapie

Classical scrapie is considered as the most ancient form of TSEs affecting sheep and goats; it was described in the 18th century in Europe. The clinical signs vary between flocks and include behavioural abnormalities, visual impairment, ataxia, uncoordinated movement, hyperexcitability, pruritus, and tremors [60]. The neuropathological presentation consists of spongiform changes, gliosis, and PrP^{Sc} deposition in the brain [61]. Apart from the brain, in scrapie-infected sheep, PrP^{Sc} has been detected in the spleen, lymph nodes, rectoanal mucosa-associated lymphoid tissue (RAMALT), tonsils, salivary glands and placenta [62-65]. Moreover, PrP^{Sc} has also been found in the blood, milk, and feces of scrapie infected-animals [66-68]. Scrapie is horizontally transmitted from an infected sheep to an uninfected animal by direct contact, orally, or through a mucosal route from a contaminated environment, even in suckling lambs via milk. Transmission has also

been demonstrated in utero [67, 69, 70]. Scrapie prions are very resistant and can remain in the environment for more than a decade [71].

Besides classical scrapie, atypical forms of scrapie have also been reported. For example, Nor98, first identified in Norwegian sheep, had different biological properties than classical scrapie in terms of clinical signs, PK sensitivity of PrP^{Sc}, banding profile in SDS-PAGE, and neuropathology [72]. Though the PrP^{Sc} was not detected in lymphoid tissues and muscles in atypical scrapie-infected sheep, these tissues contained infectivity [73].

1.3.2.2. Bovine spongiform encephalopathy

Classical BSE (C-BSE) was first identified as TSE in cattle in the UK in the 1980s where it later became epizootic, reaching its peak in 1992 with more than 37,000 confirmed cases [6, 74]. It was spread to at least 28 countries, mostly in Europe, the United States (US), Canada, and Japan. The transmission was believed to have been through the export of infected animals or contaminated meat and bone meal (MBM) containing feed, although the origin of BSE is unknown [6]. Legislation regarding the ban of the use of MBM in livestock feed in the UK and Europe played a significant role in substantially reducing BSE cases and controlling disease transmission [6]. BSE poses a serious public health concern, as it is the only prion disease known to have zoonotic potential. BSE prions resulted in vCJD in humans via animal-to-human transmission [13]. It can also cross the interspecies transmission barrier to other animals, not just livestock [6].

The C-BSE epizootic created a huge economic crisis in the countries affected. In Canada, the first C-BSE case in 2003 highly impacted the Canadian beef industry, resulting in a financial loss of around $6.3 billion in early 2004 due to international trade bans [75].

The clinical presentation of C-BSE includes tremors, gait abnormalities with hind limb ataxia, aggressiveness, apprehension, and hypersensitivity to stimuli. The incubation period of BSE is between two and eight years with most cases identified in dairy cattle that are four to five years old [76]. The active surveillance program implemented for TSE in livestock resulted in the identification of two atypical BSE cases namely H-BSE and L-BSE in 2004, which were mainly found in older cattle. They were thought to have occurred sporadically due to the lack of a link with an infectious source, and were distinguished from C-BSE based on the histopathology and biochemical properties of PK-resistant PrP^{Sc} [77-79].

1.3.2.3. Transmissible mink encephalopathy

TSE was first noticed in 1947 in a mink ranch in Brown County, Wisconsin, USA where the death rate was 100% in adult mink [80]. When over 100 pregnant dams were relocated to another farm, all of them developed the disease, while their newborn kits and the mink in the recipient farm remained unaffected [80]. Based on these observation, the nature of disease was indicated to be non-transmissible vertically and the affected animals were exposed to the infectious agent before their transfer to the new farm [80]. Several outbreaks of TME were then observed in different farms in Wisconsin [81, 82]. TME was originally thought to be transmitted via ingestion of infectious agent as the affected farms were using commercial feed mix from a common feed plant [83, 84]. Later, TME was described as TSE with similarity in clinical course and neuropathology to that of scrapie in sheep [83]. Several TME outbreaks had also been reported in Canada and Europe [85]. During the clinical onset, lack of animal cleaniness and urine- and feces-soiled pens were observed which later was followed by clinical signs such as behavioural changes,

difficulty in eating and swallowing, curved tail, uncoordinated hind limb movement, occasional tremors, ataxia, epileptic seizures, and self-mutilation [85].

The epidemiological studies demonstrated that TME to be associated with mink diet supplemented with carcasses and by-products of cattles and sheep. Experimental transmission studies of various scrapie isolates into mink suggested that transmission is possible via intracerebral and intramuscular routes but not oral route [86]. Even the mink which developed neurological disease after intracerebral scrapie inoculation had different incubation periods compared to that of natural TME [86]. Furthermore, the use of meat from downer cattle in the mink diet in various farms, where the TME outbreaks were recorded, led to the possibility of BSE prions to be the causative agent of TME [82]. TME isolate from mink in the Stetsonville farm, which was the last farm recorded to have TME outbreak, was inoculated into cattle intracerebrally [82]. After successful experimental transmission of TME to cattle, when the cattle-passaged TME was orally transmitted to the mink, the animals developed TME with similar incubation period as mink-passaged TME [82]. This reversible transmission nature of TME agent upon passaging in cattle suggested that the origin of TME agent could be from unrecognized scrapie-like spongiform encephalopathy of cattle [82]. However, oral transmission of BSE isolates to mink demonstrated the development of neurological disease with distinct clinical presentation and neuropathology from those of natural TME-affected mink [87]. Later, transmission studies in transgenic mouse model revealed a strong association between TME and L-BSE based on incubation period, brain lesion profile and distribution of PrP^{Sc} [88]. Identification of the TME strains ‘hyper’ and ‘drowsy” by Richard Bessen and co-workers pioneered and transformed research on prion strains [89].

1.3.2.4. Feline spongiform encephalopathy

FSE is a prion disease of both domestic cats and captive wild cats, firstly recognized in the UK [90, 91]. The BSE-contaminated feed is believed to be the source of FSE infection as the FSE cases were recognized shortly after first BSE cases appeared in cattles [91, 92]. The age of disease onset in domestic cats ranged between 4 to 9 years of age [92]. The clinical signs varied greatly among cases, most commonly included ataxia, tremors, behavioural alterations, aggression, and excessive salivation [90]. The transmission studies in mouse model suggested that FSE prions shared similarities in incubation period and brain lesion profile with that of BSE, indicating that FSE and BSE prions represent a single strain [13, 93, 94].

1.3.2.5. Exotic Ungulate Spongiform Encephalopathy

EUE is an acquired form of TSE in exotic zoo animals, such as greater kudu, nyala, elands, oryx, and gemsbok, identified in the UK during the BSE epidemic [91]. The MBM feed was fed to the EUE affected animals indicating that EUE is an acquired prion disease via ingestion [91]. The comparative transmission and strain typing studies in mouse model demonstrated similarities in incubation period and neuropathology between BSE and EUE, suggesting that EUE and BSE belong to a single strain [91].

1.3.2.6. Chronic Wasting Disease

In 1967, the first case of CWD was described in a mule deer held in captivity in Colorado, where the animal was observed with a wasting syndrome with progressive neurological dysfunction. More than ten years later, in 1978, a neuropathological analysis by late Elizabeth Williams of the affected animal's brain confirmed CWD to be a TSE in cervids [95]. Since its

discovery, CWD has become endemic to both captive and free-ranging cervid species such as mule deer, wild-tailed deer, moose, and elk in North America; it has affected animals in more than 26 states in the US and three provinces in Canada [96-98]. Until now, no case of CWD has been reported in free-ranging caribou in Canada. However, experimental oral transmission of CWD was shown in Canadian reindeer [99]. Besides North America, CWD has been reported in captive cervids in Korea as a result of the importation of subclinical animals from Canada [100]. Recently, in Norway, CWD was diagnosed in a free-ranging reindeer and three European moose from geographically different parts of the country. Following the active surveillance program for CWD implemented in Norway, additional cases were found in reindeer, and even a wild red deer was diagnosed as CWD-infected [101, 102]. More recently, CWD has been identified in moose in Sweden and Finland [103, 104]. Whether the CWD origin in Norway is related to the endemic in North America is unknown. However, the CWD strain characteristics found in Norway CWD isolates in moose were different from those of North American isolates [102]. The emergence and spread of CWD in different geographical areas are a serious matter of public concern.

CWD is highly contagious and there is evidence for horizontal transmission via the oral route either directly when naïve animals are housed in close contact with infected animals or indirectly through exposure to a contaminated environment through saliva, urine, feces, and decomposed carcasses [105-108]. Both clinically sick and asymptomatic animals can shed CWD infectivity for years through excreta and bodily fluids in the environment where infectivity resides [109-113]. The CWD prions excreted in feces by asymptomatic experimental CWD-infected mule deer transmitted disease after the intracerebral (ic) inoculation into Tg mice overexpressing elk PrP [112]. As potential environmental reservoirs, CWD prions can remain bound to the soil, taken up by plants, and be present in water sources [114-117]. CWD transmission has been investigated

using natural and experimental transmission studies using both Tg mouse and cervid models [106, 118].

Intraspecies transmission in cervids and interspecies transmission in ferrets, cats, hamster, and bank voles have been reported [119-122]. However, the risk of CWD transmission to humans is not clear yet. The link between CWD prevalence and the human incidence of an unusual or new form of TSE has been nullified so far through surveillance in CWD-endemic areas. In addition, the follow-up of individuals known to be exposed to CWD through diet demonstrated no risk of prion disease development [123, 124]. Moreover, a comparison of CJD prevalence rates between CWD-endemic and non-endemic areas in the US suggested a negligible contribution of CWD in human disease [125]. The *in vivo* CWD transmission failure to Tg mice expressing human PrP signifies a high interspecies transmission barrier [118, 126]. Of note, after prion strain adaptation using PMCA and transgenic mice overexpressing cervid PrP, CWD prions were successful in converting human PrP substrate into a new form of PrP^{Sc} [127]. CWD transmission in non-human primates has been contradictory. Squirrel monkeys were susceptible to both the intracerebral and oral transmission of CWD infection; however, CWD transmission failed in cynomolgus macaques [98, 128]. Recently, in contrast, another consortium with our participation reported the ability of CWD prions to transmit and develop disease in some cynomolgus macaques [103]. Although it seems there is a lack of a clear link between CWD prions and human transmission, considering the long incubation period and presence and emergence of different strains, the zoonotic potential of CWD prions is still an open question, making CWD a public health concern.

The age of CWD disease onset ranges between three and seven years [129, 130]. Although the exact incubation period in natural CWD cases is unknown, there is the possibility of an average incubation period within two to four years [129]. In experimental transmission via the oral route,

the period for the appearance of clinical signs has been reported to be approximately 15 months in mule deer and between 12-34 months in elk [130]. Clinical signs may include weight loss, emaciation, behavioural abnormalities, excessive salivation, posterior ataxia, depression, loss of fear, polyuria, polydipsia, and teeth grinding [130]. The gold standard for CWD diagnosis is to detect pathological PrP^{Sc} accumulation in immunohistochemistry (IHC) analysis in the obex sections [131]. The ante-mortem diagnosis is based on an enzyme-linked immunosorbent assay (ELISA) for rapid screening or IHC-based detection in tonsil or RAMALT biopsies [131-133]. Regarding non-invasive methods and pre-clinical diagnosis, ultrasensitive assays such as PMCA or real-time quaking-induced conversion (RT-QuIC) have been employed to detect the pathological PrP protein in the body secretions, excreta, and biopsied tissue from CWD-infected animals [134-137]. However, these techniques are yet to be federally approved in the North American or European countries [137].

Studies regarding CWD pathogenesis reveal that following oral exposition, PrP^{Sc} deposition is found in the peripheral nervous system (PNS) and lymphoid tissues prior to the CNS [138, 139]. After oral exposure, CWD prions reach the tonsils and gut-associated lymphoid tissues (GALT) through the lymphoreticular system and enteric nervous system [140]. After replication in the lymphoid tissues, prions proceed to the CNS following neuroinvasion via the autonomic nervous system [140]. As with other prion diseases, lesions such as vacuolation, neuronal loss, and gliosis are confined to the CNS [141]. Neuropathology consisting of florid amyloid plaques, which are amyloids surrounded by vacuoles, are found in the brain of CWD-affected deer and the frequency varies in different brain regions [142]. Although the characteristic PrP^{Sc} deposition in lymphoid tissues, especially in GALT, early during infection is prominent in CWD cases, it varies between species with elk having fewer PrP^{Sc} deposits than deer [143]. The other tissues consisting

of PrP^{Sc} deposits in CWD-affected animals are skeletal muscles, salivary glands, tongue, liver, kidneys, pancreas, adrenal glands, blood, adipose, and antler velvet [144-149].

1.4. Prion strains

Prion strains, when inoculated in hosts with the same genetic background, produce distinct pathology and clinical disease. The concept of prion strains emerged in 1961 when Pattison and Millson inoculated a scrapie agent into goats [150]. To their surprise, they observed different clinical phenotypes in the goats, which they called “scratching” and “drowsy”, and which were maintained upon successive transmission [150]. Earlier it had been thought that different phenotypes resulting from different prion strains might be due to distinct genetic information encoded in the prion agent, a concept that conflicted with the protein-only hypothesis. However, the studies have now suggested, in line with the protein-only hypothesis, that the molecular basis of prion strains lies in distinct conformations of PrP^{Sc} molecules [89, 151-153]. Moreover, each conformation exhibits different biochemical properties [89, 151-153].

Scrapie strains are extensively studied in inbred mouse models. For example, the successive transmission of Suffolk sheep scrapie isolate in mice resulted in the Me7 strain [154]. Similarly, Cheviot sheep-derived scrapie isolate (SSBP/1: scrapie brain pool 1) resulted in various scrapie strains such as 22C, 22L, and 22A after successive passaging in mice [155, 156]. Furthermore, Dickinson’s group found that the scrapie strains were consistent in producing the strain-specific degree and localization of vacuolation measured as an intensity of brain lesions in various brain regions and that these characteristics remained stable upon subsequent passages [157]. Such profiling of brain lesions in different brain regions was extensively used later as one of the means to differentiate prion strains [158]. For example, the brain lesion profile study

confirmed that the causative agent of both BSE and vCJD was a single prion strain [13]. Markedly, vCJD and BSE prions were indistinguishable in their lesion profiles when both were transmitted to WT mice, suggesting that vCJD is caused by a BSE agent after interspecies transmission [13]. On the other hand, although both vCJD and sCJD prions produce disease in a human host, vCJD could be differentiated from sCJD in terms of age of onset, incubation time, deposition of PrP^{Sc}, and neuropathology, indicating that vCJD and sCJD are different prion strains in humans. Besides, sCJD and vCJD showed different transmission patterns in mouse models; whereas vCJD prions transmitted efficiently in WT mice, unlike in Tg mice expressing human PrP^{C}, the opposite was the case for sCJD prions [14].

In 1992, Bessen and Marsh conducted TME-associated interspecies transmission experiments in Syrian hamsters and identified two TME strains, hyper (HY) and drowsy (DY), based on clinical presentation [159]. Additionally, they found a distinct migration pattern of a PK-resistant fragment associated with these strains [159]. While HY showed a hyperexcitability phenotype in hamsters and its PK-resistant core fragment migrated at 21 kDa, DY on the other hand showed a lethargic phenotype with a PK-resistant fragment detected at 19 kDa. Moreover, the rate of PK digestion was found to be strain-specific, with DY PrP^{Sc} being more sensitive than HY [159]. These data suggested that either different strains co-exist in a single original host or a new strain is generated when transmitted in a new host [159]. The generation of the unique PK-resistant fragments related to HY and DY strains was attributed to different PK cleavage sites of different conformations of PrP^{Sc} [160]. The electrophoretic mobility of the PK-resistant fragment of PrP^{Sc} thus became a reliable tool to differentiate prion strains. Additionally, different prion strains, which appeared similar in terms of the incubation period and size of the PK-resistant PrP^{Sc} fragment, such as HY and Sha(Me7) in hamsters, had different conformations based on limited

protease digestion and guanidine hydrochloride (GdnHCl) denaturation by conformation-dependent immunoassay (CDI) [153]. CDI measures both PK-sensitive ($sPrP^{Sc}$) and PK-resistant ($rPrP^{Sc}$) forms of PrP^{Sc}. Such GdnHCl denaturation profile is also used as a tool to differentiate prion strains [153].

The strain typing based on the electrophoretic mobility profile of PK-resistant PrP^{Sc} fragments was utilized for BSE prions. Three BSE strains were distinguished in an immunoblot based on the size of the PK-resistant fragments, C-BSE (18 kDa for unglycosylated form), H-BSE (20 kDa), and L-BSE (17 kDa) [161].

More interestingly, strain properties have also been studied in various human prion diseases, such as FFI, fCJD, and sCJD. The study on the D178N PrP mutation associated with both the FFI and fCJD phenotypes demonstrated that codon 129, along with mutation, plays a role in disease phenotypes [39]. M at 129 and a D178N mutation give rise to FFI and a 19 kDa deglycosylated PK-resistant PrP^{Sc} fragment, whereas V at 129 and D178N result in fCJD-associated phenotype and 21 kDa fragment. Thus, a 129M/V polymorphism linked to a single mutation can exert an effect on a PrP^{Sc} conformation and its biochemical properties, resulting in a prion strain-specific distinct clinical phenotype [39]. Moreover, the study, involving the transmission of either FFI- or fCJD (with E200K mutation)-infected brain extracts in the Tg mice expressing a human-mouse chimeric PrP, showed a retention of the original strain-specific property [151]. A PK-resistant PrP^{Sc} fragment generated in these infected-mice depended on the inoculum used, with a molecular size of 19 kDa seen for the FFI and 21 kDa for the fCJD transmission [151]. In the case of sCJD, Parchi and coworkers reported six distinct subtypes of sCJD based on the clinical features, molecular size of PK-resistant PrP^{Sc}, and a specific genotype at codon 129 [35]. Among these subtypes, MM1 and MV1 are indistinguishable from each other.

Two PrP^{Sc} types in sCJD cases were examined, where the electrophoretic mobility of type 1 was at 21 kDa with a cleavage site at residue 82 with glycine (G) and type 2 migrated at 19 kDa with a cleavage at 97 with serine (S), suggesting that conformational variability might lead to distinct protease cleavage sites [35, 162]. Of note, both PrP^{Sc} types can exist in the same brain of some sCJD patients [163]. Besides, two human sporadic prion strains, MM2 sCJD and sporadic familial insomnia (sFI), share the same polymorphism at codon 129 (M) and type 2 PrP^{Sc} (19 kDa band) in an immunoblot, but they differ in clinical presentation and affected brain regions. sFI presents with insomnia and thalamus atrophy whereas in MM2 sCJD, the cerebral cortex is severely affected [35, 164].

In addition to an electrophoretic mobility profile for strain typing, glycoform ratios have also been used to distinguish strains. While the predominant glycoform of sCJD-associated PrP^{Sc} is a monoglycosylated form, that of vCJD PrP^{Sc} is diglycosylated [165]. Moreover, in the case of two CWD strains, CWD1 and CWD2, identified in Tg mice expressing cervid PrP^{C}, both exhibited similar electrophoretic profiles and glycoform ratios [166]. However, they differed in the localisation of PrP^{Sc} deposits and the incubation period. While CWD1 showed a symmetrical PrP^{Sc} deposition in both hemispheres with a short incubation period, CWD2 exhibited an asymmetrical deposition with a long incubation period [166]. The glycoform ratio of different BSE types, C-BSE, L-BSE, and H-BSE prions also differed from each other [161].

Another property of prion strains is their differential tropism, either in different brain regions or different tissues. Based on tissue tropism, prion strains can be neurotropic, which primarily target the CNS; or lymphotropic, which propagate in the lymphoid organs prior to neuroinvasion [158]. Classical scrapie exhibits PrP^{Sc} distribution in both the CNS and lymphoid organs, whereas no PrP^{Sc} accumulation was observed in the lymphoid organs for atypical scrapie

[167]. Of note, later it was reported that although there were no detectable PrP^{Sc} deposits in lymphoid tissues in atypical scrapie-infected sheep, the tissues contained infectivity [73]. Moreover, C-BSE typically targets the CNS, yet prions can be present in Peyer's patch and tonsils at the terminal disease stage but not in other lymphoid organs. However, lymphotropic strains like vCJD and CWD replicate in both the CNS and the lymphoid organs [158].

1.5. Prion transmission and species barrier

Intraspecies transmission of prions is much more efficient than interspecies transmission. For example, the transmission of mouse-adapted scrapie in mice was very efficient, while a more extended incubation period, attributed to the "species barrier," was observed during transmission to hamsters and rats [168]. To overcome this barrier, subsequent passages were needed in order for mouse-adapted scrapie prions to adapt to the new host [155, 168]. Some strains, after crossing the species barrier, gain reversible adaptation. Included in this category is the DY TME strain, which retains its pathogenicity to the original mink host while also gaining adaption through passaging in hamsters [169].

Prion transmission greatly depends on the PrP primary structure of the host and the propagating prion strain [72, 170-172]. For example, the species-specific hamster prion strain was transmitted to Tg mice expressing hamster PrP but not to the WT mice [173]. The levels of PrP expression in the host can also alter the efficiency of prion transmission. For example, Tga20 mice overexpressing PrP had a very short incubation period when inoculated with RML prions, while *Prnp*$^{+/0}$ mice with 50% less PrP expression than WT mice had a longer incubation period [174]. Moreover, the host PrP polymorphism has been reported to modulate susceptibility to prion transmission [170]. An early study by the Dickinson group showed a difference in the survival

period of mice to the Me7 scrapie strain infection depended on the *sinc* gene (for scrapie incubation) with two alleles, s7 (short) and p7 (prolonged) [175]. Later it was found that the *sinc* gene corresponds to the *Prnp* gene encoding PrP, and that s7 and p7 mice differ in their PrP primary structure due to two amino acid polymorphisms [176, 177]. However, the 22A scrapie strain showed the opposite effect on the s7 and p7 mice compared to Me7, suggesting that it is not only the host PrP primary structure that dictates prion transmission, the invading prion strain also plays a role [171].

Furthermore, in sheep as well, the PrP polymorphism and prion strain determine the transmissibility; the animals expressing the V_{136} Arginine $(R)_{154}$ Glutamine $(Q)_{171}$ (VRQ), $A_{136}R_{154}Q_{171}$ (ARQ) and $A_{136}R_{154}$ Histidine $(H)_{171}$ (ARH) PrP were found more susceptible to scrapie, while the sheep expressing the $A_{136}R_{154}R_{171}$ (ARR) and $A_{136}H_{154}Q_{171}$ (AHQ) were resistant [178]. On the other hand, the ARR sheep were susceptible to atypical scrapie [72].

A polymorphism at codon 129 (M/V) in human PrP is also correlated to vCJD susceptibility, resulting from the interspecies transmission of BSE to humans [13]. The majority of vCJD patients were methionine homozygous at codon 129 and only two clinical cases was reported to be heterozygous at codon 129 [47]. Consistent with this data, transmission studies using transgenic mice expressing 129MM-human PrP with either BSE or vCJD prions showed successful propagation [170, 179]. However, a substantial species barrier to BSE and vCJD prions was observed in 129VV-human PrP mice; even when infected, a distinct disease phenotype was observed [170].

Interestingly, a human 129M/V equivalent polymorphism exists in elk PrP^C at codon 132 (M/L), which dictates intraspecies CWD and interspecies scrapie transmission [180-182]. CWD oral transmission studies in elk expressing polymorphisms at 132 showed varying incubation

periods, with 132MM having the shortest and 132LL having the longest, with one out of four 132LL elk remaining clinically healthy at 64 months post-inoculation during the termination of the experiment [180, 181]. Additionally, PrP^{Sc} from CWD-affected 132LL elk had a distinct conformation with a shift in the PK-cleavage site, resulting in migration at a lower molecular weight band in the SDS-PAGE as compared to that from 132MM [181]. Moreover, Tg mice expressing cervid PrP with 132LL were resistant to elk CWD and susceptible to SSBP/1 sheep scrapie prions, suggesting the role of the elk 132 polymorphism at the prion strain selection [182]. In mule deer, a serine (S)/ phenylalanine (F) polymorphism at codon 225 of the *Prnp* gene was shown to be associated with CWD susceptibility, with a longer incubation period in heterozygous F225-PrP animals than WT (SS225) [183]. Moreover, the CWD-protective effect of the F225 polymorphism in deer could be explained by the F225-mediated alteration of orientations of amino acids at codon 170 (at the β2–α2 loop) and 228 (at the distal region of α-helix 3) that led to the stabilization of the region formed from the interactions between the two regions of deer PrP [184]. In WTD populations, the various polymorphisms in the cervid *Prnp* gene that have been reported to be associated with CWD are Q/ H at codon 95, G/ S at 96, and A/ G at 116, with the WT allele $Q_{95}G_{96}A_{116}$ found most frequently in the natural CWD-affected population [185-187]. Either Q95H or G96S allelic variants contributed to extended survival against a CWD oral challenge, suggesting the significant role of these polymorphisms in reduced CWD susceptibility in WTD populations [188].

During interspecies transmission, the structural difference in the β2-α2 loop region (residues 165-175; human numbering), due to amino acid changes, plays a significant role in dictating the species barrier [189]. CWD prions transmitted disease in Tg mice expressing human PrP, otherwise resistant to transmission, after four amino acid substitutions at the β2-α2 loop region

that resembled the loop of elk PrP. Of note, such modification in the β2-α2 loop region rendered these mice comparably less susceptible to human prions [189]. More interestingly, a single amino acid difference between deer and elk PrP at codon 226 (glutamatic acid (E) in elk and Q in deer) had an impact on the interspecies prion susceptibility and selection of CWD strains [166, 184]. The elk PrP-expressing Tg mice were resistant to the scrapie strain, SSBP/1, unlike the deer PrP-expressing animals, suggesting the effect of residue 226 on prion pathogenesis [184].

There are prion strains that can transmit in a wide range of hosts, such as BSE prions [172]. Interestingly, host species capable of overcoming transmission barriers and propagating various prion strains has been reported, such as bank voles. Bank voles are considered a "universal host" and bank vole PrP a universal acceptor for most of the prions such as human CJD, BSE, scrapie, and CWD [190].

1.6. Cellular prion protein

The *PRNP* gene in humans encodes the cellular prion protein, PrP^{C}. It is located on chromosome 20 and consists of two exons. The open reading frame (ORF) in the terminal exon encodes about 253 amino acids comprising PrP protein [191, 192]. The length of the PrP polypeptide chain varies depending on the species. However, the primary structure of PrP^{C} remains highly conserved among mammalian species [193]. Like other membrane-located glycoproteins, PrP^{C} follows the same secretory pathway including synthesis in the rough endoplasmic reticulum (ER) and transportation on to the cell surface via the Golgi apparatus. A mature PrP^{C} protein consists of two N-linked oligosaccharide chains attached at residues 181 and 197 and an intramolecular disulfide bond between cysteine (C) residues 179 and 214. A glycophosphatidylinositol (GPI)-anchor is attached at position 231 after the cleavage of the

COOH-terminal (C-terminal) hydrophobic peptide. In the plasma membrane, the GPI anchor helps PrP^{C} to attach to the outer leaflet of lipid rafts [194, 195]. Fig 1.2 shows the schematic diagram representing the primary structure of the cellular PrP protein along with its post-translational modifications.

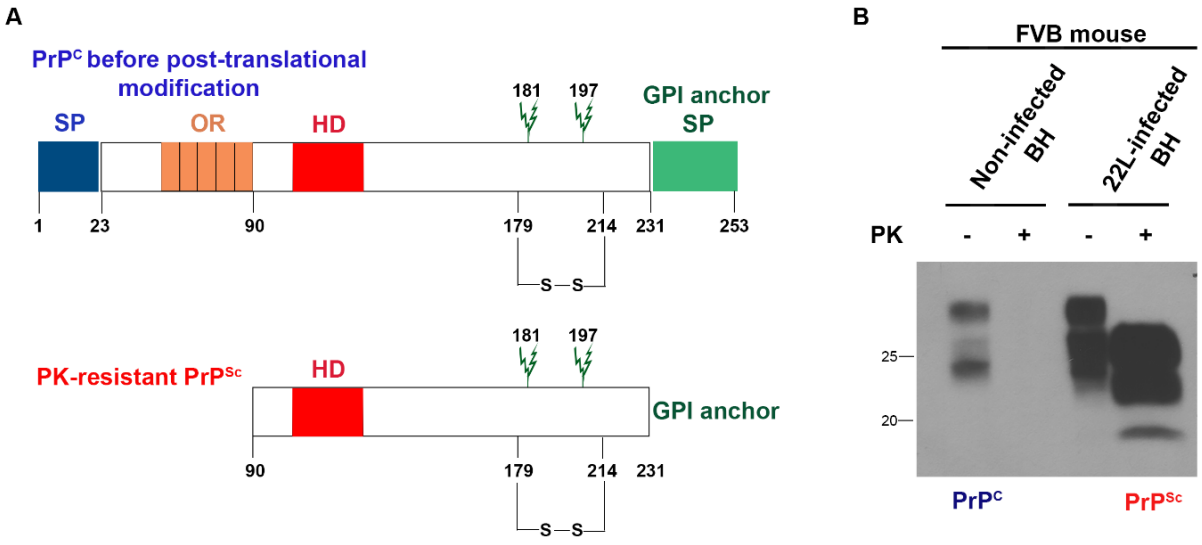

Figure 1. 2. Schematic diagram showing the primary structure of PrP^{C} and PK-resistant PrP^{Sc}. (A) PrP^{C} before post-translational modification consists of ER-targeting N-terminal signal peptide (SP) that is absent from a mature protein. In a mature PrP protein, octapeptide repeat (OR), hydrophobic domain (HD), two N-linked glycosylation sites at residue 181 and 197, a disulfide bond between residues 179 and 214, and a GPI anchor is attached after the cleavage of GPI anchor SP at the C-terminal (Adapted from Acevedo-Morantes and Wille [196]). The PK resistant pathological PrP^{Sc} represents the partially digested core fragment PK-cleaved at N-terminal. (B) Immunoblot showing the distinction between PrP^{C} and PrP^{Sc} based on PK digestion. PK digestion of non-infected brain homogenate (BH) resulted in complete digestion of PrP^{C}, whereas partially

resistant core of PrP^{Sc} is visible in case of 22L-infected BH. The characteristic three-banding pattern represents the di-, mono- and un-glycosylated forms.

1.6.1. Localization of PrP^{C}

PrP^{C} is found predominantly in the CNS, especially in neuronal and glial cells [10, 11]. In neuronal cells, it is localized on the plasma membrane of axons, dendrites, cell bodies, and in pre- and post-synaptic compartments [197, 198]. However, studies have shown a widespread expression of PrP^{C} throughout the body such as in the heart, muscle, lymphoid tissues, kidney, lung, liver, intestinal tract, and endothelium [10, 199]. Moreover, in the PNS, PrP^{C} has been found in the dorsal and ventral root ganglia of the spinal cord, sensory and motor axons, and Schwann cells [200, 201].

1.6.2. Structure of PrP^{C}

Nuclear magnetic resonance (NMR) analysis showed that the prion protein comprises a flexible N-terminal domain (residues 23 to 124) and a globular and structured C-terminal domain (residues 125 to 228) [202, 203]. The three-dimensional (3D) structure of PrP protein from different mammalian species as well as recombinant PrP proteins revealed the common architecture of domains with highly conserved folds among different species and in recombinant PrP. This indicates that glycosylation and the GPI anchor had no effect on PrP folding [203, 204].

The unstructured N-terminal part of human PrP consists of five OR elements of glycine-rich residues, PHGGGWGQ, which can bind metal ions like Cu^{2+} and Zn^{2+} [205, 206]. There is a conserved A- and V-rich HD, which spans the neurotoxic peptide residues 106-126, and a highly amyloidogenic palindrome, AGAAAAGA, between residues 113 to 120 [207, 208]. The C-

terminal domain consists of three α-helices (α1, α2 and α3) and two anti-parallel β-sheets [203]. The disulphide bridge links α2 and α3 helices between C-179 and C-214, providing stability to the globular domain [209]. The potential N-glycosylation sites, N-181 and N-197, are present for the attachment of complex oligosaccharides. This suggests that mature PrP^C exists in three different glycoforms (di-, mono- and un-glycosylated) and that when the PrP protein is subjected to SDS-PAGE, a characteristic three-banding pattern is detected by the anti-PrP antibody [2, 203] as shown in Fig. 1.2 B. The GPI anchor of PrP^C, unlike that of other mammalian GPI-anchored proteins, consists of sialic acid which is involved in targeting PrP^C to synapses in neurons [210, 211]. Moreover, the GPI composition of PrP^C influences cellular PrP^C localization, shedding, and prion pathogenesis [212].

1.6.3. Cell biology of PrP^C

PrP^C can be found in the Golgi/ trans-Golgi Network (TGN), plasma membrane, endosomes, exosomes, and endolysosomes [213-215]. Moreover, PrP^C was reported to be present in the cytosol due to misfolding in the ER [198].

After synthesis, PrP^C with an N-terminal signal peptide enters the ER and undergoes post-translational modification such as the cleavage of the N-terminal and C-terminal signal peptides, N-glycosylation, disulfide bond formation, and the addition of the GPI anchor, and undergoes proper folding under strict protein quality control (QC) [194, 195, 216]. If not correctly folded, PrP^C is destined for degradation by the ubiquitin-proteasome system in the cytoplasm [217]. If there is proteasomal inhibition, cytosolic PrP^C has been shown to exert a neurotoxic effect, which might have implications in prion disease pathogenesis [218]. The possible mechanism by which PrP^C is destined to cytoplasm could be triggered by an inefficient ER-targeting signal, which

prevents a small fraction of synthesized PrP^C from successfully translocating into the lumen of the ER [219]. Thus, that small fraction is retained in the cytoplasm [219]. Moreover, ER stress in cells might upregulate such non-translocated cytoplasmic PrP^C [220]. Correctly folded PrP is trafficked to the plasma membrane via the Golgi complex and TGN. From the plasma membrane, it is recycled via endocytosis, where it transits between endosomes and the plasma membrane or is degraded in lysosomes [221, 222]. Regarding the internalization of PrP^C, there are several studies suggesting clathrin- and caveolin-mediated endocytosis and lipid-raft dependent endocytosis as the mechanisms [223-226].

1.6.4. Function of PrP^C

The function of PrP^C is yet to be elucidated. The lack of any significant developmental defects or complications in the embryonic PrP-knockout mice, *Prnp* $^{-/-}$, made it difficult to decipher the cellular function of PrP^C [23, 24]. Even adult-onset knockout mouse models were successfully developed with normal phenotypes after the loss of PrP^C expression [227]. In addition to the mouse model, PrP gene-knockout, genetically engineered large animal models have been successfully developed. These include PrP-expression-lacking cattle and PrP-knockout goats with normal physiology and reproductive health [228, 229]. Interestingly, a study has shown the natural existence of healthy goats lacking PrP expression was due to the presence of a variant *Prnp* gene with a premature stop codon [230]. According to the study, such goats were normal in physiology, behaviour, clinical, or reproductive phenotype. These results suggest the non-vital role of PrP^C. However, some knockout mouse models showed abnormal circadian cycles and synaptic physiology [231]. Using the embryonic $PrP^{-/-}$ mice as well as a neuron-specific post-natal PrP depletion mouse model, the long-term potentiation (LTP) impairment and impaired synapsis was

observed in animals without PrP expression [227, 232]. These electrophysiological studies suggested the involvement of PrP^C in neuronal excitability and synaptic function [227, 232]. Furthermore, the increased synaptic vesicle release was observed in *Drosophila* after PrP was expressed, suggesting the role of PrP^C in synapsis [233].

Different studies have suggested the involvement of PrP in cell adhesion, metal ion homeostasis, anti-oxidative function, neuroprotection, and cell signaling (reviewed in [234]). Due to the well-known ability of the OR region of PrP^C to bind Cu^{2+} ions, it has been proposed that PrP^C might play a role in copper homeostasis and against cellular oxidative damage caused by reactive oxygen species (ROS) generated by a redox reaction of Cu^{2+}. This was later confirmed in *in vivo* as well [235-237]. Additionally, it has been reported that copper leads to reversible endocytosis of PrP^C in cultured neuronal cells and, thus, that PrP^C might be involved in the uptake and recycling of extracellular Cu^{2+} [238]. Another putative function assigned to PrP^C is intercellular adhesion, whereby PrP^C helps the cells to adhere and form aggregates *in vitro* [239]. Moreover, PrP^C was found to interact with cell adhesion molecules such as the neural cell adhesion molecule (N-CAM) and laminin; PrP^C interaction with the latter contributed to the process of neuritogenesis [240, 241]. Interestingly, a fascinating fact regarding the role of PrP^C in cell adhesion came when a genetic knockdown of PrP-1, a mammalian PrP^C homolog in zebrafish, led to a defect in embryonic development associated with the loss of embryonic cell adhesion [242]. This phenotype was later rescued upon mouse PrP^C expression, suggesting the PrP^C-mediated cell adhesion through homophilic interactions and the E-cadherin-based adhesion [242]. Some studies demonstrated that PrP^C acts as a signal transduction molecule that triggers signaling pathways involving Fyn kinase, protein kinase A (PKA), and mitogen-activated protein kinase (MAPK), leading to neuronal survival and neuritic outgrowth [243, 244]. Furthermore, the neuroprotective

role of PrP^{C} was proposed by several research groups with regard to its anti-apoptotic effect, whereby direct PrP^{C} interaction with an anti-apoptotic Bcl-2 protein in a yeast two-hybrid system was reported [245]. Hippocampal neurons derived from $PrP^{-/-}$ mice underwent apoptosis after serum deprivation more significantly than the hippocampal neurons from WT mice [246]. The apoptosis suppression in $PrP^{-/-}$ cells was achieved following the overexpression of either Bcl-2 or PrP^{C} [246]. On the other hand, PrP^{C} acts as an amyloid-β (Aβ) oligomer receptor and is involved in Aβ –mediated signaling, leading to synaptic dysfunction [247, 248].

1.7. PrP^{Sc} : the pathological form of PrP

PrP^{Sc} is the infectious misfolded isoform of PrP and is distinguishable in terms of physical and biochemical properties [1, 3, 22]. Although the primary structures of both isoforms are the same [249], the difference lies in their three-dimensional conformation, where PrP^{C} has a high α-helix content and PrP^{Sc} is rich in β-sheets [250-252]. Unlike PrP^{C}, PrP^{Sc} is detergent-insoluble and partially protease-resistant, and thus these two isoforms are distinguishable by immunoblotting after PK digestion [19, 22], as shown in Fig. 1.2 B. In contrast to the monomeric PrP^{C}, PrP^{Sc} molecules are prone to aggregation, forming oligomers, multimers, and later amyloid fibrils [3]. The PrP^{C} and PrP^{Sc} share similarity not only in amino acid sequences but also in post-translational modifications, where both consist of N-linked glycosylation and a GPI anchor [194, 249]. Nevertheless, the proportion of the type of glycan present varies in these two identities. PrP^{Sc} has more triantennary and tetraantennary oligosaccharides and less biantennary glycans than PrP^{C} [253]. Moreover, the GPI anchor of PrP^{Sc}, unlike PrP^{C}, was found to be resistant to phosphatidylinositol-specific phospholipase C (PIPLC)-cleavage [254, 255].

Unlike PrP^{C}, PrP^{Sc} is insoluble and has propensity to form aggregates; as a result, its structure has remained unsolved using high-resolution techniques such as NMR. Analysis of PrP^{Sc} using low-resolution techniques like circular dichroism (CD) and fourier transform infrared spectroscopy (FTIR) suggest that PrP^{Sc} had a content high in β-sheets (more than 40%) and low in α-helices [250, 256]. However, a study revealed that the presence of α-helices in PrP^{Sc} is questionable based on the finding that the α-helix-associated spectral band from PrP^{Sc} was similar to that from rPrP-associated entirely β-sheeted amyloid fibrils in the FTIR spectroscopy [251]. Moreover, the same study suggested that the entire C-terminal region in PrP^{C} refolds during conversion, giving rise to a PrP^{Sc} structure consisting exclusively of β-strands and relatively short turns or loops. This argument was further supported by the study in which the α-helix-attributed FTIR band actually overlapped with the spectrum from turns and coils in the same region, thus confirming the absence of the α-helix in PrP^{Sc} [257]. Recently, cryo-electron microscopy and 3D reconstructions were utilized to decipher the structure of PrP^{Sc}. The analysis suggested a four-rung β-solenoid structure of PrP^{Sc} whereby each β-strand of PrP^{Sc} remains perpendicular to the amyloid fibril axis [258]. The amyloid fibrils consist of PrP^{Sc} molecules, which get stacked either in a head-to-head or tail-to-tail orientation along the fibril axis [258]. However, the atomic details are yet to be resolved.

Although the $rPrP^{Sc}$ (PK-resistant PrP^{Sc}) has been identified as an infectious conformer in infected tissues, the CDI confirmed the existence of $sPrP^{Sc}$ (PK-sensitive PrP^{Sc}) as well [17, 153]. Another group utilized sucrose gradient ultracentrifugation to isolate $sPrP^{Sc}$ from prion-infected brain tissues representing low molecular weight aggregates that were attributed to smaller multimers [259]. Interestingly, it was later revealed that sCJD PrP^{Sc} is comprised of both $rPrP^{Sc}$ and $sPrP^{Sc}$, out of which as much as 90% is $sPrP^{Sc}$ [260]. The role of such $sPrP^{Sc}$ in prion

pathogenesis is still not well investigated. However, one study suggested that $sPrP^{Sc}$ is completely infectious in nature like the $rPrP^{Sc}$ entity and that both share similar structural properties with a difference in their aggregate size [261]. Recently, in the case of *de novo* infectious recombinant prions generated *in vitro* consisting of a large fraction of $sPrP^{Sc}$, it was found that prion infectivity was entirely dependent on $rPrP^{Sc}$ conformation [262].

1.8. PrP^{Sc} conversion and prion replication process

Prion conversion occurs by conformational transition where the α-helical-structured PrP^{C} is refolded into structures rich in β-sheets of PrP^{Sc} [250, 255, 263]. It is well known that PrP^{C} is a prerequisite for prion replication and pathogenesis. Upon prion inoculation, mice were resistant to infection when PrP^{C} was knocked out at the embryonic stage [23]. When neuronal PrP^{C} was depleted at the adult stage, disease progression and neurodegeneration were prevented [264].

Although the exact mechanism for conformational conversion is yet to be elucidated, there are two mechanistic models suggesting prion conversion from PrP^{C} to PrP^{Sc} [265]. The "template-directed or refolding" model suggests that there is a structural interaction between endogenous PrP^{C} and spontaneously PrP^{C}-misfolded or exogenously presented PrP^{Sc}, and that PrP^{Sc} acts as a template onto which monomeric PrP^{C} is refolded into PrP^{Sc}. The spontaneous conversion is prevented by a high energy barrier. Heterodimer (PrP^{Sc}-PrP^{C}) formation is thought to lower the energy barrier, facilitating the complete conversion into PrP^{Sc} homodimers. After dissociation, newly generated PrP^{Sc} continues the cyclic cascade to convert other PrP^{C} monomers [265]. This model was supported by a study conducted by Prusiner *et al.* whereby species-specific replication of prion strains was observed in Tg mice expressing both hamster PrP and mouse PrP [266]. After inoculation with mouse-adapted prions, mouse PrP^{Sc} acted as a template for the conversion of

mouse PrP^{C} into mouse PrP^{Sc}; however, in the same mouse, inoculation with hamster prions led to the conversion of hamster PrP^{C} into hamster PrP^{Sc}. The data suggested that during prion conversion, PrP^{Sc} conformation acts as a template to select PrP^{C} depending on sequence homology for conversion [266].

The second model is the "seeding or nucleation-polymerization model," proposed by Lansbury and Caughey [267]. It suggests that PrP^{C} and PrP^{Sc} exist in a reversible equilibrium where the PrP^{C} structure is highly favored. However, a small amount of PrP^{Sc} can exist and several monomeric PrP^{Sc} molecules can come together to form a highly ordered seed, which is a rather slow process followed by rapid or exponential recruitment of monomeric PrP^{C} into a growing aggregate to form amyloid fibrils. The stabilized fibrils can undergo fragmentation to increase the nuclei or seeds for further polymerization [268, 269]. The most reliable evidence for this model comes from PMCA where a small amount of PrP^{Sc}, present as a seed in samples, recruits the PrP^{C} substrate into the growing PrP^{Sc} polymer, which then undergoes fragmentation during the sonication process to increase the number of seeds with each cycle of amplification [31].

Several studies have suggested that the conversion of PrP^{C} to PrP^{Sc} occurs in various compartments in the cell. Some have proposed that the conversion happens at the cell surface [255], while others have suggested that PrP^{Sc} uses lipid rafts to enter cells and initiate the conversion [223]. The endocytic and lysosomal pathways are also proposed to be involved in prion conversion [270, 271]. Moreover, the perinuclear region [272, 273] and the ER have been suggested as possible conversion sites [274].

Several cofactors are believed to be involved in prion conversion and prion propagation; however, this needs more investigation. Glycosaminoglycans (GAG), particularly heparan sulfate, were shown to affect prion conversion *in vitro* by aiding in the PrP^{C}-PrP^{Sc} complex formation

[275, 276]. Specifically, neuronal GPI-anchored heparan sulfate proteoglycan glypican-1 was shown to be involved in facilitating prion conversion by bringing PrP^{C} and PrP^{Sc} to close proximity in lipid rafts [277]. Additionally, through PrP-interaction studies, other molecules are proposed to be involved in conversion by stabilizing the PrP^{C} structure in a way that is required for PrP^{Sc} conversion. These molecules include laminin receptor precursor 1, neural adhesion molecules, anionic lipids, and copper ions [278]. From studies with transgenic mice, researchers have proposed a hypothetical species-specific protein called "protein X", which helps in prion propagation by interacting with cellular PrP [279]. Interestingly, the *in vitro* conversion assays have provided solid proof of the role that cofactors play in prion conversion. Studies have shown that host-encoded RNA, phosphatidylethanolamine (PE), and synthetic phospholipid 1-palmitoyl-2-oleoylphosphatidylglycerol (POPG) are cofactors for the prion-seeded or unseeded *in vitro* conversion or *de novo* generation of infectious prions from rPrP [27, 29, 30, 280]. However, in the *in vivo* context, the role of cofactors has yet to be investigated.

1.9. Prion-induced neurodegeneration and the neurotoxic entity

Prion neuropathology is characterized by distinctive histopathological brain lesions associated with spongiform changes, neuronal loss, vacuolation and astrogliosis, and the deposition of PrP^{Sc} (as shown in Fig. 1.1), either in the form of aggregates or a diffused type, depending on the host species and prion strain [1-5, 281]. However, the exact mechanism of PrP^{Sc}-induced neurodegeneration and pathology is still an open question. It has been suggested that either a loss of function of PrP^{C} or toxic gain-of-function by PrP^{Sc} and/or both during prion conversion might trigger progressive neurodegeneration.

Several neuroprotective functions, such as protection against oxidative stress and Bax-mediated neuronal apoptosis, have been attributed to PrP^{C}. These functions might be hampered during PrP^{C} conversion to PrP^{Sc} [236, 245, 282]. However, the successful generation of embryonic PrP-knockout or conditional knockout animals without abnormal development, physiological and functional phenotypes, and brain neurodegeneration provide strong evidence contradicting the view of loss of function [23, 202, 227, 229]. Of note, the expression of PrP^{C} is essential for prion replication and clinical disease to occur [23]. Another exciting study which challenged this loss-of-function theory involved the ic inoculation of prions in $PrP^{-/-}$ mice containing a neural tissue graft from mice that had PrP^{C} overexpressed [283]. The prion inoculation resulted in neuronal loss and spongiform changes only in the PrP^{C}-expressing grafts and not in the PrP^{C}-deficient area outside the graft, despite the deposition of PrP^{Sc} aggregates. This data suggests the inevitable role of PrP^{C} expression in prion-induced neurodegeneration [283]. Recently, the globular domain-binding PrP antibodies in cerebellar organotypic-cultured slices (COCS) triggered ROS production, leading to neurotoxicity, similar to what was observed with prion infection. Such an outcome was reduced using antibodies against the flexible N-terminal of PrP^{C}, suggesting that PrP^{Sc} mediates toxicity via interactions with PrP^{C} where the flexible tail exerts neurotoxicity by triggering downstream pathways [284].

The role of PrP^{Sc} in prion infectivity and disease-related neurodegeneration is not well-known. Few studies reported on the positive correlation between PrP^{Sc} deposits and spongiform appearance as well as the infectivity in the brain of scrapie-infected hamsters, suggesting the possible role of PrP^{Sc} in neurotoxicity [285]. Moreover, the human PrP peptide consisting of residues 106-126 was found to be neurotoxic *in vitro* as was the purified PrP^{Sc} at a nanomolar concentration [207, 286]. However, the association between PrP^{Sc} and neurotoxicity is rather

complicated, and controversial. Some transmission studies have showed that after ic inoculation of WT mice with 263K hamster prions, the brains of mice had a high titre of infectious prions, even though no clinical disease developed; the PrP^{Sc} were transmissible further into mice [287, 288]. These data suggested that such sub-clinical carrier animals could tolerate these significant levels of infectious PrP^{Sc} without clinical disease; thus the role of PrP^{Sc} in prion infectivity is a little vague. Furthermore, when inoculated with human brain material infected with no spongiform neurodegeneration-associated form of GSS, brain of Tg mice expressing the GSS-associated P102L mutation accumulated PrP^{Sc} amyloid deposits in the absence of clinical disease [289]. Moreover, even in the second passage, no transmissibility of disease was observed despite the presence of PrP^{Sc} deposits. This result suggests no association between PrP^{Sc} deposits and neurodegeneration [289]. In GSS, a transmembrane form of prion protein was found to cause prion disease without PrP^{Sc} deposition [290]. Additionally, prion inoculation in Tg mice expressing anchorless PrP resulted in the accumulation of infectious amyloid PrP^{Sc} in the brain without clinical prion disease, which caused spongiosis after transmission to WT mice [291]. This data showed the importance of GPI anchored PrP^{C} for PrP^{Sc}-mediated neurotoxicity.

Earlier, interesting evidence for PrP^{Sc} itself being non-toxic came when the prion infection study in PrP-overexpressing tissue grafting in PrP-knockout mice showed that the area outside the graft, although it had PrP^{Sc} accumulation, was devoid of spongiform changes [283]. Moreover, the process of neuronal loss and neuropathology was reversed in prion-infected mice after the depletion of neuronal PrP^{C}, further supporting the argument that PrP^{Sc} is not directly neurotoxic [264]. On the other hand, neuronal death was observed in BSE- infected mice without any detectable $rPrP^{Sc}$ [292]. Supporting that PrP^{Sc} is itself non-neurotoxic and that there might be an intermediate neurotoxic molecule formed when prion replication is saturated, studies involved

showed the clinical onset of prion disease was not correlated with the presence of maximum infectivity and PrP^{Sc} titres in the brain [293, 294]. Based on the size, the most infectious prion particles are suggested to comprise non-fibrillary 14-28 PrP molecules, rather than large amyloid fibrils [295]. Another study identified a soluble, partial protease-resistant, and low molecular weight oligomeric intermediate formed during PrP^{C} conversion to PrP^{Sc} as a neurotoxic entity both *in vitro* and *in vivo* [296, 297]. Additional interesting study was performed to state the correlation of the punctate-type of pathological PrP deposits, not the amyloid plaques or large deposits, with neuronal loss and astrogliosis [281]. Thus, these investigations point towards the complex and heterogeneous nature of the neurotoxic species in prion disease.

1.10. Glycoprotein quality control (QC), ER stress, and unfolded protein response (UPR)

The QC of proteins allows the transportation of only correctly folded protein out of the ER. Protein QC is considered check-point through which all newly synthesized protein pass, which further assures the maintenance of the homeostasis in the secretory pathway [298]. Various factors such as, hypoxia, nutrient deprivation, mutations in proteins, redox changes, loss in calcium homeostasis and pathological conditions could promote accumulation of misfolded protein in the ER, consequently resulting in ER stress [299]. Cells necessarily need to resolve such a situation where the consequence might lead to cellular toxicity [300].

Secretory and membrane glycoproteins undergo N-linked glycosylation in the ER. An oligosaccharide is linked to the nascent chain of glycoprotein, in which two-terminal glucose residues are removed by glucosidase I and II, respectively. The presence of only one glucose residue allows the entry of this nascent protein to the calnexin/calreticulin (CNX/CRT) cycle for the folding to happen. CNX/CRT along with ERp57 binds to the protein and assists its folding.

After the protein has reached its native conformation, it is released from the ER towards the Golgi complex. If not correctly folded, the exposed hydrophobic regions are sensed by UDP-glucose:glycoprotein glycosyltransferase (UGGT), which adds the glucose residue back to the protein chain and induces the cycling of the protein back to CNX/CRT for folding. If still not folded properly, then it will be transferred towards the ER-associated degradation (ERAD) pathway for proteasomal degradation [301, 302]. Some of the components of ER QC are chaperones, co-chaperones, and cargo receptors. Chaperones and co-chaperones help in the proper folding of proteins, prevent protein aggregation, and allow proper translocation of proteins. The ER chaperones consist of three families of heat shock proteins (HSP), HSP70, HSP40 and HSP90 [303-307]. The folding enzymes, such as CNX/CRT and thiol-disulfide oxidoreductases, one of which is ERp57, are also involved in folding and QC [308]. The cargo receptors, such as ERGIC-53, allow only correctly folded proteins to leave the ER [309]. VIP36 ensures the retrograde transport of any misfolded form from the Golgi to the ER [310].

The accumulation of misfolded protein in the ER will lead to ER stress and the up-regulation of the UPR machinery. UPR includes the attenuation of the translation of proteins, and the upregulation of chaperones and other QC molecules to cope with misfolded proteins and enhance the protein degradation [311]. Persistent ER stress can eventually result in apoptosis; caspase-12 is found responsible for ER-mediated apoptosis [312, 313]. UPR activation occurs through three different stress sensor molecules present in the ER membrane, IRE1 (inositol requiring enzyme 1), PERK (Protein kinase (PKR)-like ER kinase), and ATF6 (activating transcription factor 6). IRE1 dimerizes and autophosphorylates, leading to the splicing of the X-box binding protein1 (XBP-1) mRNA to generate the active transcription factor XBP-1s, which in turn upregulates the transcription of genes related to protein folding and ERAD. PERK

autophosphorylates and leads to the phosphorylation of the translation initiation factor, eIF2a, and the subsequent attenuation of protein translation. ATF6, after being released from the ER, gets cleaved in the Golgi and upregulates the transcription of genes of UPR-related chaperones and ERAD pathway [299, 314]. The HSP70 family includes BiP, which is a widely studied chaperone that helps in the folding of proteins, is involved in protein translocation, and regulates UPR by releasing the bound ER stress response molecules such as ATF6, IRE1, and PERK. It also activates them during stress conditions [303-307]. In the ER stress condition, there is up-regulation of BiP and activated forms of PERK, IRE1, and ATF6 (cleaved 50-kDa form of ATF6α) [315]. The upregulation of ER stress markers, BiP (signifies UPR activation), and CHOP (signifies ER stress-associated apoptosis) are induced by ATF4, which is a downstream of PERK-phosphorylated eIF2α pathway [316]. CHOP has been shown to downregulate the anti-apoptotic protein Bcl-2, and increase the expression of pro-apoptotic BH3-only protein, BIM leading to mitochondrial apoptotic signaling, as well as enhanced ROS production [317-319].

Several research groups including ours have demonstrated a complex relationship between ER stress, QC molecules, and prion replication. There have been reports suggesting that the accumulation of misfolded PrP and PrP^{Sc} leads to ER stress in prion disease models [320-323]. Various factors, such as oxidative stress, calcium dysregulation and the expression of mutated proteins, have been demonstrated to be responsible for causing ER stress [322, 324, 325]. Consequently, some studies have suggested that prion infection increases the susceptibility of cells to ER stress, which in turn facilitates the formation of misfolded PrP^{C} as an increased substrate for prion conversion [220, 286, 326]. Moreover, PrP^{Sc}-induced ER stress and subsequent neurotoxicity in the cells was found to be associated with the disruption of calcium homeostasis. When the cultured cells were treated with PrP^{Sc}-containing mouse brain homogenate, calcium

released from the ER to the cytoplasm was observed [286]. Of note, ER stress induction and calcium homeostasis dysfunction were also reported in human prion disease-associated PrP mutant-expressing cells, demonstrating the role of increased susceptibility to ER stress as one of the events in prion pathogenesis [322]. Subsequently, ER calcium depletion could impair the functional activity of chaperones and foldases, leading to increased misfolded protein accumulation in the ER [299, 322]. Moreover, PrP^{Sc}-mediated neurotoxicity was found to be associated with caspase-12 activation, both *in vitro* and in *vivo*. In cells, subsequent cell death after treatment with PrP^{Sc} was prevented by overexpressing a catalytic mutant form of caspase-12. In addition, analysis of the brains of scrapie-infected mice established a link between caspase-12 activation and neuronal loss [286]. However, caspase-12-deficient mice showed a similar incubation period as WT mice after prion infection, suggesting that the caspase-12-dependent pathway is not a sole apoptotic pathway in prion pathogenesis and that the mitochondrial apoptotic pathway could be involved [323, 327]. Additionally, the involvement of ER stress has been seen in the pathophysiology of other neurodegenerative diseases such as AD, Parkinson's, and Huntington's disease [298, 299].

The upregulation of some chaperones such as GRP58, GRP78, GRP94, HSP70, and protein disulfide isomerase (PDI) has been reported in brains of CJD patients, suggesting a role of ER chaperones in prion pathogenesis [286, 328-330]. Such upregulation was also observed in prion-infected hamsters, where levels of GRP58, GRP78, GRP94, and HSP70 increased consistently starting from the pre-clinical stage [331].

1.10.1. Protein QC as a therapeutic target against prion diseases

It is necessary to understand the molecular and cellular mechanisms of prion conversion and propagation to elucidate molecular strategies for disease control [332-334]. Numerous therapeutic approaches have been reported, including the use of pharmacological compounds, peptide aptamers, and *Prnp* gene silencing-associated gene therapy [334-336]. Some are effective *in vivo* in terms of increasing the incubation time to disease. As cellular QC ensures the production and transportation of only correctly folded proteins in cells [337], the manipulation of this process could result in correctly folded PrP^{C} reaching the plasma membrane, which is less prone to prion conversion. Such QC pathways could be manipulated to achieve anti-prion therapy. Our studies have suggested the involvement of impairment in QC mechanisms in prion conversion, and the reduction of conversion by overexpressing QC proteins such as ERGIC-53 and EDEM3 [338]. Moreover, BiP expression was found to influence prion disease propagation with BiP overexpression in RML-infected CAD5 cells [339]. This led to reduced PrP^{Sc} levels, while increasing prion replication in BiP-downregulated cells. This modulation was also prominent in a prion-infected mouse model where BiP downregulation resulted in a short incubation period [339]. Recently, HSP70 has been shown to have preventive effect against prion infection in a mouse model [340]. Interestingly, after inducing HSP70 pharmacologically in the *Drosophila* model, PrP misfolding and neurotoxicity appeared to have been prevented [341]. Additionally, it has been reported that ERp57 regulates the expression and maturation of PrP^{C} in cells and has a protective effect *in vitro* against prion toxicity [328, 342]. These data suggest that reducing prion-mediated ER stress in the cells through the modulation of QC could be a therapeutic approach to control prion infection. Furthermore, the effect of other QC proteins is yet to be elucidated. There is a gap of knowledge in elucidating the role of ERp57 and VIP36 on prion conversion *in vitro* and *in vivo*.

On the other hand, some studies have shown that chronic ER stress leading to a PERK-mediated pathway could be detrimental in prion pathogenesis [320]. During ER stress, activation of PERK phosphorylates and inactivates eIF2a, which in turn reduces the global protein translation to cope with stress [314]. However, such sustained protein translation attenuation could lead to a reduction in synaptic proteins, resulting in neurodegeneration. In RML-infected Tg37 mice, elevated levels of phosphorylated PERK (p-PERK) and phosphorylated eIF2α (p-eIF2α) was seen throughout the infection period. Moreover, the increased survival and rescue of the pathological condition in the infected mice was achieved upon the reduction of p-eIF2α, genetically, via lentivirus-mediated overexpression of stress-induced eIF2α phosphatase subunit, GADD34. Moreover, the pharmacological inhibition of protein phosphatase using salubrinal led to a decline in p-eIF2α dephosphorylation, which significantly decreased the survival and enhanced neuronal loss in in prion disease animal model [320]. However, another drug, guanabenz, which inhibits only the stress-related phosphatase subunit, prolonged the survival in transgenic mice against ovine prions [343]. This difference is because salubrinal inhibits both stress-related and non-stress-related protein phosphatase complexes, resulting in the sustained and lethal attenuation of global protein translation. In contrast, guanabenz only acts on the stress-related subunit, leaving the non-stress phosphatase to dephosphorylate p-eIF2α [344-346]. Of note, guanabenz acts as α2-adrenergic agonist which limits its use as therapeutics though it is found effective in several neurodegenerative disease mouse models [347-349].

Recently, Sephin1 was identified as a derivative of guanabenz without α2-adrenergic activity, which effectively delayed disease development in protein misfolding diseases [350, 351]. However, its anti-prion activity has not been yet determined. Some compounds such as GSK2606414 (inhibit PERK), and ISRIB, trazodone hydrochloride, and dibenzoylmethane (act

downstream of p-eIF2α to restore protein translation), were reported to be neuroprotective and showed prolongation of the survival in prion-infected mice [352-354]. On the other hand, *in vitro* data suggested a possible neuroprotective role of the transcriptional factor XBP-1 by determining the rate of PrP^C aggregation during stress [326]. However, *in vivo*, this UPR pathway had no effect on prion pathogenesis and XBP-1 signaling was not enough to protect against prion infection as the survival of XBP-1 knockdown mice was similar to that of WT mice after prion infection [355]. Thus, UPR is a very complicated process and targeting it for prion therapeutics needs to be done carefully.

1.11. Vaccination approach against CWD

The CWD management program includes the strategic depopulation of cervids through sharpshooting and seasonal hunting, which, to some extent, could help limit the disease spread among wild animals and into the environment. However, it is not a feasible method for long-term management [356, 357]. Potapov et al. demonstrated a deterministic model for CWD management and control whereby harvesting animals should be simultaneously combined with intensive vaccination to achieve an adequate reduction in CWD prevalence and spread [358]. Thus, vaccination could be an effective preventive strategy to control prion infection, limit the shedding of prions into the environment, and prevent an efficient disease spread.

The prophylactic approach, like vaccination, is challenging in prion diseases, as a self-protein has to be targeted. A vaccine should overcome self-tolerance and induce a humoral immune response without inducing autoimmunity-associated side effects [359, 360]. There have been studies reporting that passive immunization was effective *in vivo* when given immediately after prion inoculation. However, immunization during the symptomatic phase of infection was

ineffective because anti-PrP antibodies are unable to cross the blood brain barrier (BBB) [361]. Furthermore, active immunization was reported to reduce prion propagation and to prolong the incubation period in murine-adapted scrapie models, suggesting the therapeutic effect of anti-PrP antibodies [359, 362, 363]. Therefore, during peripheral prion infection, as in the case of CWD, the vaccination approach could be effective as the antibodies will block the prion conversion and mitigate the infection before neuroinvasion occurs.

There are few studies regarding the vaccination approach to control CWD. Active vaccination with synthetic peptides showed no protection against CWD in mule deer [364]. Another study reported 20% protection against orally challenged CWD infection after white-tailed deer were orally vaccinated with attenuated *Salmonella typhimurium* expressing cervid PrP [365]. Another potential CWD vaccine candidate is based on disease-specific epitopes (DSE). DSEs are identified as uniquely exposed epitopes during misfolding from PrP^{C} to PrP^{Sc}. These include the Tyrosine-Tyrosine-Arginine (YYR) epitope of the β2 strand, Tyrosine-Methionine-Leucine (YML) at the β1 strand, and the rigid loop within the β2-α2 region that confers unique conformational rigidity to the cervid PrP^{C} as compared to that of mammalian species [366, 367]. An oral vaccine was made with non-replicating human adenovirus expressing a DSE, a rigid loop region in this case (hAd5:tgG-RL), fused with truncated rabies glycoprotein G. Upon oral immunization of white-tailed deer, both systemic and mucosal PrP^{Sc}-specific antibodies were produced [368]. The same research group has developed an oral vaccine in elk based on the YYR epitope, which was evaluated against natural CWD exposure achieved by housing elk in the prion-contaminated environment. Although the vaccine induced a high antibody titre in animals, the disease progression was accelerated in vaccinated animals as compared to non-vaccinated elk, which substantially raised concern regarding the CWD vaccination approach [369]. Thus, further

development of efficient vaccine immunogens and immunization strategy is necessary to control CWD.

1.12. Rationale and research objectives

1.12.1. Therapeutic approach for prion disease

There is a complex relationship between ER stress and prion pathogenesis, where ER stress can enhance PrP^{Sc} levels in prion disease models and, on other hand, prion infection can lead to ER stress in the cells [220, 320-322, 326, 338]. Previous studies in our lab have demonstrated that ER stress and proteasomal impairment in cells result in increased PrP^{C} aggregation and PrP^{Sc} conversion in prion-infected cells [338]. Interestingly, the overexpression of some QC proteins (EDEM3 and ERGIC-53) resulted in reduced ER stress-mediated PrP^{C} aggregation and PrP^{Sc} accumulation [338]. Thus, we wanted to explore other QC proteins such as VIP36 and ERp57 and investigate their role in prion diseases *in vitro* and *in vivo*. Moreover, we wanted to investigate the role of UPR in prion diseases; specifically, we wanted to target the eIF2α phosphorylation pathway as an anti-prion strategy. Recently, a compound, Sephin1, was shown to exert protective effects on the cells against cytotoxic ER stress by prolonging the eIF2α phosphorylation, and in mouse models Sephin1-associated protection was shown against protein misfolding diseases [350]. This study made us enthusiastic to test the anti-prion effect of Sephin1 both *in vitro* and *in vivo*, considering the impact of ER stress on prion infection. Our objectives for the anti-prion therapeutic approach are listed below.

a. To investigate the impact of overexpression of ERp57 and VIP36 on prion propagation, and further formulate the mechanism involved during such manipulation (Chapter 2)
b. To investigate the anti-prion effect of Sephin1 both *in vitro* and *in vivo* (Chapter 3)

1.12.2. Prophylactic approach against CWD

Keeping in mind the contagious nature of CWD as well as its zoonotic potential, which is not yet well understood, CWD vaccination could have implications on the control of disease transmission and spread. Until now, studies examining active CWD vaccination showed no success in terms of protection against CWD, except for one, which reported 20% protection in vaccinated cervids [364, 365, 369]. This should generate support for the development of a CWD vaccine which could overcome self-tolerance against PrP, generate autoantibodies binding to host PrP^C, and interfere in prion propagation at peripheral sites of the host to prevent the prions from reaching the brain, and ultimately, protecting animals against CWD and from shedding prions into the environment. Previous studies in our lab have tested the efficacy of anti-PrP antibodies generated upon active vaccination with multimeric mouse recombinant PrP in scrapie-infected cell and animal models [359, 363]. We wanted to test the immunogens made up of aggregation-prone multimeric recombinant mouse and deer PrPs in active vaccination in Tg mice overexpressing cervid PrP against the CWD challenge and, thus, validate the immunogens before testing in the natural host. The objective of this approach is to investigate the efficacy of an active vaccination using the multimeric recombinant mouse and deer PrPs against CWD challenge in Tg mice overexpressing elk PrP (Chapter 4).

CHAPTER 2:

OVEREXPRESSION OF QUALITY CONTROL PROTEINS REDUCES PRION CONVERSION IN PRION-INFECTED CELLS

This chapter presents the manuscript published in *The Journal of Biological Chemistry*

Thapa S*, Abdulrahman BA, Abdelaziz DH, Lu L, Aissa MB and Schatzl HM. 2018. Overexpression of quality control proteins reduces prion conversion in prion-infected cells. *The Journal of Biological Chemistry*, 293(41): 16069–16082

2.1. Abstract

Prion diseases are fatal infectious neurodegenerative disorders in humans and other animals and are caused by misfolding of the cellular prion protein (PrP^{C}) into the pathological isoform PrP^{Sc}. These diseases have the potential to transmit within or between species, including zoonotic transmission to humans. Elucidating the molecular and cellular mechanisms underlying prion propagation and transmission is therefore critical for developing molecular strategies for disease intervention. We previously have shown that impaired quality control (QC) mechanisms directly influence prion propagation. In the present study, we manipulated cellular quality control pathways *in vitro* by stably and transiently overexpressing selected QC folding (ERp57) and cargo (VIP36) proteins, and investigated the effects of this overexpression on prion propagation. We found that ERp57 or VIP36 overexpression in persistently prion-infected neuroblastoma cells significantly reduces the amount of PrP^{Sc} in immunoblots and prion-seeding activity in the real-time quaking-induced conversion (RT-QuIC) assay. Using different cell lines infected with various prion strains confirmed that this effect is not cell type– or prion strain–specific. Moreover, *de novo* prion infection revealed that the overexpression significantly reduced newly formed PrP^{Sc} in acutely infected cells. ERp57-overexpressing cells significantly overcame endoplasmic reticulum (ER) stress, as revealed by expression of lower levels of the stress markers BiP and CHOP, accompanied by a decrease in PrP aggregates. Furthermore, application of ERp57-expressing lentiviruses prolonged the survival of prion-infected mice. Taken together, improved cellular QC via ERp57 or VIP36 overexpression impairs prion propagation and could be utilized as a potential therapeutic strategy.

2.2. Introduction

Prion diseases are transmissible spongiform encephalopathies (TSEs) characterized by distinctive spongiform appearance and loss of neurons in the brain. TSEs include Creutzfeldt-Jakob disease (CJD) in humans, scrapie in sheep, bovine spongiform encephalopathy (BSE) in cattle and chronic wasting disease (CWD) in cervids. These diseases are caused by accumulation of the misfolded infectious isoform (PrP^{Sc}) of the normal cellular prion protein (PrP^{C}) in the brain and other tissues [1-3]. Unlike α-helix rich PrP^{C}, PrP^{Sc} is rich in β-sheets, insoluble in detergent and partially protease resistant, making the two isoforms distinguishable by immunoblotting after proteinase K (PK) digestion [250-252, 370]. PrP^{Sc} accumulation in the brain leads to formation of aggregates which impair the normal physiology of the brain, leading to neurodegeneration. Prion diseases are unique among neurodegenerative diseases as they have the potential to be transmitted between and within species, including zoonotic transmission from animals to humans [13, 14, 371]. There is currently no treatment available for these fatal neurodegenerative diseases.

The ER plays an important role in the cell biology of PrP^{C} including its folding, post-translational modification, translocation to the secretory pathway and QC [372]. ER QC of proteins allows the transportation of only correctly folded proteins out of the ER to the target cellular compartments, ensures the degradation of misfolded proteins, and helps in maintaining the homeostasis in the secretory pathway. The accumulation of misfolded proteins in the ER [298] alters its physiological function and perturbs ER homeostasis, leading to ER stress. It is important for cells to avoid such ER stress which might lead to accumulation of misfolded proteins deposits and cellular toxicity [300]. Unfolded protein response (UPR) is a series of coordinated signaling events initiated and regulated by cells to cope with ER stress. It results in downstream effects leading to attenuation of protein translation and up-regulation of chaperones, and other QC

molecules, in order to cope with misfolded proteins and to enhance protein degradation [311]. Some of the components of ER QC are chaperones and cargo receptors. Chaperones help in correct folding of proteins, prevent protein aggregation, and allow proper translocation of proteins. For example, BiP helps in folding of proteins, is involved in protein translocation, and regulates UPR [304, 305, 307]. Folding enzymes such as calnexin, calreticulin and thiol-disulphide oxidoreductase, ERp57, are also involved in folding and QC [308]. Cargo receptors such as ERGIC-53 and VIP36 ensure that only correctly folded protein exits the ER to the Golgi apparatus [309, 310]. The latter helps in retrograde transport and brings misfolded proteins from the Golgi back to the ER.

Several reports have suggested that not correctly folded forms of PrP^{C} and PrP^{Sc} accumulate during ER stress in prion disease models [220, 321, 326, 338]. Moreover, it has been shown in *in vitro* and *in vivo* models that prion infection resulted in cells to undergo ER stress which further facilitated the formation of misfolded PrP^{C} and increased prion conversion [320, 322, 326, 338]. Previous studies in our lab have also demonstrated a direct influence of impairment in QC mechanisms on prion conversion, and overexpression of QC proteins such as ERGIC-53 and EDEM3 reduced prion conversion [338]. Another group showed that overexpression of BiP modulated prion propagation *in vitro* and in animal models [339]. Thus, the manipulation of cellular QC mechanisms could be a potential strategy for interfering in prion conversion, by ensuring that only correctly folded PrP^{C} reach the plasma membrane, which is less prone to prion conversion. Additionally, it has been reported that ERp57 has a protective effect *in vitro* against prion toxicity and regulates the expression and maturation of PrP^{C} in cells [328, 342].

In this study, we investigated the role of overexpression of proteins involved in folding (ERp57) and secretory protein cargo transport (VIP36) on prion conversion. In persistently prion-

infected cells, we found a significant reduction of PrP^{Sc} following overexpression. We used both stable and transient overexpression systems, different cell types and different prion strains to assess the effect on prion propagation. Moreover, when ERp57 or VIP36 overexpressing non-infected cells were infected with prions, we found the overexpressing cells were less susceptible to prion infection. Additionally, ERp57 overexpressing cells showed a reduced susceptibility to induction of ER stress. These results provide strong evidence towards the role of QC in prion infection. Together with our preliminary *in vivo* data, this suggests that ERp57 and VIP36 could be promising targets against prion infection. Thus, the manipulation of the protein QC mechanisms could lead to reduced PrP^{Sc} conversion.

2.3. Experimental procedure

2.3.1. Reagents and Antibodies

Proteinase K (PK) and Pefabloc (PK inhibitor) was purchased from Roche (Germany), and Lipofectamine LTX plus reagent from Invitrogen (USA). If not otherwise stated, all other reagents and chemicals were obtained from Sigma Aldrich. Primary antibodies were purchased as follows: anti-HA (Abcam, USA), anti-myc (Millipore EMD, USA), anti-BiP (Santa Cruz Biotechnology, USA), anti-CHOP (Santa Cruz Biotechnology, USA), and anti-β-actin (Sigma Aldrich, USA). The anti-PrP monoclonal antibody (mAb) 4H11 has been previously described [373]. Peroxidase-conjugated secondary antibodies were from Jackson ImmunoResearch/USA (goat anti-mouse horseradish peroxidase (HRP) and goat anti-rabbit HRP).

2.3.2. Maintenance of cell culture

The mouse neuroblastoma cell line N2a was purchased from ATCC (CCL-131) and was maintained in OptiMEM Glutamax medium (GIBCO, USA) containing 10% fetal bovine serum (FBS) (Sigma, USA), and penicillin/streptomycin in a 5% CO_2 atmosphere. Mouse embryonic fibroblasts (MEF) are immortalized fibroblasts obtained from Dr. N. Mizushima (Tokyo Medical and Dental University, Japan). MEF cell line was maintained in DMEM glutamax (GIBCO, USA) containing 10% FBS (Sigma, USA). Human embryonic kidney (HEK) cells for lentiviral transduction were purchased from Invitrogen (Karlsruhe, Germany). HEK cell line was maintained in DMEM glutamax (GIBCO, USA) containing 10% FBS (Sigma, USA).

2.3.3. Ethics statement

All animal experiments were performed strictly following the Canadian Council for Animal Care (CCAC) guidelines and were approved by the University of Calgary Health Sciences Animal Care Committee (HSACC). The experiments involving the propagation of 22L prions in C57Bl/6 mice (obtained from Charles River Laboratories, USA) were approved under protocol number AC14-0025. Studies involving prion infection and application of recombinant lentiviruses were approved under protocol number AC13-0215.

2.3.4. Primary prion infection

The mouse-adapted scrapie strain 22L was used. This prion strain was propagated in C57Bl/6 mice. To prepare brain homogenates (BH), brains were homogenized in PBS at a final concentration of 10 % (w/v) and stored at -80^{o}C. For primary prion infection of cells, 1 x 10^6 cells were seeded in a 6-cm culture dish. After 24 hour (h), culture medium was removed and cells were

overlaid with 1% BH in appropriate serum-free culture medium (900 µl). After 5 h incubation, 1 ml complete culture medium was added. Medium was removed 24 h later and cells were washed once with PBS before fresh culture medium was added to the cells. For detection of PrP^{Sc} upon primary prion infection, cells were lysed and an aliquot of the cell lysate was subjected to PK-digestion and immunoblot analysis.

2.3.5. Transient transfection with plasmid

Lipofectamine LTX was used for all plasmid transfection experiments according to the manufacturer's protocol. Briefly, cells were plated in 6-cm plates for each experiment at a density of 3 x 10^5. Plasmid and Lipofectamine plus reagent plus Optimum medium were mixed and incubated for 5 min, then added to (LTX reagent+ Optimum medium) and kept for 15 mins at room temperature (RT). This solution was added stepwise to cells and gently mixed. Cells were incubated at 37ºC overnight, and the medium was replaced by fresh complete medium. After 48 h, second transfection was done. After 96 h post first transfection, cells were lysed and processed for immunoblot analysis. The following plasmids has been used control, ERp57 and VIP36 respectively: pCDH-CMV-MCS-puro-TA-GFP (Clontech Laboratories, Inc., USA), pCDH-CMV-ERp57-puro-TA-GFP, and pCDH-CMV-VIP36-puro-TA-GFP.

2.3.6. Lentiviral transduction of cells

For stable overexpression of ERp57 and VIP36, expression vector pCDH (dual promoter) was purchased from (Clontech Laboratories, Inc., USA), envelope vector pMD2.G, and packaging vector psPAX2 for producing lentiviral particles were purchased from Addgene (www.addgene.org). For production of recombinant lentiviruses, HEK293FT cells were co-

transfected with lentiviral envelope vector, lentiviral packaging vector and either the lentiviral plasmid ERp57 or VIP36 using Lipofectamine LTX transfection reagent (according to manufacturer´s direction). Medium of HEK293FT cells containing lentiviral particles was filtered (0.45 µm) to remove cellular debris and used for transduction of recipient cells. For lentiviral transduction of N2a/ScN2a-22L cells, 5 x 10^4 cells were plated in a 12-well culture dish. For N2a cells, cells were incubated next day with 4 µg/ml polybrene solution (Sigma, Munich) for 30 min before exposure to 1 ml medium containing lentiviral particles overnight. For ScN2a-22L cells, virus was directly added without polybrene treatment. Then, cells were cultivated further in normal culture medium. The efficacy of lentiviral gene transfer was detected by analyzing GFP expression by fluorescence microscopy followed by puromycin selection.

2.3.7. Proteinase K (PK) digestion and Immunoblotting

Immunoblot analysis was done as previously described [374]. Briefly, confluent cells were lysed in cold lysis buffer (10 mM Tris-HCl, pH 7.5; 100 mM NaCl; 10 mM EDTA; 0.5% Triton X-100; 0.5% sodium deoxycholate (DOC)) for 10 mins. Aliquots of lysates were incubated with PK for 30 mins at 37 °C. Proteinase inhibitors (0.5 mM Pefabloc) was used to stop PK and samples were directly precipitated with methanol. For samples without PK treatment, pefabloc was added directly and samples were precipitated with methanol. Precipitated proteins were resuspended in TNE buffer (50 mM Tris-HCl pH 7.5; 150 mM NaCl; 5 mM EDTA). Samples were run on 12.5% SDS-PAGE (10.5% gel for ER stress markers), electroblotted on Amersham Hybond P 0.45 PVDF membranes (Amersham, USA) and analyzed in immunoblot, using Luminata Western Chemiluminescent horseradish peroxidase (HRP) Substrates (Millipore, USA). The densitometric analysis of immunoblots was done using ImageJ software.

2.3.8. Real-time quacking-induced conversion assay (RT-QuIC)

A. Preparation of recombinant protein

Recombinant prion protein was prepared as described [375]. Briefly, mouse PrP (amino acids 23-231) was produced using transformed bacteria cultured in LB media using the Overnight Express Autoinduction System (Novagen, USA) to induce protein expression. Inclusion bodies were isolated from pelleted cells using Bug Buster Master Mix (Novagen, USA) and stored at -20 °C. For purification of recombinant PrP, inclusion bodies were solubilized in (8 M guanidine-HCl, 100 mM Na-phosphate, 10 mM Tris-HCl, pH 8.0), centrifuged at 16,000 x g for 5 min, and the supernatant was added to the pre-incubated Ni-NTA Superflow resin beads (Quiagen, USA) in denaturing buffer (6 M guanidine-HCl, 100 mM Na-phosphate, pH 8.0) for 1 h at RT. Beads were then packed into a XK16 glass column (GE Healthcare Life Sciences; USA; length 200 mm). Using an Amersham ÄKTA Explorer FPLC unit running with Unicorn software (5 version, GE Healthcare Life Sciences, USA), protein was refolded by a gradient from 100% denaturing buffer to 100% refolding buffer (100 mM Na-phosphate, 10 mM Tris-HCl, pH 8.0) over 4 h. The column was washed for 30 min with refolding buffer and proteins eluted using a linear gradient from 100% refolding buffer to 100% elution buffer (500 mM imidazole, 100 mM Na-phosphate, 10 mM Tris-HCl, pH 5.8). The central portions of the A280 UV peak were collected into dialysis buffer (10 mM Na-phosphate, pH 5.8). Purified protein was filtered using a 0.22 µm filter, transferred into a Slide-A-Lyzer dialysis cassette (MW 10 kDa; Thermo- Scientific, USA) for dialysis. The dialyzed protein concentration was measured using BCA protein assay (Thermo-Scientific, USA), the solution aliquoted and kept in -80°C until use.

B. RT-QuIC assay

The Real-time Quaking Induced Conversion assay was set up as described previously [376]. Briefly, 98µl of master mix containing 20 mM Na-phosphate, pH 7.4, 300 mM NaCl, 1 mM EDTA, 10 µM Thioflavin T (ThT) and 0.1 mg/ml rPrP substrate were added to each well of a black-walled 96-well optical bottom plate (Nalge Nunc International, Nunc, USA). The seeds were prepared by tenfold serial dilutions of BH or cell homogenate in seed dilution buffer. 2 µl of seed in each dilution were added to wells in quadruplicate reactions. Plates were sealed with Nunc Amplification Tape (Nalge Nunc International) and incubated in a FLUOstar Omega (BMG Labtech, Cary, NC, USA) plate reader for 50 h at 42°C. The 1 min shaking (700 revolutions per min) and 1 min rest cycle was adopted throughout the incubation. ThT fluorescence measurements (450 nm excitation and 480 nm emission) were taken every 15 mins and the average from four replicate wells were calculated and plotted against reaction time.

2.3.9. Immunofluorescence

ScN2a-22L cells at 80-90% confluency were fixed in 4% paraformaldehyde for 30 mins at room temperature (RT), followed by quenching in 50mM NH_4Cl, 20mM Glycine at RT for 10 mins. Cells were then permeabilized in PBS containing 5% FBS and 0.5% Triton X-100 (PBST) for 30 mins before incubation of 6M GnHCl at RT for 8 mins to denature cellular prion. Cells were incubated with anti-PrP mAb 4H11 at 1:100 diluted into PBST for overnight at 4ºC, secondary antibody Cy3 goat anti-mouse (Jackson Immunoresearch/USA) were used at 1:200 to visualize the immunostaining signal. All quantitative images were captured under the 63* oil lens at the same acquisition settings from Zeiss LSM 700 confocal microscope. The overall immunofluorescence intensity of PrP^{Sc} from an image was measured from ImageJ software after the background was

filtered by the same threshold applied to the same series images. Overall intensity was divided by the number of the cells obtained from the same image quantified by ImageJ “analyze particle” command to calculate the averaged immunofluorescence intensity per cell.

2.3.10. Detergent solubility assay

The detergent solubility assay was done as previously mentioned [338]. Briefly, 0.5 mM Pefabloc and N-lauryl sarcosine (sarcosyl) at final concentration of 1% were added to the post-nuclear cell lysates. The solution was then centrifuged at 4 °C for 1 h at 100,000 × g using a Beckman TL-100 centrifuge. The supernatant fraction was collected and precipitated with methanol and the pellet was resuspended in sample loading buffer (7% SDS, 30% glycerin, 20% β-mercaptoethanol, 0.01% bromphenol blue in 90 mM Tris-HCl, pH 6.8) for immunoblotting. Both the supernatant and pellet fractions were analyzed in SDS-PAGE.

2.3.11. Mouse bioassay

Five weeks old female FVB mice (obtained from Charles River Laboratories, USA) were inoculated under anaesthesia in the right parietal lobe with 20 µl of 1% BH from terminally sick mice inoculated with prion strain 22L. For the intracerebral inoculation 25 gauge disposable needles were used. After inoculation mice were checked daily for any adverse condition. Fifty days after prion inoculation, animals were inoculated similarly in the right parietal lobe with 20 µl of recombinant lentiviruses (ERp57 or VIP36) with a titer of 2×10^6 IU/animal. Control group (CT) received control virus. The animals were monitored daily for progression of prion infection after the clinical signs started in animals. At the terminal stage of disease, animals were

anaesthetized followed by euthanasia using CO_2 overdosing. The survival time of each animal was recorded.

2.3.12. Statistical analysis

Statistical analysis was performed using GraphPad Prism (GraphPad Software, USA v 7.03) using Mann-Whitney test for pair-wise comparisons between control and treated groups. Statistical significance for all the immunoblots was expressed as (mean ± SEM). For survival, the percent survival was plotted in a Kaplan–Meier plot and Log-rank (Mantel-Cox) test was performed for statistical difference between groups *: $p \leq 0.05$, **: $p \leq 0.01$, ***: $p \leq 0.001$ considered significant.

2.4. Results

2.4.1. Stable overexpression of ERp57 or VIP36 reduces PrP^{Sc} in prion-infected neuroblastoma cells

To investigate the role of ERp57 and VIP36 in prion replication, we stably overexpressed ERp57 or VIP36 in N2a cells persistently infected with mouse-adapted scrapie prion strain 22L (ScN2a-22L) using lentiviral gene integration technique. ScN2a-22L cells were transduced with lentiviruses which integrated genes encoding ERp57 (HA-tagged) or VIP36 (myc-tagged) into the host genome allowing stable overexpression of genes. Transduced cells were selected using puromycin. When non-virally transduced cells were subjected to puromycin selection as control, all cells were susceptible to puromycin treatment. As lentiviral transduction resulted in expression of GFP along with the target gene (dual promoter construct), the successful transduction and selection of cells was confirmed by investigating GFP auto-fluorescence in fluorescence microscopy and target protein expression in immunoblot. The transduced cells were passaged, at

each passage cells were lysed, and lysates subjected to PK digestion and immunoblotting. Upon overexpression of ERp57, we found a significant reduction of PrP^{Sc} in the first passage as compared to control cells transduced with mock virus (Fig. 2.1 A and D). This reduction of PrP^{Sc} was present also in passages two and three (Fig. 2.1 B, E, C and F). Moreover, VIP36 overexpression significantly reduced PrP^{Sc} as shown in Fig 2.1. Exogenous overexpression of ERp57, tagged with HA, and VIP36, tagged with c-myc, was confirmed using anti-tag antibodies in immunoblot analysis.

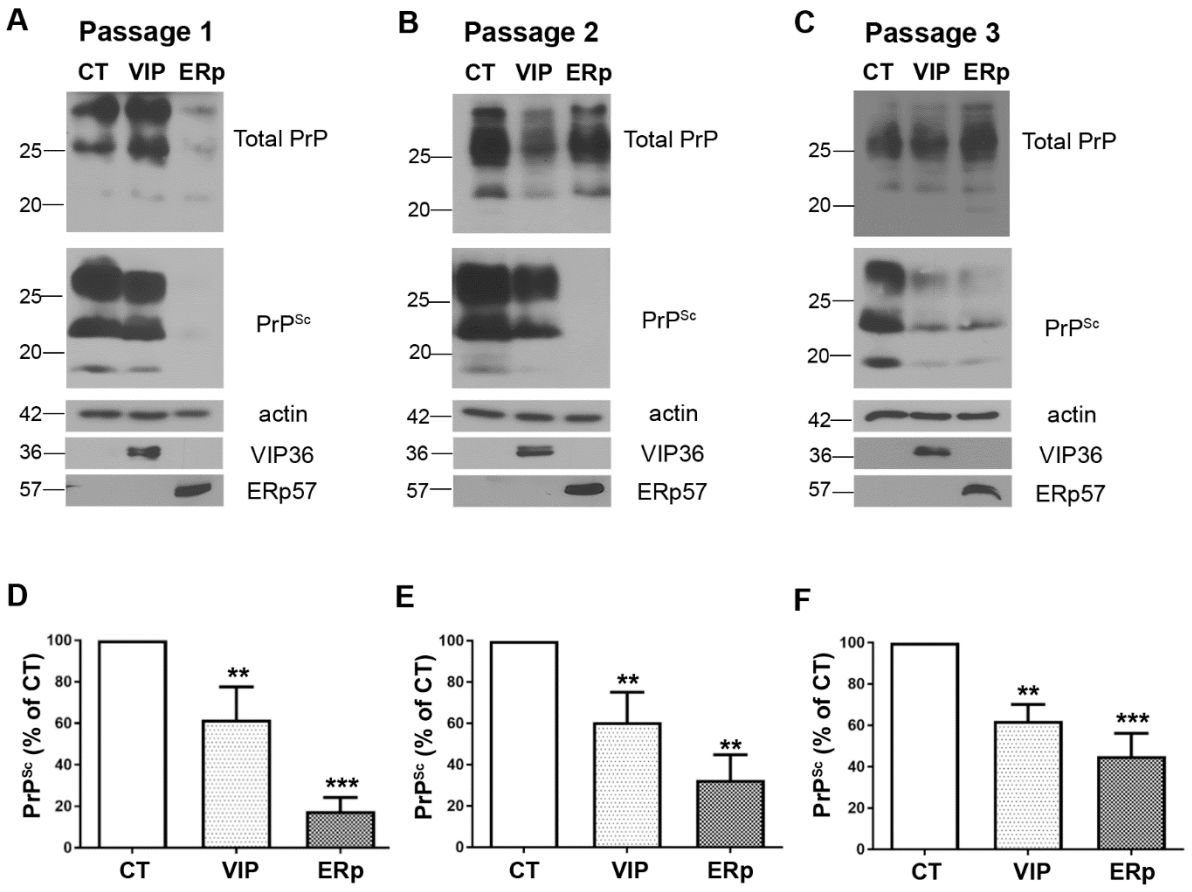

Figure 2. 1. Stable overexpression of VIP36 or ERp57 reduces PrP^{Sc} in prion-infected cells. ScN2a-22L cells were stably transduced with recombinant lentiviruses to overexpress either VIP36 or ERp57, or control GFP virus (CT). Cells were then passaged and lysed at passage 1, 2 and 3. Cell lysates were subjected to PK digestion (+PK), or not (-PK), to distinguish total PrP and PrP^{Sc}. The PrP amount analyzed by immunoblot using anti-PrP mAb 4H11. Overexpression of VIP36 and ERp57 was detected by staining with anti-HA and anti-myc antibody for exogenous ERp57 and VIP36, respectively, as shown in lower panels indicating successful transduction. Actin was used as a loading control. (A) Representative immunoblots showing the reduction of PrP^{Sc} in the first passage, (B) second passage and (C) third passage. (D) Densitometric analysis showing the amount of PrP^{Sc} in the first passage normalized by actin amount, and shown as a percentage of

control using Image J. (E) Densitometric analysis for the second passage, (F) densitometric analysis for the third passage. Data represent mean ± SEM (n=5-8). ** represents $p \leq 0.01$, *** represents $p \leq 0.001$.

Moreover, we tested cells for prion seeding activity using RT-QuIC assay. In this test, recombinant PrP substrate is converted into ThT-binding aggregates in the presence of prion seeds. Mouse rPrP was used as substrate and cell lysates in dilutions from 10^{-1} to 10^{-4} served as seed in RT-QuIC, as described previously [113]. We found a reduced prion seeding activity in cell lysates of ERp57 or VIP36 overexpressing cells compared to that of control cells (10^{-2} dilution shown) (Fig. 2.2 A and B). At passage 3, we found less seeding activity of cell lysates from ERp57 overexpressing cells (Fig. 2.2 C).

To validate immunoblot results further, we used immunofluorescence microscopy for semi-quantitative detection of PrP^{Sc} in cells. Immunofluorescence analysis involving pre-treatment with guanidine salts for epitope retrieval is widely used for specific detection of PrP^{Sc} [377]. Cells in passage three were subjected to this immunofluorescence analysis after treatment with 6M guanidine hydrochloride (GdnHCl) for PrP^{Sc}, using anti-PrP mAb 4H11 and Cy3 goat anti-mouse as primary and secondary antibodies, respectively. The mean immunofluorescence intensity per cell in PrP^{Sc} immunostaining was compared among transduction groups. Non-infected cells were used as negative control, and to eliminate background staining. Confocal microscopy analysis confirmed the reduction of PrP^{Sc} in ERp57 or VIP36 overexpressing cells (Fig. 2.2 D and E**)**.

Taken together, these data show that stable overexpression of ERp57 or VIP36 in persistently prion-infected cells reduces PrP^{Sc} and prion conversion activity.

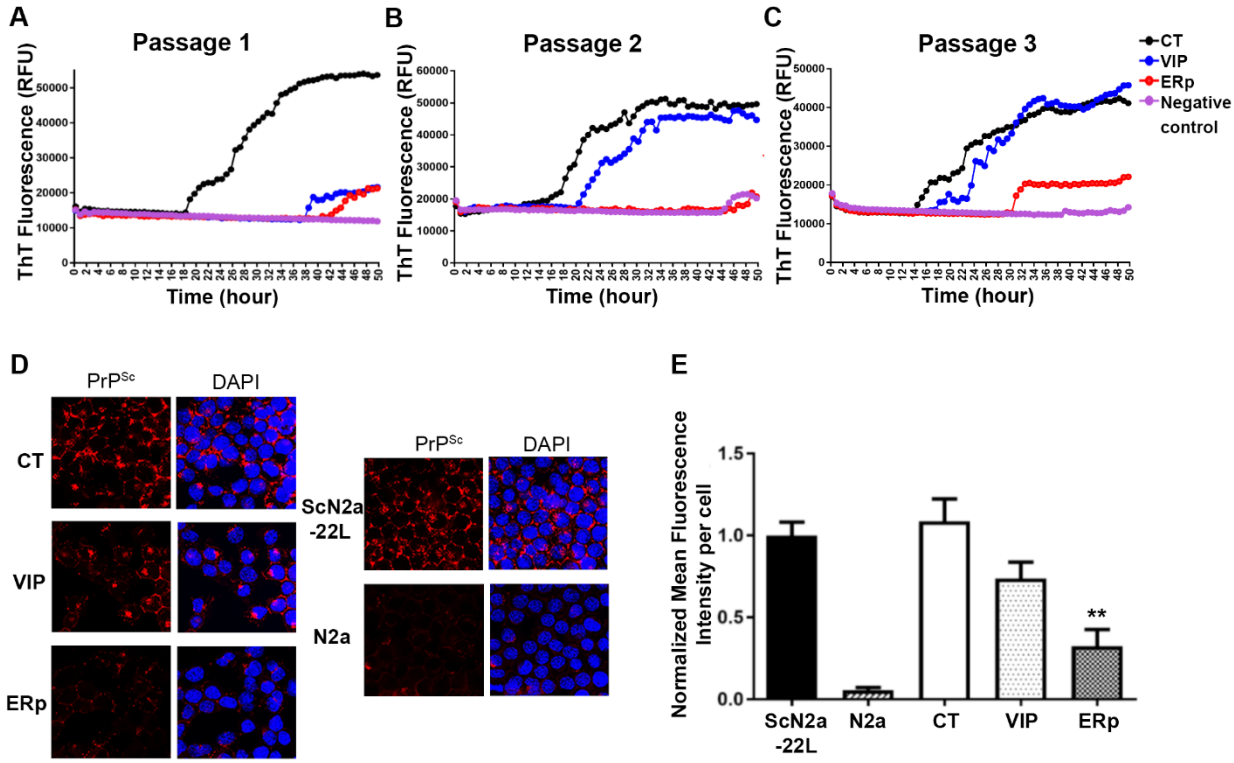

Figure 2.2. RT-QuIC analysis shows reduced prion seeding activity in VIP36 or ERp57 overexpressing prion-infected cells. ScN2a-22L cells were transduced with lentiviruses to stably overexpress VIP36 or ERp57, or control GFP virus (CT). Cells were then passaged and lysed in passages 1, 2, and 3. At each passage, cell lysates were collected and RT-QuIC analysis was performed. The y-axis shows relative ThT fluorescence units (RFU), the x-axis time in hours. N2a cell lysate was used as a negative control. The seeding activity at 10^{-2} dilution was analyzed to compare between the groups. (A) RT-QuIC analysis is shown for passage 1, (B) for passage 2, and (C) for passage 3. (D) ScN2a-22L cells stably overexpressing VIP36 or ERp57 were subjected to 6M guanidine treatment and PrP^{Sc} was stained with anti-PrP mAb 4H11 (left panels). Right panels show DAPI merge. N2a cells were used as negative control, non-transduced and control-transduced (CT) cells as positive control. Confocal microscopy revealed the PrP^{Sc} amount in cells

and (E) the mean fluorescence intensity per cell was quantified to analyse the amount of PrP^{Sc} for each group using ImageJ. ** represents $p \leq 0.01$.

2.4.2. Transient overexpression of ERp57 or VIP36 decreases PrP^{Sc} accumulation in cultured cells infected with different prion strains

Next we wanted to investigate whether the inhibitory effect of overexpression of selected molecules on prion propagation is cell type and prion strain specific. We transiently transfected ScN2a-22L, and MEF cells infected with RML or Me7 prions (ScMEF-RML and ScMEF-Me7, respectively) with plasmids expressing ERp57 or VIP36 using lipofectamine LTX plus reagent. Cells were consecutively transfected, with a 48 h interval, and lysed 96 h after first transfection. Lysates were treated with proteinase K (+ PK) and analysed in immunoblot. These studies showed that ERp57 overexpression decreased significantly PrP^{Sc} amounts in ScN2a-22L and ScMEF-Me7 cells (Fig. 2.3 A and D; Fig. 2.3 C and F). However, this effect was not significant in ScMEF-RML cells (Fig. 2.3 B, E). Similarly, VIP36 overexpression resulted in significant reduction of PrP^{Sc} in cell populations analyzed except ScMEF-RML cells (Fig. 2.3 B and E).

This data shows that overexpression of ERp57 and VIP36 reduces PrP^{Sc} in various cell types infected with different prion strains.

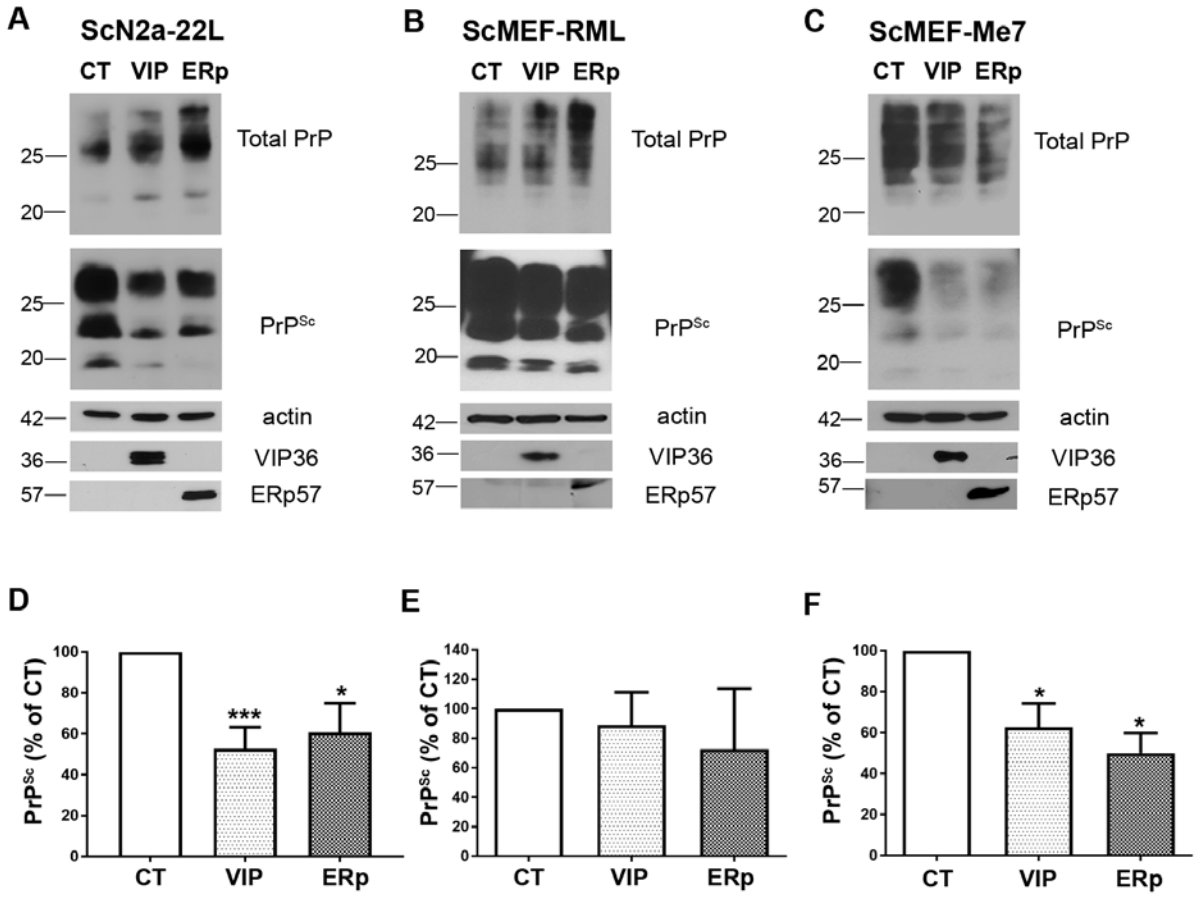

Figure 2. 3. Transient overexpression of VIP36 and ERp57 decreases PrP^{Sc} in prion-infected cells. Persistently prion-infected ScN2a-22L, ScMEF-RML, and ScMEF-Me7 cells were transfected twice with VIP36 or ERp57, or control construct, for 48 h each, and cells were lysed 96 h after first transfection. The cell lysates were then subjected to PK digestion (or not; -PK) and the amount of total PrP (-PK) and PrP^{Sc} (+PK) was investigated using immunoblotting (anti-PrP mAb 4H11). Representative immunoblots are shown for (A) ScN2a-22L cells, (B) ScMEF-RML, and (C) ScMEF-Me7 cells. Actin was used as a loading control. Transfection was confirmed by detecting the overexpression of VIP36 and ERp57 using anti-HA and anti-myc antibodies for ERp57 and VIP36, respectively, as shown in the lower panels. (D-F) Densitometric analysis showing the amount of PrP^{Sc} presented as percentage of control normalized by actin shown as

mean ± SEM in (D) ScN2a-22L (n=7), (E) ScMEF-RML (n=3), and (F) ScMEF-Me7 (n=4) cells. * represents $p \leq 0.05$ and *** represents $p \leq 0.001$.

2.4.3. Stable and transient overexpression of ERp57 results in increased levels of PrP^C in neuroblastoma cells

The previous results had shown that overexpression of the ER QC proteins ERp57 or VIP36 prevented prion propagation *in vitro* and decreased PrP^{Sc} levels. One explanation for this is that such overexpression might modulate the levels of PrP^C, which resides in the secretory pathway. A PrP^C reduction, for example, would in turn impede PrP^{Sc} propagation. Indeed, previous studies have already shown that ERp57 plays a regulatory role in the expression of PrP^C and that ERp57 overexpression increases PrP^C levels [328]. To investigate the role of ERp57 and VIP36 overexpression on PrP^C, we transiently transfected N2a cells with plasmids encoding ERp57 or VIP36. 48 h after transfection cells were lysed and lysates subjected to immunoblot analysis. ERp57 overexpressing cells showed increased amounts of PrP^C compared to control cells (Fig. 2.4 A and B). Next, stably transduced N2a cells overexpressing ERp57 or VIP36 were analyzed. Again, we found that overexpression of ERp57 significantly increased the amount of PrP^C (Fig 2.4 C and D). In contrast, VIP36 had no or little effect on PrP^C levels (Fig. 2.4). These data suggest that the reduction of PrP^{Sc} due to ERp57 or VIP36 overexpression was not due to a reduction in PrP^C levels. Moreover, qPCR data suggested that the PrP mRNA expression was unchanged in overexpressing cells as compared to control cells (data not shown). It is conceivable that overexpression helped in generating PrP^C of good quality on the cell membrane, less prone to prion conversion as described previously by us for overexpression of other QC proteins [338].

Taken together, these data clearly indicate that the decrease in PrP^{Sc} upon ERp57 or VIP36 overexpression in prion-infected cells is not due to a reduction of total levels of PrP^{C}.

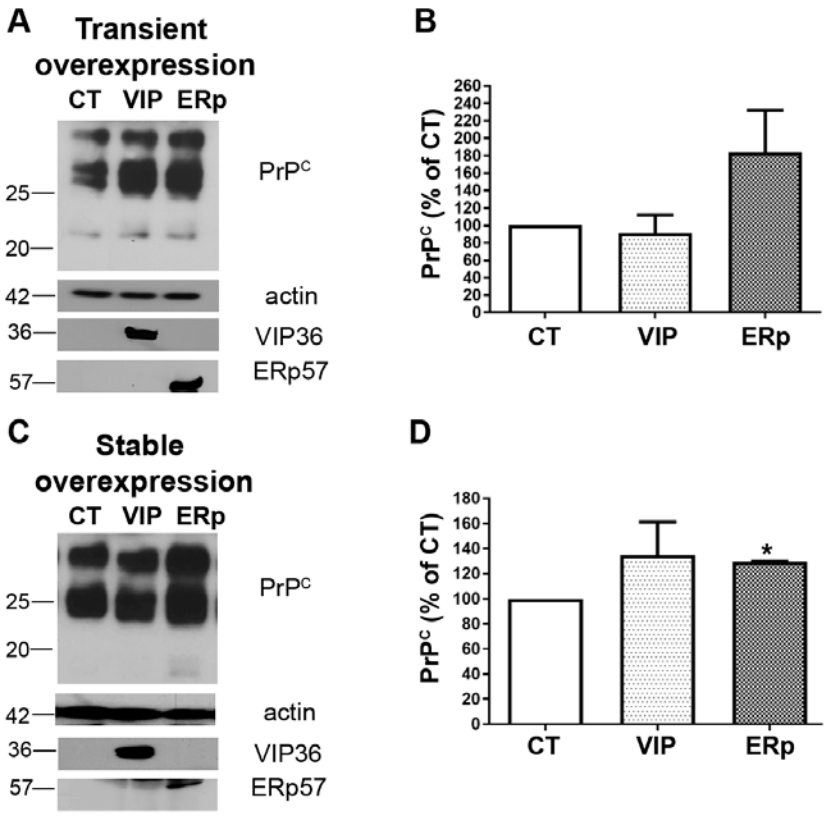

Figure 2. 4. ERp57 overexpression increases PrP^{C} expression in N2a cells. (A) N2a cells were transiently transfected with VIP36 and ERp57, or a control construct, for 48 h. Cells were then lysed and the post-nuclear lysates were used for quantifying the amount of PrP^{C} in immunblot analysis. Actin was used as a loading control and transfection was confirmed with anti-HA and anti-myc antibodies for detection of tagged ERp57 and VIP36, respectively. (B) Densitometric analysis of PrP^{C} expression represented as percentage of control. Data represent mean ± SEM (n=5). (C-D) N2a cells stably overexpressing VIP36 and ERp57, or control cells, were lysed at

passage 1 and immunoblotting was done for analysing amounts of PrP^{C} in post-nuclear lysates as above. (D) shows densitometric analysis (n=3). * represents $p \leq 0.05$.

2.4.4. ERp57 and VIP36 overexpression decrease susceptibility of cells to prion infection

Above results showed that overexpression of selected QC proteins counteracted prion propagation in cells already infected with prions. This was in line with previous studies by us and others using overexpression of QC proteins such as ERGIC-53, EDEM3 and BiP in persistently prion-infected cells [338, 339]. Next, we wanted to know whether this effect also exists in *de novo* prion infection. To investigate the impact of overexpression on susceptibility of cells to prion infection, we overexpressed ERp57 or VIP36 in uninfected N2a cells and then infected cells with BH from terminally prion-sick mice. Aliquots of cells were lysed at each passage, and lysates subjected to immunoblot analysis for PrP (+/- PK) and to RT-QuIC assay for testing seeding activity. Interestingly, we found that ERp57 overexpressing cells harbored less PrP^{Sc} in immunoblot and less seeding activity in RT-QuIC when compared with controls (Fig. 2.5). This finding was consistent until passage 5 (Fig. 2.5 C and F). Although VIP36 overexpressing cells showed minor difference in amount of PrP^{Sc} in immunoblot in this situation than controls (Fig. 2.5 A-C), their prion seeding activity was reduced compared to controls in RT-QuIC analysis (Fig. 2.5 G and H).

In summary, these results suggest that overexpression of ERp57 and VIP36 protects cells in *de novo* prion infection and reduces susceptibility to cellular prion infection.

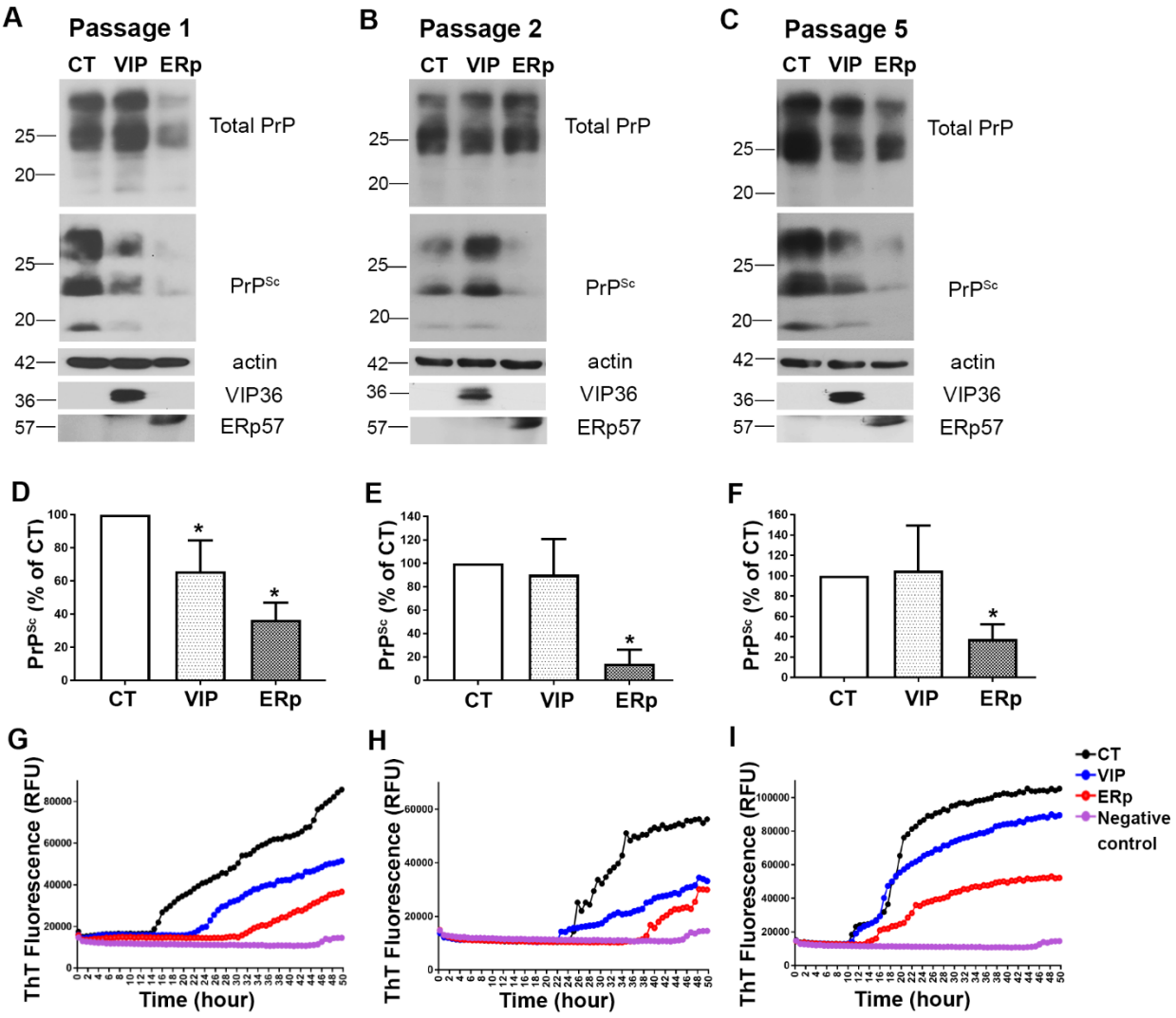

Figure 2. 5. ERp57 overexpression reduces *de novo* prion infection in cells (acute infection). Uninfected N2a cells stably overexpressing VIP36 or ERp57, or control cells (CT), were infected with 1% brain homogenate of terminally-ill 22L-infected mice. Cells were passaged and lysed at passage 1 (A) (at first splitting after infection), (B) passage 2 and (C) passage 5. The post-nuclear lysates were subjected to PK digestion, or not, to assess newly formed PrP^{Sc} in each passage. Actin was used as loading control and expression of exogenous ERp57 and VIP36 was confirmed by utilizing anti-HA and anti-myc antibodies respectively. (D-F) The densitometric analysis showing

amount of PrP^{Sc} normalized by amount of actin and expressed as a percentage of control at passage 1 (D), 2 (E) and 5 (F) (n=3-4). RT-QuIC assay was done at passage 1 (G), 2 (H) and 5 (I), using the post-nuclear lysates as seed. The seeding activity at 10^{-2} dilution was used for comparative analysis. The y-axis shows relative ThT fluorescence units, the x-axis time in hour. N2a cell lysate was used as negative control. * represents $p \leq 0.05$.

2.4.5. Overexpression of quality control proteins prevents ER stress-induced accumulation of PrP aggregates

The overexpression of ERp57 or VIP36 was successful in reducing prion infection in persistently and newly prion infected neuronal and non-neuronal cells. However, the molecular mechanisms underlying this process had to be determined. Our previous studies had suggested that ER stress caused by accumulation of misfolded proteins resulted in a deterioration in the quality of the PrP^{C} pool, PrP aggregate formation, and increased prion propagation in infected cells [338]. Consequently, we wanted to investigate whether overexpression of ERp57 or VIP36, both components of the protein QC pathway, can be beneficial in ER stress situations. We therefore transfected N2a cells with plasmids encoding ERp57, VIP36, or control constructs. After 48 h of transfection the cells were treated with tunicamycin (2.5 µg/ml) for 16 h. Tunicamycin is an ER stress inducer which inhibits the N-glycosylation during glycoprotein synthesis in the ER by blocking UDP-N-acetylglucosamine-dolichol phosphate N-acetylglucosamine-1-phosphate transferase [378]. Cells were then lysed and the post-nuclear lysates subjected to a detergent solubility assay as described previously [338]. Supernatant and pellet fractions were analysed for PrP amounts in immunoblot. ERp57 or VIP36 overexpressing cells significantly overcame ER stress induced in the cells as compared to control cells by expressing lower levels of aggregated

PrP in the pellet fraction (Fig. 2.6 A and C). Similarly, we treated cells stably overexpressing ERp57 or VIP36 with tunicamycin for 16 h after 72 h of plating, and then subjected post-nuclear lysates to the detergent solubility assay. PrP aggregate formation in ERp57 and VIP36 overexpressing cells was significantly reduced in the pellet fraction as compared to control cells (Fig. 2.6 B and D).

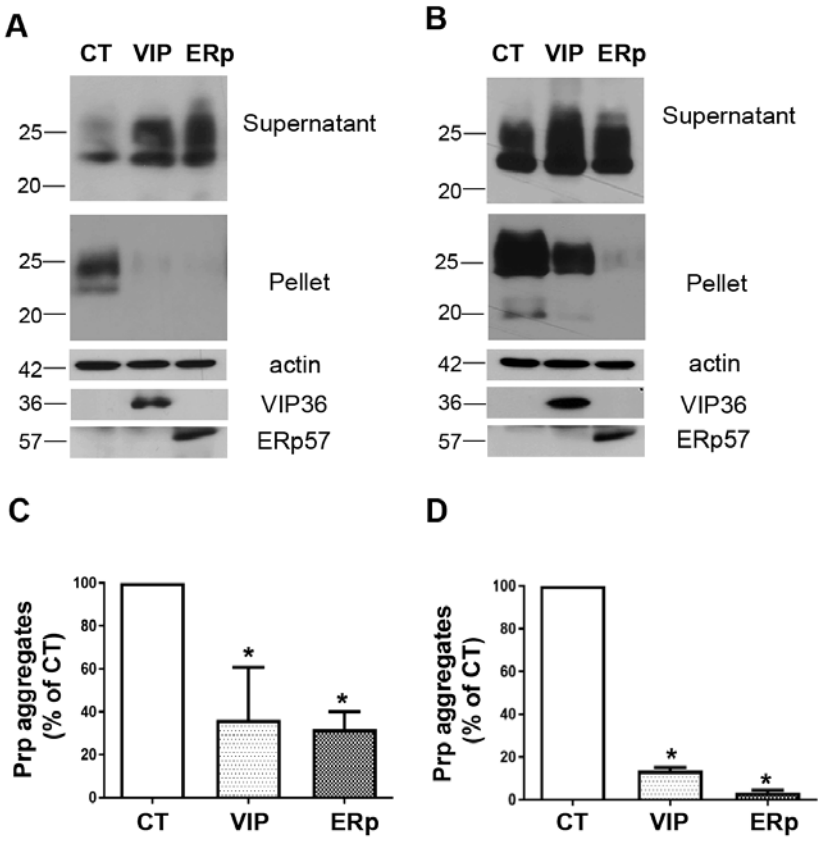

Figure 2. 6. ERp57 or VIP36 overexpression reduces PrP aggregates in cells. (A, C) N2a cells transiently overexpressing ERp57 or VIP36, or cells transfected with control plasmid (CT), were treated with tunicamycin (2.5µg/ml) after 48 h post-transfection for 16 h to induce ER stress in the cells. The cells were lysed and subjected to a detergent solubility assay. The post-nuclear lysates

were ultracentrifuged at 100,000 x g for 1 hour at 4^{o}C in the presence of 1% sarcosyl. The supernatant and pellet fractions were tested in immunoblotting for PrP (pellet and supernatant), actin and transgene expression (supernatant fraction only). (A) Representative immunoblot showing PrP distribution in pellet and supernatant fractions. (C) Densitometric analysis indicating PrP aggregates represented as percentage of control (n=3). (B, D) Induction of ER stress in stably overexpressing N2a cells at passage 2 post-transduction. Similar analysis as in (A); tunicamycin treatment was for 16 h after 72 h of plating the cells. Representative immunoblot are shown in (B) and densitometric analysis (n=3) is depicted in (D). ** represents $p \leq 0.01$.

Furthermore, we looked into ER stress markers in overexpressing cells after inducing ER stress, to delineate whether the overexpression of ERp57 and VIP36 has any effect on ER stress. As before, we transfected N2a cells with ERp57, VIP36 or control plasmids. After 48 h of transfection the cells were treated with tunicamycin. The cells were then lysed at 10, 12 and 16 h post-treatment with tunicamycin. Immunoblotting was done for ER stress markers such as BiP and CHOP (Fig. 2.7). ERp57 overexpressing cells significantly overcame ER stress induced in the cells as compared to control cells, as evidenced by lower level expression of ER stress markers, CHOP and BiP (Fig. 2.7). We found a statistically significant reduction of BiP in ERp57 overexpressing cells at 10 and 12 h post-treatment, but not at 16 h. ER stress mediated CHOP expression was delayed in ERp57 overexpressing cells at all 3 time points (10, 12 and 16 h), compared to control cells (Fig. 2.7 A, B, E, F, I, and J). VIP36 overexpression did not significantly lower the expression of ER stress markers BiP and CHOP when compared to control cells at both 10 and 12 h post-treatment, however, it significantly lowered CHOP expression at 16 h post-treatment.

Taken together, these data demonstrate that the overexpression of QC proteins like ERp57 and VIP36 has the potential to reduce the accumulation of PrP aggregates in ER stress situations. Furthermore, ER stress itself is diminished. Consequently, the pool of PrP^C amenable for cellular prion conversion is reduced, providing a mechanistic explanation for observing less prion propagation in such cells.

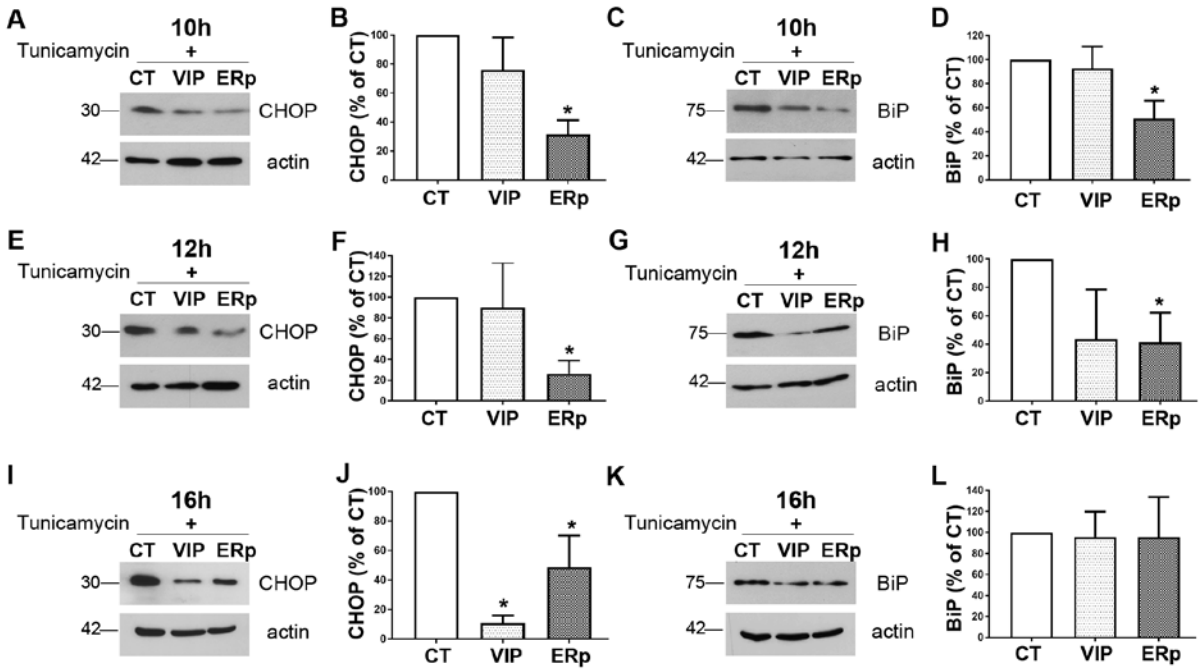

Figure 2. 7. ERp57 overexpression overcomes the ER stress in cells. N2a cells transiently transfected with ERp57 or VIP36, or cells transfected with control plasmid (CT), were treated with tunicamycin (2.5 µg/ml) 48 h after transfection to induce ER stress in the cells. Cells were lysed at 10, 12 and 16 h post starting tunicamycin treatment and cell lysates were analyzed in immunoblotting for ER stress markers BiP and CHOP. (A-B, E-F, and I-J) Representative immunoblots showing the amounts of CHOP expressed upon ER stress induction in cells and densitometric analysis represented as percentage of control (CT) at 10 h (A and B), 12 h (E and F)

and 16 h (I and J). Actin was used as loading control. (C-D, G-H, and K-L) Representative immunoblots showing the amounts of BiP expressed upon ER stress induction in cells and densitometric analysis represented as percentage of control at 10 h (C and D), 12 h (G and H) and 16 h (K and L) (n=3-4). * indicates $p \leq 0.05$.

2.4.6. Application of lentiviruses expressing ERp57 prolongs the survival time of prion-infected mice.

In order to test whether the proof-of-concept obtained in cultured cells can be validated *in vivo*, we applied recombinant lentiviruses expressing ERp57 or VIP36 into the brain of prion-infected mice. Five FVB mice per group were infected intracerebrally with prions. One group received intracerebrally ERp57-expressing virus, one virus expressing VIP36, and the control group received mock virus, all at 50 days post prion inoculation (dpi). ERp57-expressing virus inoculated mice showed statistically significant longer incubation times when compared to controls ($p = 0.0206$, ERp57 vs control group mean survival: 142.6 ± 1.8 vs. 138.8 ± 0.9), as shown in Fig. 2.8. Mice treated with lentivirus expressing VIP36 did not show a statistically significant difference in survival when compared to controls.

Taken together, these data show that application of lentiviruses expressing ERp57 has the potential to prolong the incubation time to clinical prion disease in prion-infected mice, corroborating our data *in vivo*.

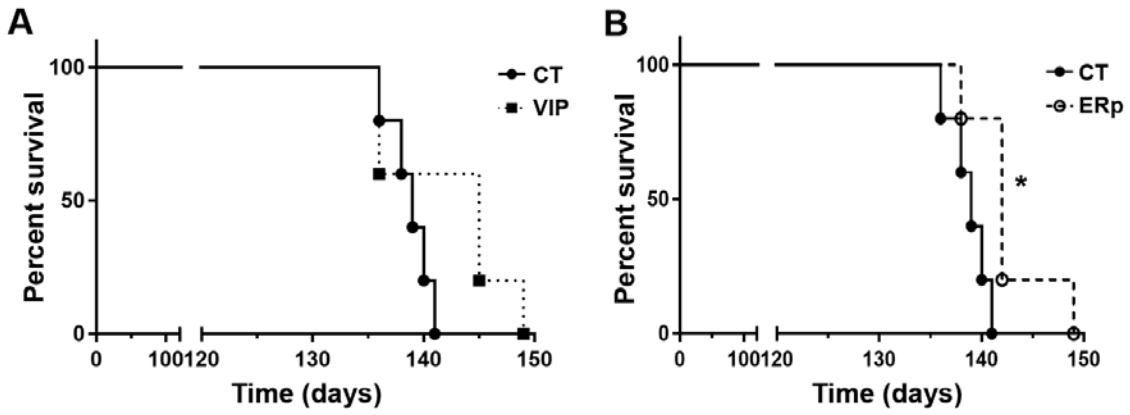

Figure 2. 8. Application of ERp57-expressing lentiviruses increases survival in prion-infected mice. Mice were inoculated intracerebrally with 1% brain homogenate from terminally sick mice infected with 22L prions and at 50 dpi mice were given ERp57 (n=5) or VIP36 (n=5) expressing lentiviruses intracerebrally. Control mice (n=5) were inoculated with mock virus. The animals were monitored for clinical prion disease and the survival of each animal was recorded. (A) Percent survival of control mice (CT) and VIP36 lentivirus-inoculated mice. (B) Percent survival of control mice (CT) and ERp57-lentivirus inoculated mice. * indicates $p \leq 0.05$.

2.5. Discussion

Protein misfolding diseases such as prion disease, Alzheimer's disease (AD), and Parkinson's disease (PD) have been associated with ER stress and activation of the unfolded protein response (UPR) in their pathogenesis [299, 320, 379-381]. The accumulation of misfolded proteins as typical for these diseases and calcium perturbation have been shown to be potential causes for induction of acute and chronic ER stress [322, 382]. Chronic ER stress in cells has been linked to upregulation of signaling pathways, which lead to apoptosis, and result in cell death and neurodegeneration [383, 384]. Several studies including ours have shown that ER stress, expression of selected ER QC molecules, and prion propagation can be interconnected [338, 339,

385]. We have previously demonstrated that detergent insoluble PrP aggregates accumulate in non-infected and infected cells upon ER stress induction, which can lead to increased PrP^{Sc} levels in prion-infected cells [338]. Under such conditions, PrP aggregates appear more prone to prion conversion, as demonstrated by another group utilizing protein misfolding cyclic amplification (PMCA) [326]. Interestingly, our previous work showed that the ER stress-mediated increase in PrP aggregates and in PrP^{Sc} can be reversed by transient overexpression of selected QC molecules such as ERGIC-53 and EDEM3 [338]. Recently, a similar approach has been described for BiP/GRP78, where the overexpression of BiP decreased prion propagation; the downregulation of it resulted in increased PrP^{Sc} levels in the cells and shortened incubation periods in prion-infected mouse models [339]. Other studies suggested that overexpression of ER chaperones such as BiP and calnexin leads to reduction of amyloid beta (Aβ) peptide production, which is involved in the pathogenesis of Alzheimer's disease *in vitro* [386]. Moreover, overexpression of the ER chaperone ERp57 in neurons was protective against toxicity induced in cells by addition of exogenous PrP^{Sc}, and regulated the expression and maturation of PrP^{C} in cells [328, 342]. Additional *in vivo* evidence comes from various studies of prion and other neurodegenerative diseases which show an increase in ER QC molecules including ER chaperones and disulfide isomerases in diseased brains [286, 329, 387-389] .

However, the direct role of these chaperones in prion disease is not fully understood. Based on these studies, we hypothesized that stable overexpression of selected QC molecules will lead to reduced PrP misfolding in the early secretory pathway which in turn will affect the propagation of prions in cells. Here, we describe the effects of overexpression of two selected QC molecules involved in folding (ERp57), and secretory protein cargo transport (VIP36).

2.5.1. Overexpression of ERp57 has anti-prion effects in persistently infected cells, reduces infection in acutely infected cells, and prolongs incubation time in prion-infected mice

ERp57 is one of the disulfide isomerases which along with calnexin and calreticulin help in folding of glycoproteins [390]. ERp57 has been found upregulated in the brain of CJD patients [329]. *In vitro*, ERp57 was neuroprotective against PrP^{Sc}-mediated cellular toxicity [342]. Moreover, axonal regeneration was promoted by ERp57 indicating its potential neuroprotective role [391]. Although it has been suggested as a possible therapeutic target before, its role in prion infection and prion propagation has not been defined yet. We wanted to transiently, and more importantly, stably overexpress ERp57 in already chronically prion-infected cells and assess whether this affects levels of PrP^{Sc}. In addition, we wanted to see whether cells with increased expression of ERp57 are less susceptible to prion infection. To stably overexpress an epitope-tagged ERp57 in persistently prion-infected neuronal cells we used a lentiviral approach. Over several passages upon transduction we found that ERp57 was overexpressed. This was correlated with a significant reduction of PrP^{Sc} up to passage 3, corresponding roughly to 15 days. Although this is consistent with previous studies using transient overexpression of QC proteins such as BiP, ERGIC-53 and EDEM3, we overexpressed such a molecule over longer periods of time in infected cells. It is the first study which addressed whether such prolonged overexpression can interfere with acute prion infection in cultured cells. Our data clearly show that ERp57 overexpressing cells are less susceptible to prion infection, an effect which was still detectable 25 days after infection.

Besides immunoblot for detection of PK-resistant PrP^{Sc}, we used RT-QuIC assay for prion seeding and conversion and PrP^{Sc}-specific confocal microscopy to confirm our results. RT-QuIC is a sensitive *in vitro* technique to detect the ability of PrP^{Sc} seed in prion-infected materials to convert a recombinant PrP^{C} substrate into ThT-positive PrP aggregates in real time [375, 392].

Using this technology, prion conversion activity has been detected in brain materials, cerebrospinal fluid (CSF), urine, feces, blood, saliva and other body fluids and tissues in various species [113, 375, 376, 393]. Moreover, we and others have used RT-QuIC to monitor the anti-prion activity of chemical compounds and anti-PrP antibodies [394, 395]. In this study, we compared the seeding activity of infected cell lysates from overexpressing and control cells. To make an easy and meaningful comparison, our analysis is based on one dilution (10^{-2}) in RT-QuIC, as shown before by a study where a single dilution was used to validate and optimize the factors for improving the assay [396]. In alignment with our immunoblotting and confocal microscopy studies, RT-QuIC data demonstrated a very pronounced reduction of prion seeding activity in ERp57 overexpressing persistently infected cells as compared to that from control cells.

Taken together, our data demonstrate that stable overexpression of ERp57 has the potential to reduce PrP^{Sc} and prion seeding activity in chronically and newly infected cells.

In vivo, local application of lentiviruses expressing ERp57 to the brain at day 50 after prion inoculation extended the survival time of prion-infected mice. Lentivirus-based RNA interference (RNAi) against PrP have been reported to down-regulate PrP expression and to mitigate prion infection [335]. The effect obtained in our study was moderate as the expected area of transgene overexpression is very local due to the non-replicating nature of the used lentiviral vector. As a system for more widespread overexpression adeno-associated virus (AAV) applied intraventricularly [397] could be more efficient in future studies.

2.5.2. Molecular mechanisms underlying the ERp57 effects on prion infection

Net changes in cellular prion infection could be due to effects on the amount and localization of PrP^{C}, on the interaction of PrP^{C} with PrP^{Sc}, or on cellular PrP^{Sc} clearance. Since a

direct interaction of ERp57 with PrP^{Sc}, whose vast majority is found in the endocytic pathway, is very unlikely we favor a direct or indirect effect of ERp57 overexpression on the quality of the PrP^{C} pool eligible for cellular prion conversion. As ERp57 is a QC protein in the early secretory pathway, its effect on proper folding of PrP^{C} could result in less misfolded or better folded PrP which reaches the cellular locale of prion conversion as described by us for ER stress situations [338]. It has been demonstrated already that PrP^{C} and ERp57 can physically interact, not surprising for a glycoprotein and an ER-resident chaperone [328]. Other indirect possibilities would be that this results in less PrP^{C} at the plasma membrane, or that ER stress caused by prion infection or other signaling pathways are involved. As reported in a previous study, ERp57 can regulate PrP expression *in vitro* and *in vivo* [328], in our system we also found that ERp57 overexpression, both transient and stable, resulted in higher PrP^{C} levels in the cells. This result clearly specifies that the decrease in PrP^{Sc} in ERp57 overexpressing prion-infected cells was not due to less PrP^{C} being available for conversion. More likely, the pool of PrP^{C} is less favorable for prion conversion. This might be the reason why we found a lowered susceptibility of ERp57 overexpressing non-infected cells to prion infection.

Our previous studies suggested that ER stress causes deterioration in the quality of PrP^{C} resulting in PrP aggregate formation, followed by enhanced production of PrP^{Sc} in infected cells. We also had found that a transient overexpression of selected QC molecules decreased detergent-insoluble PrP aggregates [338]. To be able to test the effect of transient and stable overexpression of ERp57 on ER stress, we used treatment with tunicamycin as an experimental model. As read-out we focused on PrP aggregate formation and induction of typical ER stress marker proteins. These studies showed that ERp57 overexpressing cells significantly overcame ER stress-mediated

PrP aggregate formation, resulting in less PrP aggregates in the insoluble pellet fraction as compared to control cells.

In contrast to a study where ERp57 was found not to affect the ER stress situation in cells [328], our study also suggested that ERp57 overexpressing cells significantly overcame ER stress induced in the cells. This was illustrated by lower level expression of the stress markers, BiP and CHOP. This discrepancy in the studies might be due to use of different cell lines (mouse embryonic fibroblasts and NSC34 cells in the previous study). We found in our study that after ER stress induction CHOP was reduced in VIP36 and ERp57 overexpressing cells at 16 h post-treatment. Again this might be due to different cell lines and different approaches used. We measured CHOP at the protein level in immunoblot while the previous study looked into mRNA levels.

In summary, our data strongly indicate that overexpression of ERp57 directly affects the pool of PrP which is eligible for cellular prion conversion, resulting in less prion conversion. This also impacts acute prion infection scenarios, making such cells less susceptible to infection. In addition, ERp57 overexpression improves ER stress in compromised cells, providing additive effects.

2.5.3. Anti-prion effects of VIP36 overexpression

VIP36 has not been previously described in the context of prion diseases. We found VIP36 as potential target when screening for QC molecules with anti-prion effects. VIP36 has been shown to have a role in post-ER QC of human α-1 antitrypsin and recycles between ER and Golgi [310, 398, 399]. We found that stable overexpression of VIP36 in prion-infected cells significantly reduced PrP^{Sc}, yet not as strongly as ERp57 did. Interestingly, in acute prion infection VIP36 overexpressing cells showed very slight reduction in PrP^{Sc} levels compared to control cells in

immunoblot analysis. On the other hand, in RT-QuIC analysis the seeding activity of VIP36 overexpressing cells was reduced compared to control cells, suggesting that not all PK-resistant PrP^{Sc} does correlate with prion conversion and propagation [259, 261, 400]. Similar to ERp57, VIP36 overexpression decreased detergent insoluble PrP aggregates upon ER stress induction suggesting functions of VIP36 in ER stress. The effect of VIP36 overexpression on regulation of CHOP in cells as compared to control cells was not as prominent as for ERp57 at early time-points. However, at 16 h, CHOP was significantly reduced in VIP36 overexpressing cells, suggesting functions of VIP36 in ER stress. We still have to clarify whether PrP^{C} and VIP36 directly interact.

In the transient transfection situation, we found slightly different results regarding cell type and prion strain used. ERp57 overexpression which reduced PrP^{Sc} in the stable expression condition had a consistent effect upon repetitive transient transfection in ScN2a-22L cells. In ScMEF cells, ERp57 significantly reduced PrP^{Sc} levels in Me7 infected MEFs, but not in RML infected MEFs, possibly ruling out a generalized effect of overexpression on all prion strains. Similarly, transient VIP36 overexpression significantly decreased prion infection in ScN2a-22L and ScMEF-Me7 cells, but not in ScMEF-RML cells. It will be interesting to see whether downregulation of ERp57 or VIP36 in cells results in elevated levels of PrP^{Sc} and prion conversion activity, and whether this would make cells more susceptible to infection.

Taken together, our data suggest that manipulation of ERp57 and VIP36 expression could be a promising target against prion diseases. We show that ERp57 and VIP36 overexpression modulates PrP quality control, and PrP^{Sc} propagation in acute and chronic infection. Overexpression directly affects biochemical properties of PrP and helps cells to cope with ER stress. We are in the process of validating this proof-of-concept obtained *in vitro* in mouse models infected with prions. Overexpression in the brain will be achieved using AAV delivery systems.

This will allow us also to combine VIP36 and ERp57 encoding viruses, in form of a combination therapy. Given the many similarities between prion diseases and other human neurodegenerative disorders, our approach may be also of interest for other protein misfolding diseases.

CHAPTER 3:

SEPHIN1 REDUCES PRION INFECTION IN PRION-INFECTED CELLS AND ANIMAL MODEL

This chapter presents the manuscript published in *The Journal of Molecular Neurobiology*

Thapa S*, Abdelaziz DH*, Abdulrahman BA and Schatzl HM. 2020. Sephin1 Reduces Prion Infection in Prion-Infected Cells and Animal Model. *Molecular Neurobiology*. https://doi.org/10.1007/s12035-020-01880-y

3.1. Abstract

Prion diseases are fatal infectious neurodegenerative disorders in human and animals caused by misfolding of the cellular prion protein (PrP^{C}) into the infectious isoform PrP^{Sc}. These diseases have the potential to transmit within or between species, and no cure is available to date. Targeting the unfolded protein response (UPR) as an anti-prion therapeutic approach has been widely reported for prion diseases. Here, we describe the anti-prion effect of the chemical compound Sephin1 which has been shown to protect in mouse models of protein misfolding diseases including amyotrophic lateral sclerosis (ALS) and of multiple sclerosis (MS) by selectively inhibiting the stress-induced regulatory subunit of protein phosphatase 1, thus prolonging eIF2α phosphorylation. We show here that Sephin1 dose- and time-dependently reduced PrP^{Sc} in different neuronal cell lines which were persistently infected with various prion strains. In addition, prion seeding activity was reduced in Sephin1-treated cells. Importantly, we found that Sephin1 significantly overcame the endoplasmic reticulum (ER) stress induced in treated cells, as measured by lower expression of stress-induced aberrant prion protein. In a mouse model of prion infection, intraperitoneal (ip) treatment with Sephin1 significantly prolonged survival of prion-infected mice. When combining Sephin1 with the neuroprotective drug metformin, the survival of prion-infected mice was also prolonged. These results suggest that Sephin1 could be a potential anti-prion drug selectively targeting one component of the UPR pathway.

3.2. Introduction

Prion diseases are transmissible spongiform encephalopathies (TSEs) characterized by distinctive histopathological brain lesions which include spongiform changes, neuronal loss, vacuolation, and astrogliosis [1-5]. The disease is rapidly progressive and always fatal. It is caused by the infectious and misfolded isoform, PrP^{Sc}, of the cellular prion protein (PrP^{C}). PrP^{Sc} is β-sheeted, aggregation prone, detergent insoluble, and partially protease resistant [250-252, 401]. Prion disease can be sporadic, acquired by infection to exogenous PrP^{Sc}, or familial by disease-associated mutations in the gene encoding PrP [402, 403]. Examples are Creutzfeldt-Jakob disease (CJD) in humans, scrapie in sheep and goat, bovine spongiform encephalopathy (BSE) in cattle, and chronic wasting disease (CWD) in cervids. BSE was zoonotic and crossed the species barrier to humans, resulting in vCJD in humans [13, 14]. There is no treatment available for prion diseases.

The ER plays an important role in the life cycle of PrP^{C}, where its folding, post-translational modification, translocation to the secretory pathway and quality contro (QC) occur [372]. The accumulation of misfolded proteins in the ER in response to various factors including oxidative stress, calcium dysregulation, and expression of mutated protein causes ER stress and results in dysfunction of ER homeostasis. Accumulation of misfolded proteins triggers cellular toxicity through different signaling cascades such as caspase activation, ER stress, autophagy, and calcium dysregulation; features which also have been found in prion diseases [322, 324, 325, 404]. ER stress has been reported to play a significant role in prion disease pathogenesis, not only increasing PrP^{Sc} levels in prion disease models but also leading to accumulation of not correctly folded forms of PrP^{C} which are more susceptible to prion conversion [220, 321, 326, 338]. In addition, prion infection itself can facilitate induction of ER stress in cells [320, 322].

Downstream of ER stress, UPR helps cells to cope with stress, by reducing misfolded protein deposits and cellular toxicity through a series of signaling events involved in attenuation of protein translation, upregulation of chaperones and other QC molecules, and enhancement of protein degradation [300]. Enhancing UPR and lowering ER stress in cells by overexpression of chaperones and QC molecules such as ERGIC-53, EDEM3, ERp57, VIP36, and BiP have previously been demonstrated to reduce prion conversion in *in vitro* and animal models [338, 339, 405]. However, excessive UPR can also favor prion pathogenesis [320], and thus it is very important to carefully target UPR for development of prion therapy.

One such arm of UPR to be targeted for lowering ER stress in cells could be protein phosphatases. Targeting protein phosphatases has been successful in other protein misfolding diseases [348, 350, 351, 406]. Protein phosphatase inhibitors prolong the phosphorylation of translation initiation factor 2 (eIF2α), thereby decrease protein translation and conserve cellular resources for dealing with proteostasis dysfunction, and lower protein load during ER stress conditions [344, 350]. For example, application of the chemical compound, guanabenz enhanced UPR by inhibiting the stress-induced regulatory subunit of phosphatase (PPP1R15A)-mediated dephosphorylation of p-eIF2α, thereby improving protein folding and protecting cells from protein misfolding stress. It had no effect on the related PPP1R15B-phosphatase complex, helping the cells to avoid otherwise lethal persistent attenuation of global protein synthesis [346]. Guanabenz treatment was effective in preventing disease symptoms and slowing down disease development in amyotrophic lateral sclerosis (ALS), multiple sclerosis (MS), and Parkinson's disease (PD) *in vivo* models [348, 349, 407]. Interestingly, application of guanabenz also prolonged survival against ovine prions *in vivo* [343]. Although being effective in mouse models of several neurodegenerative diseases, the side effects of guanabenz associated with its function as α2-

adrenergic agonist unfortunately limited its further use [347]. Recently, Sephin1, a derivative of guanabenz lacking the α2-adrenergic activity, was shown to inhibit the stress-induced phosphatase complex thereby preventing stress-induced damage in cells and delaying protein misfolding disease development in mouse models [350, 351].

In this study, we investigated whether Sephin1 has effects on prion infection. In prion-infected cells, we found a significant reduction of PrP^{Sc} following treatment with Sephin1, even when different neuronal cells and prion strains were used. Moreover, Sephin1-treated cells showed a reduction of ER stress-induced PrP aggregates. In addition, Sephin1 prolonged the survival of prion-infected mice. Taken together, these results suggest Sephin1 as a potential new anti-prion drug.

3.3. Experimental procedures

3.3.1. Ethics statement

Animal experiments included in this study were done under strict regulation of the Canadian Council for Animal Care (CCAC) guidelines and were approved by the University of Calgary Health Sciences Animal Care Committee (HSACC). The experiments involving the propagation of 22L and RML prions in C57Bl/6 mice (obtained from Charles River Laboratories, USA) were approved under protocol number AC18-0047. Studies involving prion infection and drug treatment were approved under protocol number AC17-0142.

3.3.2. Reagents and antibodies

Proteinase K (PK) and Pefabloc (PK inhibitor) were purchased from Roche, Germany. All reagents and chemicals, if not otherwise stated, were obtained from Sigma Aldrich, USA. The anti-

PrP monoclonal antibody (mAb) 4H11 used in this study to detect PrP has been previously described [373]. Anti-tubulin antibody was purchased from Santa Cruz Biotechnology, USA. Secondary antibody conjugated with peroxidase, goat anti-mouse HRP, was obtained from Jackson ImmunoResearch, USA.

3.3.3. Cell culture studies

The mouse neuroblastoma cell line N2a was initially obtained from ATCC (CCL-131). Cell cultures were maintained in OptiMEM Glutamax medium (GIBCO, USA) with 10% fetal bovine serum (FBS) (Sigma, USA), and penicillin/streptomycin in a 5% CO_2 atmosphere. Uninfected N2a cells and N2a cells persistently infected with mouse-adapted 22L (ScN2a-22L) or RML (RML-ScN2a) prions were used in the study. CAD5, catecholaminergic neuronal cells, optimized for prion infection [408] were a generous gift from Dr. Mahal (The Scripps Research Institute, Florida). CAD5 cells persistently infected with RML prions (ScCAD5-RML) were cultured at 5% CO_2 atmosphere in OptiMEM Glutamax medium containing 10% bovine growth serum (Hyclone, USA) and penicillin/streptomycin. For Sephin1 treatment, cells were plated at a density of 50,000 cells in 10-cm culture dishes and incubated at 37^{o}C overnight. Twenty-four-hour post-culturing, cells were treated with Sephin1. Sephin1 treatment experiments *in vitro* were performed with 5 or 10 µM drug concentration, after identifying the non-toxic dose of up to 10 µM using lactate dehydrogenase (LDH) assay. The control cells were treated with DMSO only. The media of cells were changed every 48 hours (h) with addition of fresh drug. At least three independent experiments were done, if not otherwise stated.

3.3.4. Cytotoxicity assay

The LDH kit was obtained from Roche, USA, and the assay was performed according to the manufacturer's instructions. Briefly, after drug treatment, the cell culture supernatant was collected and subjected to centrifugation to remove cell debris. 100 µl of clear supernatant was placed in a 96-well plate and 100 µl of LDH reagent was added. The mixture was incubated in dark for 10 minutes (min) for conversion of lactate to pyruvate which produces NADH and reduces a yellow tetrazolium salt turning into a red, water-soluble formazan-class dye. The reaction is blocked by addition of 50 µl of 1N HCl, and the absorbance was measured at 490 nm using BioTek Synergy HT. The absorbance measurement of red dye is directly proportional to the amount of LDH released in the culture supernatant due to cell damage. Data were expressed as optical density (OD).

3.3.5. PK digestion and immunoblotting

Immunoblot analysis was done as previously described [374]. Briefly, cells were lysed in cold lysis buffer (10 mM Tris-HCl, pH 7.5; 100 mM NaCl; 10 mM EDTA; 0.5% Triton X-100; 0.5% sodium deoxycholate (DOC)) for 10 min. One half of lysate was subjected to PK digestion (+PK) for 30 min at 37 °C and the digestion was blocked by addition of proteinase inhibitor (0.5 mM Pefabloc). For no PK-treated samples (-PK), Pefabloc was added directly. After methanol precipitation, the protein samples were resuspended in TNE buffer (50 mM Tris-HCl pH 7.5; 150 mM NaCl; 5 mM EDTA) and separated on 12.5% SDS-PAGE. Electroblotting was done on Amersham Hybond P 0.45 PVDF membranes (Amersham, USA) and analyzed using Luminata Western Chemiluminescent HRP Substrates (Millipore, USA). The densitometric analysis of immunoblots was performed using ImageJ. For brain homogenates (BH), 10% (w/v) BH from

terminally sick prion-infected mice was subjected to PK digestion at a final concentration of 50 µg/ml before loading to SDS-PAGE.

3.3.6. Real-time quaking-induced conversion assay (RT-QuIC)

We performed RT-QuIC assay as previously described and used recombinant mouse prion protein (rPrP) as a substrate, which was expressed in a bacterial expression system [376]. Briefly, 20 mM Na-phosphate (pH 7.4), 300 mM NaCl, 1 mM EDTA, 10 µM Thioflavin T (ThT) and 0.1 mg/ml mouse rPrP substrate were mixed to make a master mix. 98 µl of master mix was added to each well of a black-walled 96-well optical bottom plate (Nalge Nunc International, USA). The cell lysates were serially diluted tenfold in a seed dilution buffer and 2 µl of seed at each dilution was added to the master mix. The reactions were set up in quadruplicate and the plate was incubated in a FLUOstar Omega (BMG Labtech, Cary, NC, USA) plate reader for 30 h at 42°C at 1 min shaking (700 revolutions per min) and 1 min rest cycle. Nunc Amplification Tape (Nalge Nunc International) was used as a plate sealing material. The fluorescence at 450 nm excitation and 480 nm emission was measured every 15 min, averaged from four replicate wells and then plotted against reaction time. An uninfected cell lysate was used as a negative control on each plate. The criteria for the sample to be positive was when amplification in $\geq$2 replicates out of four was seen above the cut-off (average fluorescence of the negative controls plus 5× standard deviation (SD).

3.3.7. Detergent solubility assay

We followed the previous protocol to perform the detergent solubility assay [338]. Briefly, after addition of 0.5 mM Pefabloc and N-lauryl sarcosine (sarcosyl) at a final concentration of 1%, the post-nuclear cell lysates were subjected to ultracentrifugation at 4 °C for 1 h at 100,000 × g

using a Beckman TL-100 centrifuge. Both the supernatant and pellet fractions were collected separately. The supernatant fraction was precipitated in methanol and pellet was resuspended directly in sample loading buffer (7% SDS, 30% glycerin, 20% β-mercaptoethanol, 0.01% bromophenol blue in 90 mM Tris-HCl, pH 6.8) for immunoblotting. Both the fractions were analyzed in 12.5% SDS-PAGE.

3.3.8. Mouse bioassay

Five-week-old female FVB mice (Charles River Laboratories, USA) were inoculated intracerebrally (ic) with 20 µl of 1% (w/v) brain homogenate from a terminally-sick mouse inoculated with RML prions. Twenty-five gauge disposable needles were used for intracerebral inoculation and animals were under anesthesia during the procedure. Mice were monitored daily for health and activity after ic inoculation. Thirty days post-prion inoculation, treatment of animals with drugs was started. Each mouse was injected ip with 100 µl solution (Sephin1 in PBS) containing 100 µg Sephin1 (approximately equal to 5 mg/kg) for 60 days with 3 injections per week. After 60 days, animals were injected ip for additional 20 days with 2 injections per week. Control group received vehicle only (5 µl DMSO mixed with 95 µl PBS; total volume 100 µl). For the combination group, at 30 dpi each animal was given 100 µg Sephin1 along with 5 mg metformin (approximately 250 mg/kg) as a single injection ip for 30 days at 3 times per week. Animals were monitored daily for progression of prion disease. The terminal stage of disease was determined by two researchers, animals were euthanized following anesthesia, and their survival time was recorded.

3.3.9. Statistical analysis

GraphPad Prism (GraphPad Software, USA v 7.03) was used to perform statistical analysis. For multiple comparisons of treated groups with that of control, one-way ANOVA with post-hoc test was used. Statistical significance for all the immunoblots was expressed as mean ± SEM. The graphical representation of survival time of animals was done using a Kaplan–Meier plot by plotting percent survival for each group. Gehan-Breslow-Wilcoxon test was performed for statistical difference between groups in the survival plot with median taken into account. For comparison of mean survival, Mann-Whitney test was used for pair-wise comparisons between control and treated group. Outliers were removed before analysis using outlier calculator, GraphPad Prism. *: $p \leq 0.05$, **: $p \leq 0.01$, and ***: $p \leq 0.001$ were considered significant.

3.4. Results

3.4.1. Sephin1 reduces PrP^{Sc} in prion-infected neuroblastoma cells

To investigate whether Sephin1 affects the level of PrP^{Sc} in prion-infected cells, N2a cells persistently infected with the mouse-adapted scrapie strain 22L (ScN2a-22L) were treated with Sephin1 at concentrations of 5 or 10 µM for 7 days. The drug vehicle DMSO was used to treat control cells. The levels of PrP^{Sc} were measured in immunoblot upon PK digestion of cell lysates. We found that Sephin1 at a concentration of 10 µM decreased PrP^{Sc} significantly in treated ScN2a-22L cells ($p < 0.05$) (Fig. 3.1 B and C). Next, we analyzed the prion seeding activity of treated and non-treated cells using RT-QuIC assays. As described previously [113], we used mouse recombinant PrP as substrate. Treatment with 10 µM of Sephin1 lowered the prion seeding activity in the cells compared with that of controls (Fig. 3.1 D). To exclude drug toxicity as reason for PrP^{Sc} reduction, we performed LDH assay. LDH is a cytoplasmic enzyme which is released into

the cell culture supernatant when the plasma membrane is damaged [409]. Sephin1 concentrations of 5 and 10 µM were not cytotoxic (Fig. 3.1 A); the significant decrease of LDH in cells treated with 10 µM indicates reduced cytotoxicity and increased viability. Moreover, treatment of uninfected N2a cells with Sephin1 had no effect on the levels of PrP^{C}, indicating that the reduction of PrP^{Sc} is not due to lowering of PrP^{C} (Fig. 3.1 E).

Taken together, these data show that application of Sephin1 at a concentration of 10 µM significantly reduced PrP^{Sc} in ScN2a-22L cells.

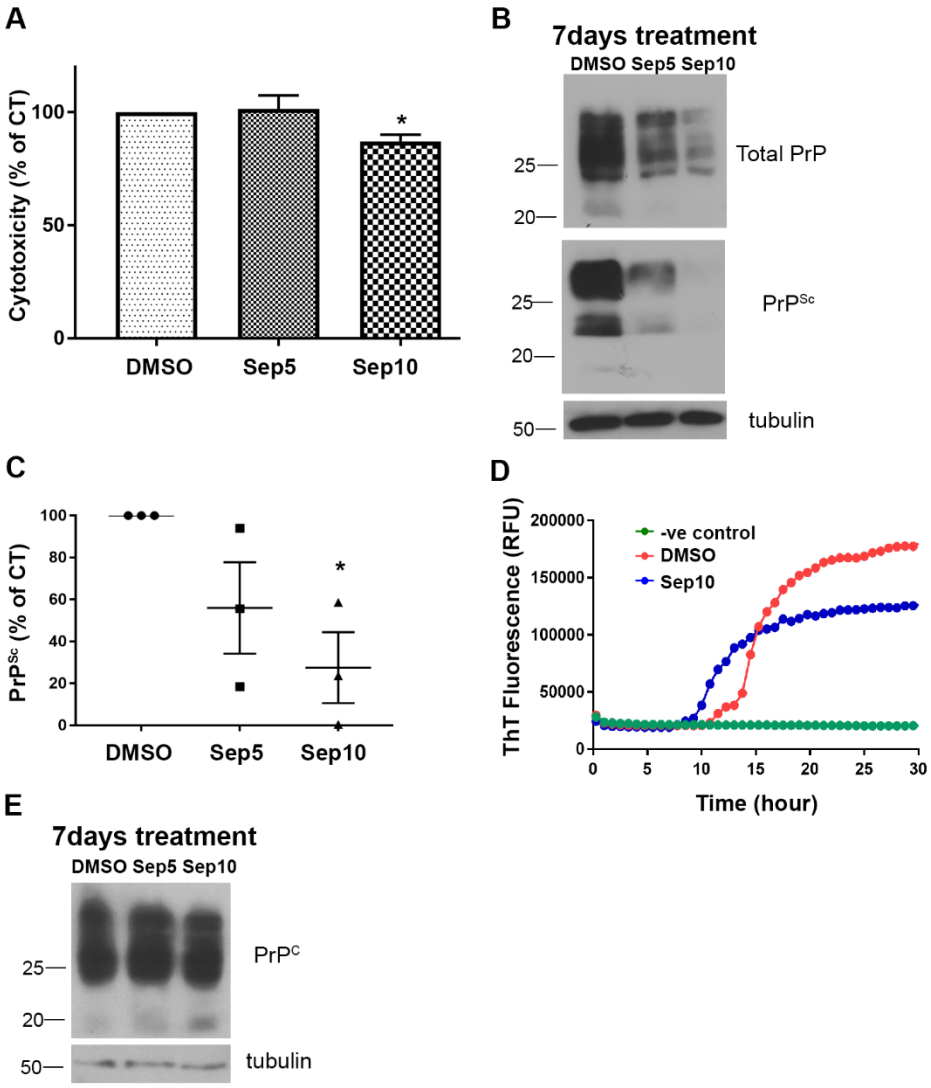

Figure 3. 1. Sephin1 reduces PrP^{Sc} in prion-infected cells. ScN2a-22L cells were treated with 5 µM (Sep5) or 10 µM (Sep10) of Sephin1 for 7 days. DMSO-treated cells were used as a control. Cells were then lysed and PK digestion of cell lysates was done to distinguish PrP^{Sc} (+PK); the amount of PrP^{Sc} was quantified from the immunoblot using anti-PrP mAb 4H11. Furthermore, cell lysates (-PK) were subjected to RT-QuIC analysis to determine prion seeding activity. (A) LDH assay was performed to determine potential drug toxicity. Y-axis represents the cytotoxicity levels in percent of the control. (B) Representative immunoblot showing the amount of PrP^{Sc} after 7 days

of treatment. Tubulin was used as a loading control. (C) Densitometric analysis showing the amount of PrP^{Sc} normalized by amount of tubulin or actin and shown as a percentage of control for 3 different independent experiments using Image J. (D) RT-QuIC analysis in which relative fluorescence units (RFU) of ThT (y-axis) were plotted against time (x-axis). N2a cell lysate was used as a negative control. Sample dilution shown is 10^{-2}. (E) Uninfected N2a cells were treated with either 5 µM (Sep5) or 10 µM (Sep10) of Sephin1 for 7 days, cell lysed and cell lysates subjected to immunoblotting to determine the levels of PrP^{C} in control and Sephin1 treated-cells. * indicates $p \leq 0.05$

3.4.2. Long-term treatment with Sephin1 controlled but did not cure prion infection in ScN2a-22L cells

Since Sephin1 treatment for 7 days significantly reduced PrP^{Sc}, we next investigated whether long-term treatment cures treated cells. We treated ScN2a-22L cells with 5 or 10 µM of Sephin1 for 7 days and then passaged the cells in the presence of the drug for 3 passages, each passage lasting 7 days. Accordingly, passage 1 indicates 14 days of treatment; passage 2, 21 days of treatment; and passage 3, 28 days of treatment. At each passage, we lysed the cells and collected the lysates. We found that Sephin1 treatment at 10 µM concentration significantly reduced PrP^{Sc} in each passage, to levels almost undetectable in immunoblot at passage 1 (Fig. 3.2 A and D), 2 (Fig. 3.2 B and E) and 3 (Fig. 3.2 C and F). At passages 1 and 2, even the concentration of 5 µM decreased the amount of PrP^{Sc} (Fig. 3.2 A, B, D, and E). RT-QuIC analysis showed decreased seeding activity of treated cells compared with controls, with a consistent decline over passaging (Fig. 3.2 G-I). However, our RT-QuIC analysis showed that the treatment did not cure the cells

from prion infection, as we still could detect some prion seeding activity in long-term Sephin1 treated cells.

Taken together, long-term treatment with Sephin1 at a 10 μM concentration successfully reduced PrP^{Sc} to levels undetectable in immunoblot. Interestingly, it did not result in complete removal of prion seeding activity as shown by RT-QuIC.

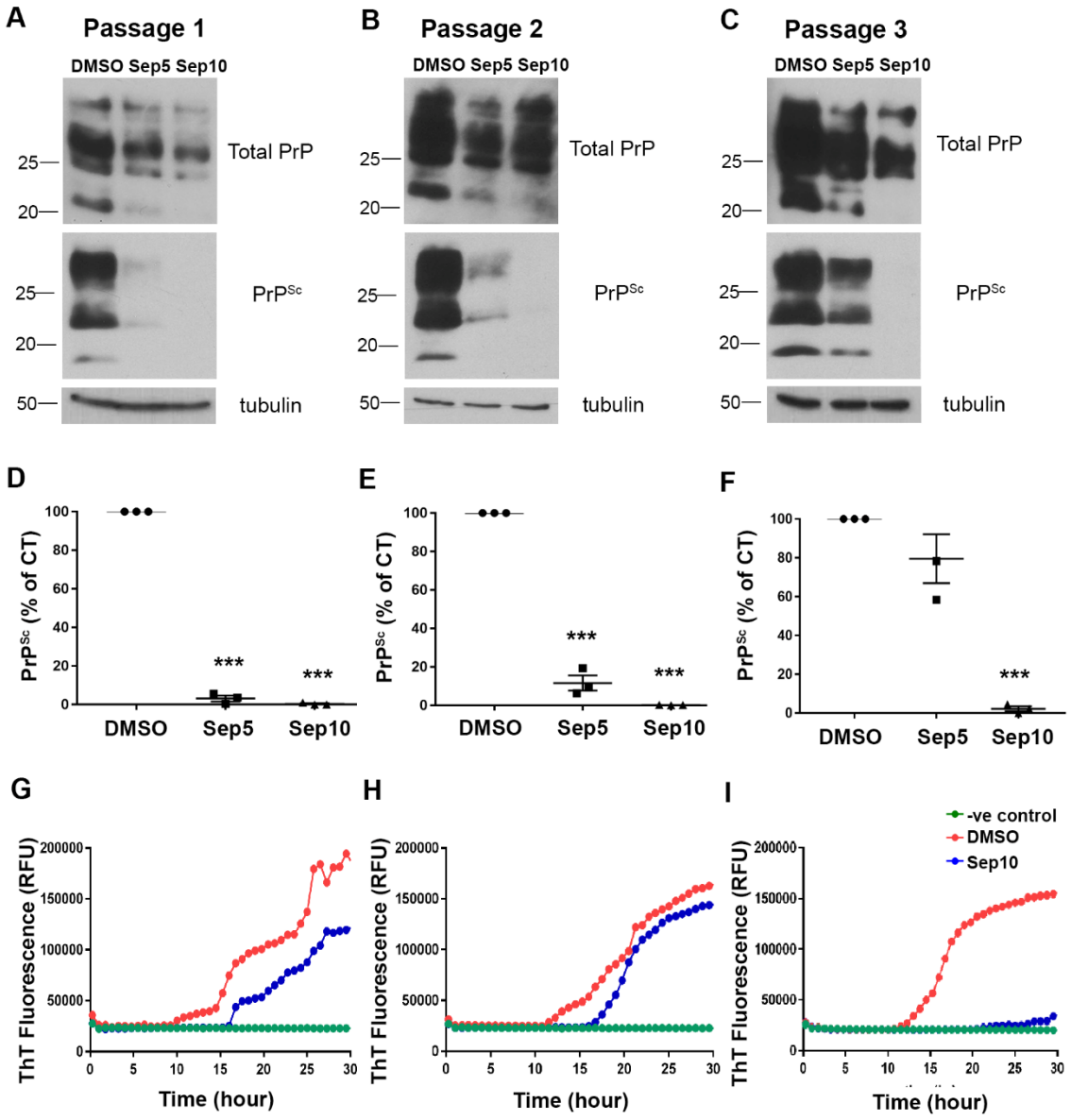

Figure 3. 2. Prolonged treatment with Sephin1 reduces PrP^{Sc} to undetectable levels. ScN2a-22L cells were treated with 5 (Sep5) or 10 µM (Sep10) of Sephin1 for 7 days. The cells were then passaged for 3 passages, each passage 7 days apart, in the presence of the drug and an aliquot lysed in each passage. Cell lysates were subjected to immunoblotting (-/+ PK digestion) using anti-PrP mAb 4H11, and to RT-QuIC analysis (-PK samples). (A) Representative immunoblot showing the amount of PrP^{Sc} in first passage; (B) second passage; and (C) third passage. Densitometric analysis

showing the amount of PrP^{Sc} in first (D), second (E), and third passage (F), shown as a percentage of control for 3 different independent experiments using Image J. (G) Seeding activity of cells at passage 1 in RT-QuIC assay; N2a cell lysate was used as negative control. (H) RT-QuIC in passage 2. (I) RT-QuIC in passage 3. Sample dilution shown is 10^{-2}. *** indicates $p \leq 0.001$

3.4.3. Sephin1 reduces PrP^{Sc} accumulation in N2a and CAD5 cells infected with RML prions

To see whether the observed anti-prion effect is cell line or prion strain specific, we next tested N2a cells persistently infected with RML prions (RML-ScN2a). Cells were treated for 7 days with 5 or 10 µM of Sephin1 and analyzed by immunoblot for PrP^{Sc}. A significant reduction was found after treatment with either dose (*$p<0.001$*) (Fig. 3.3 A and B). When cells were further passaged for 7 days with treatment, PrP^{Sc} was undetectable in cells treated with 10 µM of Sephin1 (Fig. 3.3 D and E). When prion seeding activity was compared, Sephin1-treated cells (10 µM) had less prion seeding activity than the control cells at both time points (Fig. 3.3 C and F). LDH assay suggested no cytotoxic effect of Sephin1 on RML-ScN2a cells at concentrations used in this study (Fig. 3.3 G). These results indicate that Sephin1 decreases levels of PrP^{Sc} also in N2a cells infected with a different prion strain.

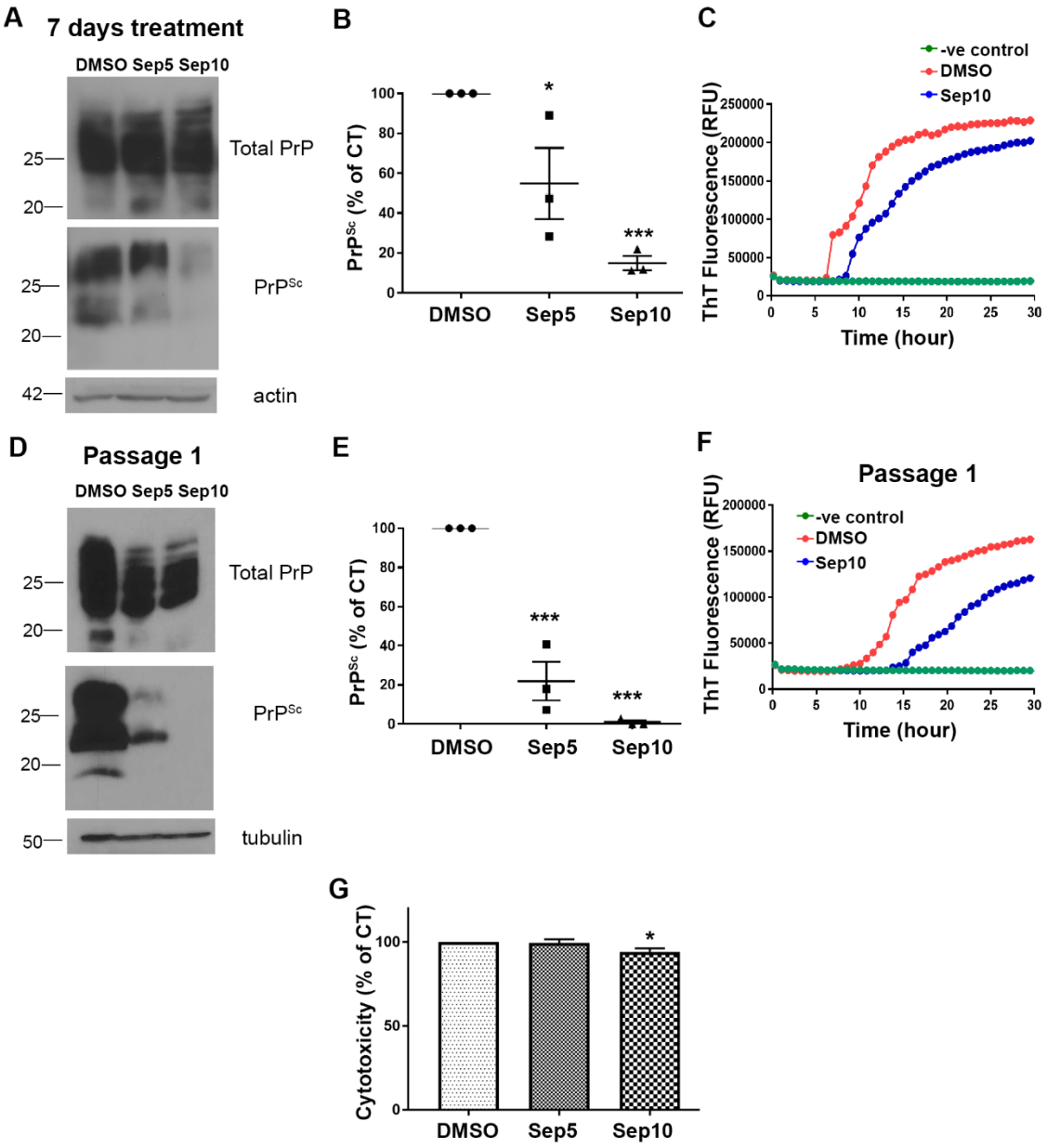

Figure 3. 3. Sephin1 decreases PrP^{Sc} in N2a cells infected with RML prions. RML-ScN2a cells were treated with Sephin1 for 7 and 14 days and an aliquot lysed at each passage. Cell lysates were analyzed in immunoblot (-/+ PK; mAb 4H11) and RT-QuIC (-PK samples). Representative immunoblots showing the amount of PrP^{Sc} after 7 (A) and 14 (D) days of treatment. Either actin or tubulin was used as a loading control. Densitometric analysis of amount of PrP^{Sc} shown as a

percentage of control after 7 (B) and 14 (E) days of treatment. Representative RT-QuIC analysis showing seeding activity of cells after 7 (C) and 14 (F) days of treatment. Sample dilution shown is 10^{-2} (G) LDH assay showing no cytotoxicity of the drug at used concentrations. * indicates $p \leq 0.05$ and *** indicates $p \leq 0.001$

Next, we tested another neuronal cell line, murine catecholaminergic CAD5 cells of the central nervous system (CNS) origin, persistently infected with RML prions (ScCAD5-RML). When treated for 5 days with Sephin1, we found a significant reduction of PrP^{Sc} in RML-CAD5 cells (Fig. 3.4 B and C). As before, the drug doses were not toxic to cells under experimental conditions used as shown by LDH assay (Fig. 3.4 A). RT-QuIC assay showed less prion seeding activity at 10 µM drug concentrations (Fig. 3.4 D). In summary, these data demonstrate that the anti-prion activity of Sephin1 is independent of the cell line and prion strain used.

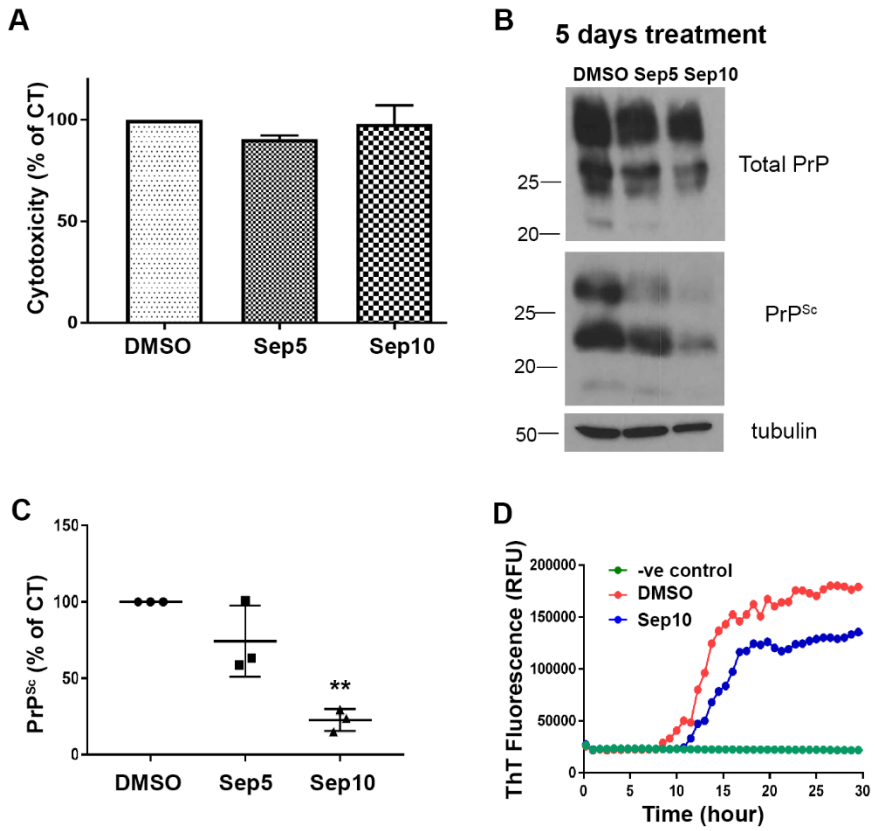

Figure 3. 4. Sephin1 decreases PrP^{Sc} in RML-infected ScCAD5 cells. ScCAD5-RML cells were treated with Sephin1 for 5 days and cells were lysed. The cell lysates were analyzed with RT-QuIC for prion seeding activity and amount of PrP^{Sc} by immunoblotting (-/+ PK digestion). Tubulin was used as a loading control. (A) Cytotoxicity measured using LDH assay, shown as percentage of control. (B) Representative immunoblot showing the amount of PrP^{Sc}. (C) Densitometric analysis of amount of PrP^{Sc} shown as a percentage of control. (D) Seeding activity in RT-QuIC. Sample dilution shown is 10^{-2}. Uninfected cell lysate was used as negative control. ** indicates $p \leq 0.01$

3.4.4. Sephin1 prevents ER stress-mediated accumulation of PrP aggregates

Our data so far suggested that Sephin1 can reduce prion infection in neuronal cells, and the next set of studies addressed the molecular mechanisms underlying this process. Our group has

previously shown that ER stress caused by accumulation of misfolded proteins can result in the deterioration of the quality of PrP^{C} which favors the production of more PrP^{Sc} in infected cells [338]. We also showed that this can be prevented by lowering ER stress by the overexpression of cellular QC proteins [405]. As Sephin1 has been reported to reduce ER stress in cells by prolonging the eIF2α phosphorylation during stress conditions and also to protect the cells from stress-related cytotoxic effects [350], we investigated whether Sephin1 affects stress-induced PrP aggregation. We treated N2a cells with Sephin1 (5 or 10 µM) or solvent only (DMSO). After 7 days of treatment, tunicamycin (2.5 µg/ml) was added to the cells followed by incubation for 16 h. Upon cell lysis, the cell lysates were subjected to a detergent solubility assay as described previously [338]. Tunicamycin induces ER stress in cells by inhibiting the N-glycosylation during glycoprotein synthesis in the ER [378], which is demonstrated in Fig. 3.5 A where N2a cells were subjected to detergent solubility assay in the presence or absence of tunicamycin treatment for 16 h. The supernatant of tunicamycin-treated cells showed a PrP which tends to be more non-glycosylated and different from the usual three-banding pattern of PrP^{C}. PrP aggregates in the pellet fraction are found prominently in tunicamycin-treated samples. When DMSO or Sephin1-treated cells were subjected to detergent solubility assay, we found that Sephin1 at 10 µM concentration significantly reduced the level of stress-induced PrP aggregates in the pellet fraction (Fig. 3.5 B and C).

Taken together, this indicates that Sephin1 helps the cells in coping with stress-induced PrP aggregation.

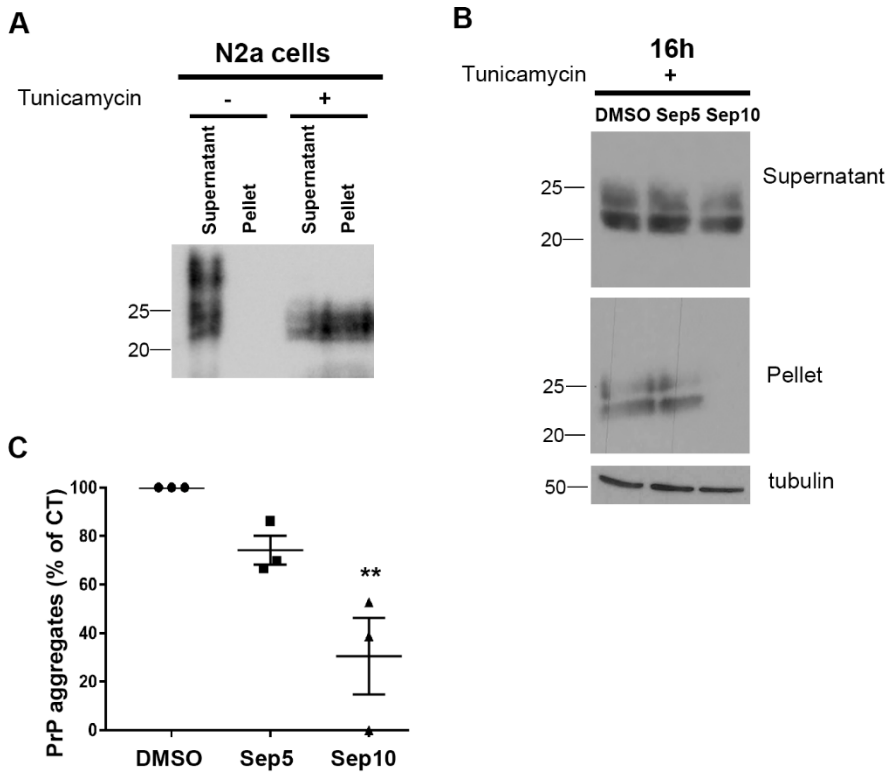

Figure 3. 5. Sephin1 decreases ER stress in the cells. N2a cells were treated with tunicamycin (2.5 µg/ml) for 16 h, to induce ER stress in the cells. Cells were then lysed and subjected to a detergent solubility assay. In the presence of 1% sarcosyl, the post-nuclear lysates were ultracentrifuged at 100,000 g for 1 h. Supernatant and pellet fractions were separated and immunoblotting was done using anti-PrP mAb 4H11. (A) Immunoblot showing the supernatant and pellet fractions of N2a cell lysates in the presence or absence of tunicamycin (B) Immunoblot showing PrP aggregates in the pellet fraction when cells were treated either with DMSO or Sephin1 for 7 days prior to tunicamycin addition and detergent solubility assay (C) Densitometric analysis of PrP aggregates in DMSO and Sephin1 treated groups represented as percentage of control after normalization with levels of tubulin using ImageJ. ** indicates $p \leq 0.01$.

3.4.5. Sephin1 prolongs the survival of prion-infected mice

Our *in vitro* data suggested that Sephin1 is capable of reducing prion propagation; however, findings in prion-infected cultured cells sometimes cannot be recapitulated in animal models of prion infection. In order to test whether the proof-of-concept obtained in cultured cells can be validated *in vivo*, we next treated prion-infected mice with Sephin1. FVB mice were infected ic with mouse-adapted RML prions. One group of mice received intraperitoneally 100 µg of Sephin1, and the control group received vehicle only (DMSO). The drug treatment was started 30 days after prion infection (dpi) and was done 3 times per week for the next 60 days. After 60 days of treatment, the treatment was reduced to two ip injections per week for another 20 days. The schematic for treatment is shown in Fig. 3.6 A. Sephin1-treated mice showed statistically significant longer incubation times when compared with controls as shown in Fig. 3.6 B and D (Gehan-Breslow-Wilcoxon test , $p = 0.0470$; Sephin1 vs. control group mean survival: 156.9 ± 1.575 vs. 150.3 ± 2.407).

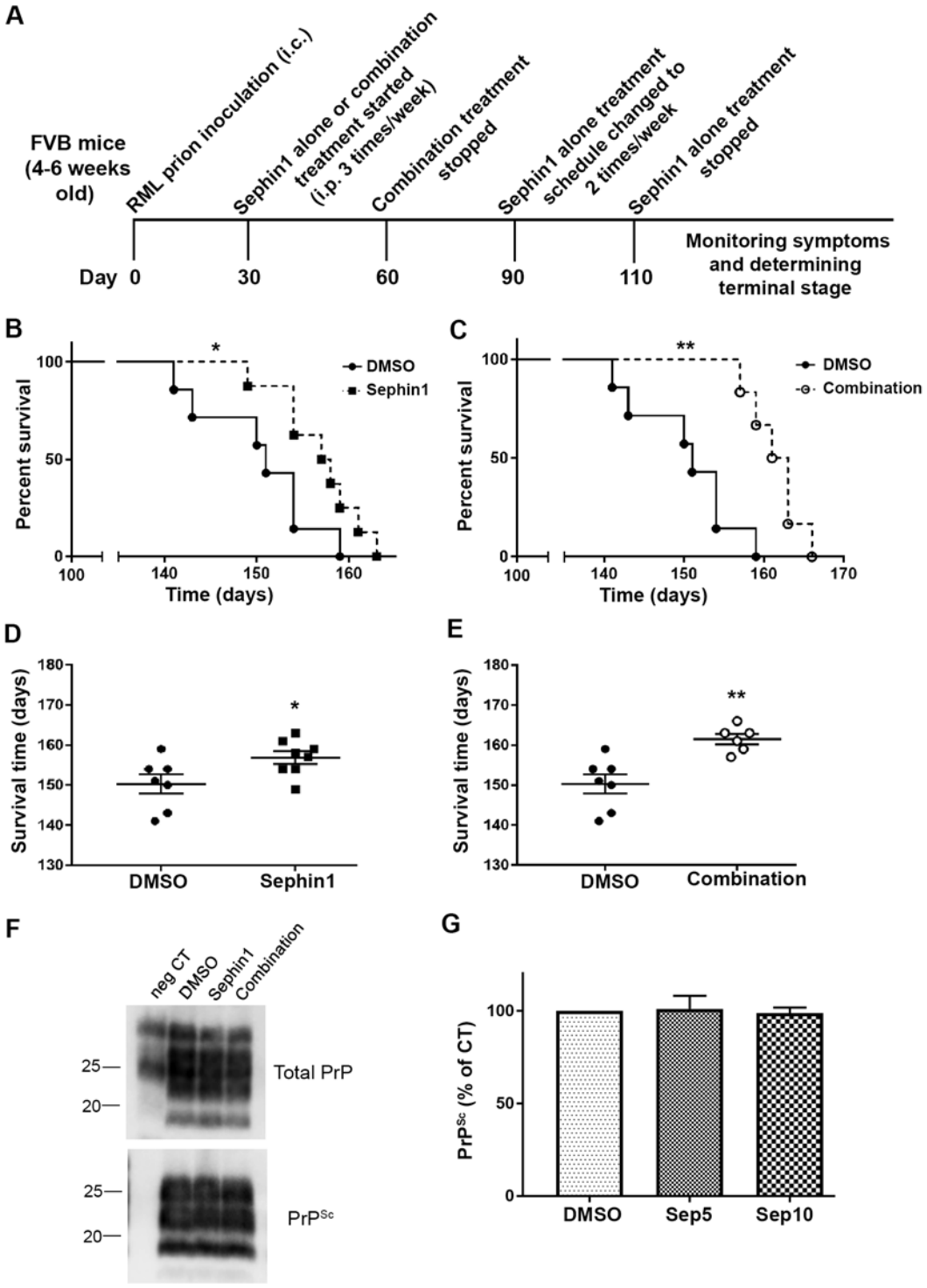

Figure 3. 6. Sephin1 extends the survival time in mice infected with RML prions. (A) RML-infected FVB mice were intraperitoneally treated with Sephin1 (100 µg/mouse), or DMSO only

as control, for 80 days starting at 30 dpi. For the combination treatment group, Sephin1 was combined with metformin and FVB mice were treated ip for 30 days (day 30 to 60 dpi). (B) Percent survival of control mice (DMSO) and Sephin1-treated mice showing a Kaplan–Meier plot with Gehan-Breslow-Wilcoxon test. (C) Percent survival of control mice (DMSO) and combination group (Sephin1 and metformin) presented as a Kaplan-Meier plot, using Gehan-Breslow-Wilcoxon test for statistical analysis. (D) Mean survival time with SEM for control mice (DMSO) and Sephin1-treated mice. (E) Mean survival time with SEM for control mice (DMSO) and combination group. (F) Representative immunoblot showing levels of PrP^{Sc} in the brains of terminally sick DMSO, Sephin1, or combination-treated mice after PK digestion (50 µg/ml) of 10% (w/v) BH. The negative control is BH from a FVB mouse with no prion infection (neg CT). (G) Densitometric analysis of PrP^{Sc} in the brains of terminal mice (3 animals/group) represented as percentage of control. * indicates $p \leq 0.05$ and ** indicates $p \leq 0.01$.

The mechanism of action known for Sephin1 is that it inhibits the stress-induced regulatory subunit of the protein phosphatase complex and in turn prolongs phosphorylation of eIF2α during stress, and thus protects the cells from proteostasis damage [350, 351]. Although the global protein translation is not attenuated by Sephin1 [350], still we wanted to combine it with the neuroprotective drug metformin [410] *in vivo.* This also should investigate whether such a combination has more beneficial effects. Another group of mice was treated with Sephin1 along with metformin (5 mg/mouse) as a single mixture intraperitoneally for 30 days, at 3 times a week starting at 30 dpi. We found that mice treated with both Sephin1 and metformin simultaneously had a higher survival time compared with controls (Fig. 3.6 C and E) (*$p=0.0034$*; combination vs control group mean survival: 161.5 ± 1.31 vs. 150.3 ± 2.407). Although the survival time of the

combination group was higher than that of Sephin1 treatment alone (*p=0.0615;* 161.5 ± 1.31 vs. 156.9 ± 1.575), this difference was not statistically significant. Of note, the combination group was treated for only 30 days. Moreover, we analyzed the brains sampled from terminally sick DMSO, Sephin1 or combination-treated mice in immunoblot to look for effects on PrP^{Sc}. As expected, we did not see any difference in the amount of PrP^{Sc} in the brain between treatment groups (Fig. 3.6 F and G), as the brains were sampled at the terminal stage of each animal.

Taken together, these data show that application of Sephin1 has the potential to extend the survival time in prion-infected mice, alone or in combination with metformin.

3.5. Discussion

In this study, we demonstrate that Sephin1 is effective in reducing PrP^{Sc} in different prion-infected cell models and prolongs the survival in prion-infected mice. Combination with a neuroprotective drug yielded additive effects in delaying disease progression. Mechanistically, Sephin1 prevents ER stress-mediated aggregation of PrP in the cells. Our data support the idea that selective inhibition of the stress-related subunit of protein phosphatase by Sephin1 could be a novel therapeutic approach against prion disease as has been shown for other protein misfolding diseases [350, 351].

Numerous protein misfolding diseases have been associated with ER stress, among them are prion disease, Alzheimer's disease (AD), PD, Huntington's disease, and ALS [299, 387, 411-413]. ER stress can be triggered by accumulation of misfolded proteins leading to ER dysfunction and cytotoxicity [414, 415]. With the purpose to cope with such a dysfunction, UPR response is generated in the cells. UPR response includes attenuation of protein translation, upregulation of the expression of QC molecules (chaperones and foldases), and enhancement of ER-associated

degradation, and provides the cells the necessary time to get rid of the accumulated protein load, relieve the stress, and re-establish cellular homeostasis [416]. However, chronic ER stress can overwhelm the QC system leading to apoptosis and ultimately results in cell death and neurodegeneration [417].

In prion disease, we and others have demonstrated a complex relationship that exists between ER stress, ER QC molecules, and prion propagation. We previously found that ER stress induction leads to increased accumulation of detergent insoluble PrP aggregates in cells which increases PrP^{Sc} in prion-infected cells [338]. Another group found that such PrP aggregates are more susceptible to prion conversion in protein misfolding cyclic amplification (PMCA) [326]. Importantly, we found that overexpression of selected QC molecules can reduce ER stress in cells and subsequently reverse the increase of ER stress-mediated PrP aggregates and PrP^{Sc} accumulation [338, 405]. In line with this, downregulation of BiP expression enhanced prion propagation in *in vitro* and *in vivo* prion models [339]. However, such genetic manipulations are difficult to implicate as therapy, due to limitation in efficient delivery and possible side effects related to gene integration or knockdown, and thus, a pharmacological approach to reduce ER stress and protect cells from proteostasis failure might be preferable.

Attenuation of protein translation during UPR is executed in cells by phosphorylating eIF2α. Modulation of this pathway has been studied as an attractive therapeutic approach for protein misfolding diseases, with the aim to protect cells from ER stress [344, 350]. This approach seems promising against neurodegenerative diseases, although it is conceivable that prolonged protein translation attenuation due to eIF2α phosphorylation might result in cytotoxicity [320, 348, 349]. For example, some studies have suggested that the chemical compounds guanabenz and salubrinal, which inhibit the protein phosphatase complex and prolong eIF2α phosphorylation, are

neuroprotective and alleviate the progression in various neurodegenerative diseases, including prion disease, ALS, PD, and Huntington's Disease [343, 348, 349, 418]. However, other studies have demonstrated that salubrinal accelerated prion disease propagation in mice and increased accumulation of Aβ in an AD *in vitro* model [320, 419]. This discrepancy can be attributed to the fact that salubrinal inhibits both stress-related and non-stress-related protein phosphatase complexes, leading to sustained eIF2α phosphorylation and potentially lethal protein translation repression [344, 345], whereas guanabenz only inhibits stress-related phosphatase [346]. On the other hand, guanabenz also exerts a number of side effects which are related to its α2-adrenergic action. Devoid of such α2-adrenergic activity, Sephin1 is a derivative of guanabenz which inhibits the stress-induced subunit of protein phosphatase and thus helps in preventing the dephosphorylation of eIF2α, reduces ER stress, and provides protection to cells from damaging effects of protein misfolding stress [350].

We show here that Sephin1 can reduce prion propagation and conversion *in vitro* and increase survival in prion-infected animal models, without generating unwanted side effects. Sephin1 prolongs eIF2α phosphorylation in ER stress condition and thereby protects cells from toxicity [350, 351]. As expected, Sephin1 treatment led to prolongation of phosphorylation of eIF2α in cultured cells in stressed condition, and preliminary studies suggest that this was also the case *in vivo* after prion infection (data not shown). Of note, Sephin1 was effective in various neuronal cell lines infected with different prion strains. Mechanistically, we anticipated that Sephin1 reduces prion-infection mediated ER stress in cells. To test this in our system, we measured PrP aggregates in ER-stressed cells after treatment with Sephin1. Our previous studies have shown that ER stress negatively affects the quality of PrP^{C} and triggers PrP aggregate formation; overcoming ER stress in cells by overexpression of QC molecules prevented formation

of such detergent-insoluble PrP aggregates [338, 405]. In line with this, application of Sephin1 significantly overcame production of stress-mediated PrP aggregates in the cells, thereby likely decreasing the more susceptible PrP substrate for prion conversion. This might explain why we observed less PrP^{Sc} in prion-infected cells after Sephin1 treatment. Of note, the reduction in PrP^{Sc} in Sephin1-treated prion-infected cells was not due to less PrP^{C} being available for conversion, as the PrP^{C} levels remained unaltered in non-infected N2a cells after treatment with Sephin1. Interestingly, although Sephin1 very profoundly reduced PK-resistant PrP^{Sc} in immunoblot, down to undetectable levels, long-term treatment could not completely eliminate prion-seeding activity as tested in RT-QuIC assay. This suggests that at the dose and time used here, Sephin1 was not capable of curing prion infection in the cells. Although the two techniques used here measure different aspects of PrP^{Sc}, where immunoblotting quantifies PK-resistant PrP^{Sc} and RT-QuIC detects the ability of PrP^{Sc} to convert recombinant PrP substrate to PrP aggregates, this is a clear indication for the necessity of utilizing multiple relevant techniques when studying therapeutic effects in prion-infected cells. RT-QuIC has been occasionally utilized to screen the anti-prion activity of compounds *ex vivo* [394, 395], however, we used this technique as a read-out to investigate if Sephin1 reduced the prion seeding activity in the cells.

In vivo, Sephin1 given ip starting 30 days after ic prion inoculation prolonged the survival time in prion-infected mice. As Sephin1 was reported to cross the blood brain barrier (BBB) and to be safe *in vivo* [350], we used the ip route for drug treatment, anticipating efficient absorption and bioavailability of compound. Notably, the pharmacokinetics of ip route application is similar to that of oral administration in animals [420]. We observed no unwanted side effects in the mice treated with Sephin1, in line with other reports which even used higher concentrations of Sephin 1 *in vivo* [351]. A potential limitation of our study is that we used only one dose and route of drug

administration. It would be interesting to utilize different concentrations and other routes for optimal pharmacological delivery. In support of our study, the drug guanabenz was shown to prolong survival against ovine prions; however, unlike Sephin1, guanabenz had severe side effects [343].

Of note, there are reports which show that prolonged eIF2α phosphorylation reduces synaptic protein translation and leads to neuronal death in prion-infected mouse models, and that restoring translation rates genetically or pharmacologically to restore repressed protein translation rates is beneficial [320, 352-354]. The obvious contradiction between these studies and our study might be due to the different genotypes of mice used. Whereas we used PrP wild-type mice, these studies used Tg37 PrP-overexpressing transgenic mice. Another explanation is the differences in which phase of disease progression the drug was administered. Tg37 mice highly overexpress PrP and thus, the time to reach terminal prion disease is rapid around 85 dpi. In this model, drug administration was started around 50 dpi which is in the third quarter of incubation time. In our study, wild-type mice were used which show terminal disease around 150 dpi, and we started drug administration early after 30 dpi roughly in the first quarter of incubation time. This is reminiscent to another study. When Sephin1 was used early in a MS animal model, it protected oligodendrocytes and decreased clinical disease severity, while at a later stage of disease, it was not effective [351]. Although Sephin1 enhanced eIF2α phosphorylation and protected cells from stress, at a later stage of MS disease the system might have been overwhelmed with excessive cellular stress leading to apoptosis. To achieve a specific goal in therapy, it is therefore very important to determine the optimal time of drug administration in such long incubation protein misfolding diseases. Modulation of different molecular pathways or targeting different mechanism may be beneficial, which ultimately requires a drug combination approach. For Sephin1

specifically, in animal models of MS, a more efficient delay of disease was observed after combining it with interferon-β treatment, better than with each drug alone [351].

Keeping in mind the potential risk of repression of synaptic protein translation and ultimate neurodegeneration arising from modulation of eIF2α phosphorylation pathway in prion disease [320, 354], we decided to combine Sephin1 with the potentially neuroprotective drug metformin. Metformin is an anti-diabetic drug shown to have neuroprotective function in different neurodegenerative diseases. Although the exact mechanism of neuroprotection is unknown, it is believed to exert its effect by counteracting protein hyperphosphorylation, oxidative stress, and neuroinflammation [410, 421]. When Sephin1 and metformin were used in combination to treat prion-infected mice, for 30 days starting at 30 dpi, this regimen delayed clinical disease more than when using the two drugs alone. For the metformin alone treatment group, at the dose we used here, there was no difference in survival compared with that of the control (data not shown). For the Sephin1 group, the mean survival was less than compared with that of the combination group. Of note, combination therapy was only given for 30 days, while drugs alone were given continuously for 80 days. These data clearly indicate the advantage of combination therapy; however, we have to perform further investigation regarding dose optimization and toxicity.

Taken together, these data suggest that Sephin1 could be a novel therapeutic agent against prion disease. We show that Sephin1 significantly reduces PrP^{Sc} propagation in various neuronal cells infected with different prion strains. The effect on PrP^{Sc} is due to modulation of stress-mediated effects on PrP; however, other possibilities are yet to be elucidated. When used in a mouse model of prion disease, Sephin1 treatment prolonged the survival of animals. Combination therapy of Sephin1 with the neuroprotective drug metformin yielded slightly better *in vivo* effects.

In line with this, we are currently examining other drugs which target different cellular pathways for combination therapy.

CHAPTER 4:

RECOMBINANT PRION PROTEIN VACCINATION OF TRANSGENIC ELK PrP MICE AND REINDEER OVERCOMES SELF-TOLERANCE AND PROTECTS MICE AGAINST CHRONIC WASTING DISEASE

This chapter presents the manuscript published in *The Journal of Biological Chemistry*

Abdelaziz DH[*], Thapa S[*], Brandon J, Maybee J, Vankuppeveld L, McCorkell R and Schatzl HM. 2018. Recombinant prion protein vaccination of transgenic elk PrP mice and reindeer overcomes self-tolerance and protects mice against chronic wasting disease. *The Journal of Biological Chemistry*, 293 (51): 19812-19822 (Shared first authorship by Thapa S)

The "Results" and "Discussion" sections are re-written with the consent of other authors.

4.1. Abstract

Chronic wasting disease (CWD) is a fatal neurodegenerative disease that affects cervids in North America and now Europe. No effective measures are available to control CWD. We hypothesized that active vaccination with homologous and aggregation-prone recombinant prion protein (PrP) could overcome self-tolerance and induce autoantibody production against the cellular isoform of PrP (PrP^C), which would be protective against CWD infection from peripheral routes. Five groups of transgenic mice expressing elk PrP (TgElk) were vaccinated with either the adjuvant CpG alone or one of four recombinant PrP immunogens: deer dimer (Ddi), deer monomer (Dmo), mouse dimer (Mdi), and mouse monomer (Mmo). Mice were then challenged intraperitoneally with elk CWD prions. All vaccinated mice developed ELISA-detectable antibody titers against PrP. Importantly, all four vaccinated groups survived longer than the control group, with the Mmo-immunized group exhibiting 60% prolongation of mean survival time compared with the control group (183 vs. 114 days post-inoculation). We tested for prion infection in brain and spleen of all clinically sick mice. Notably, the attack rate was 100% as revealed by positive CWD signals in all tested tissues when assessed with Western blotting, real-time quaking-induced conversion (RT-QuIC), and immunohistochemistry (IHC). Our pilot study in reindeers indicated appreciable humoral immune responses to Mdi and Ddi immunogens, and the post-immune sera from the Ddi vaccinated reindeer mitigated CWD propagation in a cell culture model (CWD-RK13). Taken together, our study provides very promising vaccine candidates against CWD, but further studies in cervids are required to investigate vaccine efficacy in the natural CWD hosts.

4.2. Introduction

Prion diseases are fatal transmissible spongiform encephalopathies (TSEs) in human and animals characterized by distinctive spongiform appearance and neuronal loss in the brain. These diseases are caused by accumulation of the pathological isoform (PrP^{Sc}) of the cellular prion protein (PrP^{C}) [1, 2, 422]. CWD is considered the most contagious prion disease and affects both free-ranging and farmed cervids (deer, elk, moose and reindeer) [99, 423-425]. Firstly described and reported to be a prion disease in USA, until now it has been detected in North America, South Korea and recently in Norway and Finland [100, 101, 426]. The substantial shedding of CWD prion infectivity via urine, feces and saliva into the environment and prion resistance for many years are driving forces for CWD transmission [109, 147, 376]. Due to the horizontal transmission nature of the disease via mucosal/oral route and the occurrence in wildlife, the control of disease spread is extremely challenging. Moreover, the potential of zoonotic transmission into humans is an alarming issue and is still an open question [427, 428]. Yet, studies have shown its transmissibility into non-human primates (squirrel monkeys), both by intracerebral and oral route [128, 429]. There are no preventive or therapeutic measures available against CWD, like it is the case for other prion diseases (Creutzfeldt-Jakob disease (CJD) in humans, scrapie in sheep and bovine spongiform encephalopathy (BSE) in cattle.

The concept of active and passive immunization has already been introduced for prion disease, and reduced prion propagation *in vitro* and *in vivo* and prolonged the incubation period in murine adapted scrapie prion models after immunization [359, 361-363, 430, 431]. Vaccination in prion disease would be useful to prevent peripheral infection before prions reach the brain, as the vast majority of antibodies cannot cross the blood brain barrier (BBB) [361, 432]. Of note, targeting cellular PrP in active immunization is complicated by the necessity to overcome self-

tolerance against PrP and by the risk to induce thereby undesirable side effects. However, there is already a proof-of-concept that active immunization can break the self-tolerance against host prion protein to produce auto-antibodies, without inducing side effects [359, 395, 433].

For CWD, there is a very limited number of studies investigating active immunization. A study has reported that active vaccination with synthetic peptides against CWD was not successful in terms of protection in mule deer [364]. However, another study reported partial protection against orally challenged CWD infection (around 20%) provided by oral vaccination of white-tailed deer with attenuated *Salmonella typhimurium* vaccine expressing cervid PrP [365]. A recent study described a potential CWD vaccine consisting of a non-replicating human adenovirus which expresses a truncated rabies glycoprotein G fused with postulated disease specific epitopes (DSEs), here the rigid loop region (hAd5:tgG-RL). This vaccine was successful in inducing humoral immune responses, both systemic and mucosal, upon oral immunization of white-tailed deer [368].

Our objective in this study was to develop a CWD vaccine which overcomes self-tolerance and induces self-antibodies against cervid prion protein to impede peripheral prion infection. For this purpose we used multimeric and aggregation-prone recombinant PrPs (both mouse and deer), as our lab had already provided a proof-of-principle that this approach can induce a robust humoral immunity against PrP^{C}, both mouse and cervid [359, 395, 433], and protect some immunized mice against scrapie challenge [363]. In the current study, we tested these recombinant immunogens for their potential to induce immune responses in transgenic mice expressing elk PrP (TgElk) and in reindeers, and then studied the vaccination effect in TgElk mice against CWD challenge.

4.3. Experimental Procedures

4.3.1. Ethics statement

The animal use in the experiments strictly followed the guidelines of the Canadian Council for Animal Care (CCAC). The animal protocol was approved by the institutional Health Sciences Animal Care Committee (HSACC). For vaccination of mice the protocol was under the number AC14-0122, and for reindeer it was AC17-0088.

4.3.2. Reagents and antibodies

Proteinase K (PK) and Pefabloc (PK inhibitor) were commercially obtained from (Roche, Germany). Primary antibodies used were as follows: anti-PrP mAb 4H11 [373], anti-PrP mAb 8H4 (Sigma, USA), anti-PrP mAb BAR224 (Cayman Chemical, USA) and anti-β-actin (Sigma Aldrich, USA). As secondary peroxidase-conjugated antibodies, goat anti-mouse horseradish peroxidase (HRP) (Jackson ImmunoResearch/USA) and rabbit anti-deer HRP (KPL, USA) were used.

4.3.3. Mice

The transgenic mouse line used in this study (TgElk mice) were kindly provided by Dr. Debbie McKenzie, Centre for Prions and Protein Folding Diseases, University of Alberta, Edmonton, Canada. The development of transgenic mice, genotyping, maintenance of homozygous line for the Rocky Mountain elk (*Cervus elaphus nelsoni*) PrP and their susceptibility to CWD prions have been described previously [434]. In our facility, the transgenic line was maintained on homozygous background and only female mice were used in this study.

4.3.4. Immunogen preparation

The preparation of immunogens is described elsewhere [395]. Briefly, pQE30 (Qiagen) expression vector was used to express the monomeric and dimeric constructs in *Escherichia coli* strain BL21-Gold(DE3) pLysS (Stratagene) as previously described [359, 433]. Ni-NTA superflow resin beads (Quiagen) was used to separate His-tagged proteins from the bacterial lysate. After elution and refolding of protein by dialysis, the concentration of protein was determined using the BCA kit (Pierce, ThermoFisher Scientific, Rockford, IL, USA).

4.3.5. Mice vaccination and prion challenge studies

The female TgElk mice used in the study were immunized via subcutaneous (sc) route by injecting 100 µg protein/mouse, starting with 4 to 6 week-old mice. After this first priming dose, each mouse was subjected to four booster doses of 50 µg, each within 3-weeks interval. The oligodeoxynucleotide CpG (5 µM) (InvivoGen, San Diego, CA, USA) was used as an adjuvant for all immunogens and the control group received only CpG. The bleeding schedule for all mice was maintained twice, before immunization (zero sera) and 10 days after the last boost (post-immune sera). Five days after the post-immune bleeding, all mice were inoculated with mouse-adapted elk CWD prions by injecting 100 µl of 1% brain homogenate (BH) intraperitoneally (ip). The inoculum was obtained from terminal prion-sick TgElk mice inoculated with elk CWD intracerebrally. For the preparation of BH, mouse brains were homogenized in PBS at a final concentration of 10 % (w/v) and stored at -80°C. Two booster doses were given to each mouse after prion inoculation at 6-week intervals. The mice were monitored daily after start of first disease signs. Two researchers were involved in monitoring animals, recording and scoring clinical signs, and making decision for euthanasia of animals. The weight of animals was also recorded

every day. Brain and spleen samples were collected from terminally sick mice, 10% homogenate was prepared using PBS and kept at -80°C until use. Half of the brain from each animal was kept in formalin for histology examination.

4.3.6. Reindeer immunization study

Seven reindeers (*Rangifer tarandus*) accommodated in the Veterinary Sciences Research Station (VSRS) at the University of Calgary Spy Hill Campus were vaccinated 3 times with either Mdi (4 animals) or Ddi (3 animals) immunogens with 4-week intervals (one priming and two booster doses). The animals were immunized with 500 µg of Mdi or Ddi with 5µM CpG added as adjuvant via sc route with animals being restrained in chutes. Animals and injection sites were monitored for any adverse effects of immunization. Blood sampling was performed either before starting vaccination (pre-immune) or 21 days after the second booster dose (post-immune).

4.3.7. Enzyme linked immunosorbent assay (ELISA)

ELISA was done following the procedure described previously [395]. Briefly, 1 µg recombinant protein in sodium-carbonate buffer (pH 9.5) was used to coat the wells of high binding 96-well plates (Greiner Bio-One GmbH- Frickenhausen-Germany) for overnight. Blocking was done using 3% bovine serum albumin (BSA) in PBS containing Tween X-100 (PBST) for 2 h at 37°C after washing with PBST. A serial dilution of sera in 3% BSA was prepared and plates were incubated with sera for 1h. Following the washing step, either HRP-labeled anti-mouse-IgG antibody (Jackson Immuno-research Lab, West Grove, PA, USA) or rabbit anti-deer HRP (KPL, USA) was added as secondary antibody. ABTS (2,2'-Azino-bis(3-Ethylbenzthiazoline-6-Sulfonic

Acid) peroxidase (KPL, Gaithersburg, USA) was used as substrate for signal detection and OD was measured at 405nm using a BioTek Synergy HT reader.

4.3.8. Cell culture experiments and PK digestion

Cervid PrP expressing RK13 cells (cerRK13) were kindly obtained from Dr. Glenn Telling's lab (Colorado State University, Fort Collins, Colorado, USA). DMEM media (GIBCO, Rockford, IL, USA) with 10% fetal bovine serum (FBS), 1% penicillin/streptomycin, 1µg/ml puromycin and 200 µg/ml G148 was used for maintenance of cerRK13 cells. To boost the infection, cells were infected again with 10% brain homogenate (BH) from white-tailed deer CWD-infected terminally sick Tg (cerPrP) 1536 +/+ mice and this persistently infected CWD-cell culture model was used for cell experiments. Cells were cultured in medium with a 1:100 dilution of sera from Mdi or Ddi vaccinated reindeer, and pre-immune sera were used as control. After 5 days, cells were lysed in cold lysis buffer (10 mM Tris-HCl, pH 7.5; 100 mM NaCl; 10 mM EDTA; 0.5% Triton X-100; 0.5% sodium deoxycholate (DOC)) and lysates were digested with 20 µg/ml PK at 37°C for 30 min. PK digestion was blocked using 0.5 mM Pefabloc and samples were subjected to methanol precipitation. Precipitated proteins were dissolved in TNE buffer (50 mM Tris-HCl pH 7.5; 150 mM NaCl; 5 mM EDTA).

4.3.9. Sodium phosphotungstic acid (NaPTA) precipitation

BH or spleen homogenate (SH) was prepared in PBS using a gentle MACs Dissociator (Miltenyl Biotech) in a 10% w/v dilution. For immunoblotting and RT-QuIC, 250 µl and 50 µl, respectively of BH or SH was mixed with sarcosyl to make the final concentration to 2%, and incubated by shaking at 37°C for 30 min. For immunoblotting, BH was digested with 40 µg/ml

PK at 37°C for 30 min before adding sarcosyl; for SH 50 µg/ml PK was used for 1h. Then, 0.5 mM Pefabloc was added to stop PK digestion. After incubation in sarcosyl, 1/12.5 volume of sodium phosphotungstic acid (NaPTA) stock solution (20 mM phosphotungstic acid, 400 mM MgCl2, 200 mM NaOH; pH: 7.4) was added and incubated at 37°C for 2 h by shaking. Following centrifugation at 21,000 x g for 30 min at 8°C, the pellet was washed with cell lysis buffer (10 mM Tris-HCl, pH 7.5; 100 mM NaCl; 10 mM EDTA; 0.5% Triton X-100; 0.5% sodium deoxycholate) containing 1% sarcosyl. The solution was again centrifuged for 15 min and the pellet was either dissolved in RT-QuIC seed dilution buffer for RT-QuIC or in sample buffer for immunoblotting.

4.3.10. Immunoblotting

Immunoblot analysis was performed as mentioned in our previous studies [395]. Briefly, protein precipitated from cell lysate, BH or SH after NaPTA precipitation was separated on 12.5% SDS-PAGE. The electroblotting was done on Amersham Hybond P 0.45 PVDF membranes (Amersham, USA) and analyzed using Luminata Western Chemiluminescent HRP Substrates (Millipore, USA). ImageJ software was used to perform densitometric analysis.

4.3.11. Real-time quaking induced conversion assay (RT-QuIC)

RT-QuIC was performed as previously described, including the procedure for preparation of recombinant prion protein using a bacterial expression system [376, 395]. Briefly, master mix was prepared with 20 mM Na-phosphate (pH 7.4), 300 mM NaCl, 1 mM EDTA, 10 µM Thioflavin T (ThT) and 0.1 mg/ml mouse rPrP substrate, from which 98 µl was taken in each well of a black-walled 96-well optical bottom plate (Nalge Nunc International, Nunc, USA). Either BH after NaPTA precipitation, SH without NaPTA precipitation or cell lysates were used at tenfold serial

dilutions in seed dilution buffers. Reactions included 2 µl of seed in each dilution and were set up in quadruplicate. After sealing with Nunc Amplification Tape (Nalge Nunc International), plates were incubated in a FLUOstar Omega (BMG Labtech, Cary, NC, USA) plate reader for 30 h at 42°C at 1 min shaking (700 revolutions per min) and 1 min rest cycle. Finally, fluorescence measurements (450 nm excitation and 480 nm emission) obtained every 15 min were averaged from four replicate wells and plotted against reaction time. A positive and a negative control were run on each plate. A reaction cut-off was calculated as average fluorescence of the negative controls plus 5× standard deviation (SD). Reactions were considered positive when >2 replicates out of 4 were reactive (>cut-off).

4.3.12. Immunohistochemistry (IHC)

The immunohistochemical analysis of brain sections was kindly performed by the Histology Core Facility at the Centre for Prions and Protein Folding Diseases, University of Alberta, following the procedure as described previously [435]. Briefly, formalin fixed and paraffin embedded brain tissues were sectioned (4.5 to 6 µm thick) to get sagittal sections on colorfrost plus slide (Thermofisher, USA) and left overnight at 37°C. The slides were used for immunostaining and hematoxylin and eosin staining (H&E) to investigate the deposition of PrP^{Sc} (CWD) and spongiform changes, respectively. Anti-PrP monoclonal antibody BAR224 (Cayman Chemical, USA) was used for PrP^{Sc} staining at a dilution of 1:2000. Brain slides were deparaffinised and hydrated using xylene and ethanol dip cycles (100%-70% ethanol) and then heated at autoclaving temperature (121°C) and pressure in 10mM citric acid buffer (pH 6.0) for 30 min. The slides were cooled at room temperature and incubated in 98% formic acid for 30 min followed by treatment with 4M guanidine thiocyanate for 2 h at room temperature. 3% hydrogen

peroxide was used to remove endogenous peroxidase activity in the tissue. Biotinylation of antibody was done using a kit (DAKO ARKTM, ARK animal research kit) following the manufacturer's protocol and slides were incubated in antibody for overnight at 4°C in humidifying chamber. Immunostaining detection was done using a streptavidin-peroxidase system (Invitrogen, USA) and DAB (BD Pharmingen, USA) for enzymatic activity detection. Tissue sections were incubated in Mayers hematoxylin (Thermofisher, USA) for counterstaining and scanned using a NanoZoomer 2.0RS scanner (Hamamatsu Photonics, Japan). NanoZoomer digital pathology software (Hamamatsu Photonics, Japan) was used for image processing.

4.3.13. Statistical analysis

Statistical analysis was done using GraphPad Prism (Graph Pad software Inc., V 7.03, USA.) using nonparametric Kruskal-Wallis test for multiple comparisons among groups. Statistical significance for the immunoblots was expressed as (mean ± SEM). The percent survival was plotted in Kaplan-Meier plot and Log-rank (Mantel-Cox) test was performed for statistical difference between groups. *: $p \leq 0.05$, **: $p \leq 0.01$ considered significant.

4.4. Results

4.4.1. Anti-PrP antibody induction in TgElk mice following immunization with recombinant mouse and deer PrP-based immunogens

TgElk mice used in this study are homozygous for elk PrP and express 2.5 times more PrP in the brain than do WT mice [434]. These mice were vaccinated with one of four recombinant PrP immunogens: Mmo, Mdi, Dmo, and Ddi. The structure and immunogenicity of these immunogens have been well described by our group [359, 395, 433]. Each vaccine preparation

consists of type B CpG as an adjuvant in order to overcome the self-tolerance against PrP. The control group received CpG only. The vaccination strategy in Fig. 4.1 A included one priming dose containing 100 ug of protein mixed with 5 uM CpG, followed by four boosting doses (50 ug protein and 5 uM CpG), each dose given subcutaneously at four-week intervals until intraperitoneal CWD prion inoculation. Following prion inoculation, two boosting doses were given to the mice six weeks apart.

In order to test the ability of the immunogens to induce anti-PrP antibodies in the mice, we used ELISA and investigated the immunoreactivity of post-immune sera from the vaccinated and control animals against deer rPrP. We found that all the immunogens were successful in producing high titres of anti-PrP antibodies in the vaccinated animals as shown in Fig. 4.1 B. However, Ddi induced the lowest antibody titre, indicating that self-immunogens are less efficient in inducing a humoral immune response and overcoming self-tolerance against cervid PrP expressed in our TgElk mouse model. Moreover, in the immunoblot, we were able to detect the elk PrP present in the BH of elk CWD-infected TgElk mice using the post-immune sera from all vaccinated groups as a primary antibody. Interestingly, the sera from Mdi-vaccinated group was more efficient in detecting both total PrP (-PK) and elk CWD PrP^{Sc} (+PK) (data not shown).

Taken together, all four immunogens used to vaccinate the animals successfully induced generation of anti-PrP antibodies in TgElk mice, which showed immunoreactivity against both recombinant and native cervid PrP.

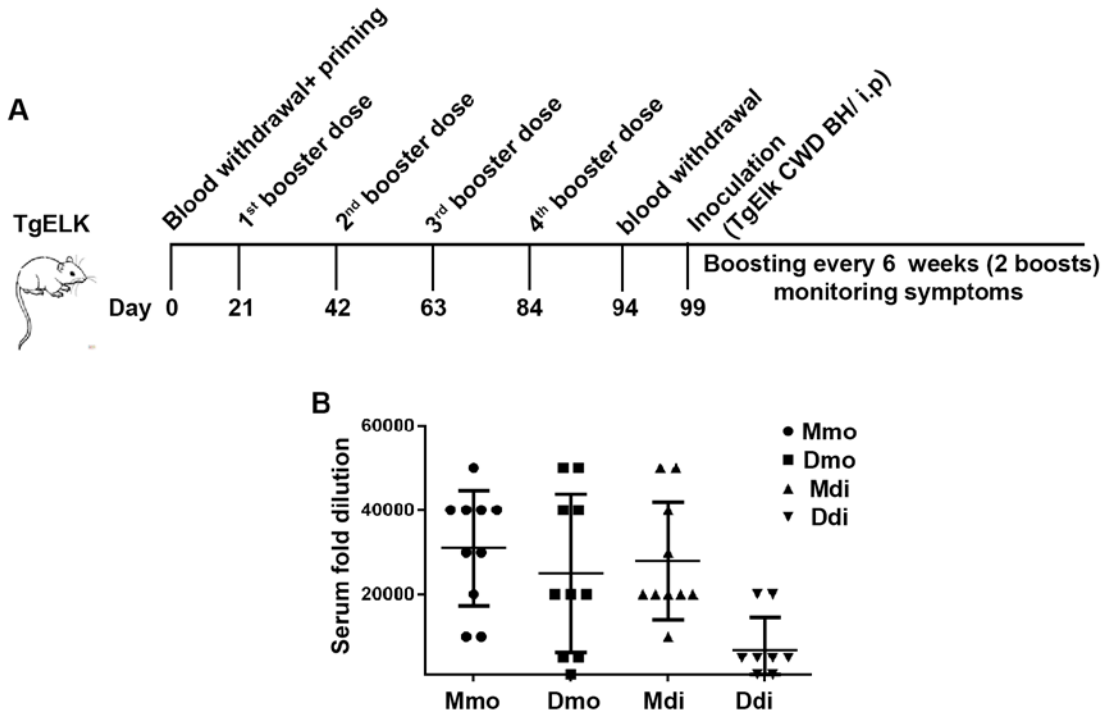

Figure 4. 1. High antibody titres produced by immunization of TgElk mice with monomeric or dimeric recombinant PrP. (A) TgElk mice were immunized with four different immunogens at three-week intervals five times (one priming and four booster doses), and blood sampling was performed either before starting vaccination or 10 days after the fourth booster dose. The animals were inoculated ip at day 99 with 1% brain homogenate (BH) from terminally ill CWD-infected TgElk mice and the animals received two more booster doses post-inoculation at six-week intervals. (B) Antibody titres using end-point ELISA from the four vaccinated groups. Mice were vaccinated with Mmo-, Dmo-, Mdi-, or Ddi-recombinant PrPs, and CpG was used as adjuvant for all groups. The antibody titre for each individual mouse was determined by end-point dilution. The y-axis indicates the serum fold dilution. The cut-off was calculated as three times the average optical density (OD) (405 nm) of the pre-immune sera.

4.4.2. Vaccination leads to significant prolongation of survival time in vaccinated animals as compared to controls

We next investigated the efficiency of the vaccination-mediated anti-PrP antibodies in protecting the animals against a CWD challenge. Following the post-immune sera collection, we inoculated all the mice with 1% BH from terminally ill TgElk mice infected with elk CWD through the ip route. The animals were monitored for the clinical disease and survival time was recorded for each animal. As the rationale behind our vaccination strategy is to achieve interference in prion replication at the periphery before prions invade the nervous system, we utilized the ip route for CWD inoculation. Of note, the antibodies cannot cross the BBB under normal circumstances [436]; thus, interference before neuroinvasion is beneficiary. Moreover, the ip infection route is preferred to the ic route to mimick the natural CWD infection route.

A complete attack rate was seen after the ip infection of TgElk mice with mouse-adapted CWD prions; all animals displayed similar progressive clinical signs including ataxia, severe weight loss, uncoordinated and slow movement, kyphosis, and dragging of the hind limbs. However, the animals differed in the survival time. The mean survival period of all vaccinated and control groups is shown in Table 4.1. All of the vaccinated groups showed remarkable prolongation in survival time as compared to the control group (CpG), as shown in Fig. 4.2. Among the groups, the Mmo-vaccinated one accounted for a 60% increased survival time as compared to that of the CpG group (Fig. 4.2 A), for which the difference in survival was statistically significant (Mmo vs CpG; $p=0.0002$). Similarly, when compared to that of CpG group, the Dmo and Ddi-vaccinated groups showed a 28.4% and 24.1% increase in survival time respectively (Fig. 4.2 A and B). Although the difference in survival time between the Ddi-vaccinated and CpG group was found to be statistically significant (Ddi vs CpG; $p=0.031$), this was not the case for the Dmo-

vaccinated group (Dmo vs CpG; *p=0.0509*). The least effective vaccinated group in terms of survival time against CWD was the Mdi-vaccinated group which exhibited only a 15.9% increase in survival time (Fig. 4.2 B) which was not significant statistically (Mdi vs CpG; *p=0.198*).

Although all of the vaccinated animals, like the control, succumbed to terminal prion disease, the survival times varied greatly with the vaccinated animals showing a prolongation in survival up to 60%, for example in the Mmo group. Once the mice reached the terminal stage, there was no notable difference in clinical signs among the groups.

Table 4. 1. Mean survival time and attack rate of the TgElk vaccinated groups

Vaccination groups	**Attack rate**	**Survival time (dpi) (Mean±SEM)**
CpG	10/10	114.8±10.0
Mmo	10/10	183.6±8.8
Mdi	10/10	133.1±15.0
Dmo	9/9	147.4±13.4
Ddi	8/8	142.5±5.8

Mmo: mouse monomeric recombinant PrP; Mdi: mouse dimeric recombinant PrP; Dmo: deer monomeric recombinant PrP; Ddi: Deer dimeric PrP; dpi: days post CWD inoculation

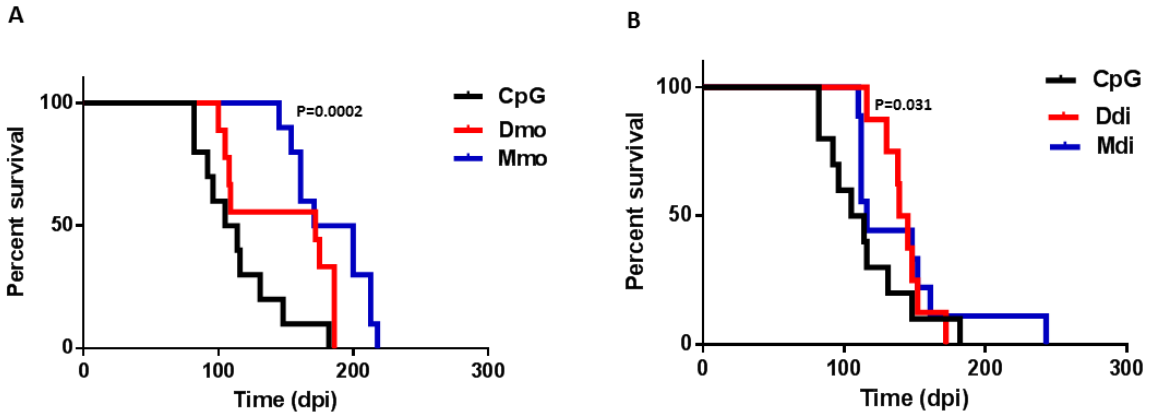

Figure 4. 2. Immunization with monomeric or dimeric recombinant PrPs prolongs the survival in a CWD-infected TgElk mouse model. (A-B) Kaplan-Meier survival curves of Dmo-, Mmo-, Ddi- and Mdi-vaccinated groups compared to control group (CpG-only) of female TgElk mice, inoculated via ip route with 1% BH of terminally ill CWD-infected TgElk mice. (A) The CpG control group, n=10, median incubation time 109 days post inoculation (dpi). Dmo-vaccinated group, n=9, median incubation time 172 dpi (*p=0.0509*; log rank test). Mmo-vaccinated group, n=10, median incubation time 185 dpi (*p=0.0002*; log rank test). (B) CpG control group, n=10, median incubation time 109 dpi. Ddi-vaccinated group, n=8, median incubation time: 142 dpi (*p=0.031*; log rank test). Mdi-vaccinated group, n=10, median incubation time 116 dpi (*p=0.198*; log rank test).

4.4.3. PK-resistant PrP^{CWD} in the brain of intraperitoneally infected TgElk mice show similar electrophoretic profile as that of inoculum

Further characterization of the CWD infection in TgElk via the ip route was achieved by accessing the brain of terminally sick mice using various read-outs. The immunoblot analysis showed the presence of PrP^{Sc} in the brain homogenate following PK digestion and a NaPTA

concentrating step (Fig. 4.3 H). We found no difference in the PK-digested PrP^{CWD} signature in the brain of ip-infected TgElk and in the inoculum. Next, RT-QuIC was utilized to investigate the prion conversion activity *in vitro* of PrP^{CWD} present in the brain. The BH from the terminally sick mice in our study demonstrated prion conversion activity in RT-QuIC after NaPTA precipitation. Representative ThT fluorescence curves from each vaccinated and control group are shown in Fig. 4.3 C-G. For negative and positive controls, a mock BH from an uninfected TgElk mouse and BH from terminally sick TgElk mice infected with elk-CWD prions through the ic route respectively were used (Fig. 4.3 A and B). Interestingly, when initially the crude BH from ip infected TgElk mice was used in the RT-QuIC assay, very weak positive signals were obtained (Fig. S4.1). Using the NaPTA purification method allowed us to have a better seeding activity signals (Fig. 4.3 and Fig. S4.1). Unlike the brain, the RT-QuIC analysis of SH obtained from clinically sick ip-infected TgElk mice demonstrated strong conversion activity without the need for NaPTA enrichment. Signals were comparable to that of SH from ic-infected TgElk mice (Fig. S4.2). Moreover, an immunoblot of SH revealed the presence of PK-resistant PrP^{Sc} in the spleen of ip-infected TgElk mice as shown in Fig. S4.2 H, suggesting a substantial amount of infectivity in the spleen of TgElk mice following the ip infection.

Furthermore, PrP^{Sc} deposits were detected in the brain sections from ip-infected vaccinated and control TgElk mice in IHC analysis. The representative IHC staining image of brain sections from both Mmo-vaccinated and CpG-control mice is shown in Fig. 4.3 I and K. The PrP^{Sc}-positive staining was predominantly found in the prefrontal cortex, temporal lobes, and occipital lobe. H&E staining revealed the spongiform neuropathology in the brain sections with no difference between the vaccinated and CpG control group (Fig. 4.3 J and L). Of note, all the animals were euthanized at their terminal clinical stage. No characteristic difference could be detected in terms of PrP^{Sc}

staining patterns and distribution as well as the degree of spongiform changes in the brains of the vaccinated and control mice.

In summary, ip CWD-infection of TgElk mice results in prion pathogenesis as demonstrated by immunoblot, RT-QuIC, and IHC analysis. There was no difference in PrP^{Sc} deposition between the vaccinated and control groups during their terminal disease stage.

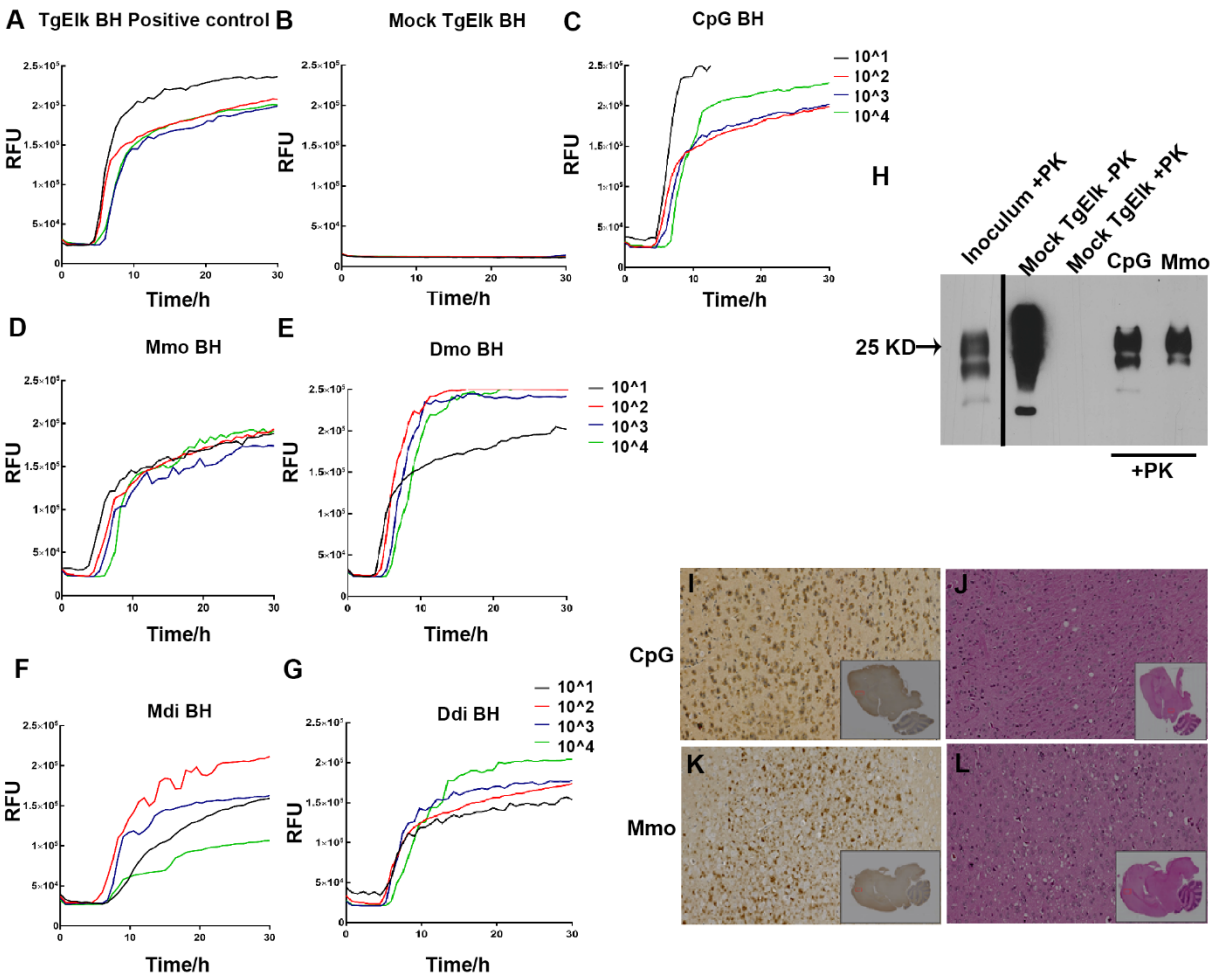

Figure 4. 3. Prion conversion activity and PrP^{Sc} in brain homogenates of ip-inoculated TgElk mice. (A) CWD positive control for RT-QuIC in which the seed was 10% brain homogenate (BH) of ic-inoculated TgElk mouse (terminally ill) after NaPTA enrichment. (B) Brain homogenate of an uninfected TgElk mouse purified using NaPTA was used as a negative control. (C-G) RT-QuIC

assay of one representative BH from every group upon NaPTA enrichment (C) CpG-only, (D) Mmo-, (E) Dmo-, (F) Mdi-, and (G) Ddi-immunized groups. Mouse rPrP was used as substrate for all reactions. Four tenfold dilutions of seed were analyzed (10^{-1} to 10^{-4}), and each curve plotted as an average of four technical replicates against time. (H) Western blot analysis using mAb 8H4 of brain homogenate samples (CpG and Mmo-vaccinated mice) treated with PK followed by NaPTA enrichment. The inoculum is brain homogenate from a terminally ill TgElk mouse which was ic-infected with elk CWD. Mock-infected TgElk brain homogenate was used as a negative control. (I, K) Immunohistochemistry for PrP^{Sc} using a BAR224 antibody in representative brain sections from the CpG control group (I) and Mmo-vaccinated group (K). The sections showed positive staining in different areas of the brain. High magnification (20X) areas are shown by boxes in the whole hemisphere sagittal section inlet. (J, L) The brain sections were stained with hematoxylin and eosin to detect spongiform pathological changes in sections from one representative CpG control (J) and one representative Mmo-vaccinated brain (L).

4.4.4. Anti-PrP antibody response in reindeer to vaccination with multimeric immunogens

After achieving successful vaccination in a TgElk mouse model with recombinant PrP immunogens, we tested the immunogenicity of the dimeric PrP immunogens in reindeer. A reindeer is a relevant large animal model for CWD. Table 4.2 shows the *Prnp* genotypes of the reindeer used in this study. We vaccinated seven reindeer subcutaneously with three doses given four weeks apart. Each dose consisted of 500 µg/animal of either Mdi (n=4) or Ddi (n=3) immunogen along with CpG as an adjuvant. The schematic for the vaccination strategy is depicted in Fig. 4.4 A. The ELISA assay using the pre- and post-immune sera was performed to determine the titres of anti-PrP antibodies in the vaccinated animals. We found that there was successful

induction of humoral immune response against PrP in all four Mdi-vaccinated reindeer (Fig. 4.4 B). However, in the Ddi group sera, one animal out of three showed the presence of anti-PrP antibodies (Table 4.2). Interestingly, this responding reindeer in the Ddi group had two polymorphisms in cellular PrP at position 176 and 225 as shown in Table 4.2, while the other two reindeer exhibited wild-type PrP. These polymorphisms might have an influence in the animal responding to the vaccination and could result in shifting the Ddi immunogen, to some extent, towards being less non-self when compared to the host cellular PrP.

When the antibody titre in animals from the two groups was compared using end-point ELISA, Mdi-vaccinated animals had higher titres, even up to 1/5000, while Ddi-vaccinated animals had low or undetectable titres as indicated in Table 4.2. Although this result suggests that the non-self Mdi immunogen was more effective in inducing a PrP-specific humoral immune response than Ddi under the indicated vaccination conditions, it was the Ddi-induced anti-PrP antibodies in the sera which had higher efficiency for the detection of recombinant deer PrP in an immunoblot (Fig. 4.4 C).

The protective effect of vaccination against CWD was not tested in reindeer, as our facility does not allow this. It is noteworthy that no vaccine-induced unwanted side-effects were observed in these reindeer.

Taken together, our vaccination study in reindeer demonstrated the ability of our dimeric recombinant PrP immunogens to overcome self-tolerance, even in a large animal model.

Table 4. 2. Vaccinated reindeer genotypes and response to immunogens

Deer ID	Genotype	Immunogen	Antibody titre (Serum fold dilution)
2S	WT	Mdi	1/5000
15S	225Y	Mdi	1/100
X	225Y+138 N	Mdi	1/1000
2Y	225Y	Mdi	1/1000
3WD	225Y+176D	Ddi	1/100
3YD	WT	Ddi	NR
5XD	WT	Ddi	NR

WT: wild-type; Mdi: dimeric mouse recombinant PrP; Ddi: dimeric mouse recombinant PrP; NR: non- responder; Y: tyrosine; N: asparagine; D: aspartic acid. The antibody titre for individual deer was determined by end-point dilution. The cut-off was calculated as 3 times average OD (405 nm) of pre-immune sera.

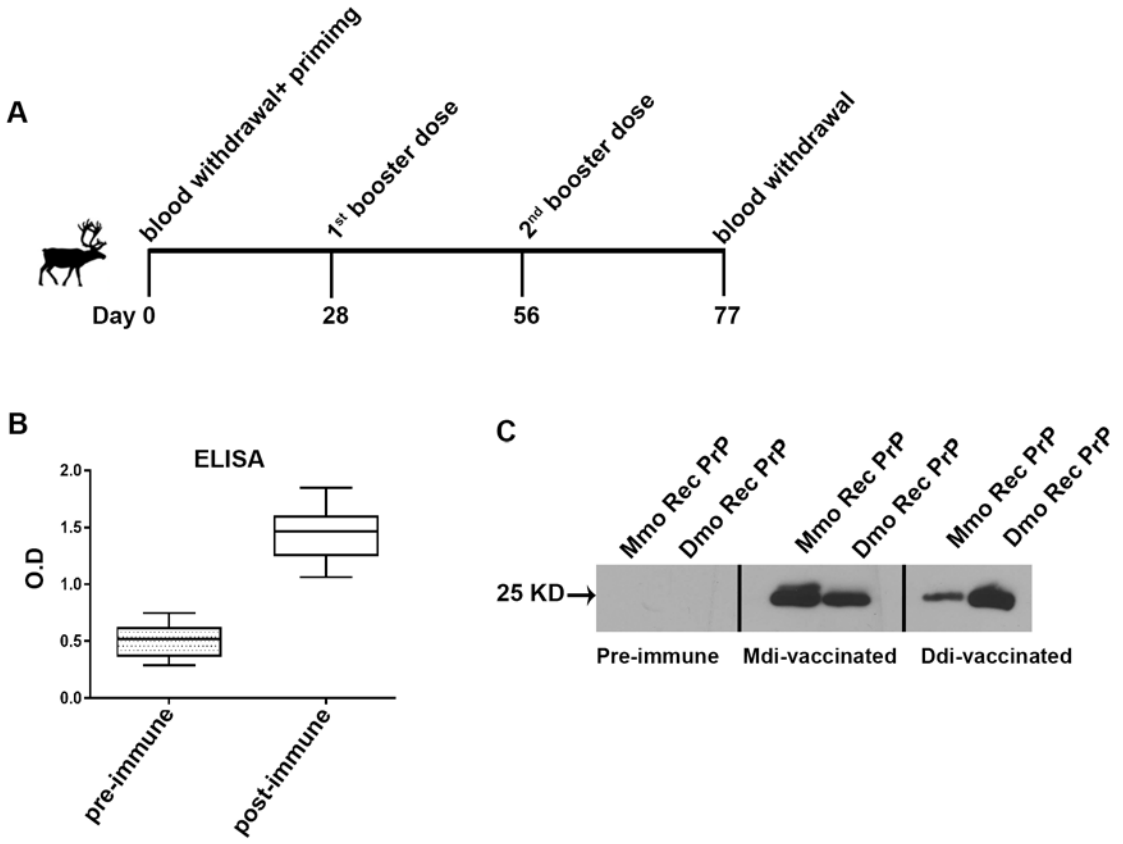

Figure 4. 4. Immunization of reindeer with dimeric recombinant PrP induces anti-PrP antibodies. (A) Seven reindeer were vaccinated three times with either Mdi (four animals) or Ddi (three animals) immunogens at four-week intervals (one priming and two booster doses) and blood sampling was performed either before starting vaccination (pre-immune) or 21 days after the second booster dose (post-immune). (B) ELISA for post-immune sera of the Mdi-vaccinated reindeer (1:100 dilution shown), compared to the respective pre-immune sera. The y-axis represents the optical density (405 nm). (C) Both mouse and deer monomeric recombinant PrP were subjected to immunoblot analysis. As primary antibodies, the pre-immune sera (reindeer ID: 15S) and post-immune sera of reindeer vaccinated with Mdi (reindeer ID: 15S) or Ddi (reindeer ID: 3WD) immunogens with comparable post-immune antibody titres, all in 1:500 dilution, were used.

4.4.5. Anti-PrP antibodies from Ddi-vaccinated reindeer reduce prion propagation in CWD-infected RK13 cells

Given the lack of a bioassay for testing the protective effect of reindeer vaccination against CWD, we investigated the efficacy of sera from vaccinated reindeer in reducing CWD propagation *in vitro*. The cervid PrP-overexpressing RK13 cells persistently infected with CWD prions were treated with sera from either Mdi- or Ddi-vaccinated reindeer and pre-immune sera was used as a control. After treatment with sera from the Ddi-vaccinated reindeer, PrP^{Sc} was significantly reduced in the cells, as detected in the immunoblot. This was not the case with sera from the Mdi-vaccinated animals (the group which had the highest PrP-specific antibody titre). The decline in PrP^{Sc} in the Ddi-vaccinated reindeer cells was even seen upon cell passaging (Fig. 4.5 A-D). Furthermore, the RT-QuIC analysis suggests less seeding activity of the cell lysates from cells treated with sera from Ddi-vaccinated reindeer than those from Mdi-vaccinated animals (Fig. 4.5 E and F). This might be due to the strong ability of PrP-specific antibodies, particularly those produced in reindeer following vaccination with Ddi, to bind to native and authentic cervid PrP^{C}, thereby reducing the prion conversion in CWD-infected RK13 cells.

Thus, these data suggest that self-antibodies induced in vaccinated reindeer significantly reduced CWD prion propagation in a CWD cell culture model.

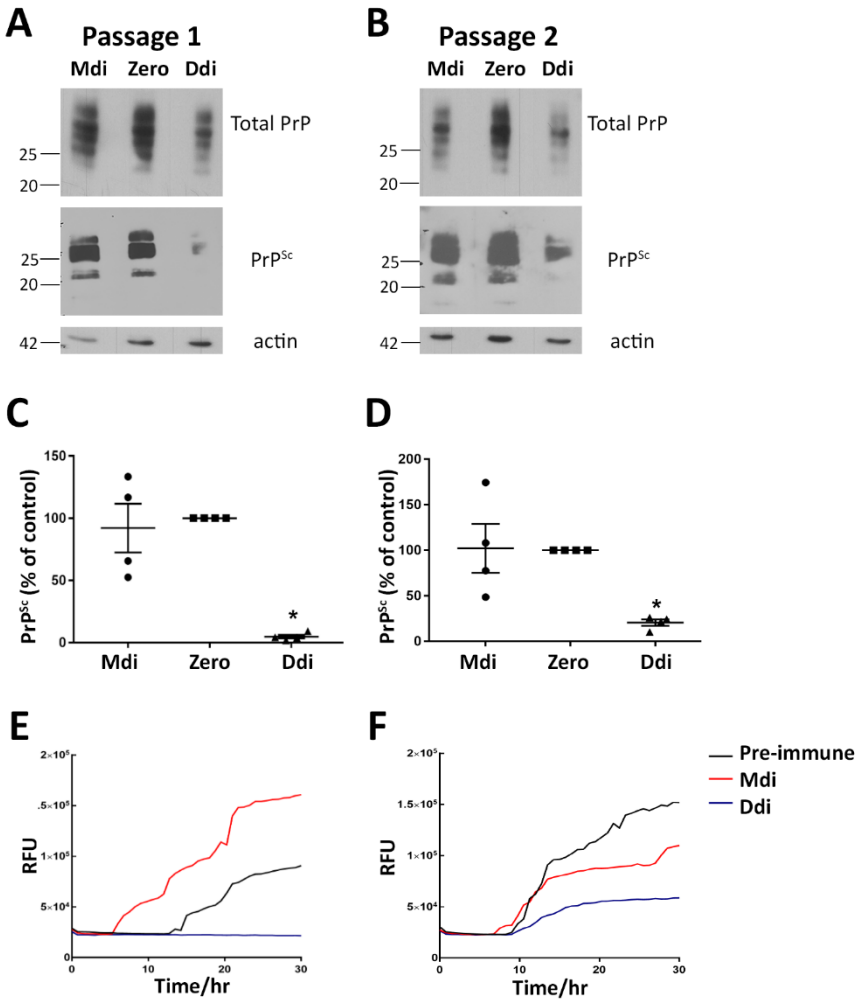

Figure 4. 5. Post-immune sera of Ddi-immunized reindeer reduce PrP^{Sc} propagation in CWD-infected RK13 cells. (A-B) CWD-infected RK13 cells expressing cervid PrP^{C} (CWD RK13) were treated with post-immune sera with comparable titres from reindeer vaccinated with Mdi (reindeer ID: 15S) or Ddi (reindeer ID 3WD), while passaging the cells every seven days for two passages. Treatment with pre-immune sera (here denoted as zero time sera) from reindeer ID: 15S was used as a control. Sera were used at a dilution of 1:100 in culture media. Cells from every passage were lysed and subjected to PK digestion (+PK) or not (-PK). The lysates were immunoblotted with mAb 8H4, and actin was used as a loading control. (C-D) Densitometric

analysis of immunoblots from treated CWD RK13 cells. Data are represented as a percentage of control (pre-immune sera) and normalized with the amount of actin. * $p \leq 0.05$ is considered significant. (E-F) RT-QuIC assay was performed on passages 1 (E) and 2 (F) of CWD-RK13 cells treated with post-immune sera from reindeer vaccinated with Mdi or Ddi. Treatment with pre-immune sera (zero) was done for comparison. Post-nuclear lysates were used as seeds and mouse recombinant PrP as substrate for RT-QuIC. The seeding activity at the 10^{-4} dilution was used for comparative analysis (shown here). The y-axis shows relative ThT fluorescence units (RFU). The x-axis represents time in hours.

4.5. Discussion

In our study, we vaccinated the TgElk mice using recombinant multimeric PrP immunogens along with CpG as an adjuvant against intraperitoneal CWD infection, and achieved prolongation of survival in the vaccinated animals. All the immunogens induced systemic PrP-specific antibodies as measured in ELISA. Both recombinant mouse monomeric and dimeric PrP vaccination resulted in a higher antibody titre as compared to deer PrP. This difference may be due to the less self-nature of mouse immunogen in TgElk mice, compared to deer immunogen. Despite the amino acid sequence homology between mouse and deer PrP, variation in 20 amino acids may have led to a difference in the induction of the humoral immune response in the animals. This scenario was seen not only in the mouse model, but also in the cervid model, i.e., in reindeer, where Mdi was more efficient in producing higher antibody titres in all vaccinated animals than Ddi that resulted in low or undetectable anti-PrP antibody production. Similar to our results, achieving induction of the humoral response in the cervid model through vaccination has been reported by various groups using different vaccination strategies [364, 365, 368]. A study was

reported where intramuscular injection with synthetic peptides conjugated to blue carrier protein in mule deer produced a strong antibody response measured at five weeks post-vaccination [364]. Similarly, another study, including oral vaccination of white-tailed deer with attenuated *Salmonella* expressing PrP, resulted in the generation of anti-PrP antibodies in the host [365].

Infection with prion agent, unlike classical pathogens, does not elicit any detectable immune response in the host, due to the fact that the pathogenic PrP^{Sc} shares the same primary sequence as PrP^{C}. This challenges the development of an effective vaccine against CWD that aims to overcome the self-tolerance to PrP in the host, which could be an effective strategy for CWD vaccine development. Yet breaking the self-tolerance could lead to auto-immunity-related side effects, which needs to be assessed [437]. In the line with CWD vaccine development, several approaches have been introduced to break the self-tolerance in cervids by using peptide-conjugates, attenuated *Salmonella*-expressing cervid PrP, or two tandem copies of mouse PrP and non-replicating human adenovirus expressing a truncated rabies glycoprotein G fused with postulated DSEs [364, 365, 368]. Likewise, in our study, we used both monomeric and dimeric forms of either mouse or deer recombinant PrPs along with an adjuvant, CpG, to break the self-tolerance and induce anti-PrP antibodies in TgElk mice and reindeer. The proof-of-concept regarding the ability of these immunogens to break tolerance to PrP and induce an antibody response in both WT and transgenic mouse models has already been described by our group [359, 395]. Moreover, the post-immune sera effectively reduced the prion propagation in persistently prion-infected cell culture models, including CWD-infected RK13 cells. Furthermore, no detectable side-effect had been seen with these immunogens [359, 395, 433].

The most important finding from our study is the prolongation of survival we identified upon the intraperitoneal CWD challenge in the vaccinated TgElk mice. Our previous study

indicated prolongation of survival in only a fraction of vaccinated mice when WT mice with mouse PrP were vaccinated against mouse-adapted scrapie prions [363]. Interestingly, in the current study, we observed more of a group effect of vaccination rather than an individual effect, where all the vaccinated groups showed increased survival with some variability compared to the control group. Mmo-vaccinated animals showed the highest prolongation in survival compared to the control (CpG only). The increase in mean survival for the Mmo-vaccinated group was up to 60%. Consistently, sera from Mmo-vaccinated animals detected the total TgElk PrP in the immunoblot more efficiently, which could partially explain the efficacy of the Mmo immunogen in increasing the survival in CWD-infected TgElk mice. On the other hand, while the Mdi immunogen induced a high antibody titre in the vaccinated mice, the prolongation in survival time was only 15.9%. In line with this result, a CWD vaccine study in mule deer reported the lack of correlation between ELISA-detected vaccine-induced anti-PrP antibody titres and CWD infection [364]. This is also supported by our previous results using the same immunogens in WT and Tg mice, where a clear indication correlating ELISA-detected antibody titres and PrP^{Sc} reduction in prion-infected cell culture models was lacking [359, 395, 433]. However, the CWD-vaccination study by Goni *et al*. found that the one vaccinated white-tailed deer that showed protection against CWD had the highest anti-PrP antibody titre [365]. The Dmo- and Ddi-vaccinated groups displayed an extension of the mean survival time by 28.4% and 24.1%, respectively, when compared to the CpG-only control group. Of note, sera from Ddi-vaccinated groups showed the least immunoreactivity in ELISA. Surprisingly, we found no difference in the immunoreactivity in linear epitope mapping among the vaccinated groups (data not shown).

There are only few studies testing the efficacy of vaccination against CWD. Among them, one study reported that the intramuscular vaccination in mule deer with synthetic peptide-

conjugates failed to provide protection against CWD challenge [364]. Another study by Goni *et al.* described a CWD-protective approach using an oral vaccination in white-tailed deer with attenuated *Salmonella* expressing PrP where 20% protection was reported against CWD challenge [365]. This study provides solid support for the effectiveness of a vaccine approach in cervids for the containment of CWD. Our vaccination and CWD challenge study used TgElk mice overexpressing elk PrP. A relatively fast and feasible CWD model, TgElk mice has provided a proof-of-concept on the efficacy of our vaccine approach. However, future studies assessing protection against CWD will need a cervid animal model.

Another benefit that CWD vaccination could provide is the reduction of CWD spreading by lowering the peripheral shedding of CWD prions by the infected animals into the environment. Keeping this in mind, our experimental approach involves the antibody-mediated blocking of prion propagation at the periphery, which could have an impact on pathogenesis in the brain and CWD shedding into the environment. There is very limited information on effect of a vaccine on CWD prions shed by infected animals into the environment. In line with this, we have sampled the urine from infected TgElk mice and are trying to detect the prion shedding by RT-QuIC. However, we faced difficulty in detecting prions in the excreta of TgElk mice so far, probably due to the limited sample size and the inefficient reproducibility by transgenic mice of CWD pathogenesis and shedding, both of which are characteristic of CWD infection in cervids. The TgElk mouse model overexpressing elk PrP has been reported to propagate deer and elk CWD prions when inoculated intracerebrally, where the ic inoculation resulted in a shorter incubation time of around 90-95 days [434, 438]. The short incubation period is the significant advantage of using TgElk mice in CWD studies where other CWD mouse models may even exceed 250 days of incubation period following ic inoculation [434, 438, 439]. We used the ip route for the CWD challenge in TgElk mice as our

vaccination approach. This induces antibody production, which targets PrP^{C} at the peripheral sites outside the CNS. We had also infected deer PrP-overexpressing Tg(cerPrP)$1536^{+/+}$ mice with CWD prions and found that in this CWD mouse model, ip inoculation results in an incomplete attack rate (data not shown). However, TgElk mice displayed a complete attack rate and showed typical prion clinical signs such as weight loss, ataxia, gait abnormalities, and very slow, uncoordinated movement. The average incubation period observed for the control (CpG) group after intraperitoneal CWD infection in our current study is 114 days, which is longer than the incubation period reported earlier for ic infection (90-95 days). This difference is due to the route of infection, as ip infection usually takes longer than ic inoculation to initiate infection in the brain as previously reported for scrapie transmission studies in rodents [440]. Of note, CpG itself prolonged survival in mice infected peripherally with RML prions when used for post-exposure prophylaxis by injecting very high doses repeatedly in animals within hours of prion inoculation [441]. Notably, we observed a pronounced intra-group variation in the survival times. This might be somewhat explained by the route of infection, treatment procedure, or the age of the animals at the time of CWD inoculation: 14-15 week-old mice were inoculated with CWD prions in this study, while for ic inoculation, mice aged four to six weeks are usually used. To resolve this notion, the inclusion of CWD inoculated non-CpG ic and non-CpG ip groups in our study would have been advantageous.

We used an immunoblot, RT-QuIC, and IHC to investigate the PrP^{Sc} in the brain of TgElk mice infected intraperitoneally with CWD prions. RT-QuIC is a sensitive technique to detect the seeding activity of PrP^{Sc} present in various samples of infected animals. It has also been used to detect CWD prions [396]. So far, ip-inoculated CWD pathogenesis in TgElk mice has not been characterized. As the brains were sampled at the terminal stage for both the vaccinated and control

groups, we found, as expected, no difference in pathogenesis between the groups except for the survival period. The BH from all ip-inoculated mice were positive in RT-QuIC, though the signals were weaker than from the ic-infected TgElk BH. The weaker signals in RT-QuIC became stronger after the BH from the ip–infected TgElk mice were subjected to NaPTA-based PrP^{Sc} enrichment before the RT-QuIC assay. This indicates that either the route of CWD inoculation or the vaccination procedure might have affected the prion pathogenesis and infectivity in the brain of TgElk mice, even when same inoculum is used for infection. Consistent with this even in an immunoblot, while the NaPTA precipitation step was not required for detection of PrP^{Sc} in the brain of ic-infected animals, we detected PK-resistant PrP^{Sc} in BH from ip-infected mice only after enrichment with NaPTA. Moreover, PrP^{Sc} in BH from ip-infected mice were more susceptible to PK digestion than that from ic-infected mice, which might indicate towards the influence in prion conformational properties. The comparison of the conformational stability profile of the prions using guanidine hydrochloride (GdnHCl) denaturation [442], and serial transmission studies in bioassay are missing in our study and would be beneficial to elucidate the effect of route of CWD infection in prion conformation.

As a pilot study, we tested our dimer immunogens for their efficacy in inducing a humoral response in reindeer. The sera from all the Mdi-vaccinated reindeer had anti-PrP antibody titres as detected in ELISA. However, for the Ddi-vaccinated group, only 33% (one of three) of the animals responded to vaccination in terms of antibody production with a lower titre than most of the Mdi-vaccinated animals. We found that this responding Ddi animal had two polymorphisms in the *Prnp* gene at position 225 and 176, which could explain the response to the self-Ddi immunogen. Moreover, such variability in inducing a humoral immune response to the vaccine was seen in the case of the PrP^{Sc}-specific vaccine approach in white-tailed deer. It is also quite common with

commercial vaccines used within an outbred population [368]. Nevertheless, optimizing a proper vaccine dose and vaccination schedule could help to achieve a better response. We used only one dose (500 ug/ animal) for three times. Moreover, it is quite normal to observe variations in animals' responses to vaccines in a given population; included in that population will be animals who will not respond. Next, we are planning on doing a recall experiment by vaccinating reindeer with two additional boosts after a year to investigate whether we have non-responders or low responders. Although the anti-PrP titre was low in the sera of the Ddi-vaccinated animal, it was more effective in reducing prion propagation in persistently CWD-infected RK13 cells. This could be explained by the efficient binding of self-antibodies present in the Ddi post-immune sera to the recombinant deer PrP in the immunoblots. Meanwhile, the antibodies in the Mdi post-immune sera showed weak binding to deer PrP. This is in agreement with our previous study in which post-immune sera from Dmo-vaccinated Tg (cerPrP) 1536+/+ mice, not from Mmo-vaccinated mice, significantly reduced the PrP^{Sc} levels in CWD-infected RK13 cells. However, it is still important to examine if our immunogens' induced antibody responses in reindeer is protective to the CWD infection *in vivo*. We were unable to test the efficacy of Mmo and Dmo as immunogens in reindeer due to unavailability of number of animals needed for such experimentation. Besides, parenteral vaccination route can be used for farmed animals, yet oral route would be more suitable for wildlife vaccination. Thus, as an alternative, we are trying to make oral preparations of our immunogens by encapsulating them in polylactic-co-glycolic acid (PLGA) microspheres [443], as well as plant-based expressions of PrP.

In conclusion, we present promising CWD vaccine candidates, which extended the survival of vaccinated TgElk mice up to 60%. Moreover, these candidates induced a humoral immune response in reindeer in our pilot study, indicating proof-of-concept for utilizing our approach for

feasible and efficient vaccination in cervids. Yet, testing the efficacy of our vaccine candidates to provide protection against CWD needs to be done in a cervid model, as cervids are natural hosts for CWD.

Supplementary Figures:

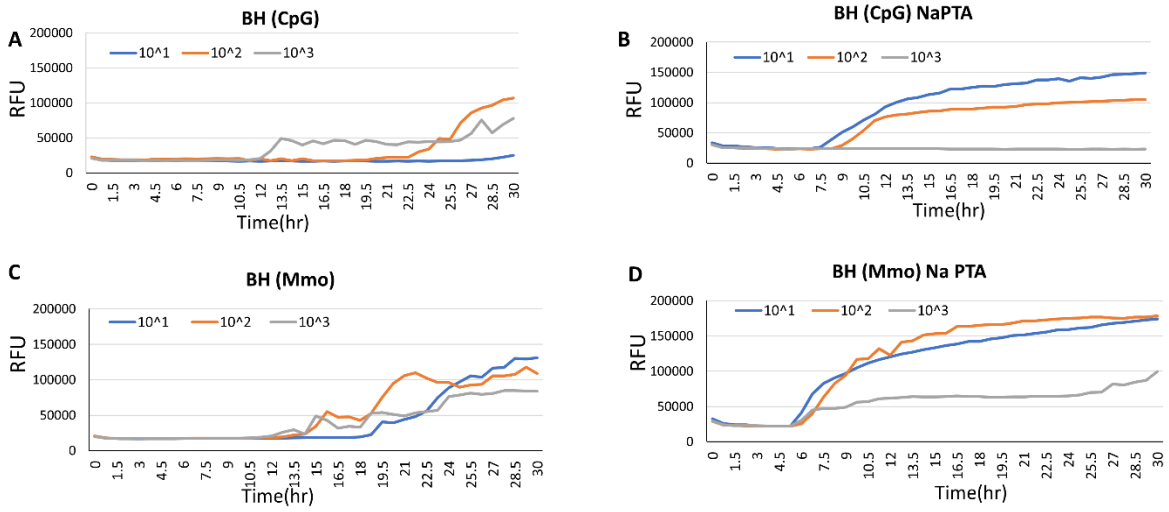

Figure S4. 1. Prion conversion activity in brain homogenates of intraperitoneally inoculated TgElk mice. (A) RT-QuIC expressed as relative fluorescence units (RFU) per hour in which the seed was 10% BH of a terminally ill CWD-infected CpG control TgElk mouse. (B) RT-QuIC in which the seed was 10% BH of the same mouse in panel A enriched by NaPTA precipitation. (C) RT-QuIC in which the seed was 10% homogenate of a terminally-ill CWD-infected Mmo-vaccinated TgElk mouse. (B) RT-QuIC in which the seed was 10% homogenate of the same mouse in panel C enriched with NaPTA precipitation. Mouse rPrP was used as substrate for the reactions, four tenfold dilutions of seed were analyzed (10^{-1} to 10^{-4}), and each curve represents the average of 4 technical replicates.

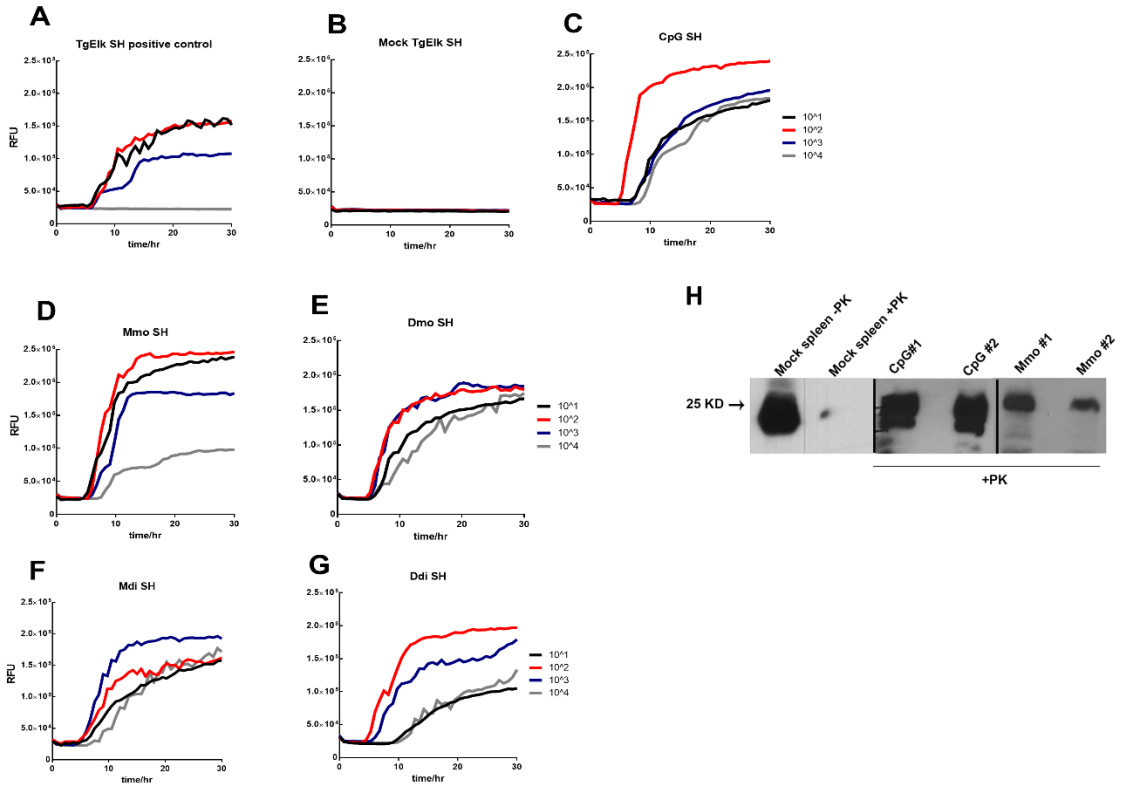

Figure S4. 2. Prion conversion activity and PrP^{Sc} in spleen homogenates of ip-inoculated TgElk mice. (A) CWD positive control for RT-QuIC in which the seed was 10% SH of a terminally ill CWD-infected TgElk mouse. (B) SH of an uninfected TgElk mouse was used as negative control. (C-G) RT-QuIC assay for one representative spleen homogenate from every group. (C) CpG-only, (D) Mmo-, (E) Dmo-, (F) Mdi-, and (G) Ddi-immunized. Mouse rPrP was used as substrate for the reactions, four tenfold dilutions of seed were analyzed (10^{-1} to 10^{-4}), and each curve represents the average of 4 technical replicates. (H) Western blot analysis using mAb 8H4 of spleen homogenate samples treated with PK followed by NaPTA enrichment. Four individual mice are shown. Mock-infected TgElk spleen homogenate was used as a negative control.

CHAPTER 5:

GENERAL DISCUSSION, LIMITATIONS AND FUTURE DIRECTIONS

5.1. Modulation of cellular pathways as a therapeutic approach in prion diseases

Prion diseases ultimately result in death and yet no treatment is available. Even several decades after describing prions as a pathogenic and infectious agent, scientists are still unable to define a therapeutic target that would result in effective therapy for these diseases. The development of an effecient therapeutic strategy would involve a better understanding of several mechanisms. Indeed, prion conversion process, PrP^{Sc} structure, prion strain existence that includes distinct conformations, and how prions exert neurotoxicity in the brain are the major hindrances for therapy development. Understanding the molecular and cellular pathways involved in prion infection might help in deciphering novel targets for intervention. Researchers have targeted different cellular pathways involved in prion disease progression using various intervention strategies. Such pathways involve targeting the ubiquitin-proteasome system (UPS), autophagy, lysosomal degradation, and unfolded protein response (UPR) (reviewed in [444, 445]). My research work contributes towards understanding the role of the secretory pathway and UPR in prion pathogenesis. Specifically, we investigated two proteins, ERp57 and VIP36, involved in protein quality control, and a compound, Sephin1, involved in UPR modulation for their effect on prion pathogenesis.

Our group has described the direct impact of proteosomal dysfunction and ER stress on the level and quality of PrP^{C} [338]. Along with others, our group has also highlighted the importance of the quality of substrate for prion conversion, where the hindrance in the quality of PrP^{C} folding exerted by ER stress and proteasomal inhibition, make the PrP^{C} more prone to conversion [338,

342]. Such cellular conditions might favor the prion conversion due to their effect on the "fitness" of the substrate, which could be relevant in the sporadic prion diseases where prion conversion occurs in the absence of *bona fide* PrP^{Sc}. Of note, with normal aging, it is believed that the accumulation of misfolded proteins in neurons occurs as a result of proteosomal and lysosomal impairment and reduced activity of molecular chaperones [446]. Interestingly, improving protein quality by overexpressing quality control (QC) proteins, such as EDEM3 and ERGIC-53, in the endoplasmic reticulum (ER) resulted in a good quality PrP^{C} population that are less efficiently converted into PrP^{Sc} in prion-infected cells [338].

Here two questions arose from the previous finding: 1) what role does protein QC play in prion propagation? and 2) what are the possible mechanisms that efficient QC exerts that interfere with prion conversion? To further elaborate on this, we investigated two proteins, ERp57 and VIP36 for their effect on prion propagation as well as to understand their mechanistic context in the prion-infection models. ERp57 and VIP36 are involved in the ER and post-ER QC respectively.

The results I described in Chapter 2 utilizes mammalian cell culture and rodent model to explain an important role of ERp57 and VIP36 of the secretory pathway in suppressing the prion propagation, which further could contribute to anti-prion therapeutic opportunities. We found that both transient and lentivirus-mediated stable overexpression of ERp57 and VIP36 reduced the PrP^{Sc} levels significantly in prion-infected neuronal cells. This effect remained even after several passages of the cells. For detection of PrP^{Sc} we used PK digestion followed by immunoblotting as it is a widely used technique in the prion field to quantify pathogenic PrP. We also used RT-QuIC and immunofluorescence as an alternative read-outs, which detect both PK-resistant and PK-sensitive PrP^{Sc}. Further investigation revealed that ERp57- and VIP36-overexpressing uninfected

cells generated lower levels of tunicamycin-mediated ER stress-induced misfolded PrP measured by detergent solubility assay, which might be the reason for the aforementioned reduction of PrP^{Sc}. This is in accordance with the study that reported that ER stress-induced misfolded PrP is more prone to prion conversion in protein misfolding cyclic amplification (PMCA) [342]. Moreover, a study has reported that ERp57 deficiency in the cells could make PrP^{C} more susceptible to aggregation [328]. Of note, tunicamycin induces ER stress in cells by inhibiting the N-glycosylation and increases PrP^{Sc} in the prion-infected cells [338, 378]. The characterization of the ER stress-induced misfolded PrP in our current study in terms of its susceptibility to prion conversion needs to be assessed in the future.

Moreover, ERp57 has been shown to be neuroprotective and to prevent cells from PrP^{Sc}-mediated neurotoxicity [342]. In cancer models as well, ERp57 depletion led to increased apoptosis in carcinoma cells [447]. This was explained by the fact that the depletion of ERp57 leads to the oxidation of protein disulfide isomerase (PDI), which resulted in the over-activation of PERK and subsequent apoptosis. Moreover, the oxidation of PDI is mediated by the ER oxidoreductase 1 protein (Ero1). In the case of high oxidation rates of PDI, Ero1 activity needs to be increased, which could lead to a high production of hydrogen peroxide, affecting cell viability [448]. However, we did not assess these neuroprotective mechanisms of ERp57 in our study. Rather, we looked into the role of ERp57 during ER stress. We found that overexpression of ERp57 resulted in the generation of less tunicamycin-induced ER stress-mediated misfolded PrP, as well as a lower expression of the ER stress markers, CHOP and BiP, both indicative of reduced ER stress in the cells. Consistent with a previous study in which ER stress induction increased PrP^{Sc} in cells, ERp57 overexpressing cells had lower amounts of PrP^{Sc}, probably due to lower stress levels. Considering the connection with ER stress, the overexpression of ERp57 might have

implications in reducing misfolded protein in other neurodegenerative diseases such as Alzheimer's disease (AD), Parkinson's disease (PD), Amyotrophic lateral sclerosis (ALS) as well as Huntington's disease, in which ER stress has been shown to be associated with disease pathology [299]. A broader therapeutic approach that would be applicable to several neurodegenerative disease models is more beneficial than one that is specific to prion disease only. Our approach is yet to be tested in other neurodegenerative disease models.

In our studies, *in vitro* results showed that VIP36 was also efficient in reducing PrP^{Sc} in prion-infected cells and in reducing the ER stress to some extent. Yet, VIP36 was not as efficient as was ERp57. Much less is known about VIP36 in the literature, which opens a platform for further study of VIP36 and its involvement in the cellular pathways. We found that the PrP^{Sc} and ER stress-mediated misfolded PrP levels was reduced in VIP36- overexpressing prion-infected cells. However, further investigation is needed to determine whether VIP36 interacts directly with misfolded PrP to bring it back to the ER from the Golgi. To that end, we tried immunofluorescence co-localization experiments using the 4H11 anti-PrP antibody and commercial anti-VIP36 antibodies. However, the anti-VIP36 antibodies we tried did not work. Further optimization is needed in this context. Immunoprecipitation can be another approach for testing the interaction between two proteins. Even for detection of exogenously expressed VIP36 in our study, we used anti-tag antibodies, a strategy that has been utilized in many other studies to detect exogenous protein expression [449]. Moreover, such tagging of proteins was advantageous in our study where commercial protein specific antibodies were inefficient in our detection assay. The pitfall for using anti-tag antibodies to detect exogenous protein expression levels is that it does not tell about how much fold change in the protein expression levels is achieved compared to the endogenous level.

We are planning to investigate the effect caused by the down-regulation of ERp57 and VIP36 using siRNA in prion-infected cells, which was not the part of this study. ERp57 is an essential protein, and ERp57 knockout was detrimental to the embryonic development of the mouse [328].

Another interesting finding I came across during my study is that such overexpression of ERp57 and VIP36 in cells to achieve efficient cellular QC makes cells less susceptible to *de novo* prion infection. Such an outcome has implications in understanding the prion infection at the cellular level, as we show that the quality of PrP^C also has a role in exogenous prion infection. *In vivo,* transgenic mouse models with the modulation of expression levels of different cellular proteins have been used to investigate the role of cellular proteins on prion susceptibility [23, 174, 339, 340]. However, we used cell culture models to assess prion susceptibility after a stable modulation of cellular proteins. The advantages of using *in vitro* models over transgenic animal models in such scenarios is their feasibility, cost-effectiveness, less time needed for experiments, easy reproducibility, and controlled experiments for mechanistic insight.

In *in vivo* experiments, the injection of a lentivirus, which mediated the overexpression of ERp57 in the brain of mice, 50 days after the ic prion inoculation, significantly prolonged the survival of FVB mice infected with 22L prion strain. A lentivirus-mediated therapeutic approach was reported in prion-infected mice where the shRNA-mediated knockdown of the *Prnp* gene expression was successful in prolonging survival in RML-infected Tg37 mice [335]. Though VIP36 overexpression showed a slight trend towards increasing survival, it was not statistically significant. With this approach, combination effect, specifically combining lentiviruses, which could help in overexpressing both VIP36 and ERp57, could be assessed in context of prion infection. In our *in vivo* experiment, we focussed only on the survival of animals as an outcome,

yet investigating the effect of ERp57 and VIP36 overexpression on PrP^{Sc} levels, biochemical properties of PrP^{Sc}, and histopathology would help in understanding the molecular role of ERp57 and VIP36. When we analyzed the PrP^{Sc} in the brain homogenates (BH) from the terminal animals in immunoblotting, we found similar levels of PrP^{Sc} in all three groups (CT, ERp57-, and VIP36-overexpressing groups) (data not shown). This was expected given that sampling was done from terminally sick animals.

We chose 50 days post-infection (dpi) for lentiviral injection to investigate the therapeutic effect of ERp57 and VIP36 overexpression, which somewhat is similar in approach we used in our experiments using persistently infected cell culture model. At the stage of 50 dpi, a significant prion propagation is already initiated in the brain following ic inoculation [450]. In prion diseases, this therapeutic window is feasible to identify due to the availability of pre-mortem diagnostic tools, such as PMCA and RT-QuIC in cerebrospinal fluid (CSF), blood, or other tissues, although are still mostly experimental [375, 451-454]. The expression for CT-, VIP36- and ERp57-lentiviruses was confirmed in the brain sections when green fluorescence protein (GFP) auto-fluorescence was detected using confocal microscopy after 10 days post virus injection (data not shown). However, data on prolonged expression level in the brain is missing in our study. The increase in survival in ERp57-overexpressing mice was less striking than expected, though significant considering the life-span of mice. Firstly, this outcome might be due to the very local delivery of the lentiviruses in the brain as the viruses were self-inactivating and non-replicative. Secondly, in this preliminary experiment, we used only one titre of virus for injection in animals, which was relatively low; this needs further optimization. Additionally, though we did not see any phenotypic side effects of lentivirus-mediated gene expression in mice due to random integration into the host genome, we cannot neglect these possibilities. To overcome this, we are considering

using Adeno-associated viruses (AAV) to express the gene of interest, as they are considered safe and remain as episomes in non-dividing cells. Moreover, the widespread expression of ERp57 and VIP36 in different regions of the brain is achievable by using intraventricularly delivered AAV in neonates. This technique is reliable as described previously [454]. I have already started experiments to achieve AAV-mediated ERp57 and VIP36 overexpression in neonates' brains via the intraventricular route, to investigate the susceptibility of those mice to prion infection. It will be more a prophylactic rather than therapeutic approach, to provide proof-of-concept *in vivo* and validate what we have achieved *in vitro* regarding prion susceptibility.

We found the efficacy of ERp57-overexpression in counteracting prion infection and reducing ER stress in the cells [405]. However, the ER stress markers were not assessed in brains of animals, as the sampling was done at the terminal stage. Performing the time-point experiment and sampling the brains at different intervals after virus injection in prion-infected mice to analyze the effect of ERp57 overexpression in prion propagation and ER homeostasis would be beneficial. This might help to dissect the role of ERp57 overexpression during disease progression. Although, we observed successful reduction of PrP^{Sc} in cells infected with different mouse-adapted scrapie prion strains after ERp57 or VIP36 overexpression, in *in vivo* experiment we used only one strain. It would be interesting to consider other prion strains in our *in vivo* study.

Our study in Chapter 2 provided a proof-of concept that targeting QC by overexpressing QC proteins is efficient in reducing prion propagation and increases survival in prion-infected mice, thus creating various interventions opportunities. For instance, EDEMs (EDEM 1, 2 and 3) involved in sorting aberrantly folded glycoprotein for ERAD-mediated degradation [338, 455], Tmp21 involved in rapid ER stress-induced export (RESET) shown to assist in lysosomal degradation of PrP following a short transit through the plasma membrane [456], and heat shock

proteins (HSPs) involved in folding and disaggregation [340, 444] can be studied in the future to see if their manipulation has an effect on prion pathogenesis. Most promising targets could be modulated in combination for more effective therapeutic intervention. Recently, a group reported two findings on HSP: that the pharmacological induction of HSP70 reduced PrP^{Sc} in the cells, and that prion disease progression was accelerated in mice that were HSP70-deficient [340]. Similarly, the role of HSP110 is being studied by our colleague, Cristóbal Marrero Winkens (PhD candidate), in the context of prion disease both *in vitro* and *in vivo*.

In addition to gene manipulation-based therapy approaches, we looked for compounds that reduce ER stress in the cells as anticipated anti-prion mechanisms. We came across Sephin1, which has been reported to inhibit the stress-induced phosphatase complex resulting in prolongation of the phosphorylation of eIF2α. In this way, it protected cells from stress-induced damage, prevented neuronal loss, and protected neurological disease in mouse models of ALS, Charcot–Marie–Tooth disease type 1B, and multiple sclerosis (MS) [350, 351].

Phosphorylation of eIF2α is downstream of the PERK pathway, which is protective to cells if moderately activated to overcome ER stress conditions but leads to cell death during chronic stress [457]. PERK exerts this dual activity, controlling the level of eIF2α phosphorylation through the regulatory subunit of protein phosphatase which helps in eIF2α dephosphorylation and resolving protein translation attenuation during UPR. Targeting the protein phosphatase to prolong eIF2α phosphorylation during ER stress conditions has been reported to prevent disease symptoms and delay disease progression in protein misfolding diseases [348-351, 407]. Recently, Sephin1 was found to protect cells from stress-induced cytotoxicity, and prevent disease pathology in a mouse model of ALS, demyelination-associated Charcot–Marie–Tooth disease type 1B, and MS [350, 351]. Using persistently prion-infected neuronal cell culture models, we found that seven

days treatment with Sephin1 at 10μM concentration significantly reduced PrP^{Sc} in the cells. Moreover, Sephin1 significantly reduced ER stress-induced misfolded PrP in the uninfected cells compared to the control. However, after long-term treatment of the cells with Sephin1, although no PK-resistant PrP^{Sc} was observed in Sephin1-treated cells in immunoblot, we still detected prion seeding activity from Sephin1-treated cells in the RT-QuIC. This might indicate that Sephin1 did not cure the cells from prion infection. Using the cell lysates from Sephin1-treated and control cells as inoculum to achieve the *de novo* prion infection of the prion susceptible uninfected cells would be considered in future.

We found that Sephin1 significantly prolonged survival in intracerebrally RML prion-infected mice. We used Sephin1 in a prion disease model and initiated ip treatment of infected mice at 30 dpi. We chose 30 dpi because this time-point lies within the early stage before the exponential phase of prion propagation following the ic challenge of FVB mice with RML prions [450]. Thus, we wanted to target the cells at an initial stage of infection so that the ER stress is coped early before the stress level becomes saturated and the system is overwhelmed. Of note, prolonged eIF2α phosphorylation at a later stage of clinical disease was reported to have an adverse effect, resulting in neuronal loss due to reduced synaptic proteins in a prion disease model [320, 354]. Also in the multiple sclerosis (MS) animal model, Sephin1 was more effective at lessening disease severity and protecting against cellular toxicity when administered as an early treatment than at a later clinical stage [351]. Similarly, in scrapie-challenged mice, the ip treatment with cannabidiol initiated at 30 dpi (time-point within the first fourth quarter of the incubation period) significantly prolonged survival, with no effect on survival observed when treatment was started late at 120 dpi (time-point at the latter half of incubation period) [458].

In contrast with previous findings by Moreno *et al.* regarding the acceleration of disease and loss of synaptic proteins in prion-infected mice when treated with the protein phosphatase inhibitor salubrinal [320], we found Sephin1 to be effective in terms of increased survival. Of note, salubrinal was neuroprotective in *in vivo* models of PD and ALS [459, 460]. Consequently, our study helps in understanding the importance of careful UPR targeting, which has been shown to be both protective and detrimental in neurodegenerative disease models. Unlike salubrinal, Sephin1 treatment was started at the very early stage of disease development, before neuropathology began. Salubrinal was used when the prion pathogenesis already existed in the animals and there was persistent ER stress and eIF2α phosphorylation. In such a situation, the use of salubrinal or other compounds that result in prolonging eIF2α phosphorylation is more likely to cause the situation to deteriorate than to improve. An investigation on the effect of time of application of Sephin1 in prion-infected mice (earlier stage vs late stage) on the prion pathogenesis is very important.

Interestingly, another inhibitor of the stress-only induced regulatory subunit of phosphatase (PPP1R15A), guanabenz, was found to prolong survival in prion-infected mice [343, 346]. Moreover, guanabenz was studied in various neurodegenerative disease models and was shown to delay disease progression and to be neuroprotective [348, 349, 407]. However, the α2-adrenergic agonist activity of guanabenz has detrimental effects on animals, which limits its clinical use [347]. Sephin1 is a derivative of guanabenz without α2-adrenergic activity. Sephin1 has been shown to cross the blood-brain barrier (BBB) and be non-toxic when given orally to animals [350, 351]. However, in our study, we did not assess the availability of Sephin1 in the brain after ip treatment. Of note, the Sephin1 dose used in our study had no phenotypic side-effects in the animals.

We analyzed the PrP^{Sc} levels in the brains of terminally sick Sephin1-treated and control prion-infected animals and found no difference between the group in terms of PK-resistant PrP^{Sc} amounts. This was expected as brains were sampled from animals at the terminal stage. It is in accordance with the study which showed that PrP^{Sc} amounts were similar in the wild-type (WT) and HSP70 knockout prion-infected mice at the terminal stage, although the prion disease acceleration was seen in HSP70 knockout mice [340]. In this study, we focussed on terminal prion disease and the effect of Sephin1 on survival. In the future, it would be very interesting to investigate whether the drug delays the prion progression and pathology during the course of the disease by analyzing brains sampled at different time-points of disease development. Moreover, we used only one dose of Sephin1 in the *in vivo* experiment, although in cell culture studies we used two concentrations of Sephin1 that are non-toxic to the cells. Thus, finding the effective dose with no toxicity effect is important. Additionally, it might be interesting to examine the effect of Sephin1 after peripheral prion inoculation, to investigate the drug effect in central versus peripheral prion pathogenesis.

Our study shown in Chapter 3 has identified Sephin1 as an anti-prion compound against mouse-adapted scrapie prion strains. Furthermore, in our preliminary study regarding the combination of Sephin1 with a neuroprotective drug, metformin [410], the increase in survival was more pronounced than when using the drugs alone, even when the duration of treatment was significantly reduced in prion-infected mice [461]. The potential of combination therapy is very encouraging in prion disease models and we plan to expand our studies by combining Sephin1 with other neuroprotective agents [462, 463]. Alternatively, without a simultaneous combination of drugs, Sephin1-treatment could be used at earlier stages of the disease, to be replaced at later stages with a neuroprotective drug. Whether such a treatment scheme will exert beneficial effect

needs further investigation. However, the major hindrance for using combination approaches is the risk of increasing side effects; it is challenging to choose the right combination, dose, and delivery methods to achieve efficacy and avoid toxicity.

Taken together, our studies provided a framework for deciphering novel targets and strategies for intervention in prion disease.

5.2. Vaccination as a prophylactic approach against CWD

The pronounced direct and environmental transmission of CWD and its ability to affect free-ranging and captive cervids are driving forces for disease spread, which make the disease management very complicated [105, 107, 108]. In addition, the zoonotic potential of CWD by subsequent transmission into humans is alarming and still an open question [427, 428, 464]. For CWD management and control in wild populations, strategic culling has been shown to limit disease spread, yet this is not effective for long-term management and controlling environmental contamination [356, 357]. A combination of disease control strategies should be applied for CWD control. One such strategy could be a vaccination approach to limit both CWD infection and prion shedding. A model was proposed that demonstrated that a combination of a cervid depopulation strategy together with vaccination would reduce CWD prevalence and spread [358]. The efficacy of CWD vaccines to prevent infection as well as reducing shedding of prions into the environment must be taken into consideration when developing a CWD vaccine.

PrP^{Sc} utilizes the host PrP^{C} for propagation, and both share the same primary structure. Thus, a prion protein displays poor immunogenicity for generating specific anti-PrP immune responses because of self-tolerance to host-encoded PrP, which makes it very difficult to develop active vaccines against prion diseases. But when transgenic mice expressing an anti-PrP antibody

(μ chain) were found to prevent prion infection upon peripheral challenge with prions, the potential for immunization looked promising for pre-exposure prophylaxis in prion disease, even without developing any adverse effect in the host [431]. Besides, anti-PrP antibodies binding to PrP^{C} significantly inhibited prion propagation in scrapie-infected cell culture models and provided protection to mice against prion infection upon passive immunization [361, 465, 466]. These studies provided encouragement for the development of a vaccine and its implication for fighting prion diseases. An ideal prion vaccine should overcome self-tolerance and induce at least a humoral immune response without inducing autoimmunity-associated side effects [359, 360, 363].

Few CWD vaccination studies have been reported so far. One showed partial protection in white-tail deer (20%), another showed no vaccine effectiveness in mule deer, and one even showed accelerated prion disease in elk [364, 365, 369]. Thus, there is need for additional vaccine candidates. In Chapter 4, we showed how we validated a vaccine strategy against CWD in a mouse model of peripheral CWD infection. We demonstrated that the active immunization strategy using oligomeric recombinant PrP as an immunogen overcame self-tolerance, induced protective antibodies against PrP, and significantly prolonged survival in CWD-infected TgElk mice (up to 60% prolongation), most likely by neutralizing prion propagation at peripheral sites of the body. Host induced anti-PrP antibodies mask PrP^{C}, a prerequisite substrate for prion conversion, thereby blocking the conversion by PrP^{Sc}. Moreover, our CWD vaccination approach was effective in peripheral CWD infection, which is a characteristic of natural CWD.

Previous active immunization studies by our group and others in murine-adapted scrapie models had shown effectiveness of anti-PrP antibodies in reducing prion propagation and prolonging survival in mice [359, 362, 363, 467, 468]. Active vaccination against CWD prepares the cervid host to mitigate peripheral prion propagation before neuroinvasion occurs. Once prions

reach the brain, the antibody-based approach will be less effective due to the relative inefficiency of antibodies to cross the BBB. A study showed that passive immunization of mice with anti-PrP antibodies intraperitoneally delayed clinical signs and reduced peripheral PrP^{Sc} levels after the ip prion challenge. However, once the mice exhibited clinical signs, no effect of immunization was seen, possibly because the antibodies did not adequately cross the BBB [361]. An interesting study has shown that when anti-PrP antibody was administered intravenously at the onset of clinical disease in scrapie-infected mice, the reduction of PrP^{Sc} levels in the brain and the prolongation of survival in the animals was observed [436]. In the same study, the injected anti-PrP antibody was found in the brain regions indicating the ability of the antibody to cross the BBB. However, at the clinical stage of scrapie prion disease, the impairment in the function of BBB has been reported [469]. Another study showed that after a single intracardial injection of an anti-PrP monoclonal antibody in rats, the antibody was already present in the blood and reached the CSF after crossing the BBB within few hours of injection [470]. In our study, after active vaccination, although we detected anti-PrP antibodies in the blood of the TgElk mice, it would have been interesting to investigate whether the antibodies could be found in the CSF. Additionally, we used our vaccines in a reindeer model to show a proof-of-concept for their efficacy in inducing anti-PrP antibodies in a large animal model. There were no phenotypic side effects related to vaccination in our study in mice and reindeer.

Mice are commonly used as universal experimental models for prion disease bioassays due to their easy management and comparatively low cost, short incubation time compared to large animal models, and feasibility in genome manipulation, the latter of which makes it possible to understand strains and the cross-species barrier [173, 471]. Transgenic mice expressing elk or deer PrP have been extensively used to study CWD, pioneered by Dr. Glenn Telling's groups [118,

166, 184, 434, 438, 439, 472]. We used TgElk mice overexpressing elk PrP in our study. The TgElk mouse model showed a complete attack rate after intraperitoneal CWD prion inoculation, which was not the case with the deer PrP-overexpressing Tg(cerPrP)$1536^{+/+}$ mice. The TgElk mice also showed typical prion clinical signs, after CWD ip infection, consistent with previous studies of ic inoculated TgElk mice [434, 438]. Moreover, we compared the survival between vaccinated and non-vaccinated animals upon ip infection and analyzed the terminal brains of vaccinated and non-vaccinated animals to confirm presence of PrP^{Sc}. We are planning to initiate a time-point experiment where we will sample spleens and brains at different times of disease progression after CWD inoculation and compare the CWD pathogenesis in the spleen and brain between vaccinated and non-vaccinated animals.

The major limitation of our CWD vaccine study is the lack of information on the effect of vaccination on prion shedding. CWD-infected cervids are well known for shedding CWD prions into the environment via their bodily fluids, excretory materials, and contaminated carcasses [147]. Thus, it is necessary to address the issue of preventing environmental contamination in addition to disease pathogenesis when considering a vaccination to contain CWD. Yet, other CWD vaccination studies in cervids have not measured the effect of vaccination on prion shedding [364, 365, 369]. An additional issue to consider is that prolonging the survival in CWD-infected animals might cause problems in terms of shedding because prolongation in survival might allow the animals more time to shed more prions into the environment over their life-time.

To address the question of whether vaccination prevents or lowers CWD prion shedding via saliva, urine, and feces is very important. Preliminarily, we tried to measure CWD prion shedding in TgElk mice. However, using RT-QuIC after NaPTA purification, we were not able to detect prions in the urine of CWD-infected TgElk mice. Of note, RT-QuIC has been extensively

reported to be a reliable and sensitive tool for detecting prions in the urine and feces of CWD-infected cervid species [113, 376]. To sum up, more investigation is needed into the detection of prions in urine and feces of TgElk mice. More importantly, cervid-PrP overexpressing transgenic mouse models, unlike gene knock-in mice with cervid PrP expression at physiological level under the endogenous *Prnp* promotor, do not recapitulate peripheral CWD pathogenesis well [473]. Thus, in the future, we are looking forward to extending our vaccine study in the gene-targeted cervid PrP expressing mice and in the cervid model itself. The *Prnp* gene-targeted cervid PrP expressing mice better recapitulate peripheral CWD pathogenesis as these mice expressed either deer or elk PrP^C at the normal physiological level and produced pathogenesis upon ip CWD challenge and supported horizontal transmission [473]. Neither of these results had been observed in previous Tg mouse models overexpressing cervid PrP^C.

We have used recombinant PrP monomers and dimers of mouse and deer origin as immunogens in our study. Our group has used recombinant Mdi in an active vaccination study in a scrapie mouse model [359, 363]. Moreover, the biochemical characterization of PrP dimers, as well as the side-effect of vaccination in mice, were assessed in previous studies [433]. Recombinant Mdi PrPs were found to have more β-sheeted structure than monomer and, in the presence of CpG, PrP dimers formed aggregates [433]. Similar characterization of recombinant Dmo and Ddi were not done in this study, yet we do not expect many differences as compared to recombinant mouse entities. Although in our current study we did not observe systemic side effects of vaccination in mice, it would be beneficial to investigate the autoimmunity-mediated adverse effect in the spleen and lymph nodes using histopathology. Future experiments should include a hematoxylin and eosin (H&E) staining of the lymphoid organs to exclude any side effects at the organ level. However, in previous studies with Mdi and CpG, no signs of histopathological

changes were observed in the spleen, kidney, brain, lymph node, and Peyer's patches in the gut lumen of immunized animals [433].

In *in vitro*, both Ddi-induced anti-PrP antibodies in reindeer (our current study) and Dmo-induced antibodies in Tg(cerPrP)$1536^{+/+}$ mice (in our previous study [395]) were efficient at reducing PrP^{Sc} in deer PrP-expressing CWD-infected RK13 cells, which can be explained by the efficacy of self-antibodies detecting and reacting with the self-PrP. Similar observations had been made where Mdi-induced antibodies in WT mice were effective in neutralizing PrP^{Sc} propagation in mouse PrP expressing 22L-infected ScN2a cells [359]. However, in TgElk mice, we found that the Mmo vaccinated group showed a significant prolongation of survival in CWD-infected mice as compared to the control group, which was better than any other vaccinated group. This discrepancy in *in vitro* and *in vivo* models is not unusual as it has been seen for many potential therapeutic compounds in prion disease models [474]. Moreover, the median survival time in CWD-infected TgElk mice in the Mmo- and Ddi- or Dmo-vaccinated groups was not significantly different. For further interpretation on the efficacy of using immunogens in a CWD vaccine, all four immunogens need to be tested in cervids, as cervids are a natural host for CWD infection. This experiment will validate the proof-of-concept for CWD vaccination, which we have achieved in TgElk mice, as described in Chapter 4. Furthermore, the efficacy of mouse PrP immunogen *in vivo* and deer PrP *in vitro* has encouraged us to test *in vivo*, in future, a recombinant heterodimer containing both mouse PrP and deer PrP as a vaccine against CWD.

In our TgElk mouse model, we used the subcutaneous (sc) route to deliver the vaccine in order to validate its immunogenicity and efficacy against CWD infection. However, to implement a CWD vaccine in wildlife, the oral route of vaccination is the most suitable. To achieve oral delivery, vaccine candidates can be encapsulated in polylactic-co-glycolic acid (PLGA)-based

microspheres/nanospheres to enhance bioavailability by a controlled release and to protect the vaccine from degradation in the gastrointestinal tract [443]. We encapsulated the monomers and dimer PrP of mouse and deer along with CpG successfully in PLGA-based nanospheres using the solvent evaporation technique [433] and tested their efficacy in Tg(cerPrP)$1536^{+/+}$ mice expressing deer PrP. After sc injection of PLGA-encapsulated immunogens, successful production of anti-PrP antibodies was detected, comparable to that induced by non-capsulated immunogens [395]. However, due to the incomplete attack rate seen in Tg(cerPrP)$1536^{+/+}$ mice after an ip CWD challenge, the investigation regarding the efficacy of PLGA-encapsulated immunogens against CWD was inconclusive. Since TgElk mice were susceptible to ip CWD infection, we are planning to test such a PLGA-encapsulated vaccine in this model. The investigation of the protective effect of such PLGA-encapsulated immunogens would be of great interest, as they could be further formulated in animal feed and used for oral vaccination. Another approach we tried was a plant-based expression of our deer dimer PrP, to use it as a vaccine against CWD. We collaborated with Dr. Joenel Alcantara at the Faculty of Medicine, University of Calgary, in an attempt to express deer dimer PrP on the surface of oil bodies conjugated with oleosins that coat the oil bodies residing in the seeds of *Arabidopsis thaliana* [475]. Dr. Alcantara's group provided the oil bodies expressing Ddi PrP, which we mixed with emulsigen-D to vaccinate the TgElk mice via sc route. In this preliminary experiment, the injection dose was not comparable to that of our study, with only two booster doses of the oil bodies given to the animals. Although this might have been due to the dose insufficiency, the successful induction of the anti-PrP antibodies was not seen in the animals vaccinated with Ddi-expressing oil bodies. Further optimization is needed in this study.

Moreover, in our TgElk vaccination study, we did not attempt to perform antibody isotyping, although in a previous study, Mdi-induced anti-PrP antibodies were revealed to be

mainly IgGs and not IgA or IgM [433]. However, as CWD mainly occurs through an oral route, early antibody-mediated interference of prion propagation in the oral cavity and gastrointestinal tract would be preferred before entering the lymphoreticular system. In this premise, IgA, in addition to IgG, is an important antibody type, which is present in body secretions and mucosal surfaces. Thus, it is important to assess the isotypes of antibodies induced by active vaccination. In our case, optimization or combination with a vaccine candidate reported to induce IgAs by Goni *et. al* [365] might be beneficial. Alternatively, oral vaccine application combined with mucosal adjuvants like synthetic macrophage-activating lipopeptide of 2 kDa from *Mycoplasma* (MALP-2) which induce well IgA antibodies can be used as as previously described by our group [476].

Furthermore, polymorphisms in the cervid *Prnp* gene play a significant role in determining the PrP structure and CWD susceptibility [181-188]. Our CWD vaccine candidates induced a humoral immune response in Tg mice overexpressing either deer or elk PrP. In addition, the anti-PrP antibodies could detect mule deer and elk PrP in the cervid brain homogenate [395, 477]. However, we have yet to test how effective the induced anti-PrP antibodies are at binding to different polymorphic PrP variants in cervids.

Thus, we successfully demonstrated in Chapter 4 the immunogenicity of new vaccine candidates in Tg mice expressing elk PrP, which effectively prolonged survival in immunized mice challenged peripherally with CWD prions. This study in mice provides a strong basis for the translation of our work into cervid models of CWD infection. Overall, this study has implications for developing a vaccine candidate against CWD. Such an anti-PrP vaccine could have implications in AD as well. As a receptor for an amyloid beta (Aβ) oligomer, PrP^{C} triggered Aβ-mediated synaptic dysfunction, which was rescued by the addition of anti-PrP antibodies in the hippocampal slices [247]. In addition, the PrP^{C}- Aβ interaction mediates the synaptic dysfunction

and memory deficit in AD animal models [248]. In line with these data, the intracardiac injection of anti-PrP monoclonal antibody in rats was shown to provide protection against amyloid-β-related synaptotoxicity [470]. Thus, the anti-PrP vaccine targeting PrP^{C} could have a dual application in both prion diseases and AD.

5.3. Conclusion

There is currently no treatment or prophylactic means available for prion diseases. It is therefore critical to understand the molecular and cellular mechanisms of prion infection to elucidate molecular strategies for controlling these diseases. My research points towards potential candidates involved in cellular pathways, which could be manipulated in favour of counteracting prion propagation. Moreover, my research helps in understanding the relation between ER stress and prion propagation in cells and how lowering ER stress would reduce PrP^{Sc} in cells. Overall, studies mentioned in Chapters 2 and 3 suggest an approach that could be applied to developing therapeutic anti-prion strategies. Additionally, my research described in Chapter 4 describes new CWD vaccine candidates whose immunogenicity in terms of a humoral immune response is validated in a CWD mouse model as well as a cervid model. Moreover, my research established that certain vaccine candidates are very effective in extending survival in CWD-infected animals. Overall, the study provides a proof-of-principle for CWD vaccination and suggests a basis for translational implementation for developing a vaccine suitable for farmed cervids and wildlife, one that would reduce mortality in cervids and contain the transmission of CWD. Most importantly, with the zoonotic potential of CWD still not known, there is an urgent need to develop a vaccine against CWD. Altogether, my work has a significant impact on the development of novel therapeutic and prophylactic anti-prion strategies.

REFERENCES

1. Prusiner, S.B., *Novel proteinaceous infectious particles cause scrapie.* Science, 1982. **216**(4542): p. 136-44.
2. Prusiner, S.B., *Prions.* Proc Natl Acad Sci U S A, 1998. **95**(23): p. 13363-83.
3. Prusiner, S.B., *Biology and genetics of prions causing neurodegeneration.* Annu Rev Genet, 2013. **47**: p. 601-23.
4. DeMarco, M.L. and V. Daggett, *From conversion to aggregation: protofibril formation of the prion protein.* Proc Natl Acad Sci U S A, 2004. **101**(8): p. 2293-8.
5. Budka, H., *Neuropathology of prion diseases.* Br Med Bull, 2003. **66**: p. 121-30.
6. Houston, F. and O. Andreoletti, *Animal prion diseases: the risks to human health.* Brain Pathol, 2019. **29**(2): p. 248-262.
7. Babelhadj, B., et al., *Prion Disease in Dromedary Camels, Algeria.* Emerg Infect Dis, 2018. **24**(6): p. 1029-1036.
8. Brown, K. and J.A. Mastrianni, *The prion diseases.* J Geriatr Psychiatry Neurol, 2010. **23**(4): p. 277-98.
9. Chen, C. and X.P. Dong, *Epidemiological characteristics of human prion diseases.* Infect Dis Poverty, 2016. **5**(1): p. 47.
10. Bendheim, P.E., et al., *Nearly ubiquitous tissue distribution of the scrapie agent precursor protein.* Neurology, 1992. **42**(1): p. 149-56.
11. Laine, J., et al., *Cellular and subcellular morphological localization of normal prion protein in rodent cerebellum.* Eur J Neurosci, 2001. **14**(1): p. 47-56.

12. Frost, B. and M.I. Diamond, *Prion-like mechanisms in neurodegenerative diseases.* Nat Rev Neurosci, 2010. **11**(3): p. 155-9.

13. Bruce, M.E., et al., *Transmissions to mice indicate that 'new variant' CJD is caused by the BSE agent.* Nature, 1997. **389**(6650): p. 498-501.

14. Hill, A.F., et al., *The same prion strain causes vCJD and BSE.* Nature, 1997. **389**(6650): p. 448-50, 526.

15. Griffith, J.S., *Self-replication and scrapie.* Nature, 1967. **215**(5105): p. 1043-4.

16. Prusiner, S.B., et al., *Molecular properties, partial purification, and assay by incubation period measurements of the hamster scrapie agent.* Biochemistry, 1980. **19**(21): p. 4883-91.

17. Bolton, D.C., M.P. McKinley, and S.B. Prusiner, *Identification of a protein that purifies with the scrapie prion.* Science, 1982. **218**(4579): p. 1309-11.

18. Prusiner, S.B., et al., *Scrapie prions aggregate to form amyloid-like birefringent rods.* Cell, 1983. **35**(2 Pt 1): p. 349-58.

19. Oesch, B., et al., *A cellular gene encodes scrapie PrP 27-30 protein.* Cell, 1985. **40**(4): p. 735-46.

20. Chesebro, B., et al., *Identification of scrapie prion protein-specific mRNA in scrapie-infected and uninfected brain.* Nature, 1985. **315**(6017): p. 331-3.

21. Basler, K., et al., *Scrapie and cellular PrP isoforms are encoded by the same chromosomal gene.* Cell, 1986. **46**(3): p. 417-28.

22. Meyer, R.K., et al., *Separation and properties of cellular and scrapie prion proteins.* Proc Natl Acad Sci U S A, 1986. **83**(8): p. 2310-4.

23. Bueler, H., et al., *Mice devoid of PrP are resistant to scrapie.* Cell, 1993. **73**(7): p. 1339-47.

24. Prusiner, S.B., et al., *Ablation of the prion protein (PrP) gene in mice prevents scrapie and facilitates production of anti-PrP antibodies.* Proc Natl Acad Sci U S A, 1993. **90**(22): p. 10608-12.

25. Legname, G., et al., *Synthetic mammalian prions.* Science, 2004. **305**(5684): p. 673-6.

26. Castilla, J., et al., *In vitro generation of infectious scrapie prions.* Cell, 2005. **121**(2): p. 195-206.

27. Deleault, N.R., et al., *Formation of native prions from minimal components in vitro.* Proc Natl Acad Sci U S A, 2007. **104**(23): p. 9741-6.

28. Barria, M.A., et al., *De novo generation of infectious prions in vitro produces a new disease phenotype.* PLoS Pathog, 2009. **5**(5): p. e1000421.

29. Wang, F., et al., *Generating a prion with bacterially expressed recombinant prion protein.* Science, 2010. **327**(5969): p. 1132-5.

30. Zhang, Z., et al., *De novo generation of infectious prions with bacterially expressed recombinant prion protein.* FASEB J, 2013. **27**(12): p. 4768-75.

31. Saborio, G.P., B. Permanne, and C. Soto, *Sensitive detection of pathological prion protein by cyclic amplification of protein misfolding.* Nature, 2001. **411**(6839): p. 810-3.

32. Jackson, W.S., et al., *Spontaneous generation of prion infectivity in fatal familial insomnia knockin mice.* Neuron, 2009. **63**(4): p. 438-50.

33. Wang, F., et al., *Self-propagating, protease-resistant, recombinant prion protein conformers with or without in vivo pathogenicity.* PLoS Pathog, 2017. **13**(7): p. e1006491.

34. Makarava, N., et al., *Recombinant prion protein induces a new transmissible prion disease in wild-type animals.* Acta Neuropathol, 2010. **119**(2): p. 177-87.

35. Parchi, P., et al., *Classification of sporadic Creutzfeldt-Jakob disease based on molecular and phenotypic analysis of 300 subjects.* Ann Neurol, 1999. **46**(2): p. 224-33.

36. Zerr, I., et al., *Updated clinical diagnostic criteria for sporadic Creutzfeldt-Jakob disease.* Brain, 2009. **132**(Pt 10): p. 2659-68.

37. Rudge, P., et al., *Imaging and CSF analyses effectively distinguish CJD from its mimics.* J Neurol Neurosurg Psychiatry, 2018. **89**(5): p. 461-466.

38. Gambetti, P., et al., *Sporadic and familial CJD: classification and characterisation.* Br Med Bull, 2003. **66**: p. 213-39.

39. Monari, L., et al., *Fatal familial insomnia and familial Creutzfeldt-Jakob disease: different prion proteins determined by a DNA polymorphism.* Proc Natl Acad Sci U S A, 1994. **91**(7): p. 2839-42.

40. Montagna, P., et al., *Familial and sporadic fatal insomnia.* Lancet Neurol, 2003. **2**(3): p. 167-76.

41. Ghetti, B., et al., *Gerstmann-Straussler-Scheinker disease and the Indiana kindred.* Brain Pathol, 1995. **5**(1): p. 61-75.

42. Will, R.G., et al., *A new variant of Creutzfeldt-Jakob disease in the UK.* Lancet, 1996. **347**(9006): p. 921-5.

43. Ritchie, D.L., et al., *Transmissions of variant Creutzfeldt-Jakob disease from brain and lymphoreticular tissue show uniform and conserved bovine spongiform encephalopathy-related phenotypic properties on primary and secondary passage in wild-type mice.* J Gen Virol, 2009. **90**(Pt 12): p. 3075-82.

44. Coulthart, M.B. and N.R. Cashman, *Variant Creutzfeldt-Jakob disease: a summary of current scientific knowledge in relation to public health.* CMAJ, 2001. **165**(1): p. 51-8.

45. Hill, A.F., et al., *Investigation of variant Creutzfeldt-Jakob disease and other human prion diseases with tonsil biopsy samples.* Lancet, 1999. **353**(9148): p. 183-9.

46. Will, R.G., et al., *Diagnosis of new variant Creutzfeldt-Jakob disease.* Ann Neurol, 2000. **47**(5): p. 575-82.

47. Mok, T., et al., *Variant Creutzfeldt-Jakob Disease in a Patient with Heterozygosity at PRNP Codon 129.* N Engl J Med, 2017. **376**(3): p. 292-294.

48. Peden, A.H., et al., *Preclinical vCJD after blood transfusion in a PRNP codon 129 heterozygous patient.* Lancet, 2004. **364**(9433): p. 527-9.

49. Wroe, S.J., et al., *Clinical presentation and pre-mortem diagnosis of variant Creutzfeldt-Jakob disease associated with blood transfusion: a case report.* Lancet, 2006. **368**(9552): p. 2061-7.

50. Gill, O.N., et al., *Prevalent abnormal prion protein in human appendixes after bovine spongiform encephalopathy epizootic: large scale survey.* BMJ, 2013. **347**: p. f5675.

51. Clewley, J.P., et al., *Prevalence of disease related prion protein in anonymous tonsil specimens in Britain: cross sectional opportunistic survey.* BMJ, 2009. **338**: p. b1442.

52. Duffy, P., et al., *Letter: Possible person-to-person transmission of Creutzfeldt-Jakob disease.* N Engl J Med, 1974. **290**(12): p. 692-3.

53. Brown, P., et al., *Iatrogenic Creutzfeldt-Jakob disease, final assessment.* Emerg Infect Dis, 2012. **18**(6): p. 901-7.

54. Gajdusek, D.C. and V. Zigas, *Degenerative disease of the central nervous system in New Guinea; the endemic occurrence of kuru in the native population.* N Engl J Med, 1957. **257**(20): p. 974-8.

55. Collinge, J., et al., *Kuru in the 21st century--an acquired human prion disease with very long incubation periods.* Lancet, 2006. **367**(9528): p. 2068-74.

56. Gajdusek, D.C., C.J. Gibbs, and M. Alpers, *Experimental transmission of a Kuru-like syndrome to chimpanzees.* Nature, 1966. **209**(5025): p. 794-6.

57. Alpers, M. and L. Rail, *Kuru and Creutzfeldt-Jakob disease: clinical and aetiological aspects.* Proc Aust Assoc Neurol, 1971. **8**: p. 7-15.

58. Wadsworth, J.D., et al., *Kuru prions and sporadic Creutzfeldt-Jakob disease prions have equivalent transmission properties in transgenic and wild-type mice.* Proc Natl Acad Sci U S A, 2008. **105**(10): p. 3885-90.

59. Alpers, M.P., *Review. The epidemiology of kuru: monitoring the epidemic from its peak to its end.* Philos Trans R Soc Lond B Biol Sci, 2008. **363**(1510): p. 3707-13.

60. Detwiler, L.A., *Scrapie.* Rev Sci Tech, 1992. **11**(2): p. 491-537.

61. Miller, J.M., et al., *Immunohistochemical detection of prion protein in sheep with scrapie.* J Vet Diagn Invest, 1993. **5**(3): p. 309-16.

62. Race, R., A. Jenny, and D. Sutton, *Scrapie infectivity and proteinase K-resistant prion protein in sheep placenta, brain, spleen, and lymph node: implications for transmission and antemortem diagnosis.* J Infect Dis, 1998. **178**(4): p. 949-53.

63. Gonzalez, L., et al., *Diagnosis of preclinical scrapie in samples of rectal mucosa.* Vet Rec, 2005. **156**(26): p. 846-7.

64. van Keulen, L.J., et al., *Immunohistochemical detection of prion protein in lymphoid tissues of sheep with natural scrapie.* J Clin Microbiol, 1996. **34**(5): p. 1228-31.

65. Vascellari, M., et al., *PrPSc in salivary glands of scrapie-affected sheep.* J Virol, 2007. **81**(9): p. 4872-6.

66. Terry, L.A., et al., *Detection of PrPsc in blood from sheep infected with the scrapie and bovine spongiform encephalopathy agents.* J Virol, 2009. **83**(23): p. 12552-8.

67. Konold, T., et al., *Evidence of scrapie transmission via milk.* BMC Vet Res, 2008. **4**: p. 14.

68. Terry, L.A., et al., *Detection of prions in the faeces of sheep naturally infected with classical scrapie.* Vet Res, 2011. **42**: p. 65.

69. Andreoletti, O., et al., *PrP(Sc) accumulation in placentas of ewes exposed to natural scrapie: influence of foetal PrP genotype and effect on ewe-to-lamb transmission.* J Gen Virol, 2002. **83**(Pt 10): p. 2607-16.

70. Foster, J.D., W. Goldmann, and N. Hunter, *Evidence in sheep for pre-natal transmission of scrapie to lambs from infected mothers.* PLoS One, 2013. **8**(11): p. e79433.

71. Georgsson, G., S. Sigurdarson, and P. Brown, *Infectious agent of sheep scrapie may persist in the environment for at least 16 years.* J Gen Virol, 2006. **87**(Pt 12): p. 3737-40.

72. Benestad, S.L., et al., *Atypical/Nor98 scrapie: properties of the agent, genetics, and epidemiology.* Vet Res, 2008. **39**(4): p. 19.

73. Andreoletti, O., et al., *Atypical/Nor98 scrapie infectivity in sheep peripheral tissues.* PLoS Pathog, 2011. **7**(2): p. e1001285.

74. Wells, G.A., et al., *A novel progressive spongiform encephalopathy in cattle.* Vet Rec, 1987. **121**(18): p. 419-20.

75. Mitra, D., et al., *The psychosocial and socioeconomic consequences of bovine spongiform encephalopathy (BSE): a community impact study.* J Toxicol Environ Health A, 2009. **72**(17-18): p. 1106-12.

76. Novakofski, J., et al., *Prion biology relevant to bovine spongiform encephalopathy.* J Anim Sci, 2005. **83**(6): p. 1455-76.

77. Casalone, C., et al., *Identification of a second bovine amyloidotic spongiform encephalopathy: molecular similarities with sporadic Creutzfeldt-Jakob disease.* Proc Natl Acad Sci U S A, 2004. **101**(9): p. 3065-70.

78. Biacabe, A.G., et al., *Distinct molecular phenotypes in bovine prion diseases.* EMBO Rep, 2004. **5**(1): p. 110-5.

79. Brown, P., et al., *On the question of sporadic or atypical bovine spongiform encephalopathy and Creutzfeldt-Jakob disease.* Emerg Infect Dis, 2006. **12**(12): p. 1816-21.

80. Hartsough, G.R. and D. Burger, *Encephalopathy of mink. I. Epizootiologic and clinical observations.* J Infect Dis, 1965. **115**(4): p. 387-92.

81. Barlow, R.M., *Transmissible mink encephalopathy: pathogenesis and nature of the aetiological agent.* J Clin Pathol Suppl (R Coll Pathol), 1972. **6**: p. 102-9.

82. Marsh, R.F., et al., *Epidemiological and experimental studies on a new incident of transmissible mink encephalopathy.* J Gen Virol, 1991. **72 (Pt 3)**: p. 589-94.

83. Marsh, R.F., et al., *A preliminary report on the experimental host range of the transmissible mink encephalopathy agent.* J Infect Dis, 1969. **120**(6): p. 713-9.

84. Burger, D. and G.R. Hartsough, *Encephalopathy of mink. II. Experimental and natural transmission.* J Infect Dis, 1965. **115**(4): p. 393-9.

85. Marsh, R.F. and W.J. Hadlow, *Transmissible mink encephalopathy.* Rev Sci Tech, 1992. **11**(2): p. 539-50.

86. Marsh, R.F. and R.P. Hanson, *On the origin of transmissible mink encephalopathy*, in *In Slow Transmissible Diseases of the Nervous System*, S.B. Prusiner and W.J. Hadlow, Editors. 1979, Academic Press: New York. p. 451-460.

87. Robinson, M.M., et al., *Experimental infection of mink with bovine spongiform encephalopathy.* J Gen Virol, 1994. **75 (Pt 9)**: p. 2151-5.

88. Baron, T., et al., *Phenotypic similarity of transmissible mink encephalopathy in cattle and L-type bovine spongiform encephalopathy in a mouse model.* Emerg Infect Dis, 2007. **13**(12): p. 1887-94.

89. Bessen, R.A., et al., *Non-genetic propagation of strain-specific properties of scrapie prion protein.* Nature, 1995. **375**(6533): p. 698-700.

90. Wyatt, J.M., et al., *Naturally occurring scrapie-like spongiform encephalopathy in five domestic cats.* Vet Rec, 1991. **129**(11): p. 233-6.

91. Kirkwood, J.K. and A.A. Cunningham, *Epidemiological observations on spongiform encephalopathies in captive wild animals in the British Isles.* Vet Rec, 1994. **135**(13): p. 296-303.

92. Pearson, G.R., et al., *Feline spongiform encephalopathy: fibril and PrP studies.* Vet Rec, 1992. **131**(14): p. 307-10.

93. Bencsik, A., et al., *Possible case of maternal transmission of feline spongiform encephalopathy in a captive cheetah.* PLoS One, 2009. **4**(9): p. e6929.

94. Fraser, H., et al., *Transmission of feline spongiform encephalopathy to mice.* Vet Rec, 1994. **134**(17): p. 449.

95. Williams, E.S. and S. Young, *Chronic wasting disease of captive mule deer: a spongiform encephalopathy.* J Wildl Dis, 1980. **16**(1): p. 89-98.

96. Spraker, T.R., et al., *Spongiform encephalopathy in free-ranging mule deer (Odocoileus hemionus), white-tailed deer (Odocoileus virginianus) and Rocky Mountain elk (Cervus elaphus nelsoni) in northcentral Colorado.* J Wildl Dis, 1997. **33**(1): p. 1-6.

97. Baeten, L.A., et al., *A natural case of chronic wasting disease in a free-ranging moose (Alces alces shirasi).* J Wildl Dis, 2007. **43**(2): p. 309-14.

98. Race, B., et al., *Lack of Transmission of Chronic Wasting Disease to Cynomolgus Macaques.* J Virol, 2018. **92**(14).

99. Mitchell, G.B., et al., *Experimental oral transmission of chronic wasting disease to reindeer (Rangifer tarandus tarandus).* PLoS One, 2012. **7**(6): p. e39055.

100. Kim, T.Y., et al., *Additional cases of Chronic Wasting Disease in imported deer in Korea.* J Vet Med Sci, 2005. **67**(8): p. 753-9.

101. Benestad, S.L., et al., *First case of chronic wasting disease in Europe in a Norwegian free-ranging reindeer.* Vet Res, 2016. **47**(1): p. 88.

102. Pirisinu, L., et al., *Novel Type of Chronic Wasting Disease Detected in Moose (Alces alces), Norway.* Emerg Infect Dis, 2018. **24**(12): p. 2210-2218.

103. Osterholm, M.T., et al., *Chronic Wasting Disease in Cervids: Implications for Prion Transmission to Humans and Other Animal Species.* MBio, 2019. **10**(4).

104. Rivera, N.A., et al., *Chronic Wasting Disease In Cervids: Prevalence, Impact And Management Strategies.* Vet Med (Auckl), 2019. **10**: p. 123-139.

105. Miller, M.W. and E.S. Williams, *Prion disease: horizontal prion transmission in mule deer.* Nature, 2003. **425**(6953): p. 35-6.

106. Moore, S.J., et al., *Horizontal Transmission of Chronic Wasting Disease in Reindeer.* Emerg Infect Dis, 2016. **22**(12): p. 2142-2145.

107. Miller, M.W., et al., *Environmental sources of prion transmission in mule deer.* Emerg Infect Dis, 2004. **10**(6): p. 1003-6.

108. Mathiason, C.K., et al., *Infectious prions in pre-clinical deer and transmission of chronic wasting disease solely by environmental exposure.* PLoS One, 2009. **4**(6): p. e5916.

109. Pulford, B., et al., *Detection of PrPCWD in feces from naturally exposed Rocky Mountain elk (Cervus elaphus nelsoni) using protein misfolding cyclic amplification.* J Wildl Dis, 2012. **48**(2): p. 425-34.

110. Haley, N.J., et al., *Detection of sub-clinical CWD infection in conventional test-negative deer long after oral exposure to urine and feces from CWD+ deer.* PLoS One, 2009. **4**(11): p. e7990.

111. Henderson, D.M., et al., *Longitudinal Detection of Prion Shedding in Saliva and Urine by Chronic Wasting Disease-Infected Deer by Real-Time Quaking-Induced Conversion.* J Virol, 2015. **89**(18): p. 9338-47.

112. Tamguney, G., et al., *Asymptomatic deer excrete infectious prions in faeces.* Nature, 2009. **461**(7263): p. 529-32.

113. Cheng, Y.C., et al., *Early and Non-Invasive Detection of Chronic Wasting Disease Prions in Elk Feces by Real-Time Quaking Induced Conversion.* PLoS One, 2016. **11**(11): p. e0166187.

114. Johnson, C.J., et al., *Prions adhere to soil minerals and remain infectious.* PLoS Pathog, 2006. **2**(4): p. e32.

115. Johnson, C.J., et al., *Oral transmissibility of prion disease is enhanced by binding to soil particles.* PLoS Pathog, 2007. **3**(7): p. e93.

116. Nichols, T.A., et al., *Detection of protease-resistant cervid prion protein in water from a CWD-endemic area.* Prion, 2009. **3**(3): p. 171-83.

117. Pritzkow, S., et al., *Grass plants bind, retain, uptake, and transport infectious prions.* Cell Rep, 2015. **11**(8): p. 1168-75.

118. Tamguney, G., et al., *Transmission of elk and deer prions to transgenic mice.* J Virol, 2006. **80**(18): p. 9104-14.

119. Raymond, G.J., et al., *Transmission and adaptation of chronic wasting disease to hamsters and transgenic mice: evidence for strains.* J Virol, 2007. **81**(8): p. 4305-14.

120. Perrott, M.R., et al., *Mucosal transmission and pathogenesis of chronic wasting disease in ferrets.* J Gen Virol, 2013. **94**(Pt 2): p. 432-42.

121. Mathiason, C.K., et al., *Susceptibility of domestic cats to chronic wasting disease.* J Virol, 2013. **87**(4): p. 1947-56.

122. Di Bari, M.A., et al., *Chronic wasting disease in bank voles: characterisation of the shortest incubation time model for prion diseases.* PLoS Pathog, 2013. **9**(3): p. e1003219.

123. Anderson, C.A., et al., *Colorado surveillance program for chronic wasting disease transmission to humans: lessons from 2 highly suspicious but negative cases.* Arch Neurol, 2007. **64**(3): p. 439-41.

124. Olszowy, K.M., et al., *Six-year follow-up of a point-source exposure to CWD contaminated venison in an Upstate New York community: risk behaviours and health outcomes 2005-2011.* Public Health, 2014. **128**(9): p. 860-8.

125. Mawhinney, S., et al., *Human prion disease and relative risk associated with chronic wasting disease.* Emerg Infect Dis, 2006. **12**(10): p. 1527-35.

126. Sandberg, M.K., et al., *Chronic wasting disease prions are not transmissible to transgenic mice overexpressing human prion protein.* J Gen Virol, 2010. **91**(Pt 10): p. 2651-7.

127. Barria, M.A., et al., *Generation of a new form of human PrP(Sc) in vitro by interspecies transmission from cervid prions.* J Biol Chem, 2011. **286**(9): p. 7490-5.

128. Race, B., et al., *Susceptibilities of nonhuman primates to chronic wasting disease.* Emerg Infect Dis, 2009. **15**(9): p. 1366-76.

129. Miller, M.W., M.A. Wild, and E.S. Williams, *Epidemiology of chronic wasting disease in captive Rocky Mountain elk.* J Wildl Dis, 1998. **34**(3): p. 532-8.

130. Williams, E.S. and M.W. Miller, *Chronic wasting disease in deer and elk in North America.* Rev Sci Tech, 2002. **21**(2): p. 305-16.

131. Williams, E.S., *Chronic wasting disease.* Vet Pathol, 2005. **42**(5): p. 530-49.

132. Spraker, T.R., et al., *Detection of PrP(CWD) in postmortem rectal lymphoid tissues in Rocky Mountain elk (Cervus elaphus nelsoni) infected with chronic wasting disease.* J Vet Diagn Invest, 2006. **18**(6): p. 553-7.

133. Wild, M.A., et al., *Preclinical diagnosis of chronic wasting disease in captive mule deer (Odocoileus hemionus) and white-tailed deer (Odocoileus virginianus) using tonsillar biopsy.* J Gen Virol, 2002. **83**(Pt 10): p. 2629-34.

134. Kurt, T.D., et al., *Efficient in vitro amplification of chronic wasting disease PrPRES.* J Virol, 2007. **81**(17): p. 9605-8.

135. Haley, N.J., et al., *Detection of CWD prions in urine and saliva of deer by transgenic mouse bioassay.* PLoS One, 2009. **4**(3): p. e4848.

136. John, T.R., H.M. Schatzl, and S. Gilch, *Early detection of chronic wasting disease prions in urine of pre-symptomatic deer by real-time quaking-induced conversion assay.* Prion, 2013. **7**(3): p. 253-258.

137. Haley, N.J., et al., *Cross-validation of the RT-QuIC assay for the antemortem detection of chronic wasting disease in elk.* Prion, 2020. **14**(1): p. 47-55.

138. Sigurdson, C.J., et al., *Oral transmission and early lymphoid tropism of chronic wasting disease PrPres in mule deer fawns (Odocoileus hemionus).* J Gen Virol, 1999. **80 (Pt 10)**: p. 2757-64.

139. Fox, K.A., et al., *Patterns of PrPCWD accumulation during the course of chronic wasting disease infection in orally inoculated mule deer (Odocoileus hemionus).* J Gen Virol, 2006. **87**(Pt 11): p. 3451-61.

140. Sigurdson, C.J., et al., *PrP(CWD) lymphoid cell targets in early and advanced chronic wasting disease of mule deer.* J Gen Virol, 2002. **83**(Pt 10): p. 2617-28.

141. Williams, E.S. and S. Young, *Neuropathology of chronic wasting disease of mule deer (Odocoileus hemionus) and elk (Cervus elaphus nelsoni).* Vet Pathol, 1993. **30**(1): p. 36-45.

142. Liberski, P.P., et al., *Deposition patterns of disease-associated prion protein in captive mule deer brains with chronic wasting disease.* Acta Neuropathol, 2001. **102**(5): p. 496-500.

143. Race, B.L., et al., *Levels of abnormal prion protein in deer and elk with chronic wasting disease.* Emerg Infect Dis, 2007. **13**(6): p. 824-30.

144. Angers, R.C., et al., *Prions in skeletal muscles of deer with chronic wasting disease.* Science, 2006. **311**(5764): p. 1117.

145. Haley, N.J., et al., *Detection of chronic wasting disease prions in salivary, urinary, and intestinal tissues of deer: potential mechanisms of prion shedding and transmission.* J Virol, 2011. **85**(13): p. 6309-18.

146. Sigurdson, C.J., et al., *PrP(CWD) in the myenteric plexus, vagosympathetic trunk and endocrine glands of deer with chronic wasting disease.* J Gen Virol, 2001. **82**(Pt 10): p. 2327-34.

147. Mathiason, C.K., et al., *Infectious prions in the saliva and blood of deer with chronic wasting disease.* Science, 2006. **314**(5796): p. 133-6.

148. Race, B., et al., *Prion infectivity in fat of deer with chronic wasting disease.* J Virol, 2009. **83**(18): p. 9608-10.

149. Angers, R.C., et al., *Chronic wasting disease prions in elk antler velvet.* Emerg Infect Dis, 2009. **15**(5): p. 696-703.

150. Pattison, I.H. and G.C. Millson, *Scrapie produced experimentally in goats with special reference to the clinical syndrome.* J Comp Pathol, 1961. **71**: p. 101-9.

151. Telling, G.C., et al., *Evidence for the conformation of the pathologic isoform of the prion protein enciphering and propagating prion diversity.* Science, 1996. **274**(5295): p. 2079-82.

152. Tanaka, M., et al., *Conformational variations in an infectious protein determine prion strain differences.* Nature, 2004. **428**(6980): p. 323-8.

153. Safar, J., et al., *Eight prion strains have PrP(Sc) molecules with different conformations.* Nat Med, 1998. **4**(10): p. 1157-65.

154. Zlotnik, I. and J.C. Rennie, *Further observations on the experimental transmission of scrapie from sheep and goats to laboratory mice.* J Comp Pathol, 1963. **73**: p. 150-62.

155. Dickinson, A.G., *Scrapie in sheep and goats.* Front Biol, 1976. **44**: p. 209-41.

156. Kimberlin, R.H., C.A. Walker, and H. Fraser, *The genomic identity of different strains of mouse scrapie is expressed in hamsters and preserved on reisolation in mice.* J Gen Virol, 1989. **70 (Pt 8)**: p. 2017-25.

157. Fraser, H. and A.G. Dickinson, *Scrapie in mice. Agent-strain differences in the distribution and intensity of grey matter vacuolation.* J Comp Pathol, 1973. **83**(1): p. 29-40.

158. Aguzzi, A., M. Heikenwalder, and M. Polymenidou, *Insights into prion strains and neurotoxicity.* Nat Rev Mol Cell Biol, 2007. **8**(7): p. 552-61.

159. Bessen, R.A. and R.F. Marsh, *Biochemical and physical properties of the prion protein from two strains of the transmissible mink encephalopathy agent.* J Virol, 1992. **66**(4): p. 2096-101.

160. Bessen, R.A. and R.F. Marsh, *Distinct PrP properties suggest the molecular basis of strain variation in transmissible mink encephalopathy.* J Virol, 1994. **68**(12): p. 7859-68.

161. Jacobs, J.G., et al., *Molecular discrimination of atypical bovine spongiform encephalopathy strains from a geographical region spanning a wide area in Europe.* J Clin Microbiol, 2007. **45**(6): p. 1821-9.

162. Parchi, P., et al., *Genetic influence on the structural variations of the abnormal prion protein.* Proc Natl Acad Sci U S A, 2000. **97**(18): p. 10168-72.

163. Cali, I., et al., *Co-existence of scrapie prion protein types 1 and 2 in sporadic Creutzfeldt-Jakob disease: its effect on the phenotype and prion-type characteristics.* Brain, 2009. **132**(Pt 10): p. 2643-58.

164. Parchi, P., et al., *A subtype of sporadic prion disease mimicking fatal familial insomnia.* Neurology, 1999. **52**(9): p. 1757-63.

165. Collinge, J., et al., *Molecular analysis of prion strain variation and the aetiology of 'new variant' CJD.* Nature, 1996. **383**(6602): p. 685-90.

166. Angers, R.C., et al., *Prion strain mutation determined by prion protein conformational compatibility and primary structure.* Science, 2010. **328**(5982): p. 1154-8.

167. Benestad, S.L., et al., *Cases of scrapie with unusual features in Norway and designation of a new type, Nor98.* Vet Rec, 2003. **153**(7): p. 202-8.

168. Kimberlin, R.H., S. Cole, and C.A. Walker, *Temporary and permanent modifications to a single strain of mouse scrapie on transmission to rats and hamsters.* J Gen Virol, 1987. **68 (Pt 7)**: p. 1875-81.

169. Bessen, R.A. and R.F. Marsh, *Identification of two biologically distinct strains of transmissible mink encephalopathy in hamsters.* J Gen Virol, 1992. **73 (Pt 2)**: p. 329-34.

170. Wadsworth, J.D., et al., *Human prion protein with valine 129 prevents expression of variant CJD phenotype.* Science, 2004. **306**(5702): p. 1793-6.

171. Dickinson, A.G. and V.M. Meikle, *Host-genotype and agent effects in scrapie incubation: change in allelic interaction with different strains of agent.* Mol Gen Genet, 1971. **112**(1): p. 73-9.

172. Bruce, M., et al., *Transmission of bovine spongiform encephalopathy and scrapie to mice: strain variation and the species barrier.* Philos Trans R Soc Lond B Biol Sci, 1994. **343**(1306): p. 405-11.

173. Scott, M., et al., *Transgenic mice expressing hamster prion protein produce species-specific scrapie infectivity and amyloid plaques.* Cell, 1989. **59**(5): p. 847-57.

174. Fischer, M., et al., *Prion protein (PrP) with amino-proximal deletions restoring susceptibility of PrP knockout mice to scrapie.* EMBO J, 1996. **15**(6): p. 1255-64.

175. Dickinson, A.G., V.M. Meikle, and H. Fraser, *Identification of a gene which controls the incubation period of some strains of scrapie agent in mice.* J Comp Pathol, 1968. **78**(3): p. 293-9.

176. Carlson, G.A., et al., *Linkage of prion protein and scrapie incubation time genes.* Cell, 1986. **46**(4): p. 503-11.

177. Westaway, D., et al., *Distinct prion proteins in short and long scrapie incubation period mice.* Cell, 1987. **51**(4): p. 651-62.

178. Baylis, M. and W. Goldmann, *The genetics of scrapie in sheep and goats.* Curr Mol Med, 2004. **4**(4): p. 385-96.

179. Asante, E.A., et al., *BSE prions propagate as either variant CJD-like or sporadic CJD-like prion strains in transgenic mice expressing human prion protein.* EMBO J, 2002. **21**(23): p. 6358-66.

180. Hamir, A.N., et al., *Preliminary observations of genetic susceptibility of elk (Cervus elaphus nelsoni) to chronic wasting disease by experimental oral inoculation.* J Vet Diagn Invest, 2006. **18**(1): p. 110-4.

181. O'Rourke, K.I., et al., *Elk with a long incubation prion disease phenotype have a unique PrPd profile.* Neuroreport, 2007. **18**(18): p. 1935-8.

182. Green, K.M., et al., *The elk PRNP codon 132 polymorphism controls cervid and scrapie prion propagation.* J Gen Virol, 2008. **89**(Pt 2): p. 598-608.

183. Jewell, J.E., et al., *Low frequency of PrP genotype 225SF among free-ranging mule deer (Odocoileus hemionus) with chronic wasting disease.* J Gen Virol, 2005. **86**(Pt 8): p. 2127-34.

184. Angers, R., et al., *Structural effects of PrP polymorphisms on intra- and interspecies prion transmission.* Proc Natl Acad Sci U S A, 2014. **111**(30): p. 11169-74.

185. Johnson, C., et al., *Prion protein gene heterogeneity in free-ranging white-tailed deer within the chronic wasting disease affected region of Wisconsin.* J Wildl Dis, 2003. **39**(3): p. 576-81.

186. O'Rourke, K.I., et al., *Polymorphisms in the prion precursor functional gene but not the pseudogene are associated with susceptibility to chronic wasting disease in white-tailed deer.* J Gen Virol, 2004. **85**(Pt 5): p. 1339-46.

187. Kelly, A.C., et al., *Prion sequence polymorphisms and chronic wasting disease resistance in Illinois white-tailed deer (Odocoileus virginianus).* Prion, 2008. **2**(1): p. 28-36.

188. Johnson, C.J., et al., *Prion protein polymorphisms affect chronic wasting disease progression.* PLoS One, 2011. **6**(3): p. e17450.

189. Kurt, T.D., et al., *Human prion protein sequence elements impede cross-species chronic wasting disease transmission.* J Clin Invest, 2015. **125**(4): p. 1485-96.

190. Watts, J.C., et al., *Evidence that bank vole PrP is a universal acceptor for prions.* PLoS Pathog, 2014. **10**(4): p. e1003990.

191. Sparkes, R.S., et al., *Assignment of the human and mouse prion protein genes to homologous chromosomes.* Proc Natl Acad Sci U S A, 1986. **83**(19): p. 7358-62.

192. Lee, I.Y., et al., *Complete genomic sequence and analysis of the prion protein gene region from three mammalian species.* Genome Res, 1998. **8**(10): p. 1022-37.

193. Schatzl, H.M., et al., *Prion protein gene variation among primates.* J Mol Biol, 1995. **245**(4): p. 362-74.

194. Stahl, N., et al., *Scrapie prion protein contains a phosphatidylinositol glycolipid.* Cell, 1987. **51**(2): p. 229-40.

195. Haraguchi, T., et al., *Asparagine-linked glycosylation of the scrapie and cellular prion proteins.* Arch Biochem Biophys, 1989. **274**(1): p. 1-13.

196. Acevedo-Morantes, C.Y. and H. Wille, *The structure of human prions: from biology to structural models-considerations and pitfalls.* Viruses, 2014. **6**(10): p. 3875-92.

197. Sales, N., et al., *Cellular prion protein localization in rodent and primate brain.* Eur J Neurosci, 1998. **10**(7): p. 2464-71.

198. Mironov, A., Jr., et al., *Cytosolic prion protein in neurons.* J Neurosci, 2003. **23**(18): p. 7183-93.

199. Peralta, O.A. and W.H. Eyestone, *Quantitative and qualitative analysis of cellular prion protein (PrP(C)) expression in bovine somatic tissues.* Prion, 2009. **3**(3): p. 161-70.

200. Manson, J., et al., *The prion protein gene: a role in mouse embryogenesis?* Development, 1992. **115**(1): p. 117-22.

201. Follet, J., et al., *PrP expression and replication by Schwann cells: implications in prion spreading.* J Virol, 2002. **76**(5): p. 2434-9.

202. Riek, R., et al., *NMR structure of the mouse prion protein domain PrP(121-231).* Nature, 1996. **382**(6587): p. 180-2.

203. Zahn, R., et al., *NMR solution structure of the human prion protein.* Proc Natl Acad Sci U S A, 2000. **97**(1): p. 145-50.

204. Lysek, D.A., et al., *Prion protein NMR structures of cats, dogs, pigs, and sheep.* Proc Natl Acad Sci U S A, 2005. **102**(3): p. 640-5.

205. Viles, J.H., et al., *Copper binding to the prion protein: structural implications of four identical cooperative binding sites.* Proc Natl Acad Sci U S A, 1999. **96**(5): p. 2042-7.

206. Stockel, J., et al., *Prion protein selectively binds copper(II) ions.* Biochemistry, 1998. **37**(20): p. 7185-93.

207. Forloni, G., et al., *Neurotoxicity of a prion protein fragment.* Nature, 1993. **362**(6420): p. 543-6.

208. Gasset, M., et al., *Predicted alpha-helical regions of the prion protein when synthesized as peptides form amyloid.* Proc Natl Acad Sci U S A, 1992. **89**(22): p. 10940-4.

209. Billeter, M., et al., *Prion protein NMR structure and species barrier for prion diseases.* Proc Natl Acad Sci U S A, 1997. **94**(14): p. 7281-5.

210. Stahl, N., et al., *Glycosylinositol phospholipid anchors of the scrapie and cellular prion proteins contain sialic acid.* Biochemistry, 1992. **31**(21): p. 5043-53.

211. Bate, C., et al., *Sialic Acid within the Glycosylphosphatidylinositol Anchor Targets the Cellular Prion Protein to Synapses.* J Biol Chem, 2016. **291**(33): p. 17093-101.

212. Puig, B., et al., *GPI-anchor signal sequence influences PrPC sorting, shedding and signalling, and impacts on different pathomechanistic aspects of prion disease in mice.* PLoS Pathog, 2019. **15**(1): p. e1007520.

213. Fevrier, B., et al., *Cells release prions in association with exosomes.* Proc Natl Acad Sci U S A, 2004. **101**(26): p. 9683-8.

214. Magalhaes, A.C., et al., *Endocytic intermediates involved with the intracellular trafficking of a fluorescent cellular prion protein.* J Biol Chem, 2002. **277**(36): p. 33311-8.

215. Caughey, B., *In vitro expression and biosynthesis of prion protein.* Curr Top Microbiol Immunol, 1991. **172**: p. 93-107.

216. Turk, E., et al., *Purification and properties of the cellular and scrapie hamster prion proteins.* Eur J Biochem, 1988. **176**(1): p. 21-30.

217. Ma, J. and S. Lindquist, *Wild-type PrP and a mutant associated with prion disease are subject to retrograde transport and proteasome degradation.* Proc Natl Acad Sci U S A, 2001. **98**(26): p. 14955-60.

218. Ma, J., R. Wollmann, and S. Lindquist, *Neurotoxicity and neurodegeneration when PrP accumulates in the cytosol.* Science, 2002. **298**(5599): p. 1781-5.

219. Rane, N.S., J.L. Yonkovich, and R.S. Hegde, *Protection from cytosolic prion protein toxicity by modulation of protein translocation.* EMBO J, 2004. **23**(23): p. 4550-9.

220. Orsi, A., et al., *Conditions of endoplasmic reticulum stress favor the accumulation of cytosolic prion protein.* J Biol Chem, 2006. **281**(41): p. 30431-8.

221. Shyng, S.L., M.T. Huber, and D.A. Harris, *A prion protein cycles between the cell surface and an endocytic compartment in cultured neuroblastoma cells.* J Biol Chem, 1993. **268**(21): p. 15922-8.

222. Taraboulos, A., et al., *Synthesis and trafficking of prion proteins in cultured cells.* Mol Biol Cell, 1992. **3**(8): p. 851-63.

223. Campana, V., D. Sarnataro, and C. Zurzolo, *The highways and byways of prion protein trafficking.* Trends Cell Biol, 2005. **15**(2): p. 102-11.

224. Taylor, D.R., et al., *Assigning functions to distinct regions of the N-terminus of the prion protein that are involved in its copper-stimulated, clathrin-dependent endocytosis.* J Cell Sci, 2005. **118**(Pt 21): p. 5141-53.

225. Shyng, S.L., J.E. Heuser, and D.A. Harris, *A glycolipid-anchored prion protein is endocytosed via clathrin-coated pits.* J Cell Biol, 1994. **125**(6): p. 1239-50.

226. Vey, M., et al., *Subcellular colocalization of the cellular and scrapie prion proteins in caveolae-like membranous domains.* Proc Natl Acad Sci U S A, 1996. **93**(25): p. 14945-9.

227. Mallucci, G.R., et al., *Post-natal knockout of prion protein alters hippocampal CA1 properties, but does not result in neurodegeneration.* EMBO J, 2002. **21**(3): p. 202-10.

228. Richt, J.A., et al., *Production of cattle lacking prion protein.* Nat Biotechnol, 2007. **25**(1): p. 132-8.

229. Zhu, C., et al., *Production of Prnp-/- goats by gene targeting in adult fibroblasts.* Transgenic Res, 2009. **18**(2): p. 163-71.

230. Benestad, S.L., et al., *Healthy goats naturally devoid of prion protein.* Vet Res, 2012. **43**: p. 87.

231. Tobler, I., et al., *Altered circadian activity rhythms and sleep in mice devoid of prion protein.* Nature, 1996. **380**(6575): p. 639-42.

232. Collinge, J., et al., *Prion protein is necessary for normal synaptic function.* Nature, 1994. **370**(6487): p. 295-7.

233. Robinson, S.W., et al., *Prion protein facilitates synaptic vesicle release by enhancing release probability.* Hum Mol Genet, 2014. **23**(17): p. 4581-96.

234. Wulf, M.A., A. Senatore, and A. Aguzzi, *The biological function of the cellular prion protein: an update.* BMC Biol, 2017. **15**(1): p. 34.

235. Brown, D.R., et al., *The cellular prion protein binds copper in vivo.* Nature, 1997. **390**(6661): p. 684-7.

236. Brown, D.R., C. Clive, and S.J. Haswell, *Antioxidant activity related to copper binding of native prion protein.* J Neurochem, 2001. **76**(1): p. 69-76.

237. Klamt, F., et al., *Imbalance of antioxidant defense in mice lacking cellular prion protein.* Free Radic Biol Med, 2001. **30**(10): p. 1137-44.

238. Pauly, P.C. and D.A. Harris, *Copper stimulates endocytosis of the prion protein.* J Biol Chem, 1998. **273**(50): p. 33107-10.

239. Mange, A., et al., *PrP-dependent cell adhesion in N2a neuroblastoma cells.* FEBS Lett, 2002. **514**(2-3): p. 159-62.

240. Schmitt-Ulms, G., et al., *Binding of neural cell adhesion molecules (N-CAMs) to the cellular prion protein.* J Mol Biol, 2001. **314**(5): p. 1209-25.

241. Graner, E., et al., *Cellular prion protein binds laminin and mediates neuritogenesis.* Brain Res Mol Brain Res, 2000. **76**(1): p. 85-92.

242. Malaga-Trillo, E., et al., *Regulation of embryonic cell adhesion by the prion protein.* PLoS Biol, 2009. **7**(3): p. e55.

243. Mouillet-Richard, S., et al., *Signal transduction through prion protein.* Science, 2000. **289**(5486): p. 1925-8.

244. Chen, S., et al., *Prion protein as trans-interacting partner for neurons is involved in neurite outgrowth and neuronal survival.* Mol Cell Neurosci, 2003. **22**(2): p. 227-33.

245. Kurschner, C. and J.I. Morgan, *The cellular prion protein (PrP) selectively binds to Bcl-2 in the yeast two-hybrid system.* Brain Res Mol Brain Res, 1995. **30**(1): p. 165-8.

246. Kuwahara, C., et al., *Prions prevent neuronal cell-line death.* Nature, 1999. **400**(6741): p. 225-6.

247. Lauren, J., et al., *Cellular prion protein mediates impairment of synaptic plasticity by amyloid-beta oligomers.* Nature, 2009. **457**(7233): p. 1128-32.

248. Gimbel, D.A., et al., *Memory impairment in transgenic Alzheimer mice requires cellular prion protein.* J Neurosci, 2010. **30**(18): p. 6367-74.

249. Stahl, N., et al., *Structural studies of the scrapie prion protein using mass spectrometry and amino acid sequencing.* Biochemistry, 1993. **32**(8): p. 1991-2002.

250. Pan, K.M., et al., *Conversion of alpha-helices into beta-sheets features in the formation of the scrapie prion proteins.* Proc Natl Acad Sci U S A, 1993. **90**(23): p. 10962-6.

251. Smirnovas, V., et al., *Structural organization of brain-derived mammalian prions examined by hydrogen-deuterium exchange.* Nat Struct Mol Biol, 2011. **18**(4): p. 504-6.

252. Wille, H., et al., *Natural and synthetic prion structure from X-ray fiber diffraction.* Proc Natl Acad Sci U S A, 2009. **106**(40): p. 16990-5.

253. Rudd, P.M., et al., *Glycosylation differences between the normal and pathogenic prion protein isoforms.* Proc Natl Acad Sci U S A, 1999. **96**(23): p. 13044-9.

254. Stahl, N., D.R. Borchelt, and S.B. Prusiner, *Differential release of cellular and scrapie prion proteins from cellular membranes by phosphatidylinositol-specific phospholipase C.* Biochemistry, 1990. **29**(22): p. 5405-12.

255. Caughey, B. and G.J. Raymond, *The scrapie-associated form of PrP is made from a cell surface precursor that is both protease- and phospholipase-sensitive.* J Biol Chem, 1991. **266**(27): p. 18217-23.

256. Caughey, B.W., et al., *Secondary structure analysis of the scrapie-associated protein PrP 27-30 in water by infrared spectroscopy.* Biochemistry, 1991. **30**(31): p. 7672-80.

257. Requena, J.R. and H. Wille, *The structure of the infectious prion protein: experimental data and molecular models.* Prion, 2014. **8**(1): p. 60-6.

258. Vazquez-Fernandez, E., et al., *The Structural Architecture of an Infectious Mammalian Prion Using Electron Cryomicroscopy.* PLoS Pathog, 2016. **12**(9): p. e1005835.

259. Tzaban, S., et al., *Protease-sensitive scrapie prion protein in aggregates of heterogeneous sizes.* Biochemistry, 2002. **41**(42): p. 12868-75.

260. Safar, J.G., et al., *Diagnosis of human prion disease.* Proc Natl Acad Sci U S A, 2005. **102**(9): p. 3501-6.

261. Sajnani, G., et al., *PK-sensitive PrP is infectious and shares basic structural features with PK-resistant PrP.* PLoS Pathog, 2012. **8**(3): p. e1002547.

262. Wang, F., et al., *Prion infectivity is encoded exclusively within the structure of proteinase K-resistant fragments of synthetically generated recombinant PrP(Sc).* Acta Neuropathol Commun, 2018. **6**(1): p. 30.

263. Borchelt, D.R., et al., *Scrapie and cellular prion proteins differ in their kinetics of synthesis and topology in cultured cells.* J Cell Biol, 1990. **110**(3): p. 743-52.

264. Mallucci, G., et al., *Depleting neuronal PrP in prion infection prevents disease and reverses spongiosis.* Science, 2003. **302**(5646): p. 871-4.

265. Aguzzi, A. and A.M. Calella, *Prions: protein aggregation and infectious diseases.* Physiol Rev, 2009. **89**(4): p. 1105-52.

266. Prusiner, S.B., et al., *Transgenetic studies implicate interactions between homologous PrP isoforms in scrapie prion replication.* Cell, 1990. **63**(4): p. 673-86.

267. Lansbury, P.T., Jr. and B. Caughey, *The chemistry of scrapie infection: implications of the 'ice 9' metaphor.* Chem Biol, 1995. **2**(1): p. 1-5.

268. Aguzzi, A. and C. Weissmann, *Prion research: the next frontiers.* Nature, 1997. **389**(6653): p. 795-8.

269. Jarrett, J.T. and P.T. Lansbury, Jr., *Seeding "one-dimensional crystallization" of amyloid: a pathogenic mechanism in Alzheimer's disease and scrapie?* Cell, 1993. **73**(6): p. 1055-8.

270. Borchelt, D.R., A. Taraboulos, and S.B. Prusiner, *Evidence for synthesis of scrapie prion proteins in the endocytic pathway.* J Biol Chem, 1992. **267**(23): p. 16188-99.

271. McKinley, M.P., et al., *Ultrastructural localization of scrapie prion proteins in cytoplasmic vesicles of infected cultured cells.* Lab Invest, 1991. **65**(6): p. 622-30.

272. Godsave, S.F., et al., *Cryo-immunogold electron microscopy for prions: toward identification of a conversion site.* J Neurosci, 2008. **28**(47): p. 12489-99.

273. Marijanovic, Z., et al., *Identification of an intracellular site of prion conversion.* PLoS Pathog, 2009. **5**(5): p. e1000426.

274. Beranger, F., et al., *Stimulation of PrP(C) retrograde transport toward the endoplasmic reticulum increases accumulation of PrP(Sc) in prion-infected cells.* J Biol Chem, 2002. **277**(41): p. 38972-7.

275. Yokoyama, T., et al., *Heparin enhances the cell-protein misfolding cyclic amplification efficiency of variant Creutzfeldt-Jakob disease.* Neurosci Lett, 2011. **498**(2): p. 119-23.

276. Horonchik, L., et al., *Heparan sulfate is a cellular receptor for purified infectious prions.* J Biol Chem, 2005. **280**(17): p. 17062-7.

277. Taylor, D.R., I.J. Whitehouse, and N.M. Hooper, *Glypican-1 mediates both prion protein lipid raft association and disease isoform formation.* PLoS Pathog, 2009. **5**(11): p. e1000666.

278. Gill, A.C., et al., *Structural requirements for efficient prion protein conversion: cofactors may promote a conversion-competent structure for PrP(C).* Prion, 2010. **4**(4): p. 235-42.

279. Telling, G.C., et al., *Prion propagation in mice expressing human and chimeric PrP transgenes implicates the interaction of cellular PrP with another protein.* Cell, 1995. **83**(1): p. 79-90.

280. Deleault, N.R., et al., *Isolation of phosphatidylethanolamine as a solitary cofactor for prion formation in the absence of nucleic acids.* Proc Natl Acad Sci U S A, 2012. **109**(22): p. 8546-51.

281. Faucheux, B.A., et al., *Loss of cerebellar granule neurons is associated with punctate but not with large focal deposits of prion protein in Creutzfeldt-Jakob disease.* J Neuropathol Exp Neurol, 2009. **68**(8): p. 892-901.

282. Bounhar, Y., et al., *Prion protein protects human neurons against Bax-mediated apoptosis.* J Biol Chem, 2001. **276**(42): p. 39145-9.

283. Brandner, S., et al., *Normal host prion protein necessary for scrapie-induced neurotoxicity.* Nature, 1996. **379**(6563): p. 339-43.

284. Herrmann, U.S., et al., *Prion infections and anti-PrP antibodies trigger converging neurotoxic pathways.* PLoS Pathog, 2015. **11**(2): p. e1004662.

285. Jendroska, K., et al., *Proteinase-resistant prion protein accumulation in Syrian hamster brain correlates with regional pathology and scrapie infectivity.* Neurology, 1991. **41**(9): p. 1482-90.

286. Hetz, C., et al., *Caspase-12 and endoplasmic reticulum stress mediate neurotoxicity of pathological prion protein.* EMBO J, 2003. **22**(20): p. 5435-45.

287. Hill, A.F., et al., *Species-barrier-independent prion replication in apparently resistant species.* Proc Natl Acad Sci U S A, 2000. **97**(18): p. 10248-53.

288. Race, R., et al., *Long-term subclinical carrier state precedes scrapie replication and adaptation in a resistant species: analogies to bovine spongiform encephalopathy and variant Creutzfeldt-Jakob disease in humans.* J Virol, 2001. **75**(21): p. 10106-12.

289. Piccardo, P., et al., *Accumulation of prion protein in the brain that is not associated with transmissible disease.* Proc Natl Acad Sci U S A, 2007. **104**(11): p. 4712-7.

290. Hegde, R.S., et al., *A transmembrane form of the prion protein in neurodegenerative disease.* Science, 1998. **279**(5352): p. 827-34.

291. Chesebro, B., et al., *Anchorless prion protein results in infectious amyloid disease without clinical scrapie.* Science, 2005. **308**(5727): p. 1435-9.

292. Lasmezas, C.I., et al., *Transmission of the BSE agent to mice in the absence of detectable abnormal prion protein.* Science, 1997. **275**(5298): p. 402-5.

293. Bueler, H., et al., *High prion and PrPSc levels but delayed onset of disease in scrapie-inoculated mice heterozygous for a disrupted PrP gene.* Mol Med, 1994. **1**(1): p. 19-30.

294. Sandberg, M.K., et al., *Prion propagation and toxicity in vivo occur in two distinct mechanistic phases.* Nature, 2011. **470**(7335): p. 540-2.

295. Silveira, J.R., et al., *The most infectious prion protein particles.* Nature, 2005. **437**(7056): p. 257-61.

296. Simoneau, S., et al., *In vitro and in vivo neurotoxicity of prion protein oligomers.* PLoS Pathog, 2007. **3**(8): p. e125.

297. Kazlauskaite, J., et al., *An unusual soluble beta-turn-rich conformation of prion is involved in fibril formation and toxic to neuronal cells.* Biochem Biophys Res Commun, 2005. **328**(1): p. 292-305.

298. Herczenik, E. and M.F. Gebbink, *Molecular and cellular aspects of protein misfolding and disease.* FASEB J, 2008. **22**(7): p. 2115-33.

299. Hetz, C. and B. Mollereau, *Disturbance of endoplasmic reticulum proteostasis in neurodegenerative diseases.* Nat Rev Neurosci, 2014. **15**(4): p. 233-49.

300. Broadley, S.A. and F.U. Hartl, *The role of molecular chaperones in human misfolding diseases.* FEBS Lett, 2009. **583**(16): p. 2647-53.

301. Ruddock, L.W. and M. Molinari, *N-glycan processing in ER quality control.* J Cell Sci, 2006. **119**(Pt 21): p. 4373-80.

302. Trombetta, E.S. and A.J. Parodi, *Quality control and protein folding in the secretory pathway.* Annu Rev Cell Dev Biol, 2003. **19**: p. 649-76.

303. Knittler, M.R. and I.G. Haas, *Interaction of BiP with newly synthesized immunoglobulin light chain molecules: cycles of sequential binding and release.* EMBO J, 1992. **11**(4): p. 1573-81.

304. Vogel, J.P., L.M. Misra, and M.D. Rose, *Loss of BiP/GRP78 function blocks translocation of secretory proteins in yeast.* J Cell Biol, 1990. **110**(6): p. 1885-95.

305. Shen, J., et al., *Stable binding of ATF6 to BiP in the endoplasmic reticulum stress response.* Mol Cell Biol, 2005. **25**(3): p. 921-32.

306. Okamura, K., et al., *Dissociation of Kar2p/BiP from an ER sensory molecule, Ire1p, triggers the unfolded protein response in yeast.* Biochem Biophys Res Commun, 2000. **279**(2): p. 445-50.

307. Bertolotti, A., et al., *Dynamic interaction of BiP and ER stress transducers in the unfolded-protein response.* Nat Cell Biol, 2000. **2**(6): p. 326-32.

308. Maattanen, P., et al., *ERp57 and PDI: multifunctional protein disulfide isomerases with similar domain architectures but differing substrate-partner associations.* Biochem Cell Biol, 2006. **84**(6): p. 881-9.

309. Nyfeler, B., et al., *The cargo receptor ERGIC-53 is a target of the unfolded protein response.* Biochem Biophys Res Commun, 2003. **304**(4): p. 599-604.

310. Reiterer, V., B. Nyfeler, and H.P. Hauri, *Role of the lectin VIP36 in post-ER quality control of human alpha1-antitrypsin.* Traffic, 2010. **11**(8): p. 1044-55.

311. Rutkowski, D.T. and R.J. Kaufman, *A trip to the ER: coping with stress.* Trends Cell Biol, 2004. **14**(1): p. 20-8.

312. Nakagawa, T., et al., *Caspase-12 mediates endoplasmic-reticulum-specific apoptosis and cytotoxicity by amyloid-beta.* Nature, 2000. **403**(6765): p. 98-103.

313. Hitomi, J., et al., *Apoptosis induced by endoplasmic reticulum stress depends on activation of caspase-3 via caspase-12.* Neurosci Lett, 2004. **357**(2): p. 127-30.

314. Walter, P. and D. Ron, *The unfolded protein response: from stress pathway to homeostatic regulation.* Science, 2011. **334**(6059): p. 1081-6.

315. Oslowski, C.M. and F. Urano, *Measuring ER stress and the unfolded protein response using mammalian tissue culture system.* Methods Enzymol, 2011. **490**: p. 71-92.

316. Kojima, E., et al., *The function of GADD34 is a recovery from a shutoff of protein synthesis induced by ER stress: elucidation by GADD34-deficient mice.* FASEB J, 2003. **17**(11): p. 1573-5.

317. McCullough, K.D., et al., *Gadd153 sensitizes cells to endoplasmic reticulum stress by down-regulating Bcl2 and perturbing the cellular redox state.* Mol Cell Biol, 2001. **21**(4): p. 1249-59.

318. Silva, R.M., et al., *CHOP/GADD153 is a mediator of apoptotic death in substantia nigra dopamine neurons in an in vivo neurotoxin model of parkinsonism.* J Neurochem, 2005. **95**(4): p. 974-86.

319. Puthalakath, H., et al., *ER stress triggers apoptosis by activating BH3-only protein Bim.* Cell, 2007. **129**(7): p. 1337-49.

320. Moreno, J.A., et al., *Sustained translational repression by eIF2alpha-P mediates prion neurodegeneration.* Nature, 2012. **485**(7399): p. 507-11.

321. Rane, N.S., et al., *Reduced translocation of nascent prion protein during ER stress contributes to neurodegeneration.* Dev Cell, 2008. **15**(3): p. 359-70.

322. Torres, M., et al., *Prion protein misfolding affects calcium homeostasis and sensitizes cells to endoplasmic reticulum stress.* PLoS One, 2010. **5**(12): p. e15658.

323. Brown, A.R., et al., *Gene expression profiling of the preclinical scrapie-infected hippocampus.* Biochem Biophys Res Commun, 2005. **334**(1): p. 86-95.

324. Soto, C. and N. Satani, *The intricate mechanisms of neurodegeneration in prion diseases.* Trends Mol Med, 2011. **17**(1): p. 14-24.

325. Hetz, C.A. and C. Soto, *Stressing out the ER: a role of the unfolded protein response in prion-related disorders.* Curr Mol Med, 2006. **6**(1): p. 37-43.

326. Hetz, C., J. Castilla, and C. Soto, *Perturbation of endoplasmic reticulum homeostasis facilitates prion replication.* J Biol Chem, 2007. **282**(17): p. 12725-33.

327. Steele, A.D., et al., *Prion pathogenesis is independent of caspase-12.* Prion, 2007. **1**(4): p. 243-7.

328. Torres, M., et al., *The Protein-disulfide Isomerase ERp57 Regulates the Steady-state Levels of the Prion Protein.* J Biol Chem, 2015. **290**(39): p. 23631-45.

329. Yoo, B.C., et al., *Overexpressed protein disulfide isomerase in brains of patients with sporadic Creutzfeldt-Jakob disease.* Neurosci Lett, 2002. **334**(3): p. 196-200.

330. Shyu, W.C., et al., *Creutzfeldt-Jakob disease: heat shock protein 70 mRNA levels in mononuclear blood cells and clinical study.* J Neurol, 2000. **247**(12): p. 929-34.

331. Wang, S.B., et al., *Protein disulfide isomerase regulates endoplasmic reticulum stress and the apoptotic process during prion infection and PrP mutant-induced cytotoxicity.* PLoS One, 2012. **7**(6): p. e38221.

332. Nunziante, M., S. Gilch, and H.M. Schatzl, *Prion diseases: from molecular biology to intervention strategies.* Chembiochem, 2003. **4**(12): p. 1268-84.

333. Gilch, S., C. Krammer, and H.M. Schatzl, *Targeting prion proteins in neurodegenerative disease.* Expert Opin Biol Ther, 2008. **8**(7): p. 923-40.

334. Krammer, C., et al., *Therapy in prion diseases: from molecular and cellular biology to therapeutic targets.* Infect Disord Drug Targets, 2009. **9**(1): p. 3-14.

335. White, M.D., et al., *Single treatment with RNAi against prion protein rescues early neuronal dysfunction and prolongs survival in mice with prion disease.* Proc Natl Acad Sci U S A, 2008. **105**(29): p. 10238-43.

336. Ahn, M., et al., *Convection-enhanced delivery of AAV2-PrPshRNA in prion-infected mice.* PLoS One, 2014. **9**(5): p. e98496.

337. Sitia, R. and I. Braakman, *Quality control in the endoplasmic reticulum protein factory.* Nature, 2003. **426**(6968): p. 891-4.

338. Nunziante, M., et al., *Proteasomal dysfunction and endoplasmic reticulum stress enhance trafficking of prion protein aggregates through the secretory pathway and increase accumulation of pathologic prion protein.* J Biol Chem, 2011. **286**(39): p. 33942-53.

339. Park, K.W., et al., *The Endoplasmic Reticulum Chaperone GRP78/BiP Modulates Prion Propagation in vitro and in vivo.* Sci Rep, 2017. **7**: p. 44723.

340. Mays, C.E., et al., *Prion disease is accelerated in mice lacking stress-induced heat shock protein 70 (HSP70).* J Biol Chem, 2019. **294**(37): p. 13619-13628.

341. Zhang, Y., et al., *Combined pharmacological induction of Hsp70 suppresses prion protein neurotoxicity in Drosophila.* PLoS One, 2014. **9**(2): p. e88522.

342. Hetz, C., et al., *The disulfide isomerase Grp58 is a protective factor against prion neurotoxicity.* J Neurosci, 2005. **25**(11): p. 2793-802.

343. Tribouillard-Tanvier, D., et al., *Antihypertensive drug guanabenz is active in vivo against both yeast and mammalian prions.* PLoS One, 2008. **3**(4): p. e1981.

344. Boyce, M., et al., *A selective inhibitor of eIF2alpha dephosphorylation protects cells from ER stress.* Science, 2005. **307**(5711): p. 935-9.

345. Teng, Y., et al., *Inhibition of eIF2alpha dephosphorylation enhances TRAIL-induced apoptosis in hepatoma cells.* Cell Death Dis, 2014. **5**: p. e1060.

346. Tsaytler, P., et al., *Selective inhibition of a regulatory subunit of protein phosphatase 1 restores proteostasis.* Science, 2011. **332**(6025): p. 91-4.

347. Holmes, B., et al., *Guanabenz. A review of its pharmacodynamic properties and therapeutic efficacy in hypertension.* Drugs, 1983. **26**(3): p. 212-29.

348. Jiang, H.Q., et al., *Guanabenz delays the onset of disease symptoms, extends lifespan, improves motor performance and attenuates motor neuron loss in the SOD1 G93A mouse model of amyotrophic lateral sclerosis.* Neuroscience, 2014. **277**: p. 132-8.

349. Sun, X., et al., *Guanabenz promotes neuronal survival via enhancement of ATF4 and parkin expression in models of Parkinson disease.* Exp Neurol, 2018. **303**: p. 95-107.

350. Das, I., et al., *Preventing proteostasis diseases by selective inhibition of a phosphatase regulatory subunit.* Science, 2015. **348**(6231): p. 239-42.

351. Chen, Y., et al., *Sephin1, which prolongs the integrated stress response, is a promising therapeutic for multiple sclerosis.* Brain, 2019. **142**(2): p. 344-361.

352. Moreno, J.A., et al., *Oral treatment targeting the unfolded protein response prevents neurodegeneration and clinical disease in prion-infected mice.* Sci Transl Med, 2013. **5**(206): p. 206ra138.

353. Halliday, M., et al., *Partial restoration of protein synthesis rates by the small molecule ISRIB prevents neurodegeneration without pancreatic toxicity.* Cell Death Dis, 2015. **6**: p. e1672.

354. Halliday, M., et al., *Repurposed drugs targeting eIF2α-P-mediated translational repression prevent neurodegeneration in mice.* Brain, 2017. **140**(6): p. 1768-1783.

355. Hetz, C., et al., *Unfolded protein response transcription factor XBP-1 does not influence prion replication or pathogenesis.* Proc Natl Acad Sci U S A, 2008. **105**(2): p. 757-62.

356. Mateus-Pinilla, N., et al., *Evaluation of a wild white-tailed deer population management program for controlling chronic wasting disease in Illinois, 2003-2008.* Prev Vet Med, 2013. **110**(3-4): p. 541-8.

357. Uehlinger, F.D., et al., *Systematic review of management strategies to control chronic wasting disease in wild deer populations in North America.* BMC Vet Res, 2016. **12**(1): p. 173.

358. Potapov, A., E. Merrill, and M.A. Lewis, *Wildlife disease elimination and density dependence.* Proc Biol Sci, 2012. **279**(1741): p. 3139-45.

359. Gilch, S., et al., *Polyclonal anti-PrP auto-antibodies induced with dimeric PrP interfere efficiently with PrPSc propagation in prion-infected cells.* J Biol Chem, 2003. **278**(20): p. 18524-31.

360. Sigurdsson, E.M. and T. Wisniewski, *Promising developments in prion immunotherapy.* Expert Rev Vaccines, 2005. **4**(5): p. 607-10.

361. White, A.R., et al., *Monoclonal antibodies inhibit prion replication and delay the development of prion disease.* Nature, 2003. **422**(6927): p. 80-3.

362. Schwarz, A., et al., *Immunisation with a synthetic prion protein-derived peptide prolongs survival times of mice orally exposed to the scrapie agent.* Neurosci Lett, 2003. **350**(3): p. 187-9.

363. Polymenidou, M., et al., *Humoral immune response to native eukaryotic prion protein correlates with anti-prion protection.* Proc Natl Acad Sci U S A, 2004. **101 Suppl 2**: p. 14670-6.

364. Pilon, J.L., et al., *Immunization with a synthetic peptide vaccine fails to protect mule deer (Odocoileus hemionus) from chronic wasting disease.* J Wildl Dis, 2013. **49**(3): p. 694-8.

365. Goni, F., et al., *Mucosal immunization with an attenuated Salmonella vaccine partially protects white-tailed deer from chronic wasting disease.* Vaccine, 2015. **33**(5): p. 726-33.

366. Paramithiotis, E., et al., *A prion protein epitope selective for the pathologically misfolded conformation.* Nat Med, 2003. **9**(7): p. 893-9.

367. Marciniuk, K., et al., *Development of a multivalent, PrP(Sc)-specific prion vaccine through rational optimization of three disease-specific epitopes.* Vaccine, 2014. **32**(17): p. 1988-97.

368. Taschuk, R., et al., *Induction of PrP(Sc)-specific systemic and mucosal immune responses in white-tailed deer with an oral vaccine for chronic wasting disease.* Prion, 2017. **11**(5): p. 368-380.

369. Wood, M.E., et al., *Accelerated onset of chronic wasting disease in elk (Cervus canadensis) vaccinated with a PrP(Sc)-specific vaccine and housed in a prion contaminated environment.* Vaccine, 2018. **36**(50): p. 7737-7743.

370. Butler, D.A., et al., *Scrapie-infected murine neuroblastoma cells produce protease-resistant prion proteins.* J Virol, 1988. **62**(5): p. 1558-64.

371. Hill, A.F. and J. Collinge, *Prion strains and species barriers.* Contrib Microbiol, 2004. **11**: p. 33-49.

372. Tatzelt, J. and K.F. Winklhofer, *Folding and misfolding of the prion protein in the secretory pathway.* Amyloid, 2004. **11**(3): p. 162-72.

373. Ertmer, A., et al., *The tyrosine kinase inhibitor STI571 induces cellular clearance of PrPSc in prion-infected cells.* J Biol Chem, 2004. **279**(40): p. 41918-27.

374. Gilch, S., et al., *Intracellular re-routing of prion protein prevents propagation of PrP(Sc) and delays onset of prion disease.* EMBO J, 2001. **20**(15): p. 3957-66.

375. Orru, C.D., et al., *Rapid and sensitive RT-QuIC detection of human Creutzfeldt-Jakob disease using cerebrospinal fluid.* MBio, 2015. **6**(1).

376. John, T.R., H.M. Schatzl, and S. Gilch, *Early detection of chronic wasting disease prions in urine of pre-symptomatic deer by real-time quaking-induced conversion assay.* Prion, 2013. **7**(3): p. 253-8.

377. Homma, T., et al., *Increased expression of p62/SQSTM1 in prion diseases and its association with pathogenic prion protein.* Sci Rep, 2014. **4**: p. 4504.

378. Wang, H., et al., *Tunicamycin-induced unfolded protein response in the developing mouse brain.* Toxicol Appl Pharmacol, 2015. **283**(3): p. 157-67.

379. Lindholm, D., H. Wootz, and L. Korhonen, *ER stress and neurodegenerative diseases.* Cell Death Differ, 2006. **13**(3): p. 385-92.

380. Hoozemans, J.J., et al., *Activation of the unfolded protein response in Parkinson's disease.* Biochem Biophys Res Commun, 2007. **354**(3): p. 707-11.

381. Hoozemans, J.J., et al., *The unfolded protein response is activated in Alzheimer's disease.* Acta Neuropathol, 2005. **110**(2): p. 165-72.

382. Rao, R.V. and D.E. Bredesen, *Misfolded proteins, endoplasmic reticulum stress and neurodegeneration.* Curr Opin Cell Biol, 2004. **16**(6): p. 653-62.

383. Hetz, C.A., *ER stress signaling and the BCL-2 family of proteins: from adaptation to irreversible cellular damage.* Antioxid Redox Signal, 2007. **9**(12): p. 2345-55.

384. Paschen, W. and T. Mengesdorf, *Endoplasmic reticulum stress response and neurodegeneration.* Cell Calcium, 2005. **38**(3-4): p. 409-15.

385. Hamdan, N., P. Kritsiligkou, and C.M. Grant, *ER stress causes widespread protein aggregation and prion formation.* J Cell Biol, 2017. **216**(8): p. 2295-2304.

386. Hoshino, T., et al., *Endoplasmic reticulum chaperones inhibit the production of amyloid-beta peptides.* Biochem J, 2007. **402**(3): p. 581-9.

387. Hoozemans, J.J., et al., *The unfolded protein response is activated in pretangle neurons in Alzheimer's disease hippocampus.* Am J Pathol, 2009. **174**(4): p. 1241-51.

388. Stutzbach, L.D., et al., *The unfolded protein response is activated in disease-affected brain regions in progressive supranuclear palsy and Alzheimer's disease.* Acta Neuropathol Commun, 2013. **1**: p. 31.

389. Hoozemans, J.J., et al., *Activation of the unfolded protein response is an early event in Alzheimer's and Parkinson's disease.* Neurodegener Dis, 2012. **10**(1-4): p. 212-5.

390. Rutkevich, L.A. and D.B. Williams, *Participation of lectin chaperones and thiol oxidoreductases in protein folding within the endoplasmic reticulum.* Curr Opin Cell Biol, 2011. **23**(2): p. 157-66.

391. Castillo, V., et al., *Functional Role of the Disulfide Isomerase ERp57 in Axonal Regeneration.* PLoS One, 2015. **10**(9): p. e0136620.

392. Orru, C.D., et al., *Human variant Creutzfeldt-Jakob disease and sheep scrapie PrP(res) detection using seeded conversion of recombinant prion protein.* Protein Eng Des Sel, 2009. **22**(8): p. 515-21.

393. Henderson, D.M., et al., *Rapid antemortem detection of CWD prions in deer saliva.* PLoS One, 2013. **8**(9): p. e74377.

394. Schmitz, M., et al., *Application of an in vitro-amplification assay as a novel pre-screening test for compounds inhibiting the aggregation of prion protein scrapie.* Sci Rep, 2016. **6**: p. 28711.

395. Abdelaziz, D.H., et al., *Immunization of cervidized transgenic mice with multimeric deer prion protein induces self-antibodies that antagonize chronic wasting disease infectivity in vitro.* Sci Rep, 2017. **7**(1): p. 10538.

396. Orru, C.D., et al., *Factors That Improve RT-QuIC Detection of Prion Seeding Activity.* Viruses, 2016. **8**(5).

397. Kim, J.Y., et al., *Intracerebroventricular viral injection of the neonatal mouse brain for persistent and widespread neuronal transduction.* J Vis Exp, 2014(91): p. 51863.

398. Fullekrug, J., P. Scheiffele, and K. Simons, *VIP36 localisation to the early secretory pathway.* J Cell Sci, 1999. **112 (Pt 17)**: p. 2813-21.

399. Hauri, H., et al., *Lectins and traffic in the secretory pathway.* FEBS Lett, 2000. **476**(1-2): p. 32-7.

400. D'Castro, L., et al., *Isolation of proteinase K-sensitive prions using pronase E and phosphotungstic acid.* PLoS One, 2010. **5**(12): p. e15679.

401. Madec, J.Y., et al., *Biochemical properties of protease resistant prion protein PrPsc in natural sheep scrapie.* Arch Virol, 1997. **142**(8): p. 1603-12.

402. Collinge, J., *Molecular neurology of prion disease.* J Neurol Neurosurg Psychiatry, 2005. **76**(7): p. 906-19.

403. Collinge, J., *Prion diseases of humans and animals: their causes and molecular basis.* Annu Rev Neurosci, 2001. **24**: p. 519-50.

404. Heiseke, A., Y. Aguib, and H.M. Schatzl, *Autophagy, prion infection and their mutual interactions.* Curr Issues Mol Biol, 2010. **12**(2): p. 87-97.

405. Thapa, S., et al., *Overexpression of quality control proteins reduces prion conversion in prion-infected cells.* J Biol Chem, 2018. **293**(41): p. 16069-16082.

406. Crunkhorn, S., *Neurodegenerative disease: Phosphatase inhibitor prevents protein-misfolding diseases.* Nat Rev Drug Discov, 2015. **14**(6): p. 386.

407. Way, S.W., et al., *Pharmaceutical integrated stress response enhancement protects oligodendrocytes and provides a potential multiple sclerosis therapeutic.* Nat Commun, 2015. **6**: p. 6532.

408. Mahal, S.P., et al., *Prion strain discrimination in cell culture: the cell panel assay.* Proc Natl Acad Sci U S A, 2007. **104**(52): p. 20908-13.

409. Decker, T. and M.L. Lohmann-Matthes, *A quick and simple method for the quantitation of lactate dehydrogenase release in measurements of cellular cytotoxicity and tumor necrosis factor (TNF) activity.* J Immunol Methods, 1988. **115**(1): p. 61-9.

410. Rotermund, C., G. Machetanz, and J.C. Fitzgerald, *The Therapeutic Potential of Metformin in Neurodegenerative Diseases.* Front Endocrinol (Lausanne), 2018. **9**: p. 400.

411. Jiang, P., et al., *ER stress response plays an important role in aggregation of alpha-synuclein.* Mol Neurodegener, 2010. **5**: p. 56.

412. Carnemolla, A., et al., *Rrs1 is involved in endoplasmic reticulum stress response in Huntington disease.* J Biol Chem, 2009. **284**(27): p. 18167-73.

413. Atkin, J.D., et al., *Induction of the unfolded protein response in familial amyotrophic lateral sclerosis and association of protein-disulfide isomerase with superoxide dismutase 1.* J Biol Chem, 2006. **281**(40): p. 30152-65.

414. Kaufman, R.J., *Stress signaling from the lumen of the endoplasmic reticulum: coordination of gene transcriptional and translational controls.* Genes Dev, 1999. **13**(10): p. 1211-33.

415. Tabas, I. and D. Ron, *Integrating the mechanisms of apoptosis induced by endoplasmic reticulum stress.* Nat Cell Biol, 2011. **13**(3): p. 184-90.

416. Gardner, B.M. and P. Walter, *Unfolded proteins are Ire1-activating ligands that directly induce the unfolded protein response.* Science, 2011. **333**(6051): p. 1891-4.

417. Cabral-Miranda, F. and C. Hetz, *ER Stress and Neurodegenerative Disease: A Cause or Effect Relationship?* Curr Top Microbiol Immunol, 2018. **414**: p. 131-157.

418. Reijonen, S., et al., *Inhibition of endoplasmic reticulum stress counteracts neuronal cell death and protein aggregation caused by N-terminal mutant huntingtin proteins.* Exp Cell Res, 2008. **314**(5): p. 950-60.

419. Devi, L. and M. Ohno, *PERK mediates eIF2alpha phosphorylation responsible for BACE1 elevation, CREB dysfunction and neurodegeneration in a mouse model of Alzheimer's disease.* Neurobiol Aging, 2014. **35**(10): p. 2272-81.

420. Turner, P.V., et al., *Administration of substances to laboratory animals: routes of administration and factors to consider.* J Am Assoc Lab Anim Sci, 2011. **50**(5): p. 600-13.

421. Markowicz-Piasecka, M., et al., *Metformin - a Future Therapy for Neurodegenerative Diseases : Theme: Drug Discovery, Development and Delivery in Alzheimer's Disease Guest Editor: Davide Brambilla.* Pharm Res, 2017. **34**(12): p. 2614-2627.

422. Aguzzi, A., C. Sigurdson, and M. Heikenwaelder, *Molecular mechanisms of prion pathogenesis.* Annu Rev Pathol, 2008. **3**: p. 11-40.

423. Sigurdson, C.J. and A. Aguzzi, *Chronic wasting disease.* Biochim Biophys Acta, 2007. **1772**(6): p. 610-8.

424. Gilch, S., et al., *Chronic wasting disease.* Top Curr Chem, 2011. **305**: p. 51-77.

425. Saunders, S.E., S.L. Bartelt-Hunt, and J.C. Bartz, *Occurrence, transmission, and zoonotic potential of chronic wasting disease.* Emerg Infect Dis, 2012. **18**(3): p. 369-76.

426. Argue, C.K., et al., *Epidemiology of an outbreak of chronic wasting disease on elk farms in Saskatchewan.* Can Vet J, 2007. **48**(12): p. 1241-8.

427. Waddell, L., et al., *Current evidence on the transmissibility of chronic wasting disease prions to humans-A systematic review.* Transbound Emerg Dis, 2017.

428. Haley, N.J. and E.A. Hoover, *Chronic wasting disease of cervids: current knowledge and future perspectives.* Annu Rev Anim Biosci, 2015. **3**: p. 305-25.

429. Marsh, R.F., et al., *Interspecies transmission of chronic wasting disease prions to squirrel monkeys (Saimiri sciureus).* J Virol, 2005. **79**(21): p. 13794-6.

430. Sigurdsson, E.M., et al., *Anti-prion antibodies for prophylaxis following prion exposure in mice.* Neurosci Lett, 2003. **336**(3): p. 185-7.

431. Heppner, F.L., et al., *Prevention of scrapie pathogenesis by transgenic expression of anti-prion protein antibodies.* Science, 2001. **294**(5540): p. 178-82.

432. Wisniewski, T. and F. Goni, *Immunomodulation for prion and prion-related diseases.* Expert Rev Vaccines, 2010. **9**(12): p. 1441-52.

433. Kaiser-Schulz, G., et al., *Polylactide-coglycolide microspheres co-encapsulating recombinant tandem prion protein with CpG-oligonucleotide break self-tolerance to prion protein in wild-type mice and induce CD4 and CD8 T cell responses.* J Immunol, 2007. **179**(5): p. 2797-807.

434. LaFauci, G., et al., *Passage of chronic wasting disease prion into transgenic mice expressing Rocky Mountain elk (Cervus elaphus nelsoni) PrPC.* J Gen Virol, 2006. **87**(Pt 12): p. 3773-80.

435. Duque Velasquez, C., et al., *Deer Prion Proteins Modulate the Emergence and Adaptation of Chronic Wasting Disease Strains.* J Virol, 2015. **89**(24): p. 12362-73.

436. Ohsawa, N., et al., *Therapeutic effect of peripheral administration of an anti-prion protein antibody on mice infected with prions.* Microbiol Immunol, 2013. **57**(4): p. 288-97.

437. Zabel, M.D. and A.C. Avery, *Prions--not your immunologist's pathogen.* PLoS Pathog, 2015. **11**(2): p. e1004624.

438. Jeon, Y.C., et al., *Pathological characterization of TgElk mice injected with brain homogenate from elk with chronic wasting disease.* J Vet Sci, 2013. **14**(1): p. 21-6.

439. Hannaoui, S., et al., *Destabilizing polymorphism in cervid prion protein hydrophobic core determines prion conformation and conversion efficiency.* PLoS Pathog, 2017. **13**(8): p. e1006553.

440. Kimberlin, R.H. and C.A. Walker, *Pathogenesis of scrapie (strain 263K) in hamsters infected intracerebrally, intraperitoneally or intraocularly.* J Gen Virol, 1986. **67 (Pt 2)**: p. 255-63.

441. Sethi, S., et al., *Postexposure prophylaxis against prion disease with a stimulator of innate immunity.* Lancet, 2002. **360**(9328): p. 229-30.

442. Peretz, D., et al., *Strain-specified relative conformational stability of the scrapie prion protein.* Protein Sci, 2001. **10**(4): p. 854-63.

443. Carreno, J.M., et al., *PLGA-microencapsulation protects Salmonella typhi outer membrane proteins from acidic degradation and increases their mucosal immunogenicity.* Vaccine, 2016. **34**(35): p. 4263-4269.

444. Mays, C.E. and C. Soto, *The stress of prion disease.* Brain Res, 2016. **1648**(Pt B): p. 553-560.

445. Goold, R., C. McKinnon, and S.J. Tabrizi, *Prion degradation pathways: Potential for therapeutic intervention.* Mol Cell Neurosci, 2015. **66**(Pt A): p. 12-20.

446. Muchowski, P.J., *Protein misfolding, amyloid formation, and neurodegeneration: a critical role for molecular chaperones?* Neuron, 2002. **35**(1): p. 9-12.

447. Kranz, P., et al., *PDI is an essential redox-sensitive activator of PERK during the unfolded protein response (UPR).* Cell Death Dis, 2017. **8**(8): p. e2986.

448. Oka, O.B. and N.J. Bulleid, *Forming disulfides in the endoplasmic reticulum.* Biochim Biophys Acta, 2013. **1833**(11): p. 2425-9.

449. Chiesa, R., et al., *Neurological illness in transgenic mice expressing a prion protein with an insertional mutation.* Neuron, 1998. **21**(6): p. 1339-51.

450. Sandberg, M.K., et al., *Prion neuropathology follows the accumulation of alternate prion protein isoforms after infective titre has peaked.* Nat Commun, 2014. **5**: p. 4347.

451. Concha-Marambio, L., et al., *Detection of prions in blood from patients with variant Creutzfeldt-Jakob disease.* Sci Transl Med, 2016. **8**(370): p. 370ra183.

452. Brown, P., *A New Standard for the Laboratory Diagnosis of Sporadic Creutzfeldt-Jakob Disease.* JAMA Neurol, 2017. **74**(2): p. 144-145.

453. Kramm, C., et al., *Detection of Prions in Blood of Cervids at the Asymptomatic Stage of Chronic Wasting Disease.* Sci Rep, 2017. **7**(1): p. 17241.

454. Haley, N.J., et al., *Design, implementation, and interpretation of amplification studies for prion detection.* Prion, 2018. **12**(2): p. 73-82.

455. Meusser, B., et al., *ERAD: the long road to destruction.* Nat Cell Biol, 2005. **7**(8): p. 766-72.

456. Satpute-Krishnan, P., et al., *ER stress-induced clearance of misfolded GPI-anchored proteins via the secretory pathway.* Cell, 2014. **158**(3): p. 522-33.

457. Rutkowski, D.T., et al., *Adaptation to ER stress is mediated by differential stabilities of pro-survival and pro-apoptotic mRNAs and proteins.* PLoS Biol, 2006. **4**(11): p. e374.

458. Dirikoc, S., et al., *Nonpsychoactive cannabidiol prevents prion accumulation and protects neurons against prion toxicity.* J Neurosci, 2007. **27**(36): p. 9537-44.

459. Colla, E., et al., *Endoplasmic reticulum stress is important for the manifestations of alpha-synucleinopathy in vivo.* J Neurosci, 2012. **32**(10): p. 3306-20.

460. Saxena, S., E. Cabuy, and P. Caroni, *A role for motoneuron subtype-selective ER stress in disease manifestations of FALS mice.* Nat Neurosci, 2009. **12**(5): p. 627-36.

461. Thapa, S., et al., *Sephin1 Reduces Prion Infection in Prion-Infected Cells and Animal Model.* Mol Neurobiol, 2020.

462. Dunkel, P., et al., *Clinical utility of neuroprotective agents in neurodegenerative diseases: current status of drug development for Alzheimer's, Parkinson's and Huntington's diseases, and amyotrophic lateral sclerosis.* Expert Opin Investig Drugs, 2012. **21**(9): p. 1267-308.

463. Youdim, M.B., *Why do we need multifunctional neuroprotective and neurorestorative drugs for Parkinson's and Alzheimer's diseases as disease modifying agents.* Exp Neurobiol, 2010. **19**(1): p. 1-14.

464. Czub S, S.-S.W., Stahl-Hennig C, Beekes M, Schaetzl H, Motzkus D. *First evidence of intracranial and peroral transmission of chronic wasting disease (CWD) into cynomolgus macaques: a work in progress.* . in *Prion 2017*. 2017. Edinburgh, The United Kingdom.

465. Peretz, D., et al., *Antibodies inhibit prion propagation and clear cell cultures of prion infectivity.* Nature, 2001. **412**(6848): p. 739-43.

466. Enari, M., E. Flechsig, and C. Weissmann, *Scrapie prion protein accumulation by scrapie-infected neuroblastoma cells abrogated by exposure to a prion protein antibody.* Proc Natl Acad Sci U S A, 2001. **98**(16): p. 9295-9.

467. Goni, F., et al., *High titers of mucosal and systemic anti-PrP antibodies abrogate oral prion infection in mucosal-vaccinated mice.* Neuroscience, 2008. **153**(3): p. 679-86.

468. Sigurdsson, E.M., et al., *Immunization delays the onset of prion disease in mice.* Am J Pathol, 2002. **161**(1): p. 13-7.

469. Chung, Y.L., et al., *MRI assessment of the blood-brain barrier in a hamster model of scrapie.* Neurodegeneration, 1995. **4**(2): p. 203-7.

470. Klyubin, I., et al., *Peripheral administration of a humanized anti-PrP antibody blocks Alzheimer's disease Abeta synaptotoxicity.* J Neurosci, 2014. **34**(18): p. 6140-5.

471. Brandner, S. and Z. Jaunmuktane, *Prion disease: experimental models and reality.* Acta Neuropathol, 2017. **133**(2): p. 197-222.

472. Browning, S.R., et al., *Transmission of prions from mule deer and elk with chronic wasting disease to transgenic mice expressing cervid PrP.* J Virol, 2004. **78**(23): p. 13345-50.

473. Bian, J., et al., *Primary structural differences at residue 226 of deer and elk PrP dictate selection of distinct CWD prion strains in gene-targeted mice.* Proc Natl Acad Sci U S A, 2019. **116**(25): p. 12478-12487.

474. Abdelaziz, D.H., et al., *Autophagy pathways in the treatment of prion diseases.* Curr Opin Pharmacol, 2019. **44**: p. 46-52.

475. van Rooijen, G.J. and M.M. Moloney, *Plant seed oil-bodies as carriers for foreign proteins.* Biotechnology (N Y), 1995. **13**(1): p. 72-7.

476. Schulze, K., et al., *A prime-boost vaccination protocol optimizes immune responses against the nucleocapsid protein of the SARS coronavirus.* Vaccine, 2008. **26**(51): p. 6678-84.

477. Abdelaziz, D.H., et al., *Recombinant prion protein vaccination of transgenic elk PrP mice and reindeer overcomes self-tolerance and protects mice against chronic wasting disease.* J Biol Chem, 2018. **293**(51): p. 19812-19822.

APPENDICES

Appendix 1. List of my other publications during my PhD not included in this thesis.

1. Abdelaziz DH*, **Thapa S***, Abdulrahman BA, Schatzl HM. 2020. Metformin reduces prion infection in neuronal cells by enhancing autophagy. *Biochem Biophys Res Commun.*, 523(2): 423-428. (***Shared first authorship**)
2. Engelke A*, Gonsberg A*, **Thapa S***, Jung S, Ulbrich S, Seidel RP, Basu S, Multhaup G, Baier M, Engelhard M, Schätzl HM, Winklhofer KF and Tatzelt J. 2018. Dimerization of the cellular prion protein inhibits propagation of scrapie prions. *The Journal of Biological Chemistry*, 293: 8020-8031. (***Shared first authorship**)
3. Abdelaziz DH*, **Thapa S***, Abdulrahman B, Lu L, Jain S, Schatzl HM. 2017. Immunization of cervidized transgenic mice with multimeric deer prion protein induces self-antibodies that antagonize chronic wasting disease infectivity in vitro. *Sci Rep.*, 7: 10538. (***Shared first authorship**)
4. Abdulrahman BA, Abdelaziz DH, **Thapa S**, Lu L, Jain S, Gilch S, Proniuk S, Zukiwski A and Schatzl HM. 2017. The celecoxib derivatives AR-12 and AR-14 induce autophagy and clear prion-infected cells from prions. *Sci Rep.*, 7: 17565.

Appendix 2. Permission from co-authors of the published manuscripts included in this thesis.

As the co-authors, we give our consent to use the paper "**Overexpression of quality control proteins reduces prion conversion in prion-infected cells**" published in the Journal of Biological Chemistry, 293(41), pp. 16069-16082 in 2018 as Chapter 2 of Simrika Thapa's PhD thesis entitled "Novel approaches to fight prion diseases" to be submitted to the Faculty of Graduate Studies at the University of Calgary in 2020.

Co-Author	Signature	Date
Dr. Basant A. Abdulrahman		
Dr. Dalia H. Abdelaziz		
Dr. Li Lu		
Dr. Manel Ben Aissa		
Dr. Hermann M. Schatzl		

As the co-authors, we give our consent to use the paper "**Sephin1 Reduces Prion Infection in Prion-Infected Cells and Animal Model**" published in the Journal of *Molecular Neurobiology*, https://doi.org/10.1007/s12035-020-01880-y in 2020 as Chapter 3 of Simrika Thapa's PhD thesis entitled "Novel approaches to fight prion diseases" to be submitted to the Faculty of Graduate Studies at the University of Calgary in 2020.

Co-Author	Signature	Date
Dr. Dalia H. Abdelaziz		
Dr. Basant A. Abdulrahman		
Dr. Hermann M. Schatzl		

As the co-authors, we give our consent to use the paper "**Recombinant prion protein vaccination of transgenic elk PrP mice and reindeer overcomes self-tolerance and protects mice against chronic wasting disease**" published in the Journal of Biological Chemistry, 293(51), pp. 19812-19822 in 2018 as Chapter 4 of Simrika Thapa's PhD thesis entitled "Novel approaches to fight prion diseases" to be submitted to the Faculty of Graduate Studies at the University of Calgary in 2020. We are aware that the 'Results' and 'Discussion' sections of the above mentioned published paper is re-written by Simrika Thapa in her thesis and we all permit her to do so.

Co-Author	Signature	Date
Dr. Dalia H. Abdelaziz		
Jenna Brandon		
Justine Maybee		
Lauren Vankuppeveld		
Dr. Robert McCorkell		
Dr. Hermann M. Schatzl		

Appendix 3. Permission from journals to include the published manuscripts in this thesis.

Journal of Biological Chemistry: The copyright policy for JBC (ASBMB journal) can be found here: https://www.asbmb.org/journals-news/editorial-policies#copyright. It states that the ASBMB holds an exclusive, irrevocable License to Publish the manuscript and the authors hold the copyright. In their website, they mentioned that authors do not need to take permission from the journal and authors retain the right to include all or the part of their publication in their own's thesis or dissertation. Further, the journal was contacted and they said no permission is required to include the published work in the author's thesis.

Molecular Neurobiology

RightsLink Printable License

SPRINGER NATURE LICENSE
TERMS AND CONDITIONS

Mar 11, 2020

This Agreement between University of Calgary -- Simrika Thapa ("You") and Springer Nature ("Springer Nature") consists of your license details and the terms and conditions provided by Springer Nature and Copyright Clearance Center.

License Number	4781170279581
License date	Mar 03, 2020
Licensed Content Publisher	Springer Nature
Licensed Content Publication	Molecular Neurobiology
Licensed Content Title	Sephin1 Reduces Prion Infection in Prion-Infected Cells and Animal Model
Licensed Content Author	Simrika Thapa et al
Licensed Content Date	Jan 24, 2020
Type of Use	Thesis/Dissertation
Requestor type	academic/university or research institute
Format	print and electronic
Portion	full article/chapter
Will you be translating?	no
Circulation/distribution	50000 or greater

Author of this Springer Nature content	yes
Title	Novel approaches to fight prion diseases
Institution name	University of Calgary
Expected presentation date	Apr 2020
Requestor Location	University of Calgary 3280 Hospital Dr. NW Calgary, AB T2N4Z6 Canada Attn: University of Calgary
Total	0.00 CAD